PALEOPHYSIOLOGY OF PERMIAN AND TRIASSIC SEED PLANTS

By

Andrew B. Schwendemann

Submitted to the graduate degree program in Ecology and Evolutionary Biology and the Graduate Faculty of the University of Kansas in partial fulfillment of the requirements for the degree of Doctor of Philosophy.

_____
Chairperson Thomas N. Taylor

_____
Daniel Crawford

_____
Luis Gonzalez

_____
Craig Martin

_____
Edith L. Taylor

_____
Joy Ward

Date Defended: 23 July 2012

The Dissertation Committee for Andrew B. Schwendemann
certifies that this is the approved version of the following dissertation:

PALEOPHYSIOLOGY OF PERMIAN AND TRIASSIC SEED PLANTS

Chairperson _____ Thomas N. Taylor

Date approved: 23 July 2012

ABSTRACT

This study utilized both anatomically and morphologically preserved fossil plants to investigate plant paleophysiology using known form/function relationships. The fossils examined in this project come from fossil localities ideal for studying various paleophysiological relationships. At the beginning of the Permian Period (~299 Ma), atmospheric CO_2 and O_2 concentrations were comparable to current day values. By the end of the Permian (~251 Ma), atmospheric CO_2 concentration and temperature had risen sharply as the Earth underwent a time of rapid global warming. The distinctive leaf of *Glossopteris* plants can be found at southern high paleolatitude localities throughout the Permian, allowing for changes in plant physiology to be tracked through a drastically shifting climate. The environmental conditions at the beginning of the Permian are also the same as those that are thought to have favored the evolution of the C_4 photosynthetic pathway in the Oligocene (~25 Ma). Using known relationships between leaf anatomy and the C_4 pathway, along with stable carbon isotope analysis, the presence or absence of this pathway was tested. The combination of both approaches demonstrated the C_3-C_4 intermediate photosynthetic pathway was present in *Glossopteris* during the Late Permian.

In the ancient past, plants existed in warm environments at high paleolatitudes where they were subjected to light regimes not experienced by plants today (4 months of continuous light and 4 months of continuous dark). A study of leaf economics of Permian *Glossopteris* leaves reveals that the plant possessed deciduous leaves and adaptations to continuous light environments.

Analysis of Permian and Triassic leaf hydraulic conductance demonstrates that leaf venation density in *Glossopteris* decreases in response to increasing CO_2 but does not change in response to latitude. *Glossopteris* leaves, which dominated the Permian landscapes of Antarctica,

demonstrated a higher leaf venation density than any co-occurring leaves. Such an advantage would benefit leaf hydraulic conductance. In contrast, the *Dicroidium* leaf type, which dominated the Triassic, had leaf hydraulic values similar to co-occuring leaf morphotypes.

ACKNOWLEDGEMENTS

The research described in this dissertation would not have been possible withour my advisor, Dr. Thomas N. Taylor, and Dr. Edith L. Taylor. Their support, encouragement, and guidance throughout my graduate education has made the intellectual contributions of this dissertation possible. I am also grateful for the advice from my committee members: Drs. Dan Crawford, Luis Gonzalez, Craig Martin, and Joy Ward. Dr. Martin deserves special credit for several insightful conversations about plant physiology.

I have also had the pleasure to work with a number of excellent paleobotanists in our lab. I hope I can be at least half as successful as they have been. I am especially indebted to Dr. Rudolph Serbet, whose constant encouragement and friendship have made graduate school much easier. I am also in the debt of Julie Bergene, Benjamin Bomfleur, Anne-Laure Decombeix, Ignacio Escapa, Carla Harper, Elizabeth Hermsen, Ashley Klymiuk, and Patricia Ryberg. Jeannie Houts deserves special recognition for all of the work she does behind the scenes. Without her help, I would have surely drowned in paperwork long ago.

The entire staff of the Department of Ecology and Evolutionary Biology has my gratitude as well for all of their hard work and the patience that they have shown me over the years.

Finally, I could not have made it this far without the support of my family. My parents and sister have always stood behind me and they have never questioned (at least not where I could hear) my desire to go into paleobotany. Without the support of my loving wife, Meredith (and our cat Beaker), I probably would have given up long ago. She has kept me sane throughout all the troubles of graduate school.

Table of Contents

Chapter 1

Introduction to form/function studies in plant physiology and the utility of the Permian and Triassic of Antarctica as an experimental framework

Studies in plant physiology seek to understand how plants function. This field largely deals with processes that occur within plant tissues. These processes can be chemical (e.g., the binding of oxygen and carbon dioxide to RuBisCO) or physical (e.g., the movement of water and solutes through a plant). The focus of these studies can be on small-scale interactions (e.g., the movement of electrons through the electron transport chain) or large-scale interactions (e.g., the role of hormones in plant development). At all scales, the study of plant biochemistry is frequently essential to accurately describe how the plant functions. In some cases, the structure of the plant itself can be used to infer plant function. In these cases, a detailed study of the plant biochemistry is not needed to reach an understanding of the plant physiology. These form/function relationships are crucial to understanding physiological characteristics of plants where studies of their biochemistry are either prohibitively difficult or impossible.

Fossil plants have played a fundamental role in advancing our understanding of the origin and evolution of the plant kingdom. Without paleobotany, entire plant phyla (e.g., Rhyniophyta, Zosterophyllophyta, Trimerophytophyta, Progymnospermophyta, and Pteridospermophyta) would be completely unknown (Taylor et al., 2009). The study of these ancient forms, combined with knowledge of their environment gleaned from multiple sources of geologic evidence, offers the opportunity for unprecedented insights into how and under what circumstances plants evolved. Just as the anatomy and morphology of plants have changed over time, long-term

environmental changes have resulted in modifications in plant function through time. The study of these changes can provide detail into how plants of the past have responded to long-term environmental changes, such as rising atmospheric CO_2 concentration or temperature. Relatively few studies of fossil plants have focused on the physiological aspects of the organisms. Much of the research in plant physiology concerns the roles of plant hormones and other molecular components that can only be studied indirectly in fossil plants. Only those physiological parameters that can be examined based on fundamental relationships of plant morphology, anatomy, and isotope composition can be examined directly in the study of fossil plant physiology.

1. Form/function relationships in extant plants

It is commonly recognized that plant morphology and anatomy are strongly associated with metabolic type, light exposure, water relations, and other physiological properties (Smith et al., 1997b). The following section provides a brief review of recent research using form/function relationships to study the physiology of extant plants.

1.1 Leaf hydraulics, vasculature, and models of photosynthesis

The flow of water through plants is governed largely by physical laws and the unique anatomical and morphological structure of plants. For example, fluid flow through the tracheids of a leaf has been described by the Hagen-Poiseuille equation, which relates hydraulic conductance to the radius of a tracheid and the viscosity of a fluid flowing through the tracheid (Niklas, 1992). This equation, combined with Murray's Law for branching pipes (Sherman, 1981), can describe the flow of water through the dichotomizing venation of a leaf. In systems with a significant amount of anastomosing conduits and/or particularly leaky conduits, the sufficiency of Murray's Law to explain the flow is somewhat controversial (LaBarbera, 1990;

Canny, 1993; Roth-Nebelsick et al., 2001; McCulloh et al., 2003; McCulloh and Sperry, 2005) and more complicated models are sometimes utilized (e.g., Durand, 2006; Bohn and Magnasco, 2007). Physical laws and structural relationships have even been used to model such fine-scale phenomena as the relationship of inter-vessel pit area to the trade-offs between vessel cavitation safety and transport efficiency (Hacke et al., 2005; Hacke et al., 2006). Determination of hydraulic conductance in a leaf can yield considerable information about a plant since the amount of conductance varies 65-fold across extant species and is closely related to the maximum rate of photosynthesis (Sack and Holbrook, 2006).

Zwieniecki et al. (2006) modeled the ideal hydraulic design of pine needles with respect to permeability along the needle in order to determine how similar the biological design was to a theoretical optimum. In the three pine species analyzed, it was determined that the actual structure of the pine needle was an almost perfect match to the theoretical ideal, indicating that venation design plays a significant role in overall leaf hydraulics (Zwieniecki et al., 2006). Brodribb and Hill (1997) measured the maximum stomatal conductance (g_{max}) in several Southern Hemisphere conifers by modeling the relationship between stomatal structure, stomatal density, and the diffusivity of water vapor in the air (see Parlange and Waggoner, 1970; Parkhurst, 1994); maximum stomatal conductance is directly related to the maximum photosynthetic rate. There is a close agreement between the theoretical and measured g_{max}, except for species with stomatal plugs, emphasizing the need for accurate anatomical information when applying models to living systems (Brodribb and Hill, 1997).

Using a complex mathematical model, Dauzat et al. (2001) were able to accurately predict whole tree transpiration, leaf temperature, and the water potential gradient in a coffee plant (*Coffea arabica*). Inputs for the model were stomatal conductance, stem conductance, and

petiole-leaf conductance, all of which can be modeled based on plant structure and physical constants. The model can be easily applied to other plant functions and, in particular, the authors mention the possibility of calculating plant carbon balances; photosynthesis can be calculated once the lighting, temperature, and stomatal conductance are known (Dauzat et al., 2001). Several other models of photosynthesis (e.g., Kirschbaum and Farquhar, 1984; Harley and Sharkey, 1991) and CO_2 diffusion in leaves (Terashima et al., 2001) exist that even incorporate molecular components of photosynthesis, such as the rate of carboxylation limited by Rubisco.

1.2 Leaf economics

Leaf economics is the study of the rate at which a leaf consumes its nutritional resources. These resources can include the nitrogen content of the leaf, the photosynthetic rate, the amount of resources utilized in constructing a leaf, and the length of time that the leaf will remain functional. Because of this, it can also be used to estimate whether a plant is deciduous or evergreen. Leaf economics operate independently of generalized growth form and plant functional type (Wright et al., 2004); other studies have demonstrated that shifts in leaf economic traits occur with different climates and may represent substantial selective pressures in shifting environments (Wright et al., 2005).

Leaves with a high leaf mass per area (LMA) have been shown to have longer leaf life spans (LLS) than those with a lower LMA, and a lower photosynthetic rate as well (Reich et al., 1997; Diemer, 1998; Ryser and Urbas, 2000; Westoby et al., 2002). Although leaves with a high LMA are more expensive to construct and have lower photosynthetic rates, they are less susceptible to herbivory due to their increased thickness. The trade-offs between low and high LMA leaves represent the continuum between a rapid resource acquisition strategy and a resource retention strategy (Grubb, 1998).

Scaling relationships between photosynthetic capacity, foliar dark respiration rate, stomatal conductance, specific leaf area (SLA, the inverse of LMA), and leaf nutrient content have been studied across 79 perennial species in different habitats (Wright et al., 2001). The data indicate that these scaling relationships are true across many plant species and within different environments, allowing for generalizations to be made about resource strategies in a variety of ecosystems and among many plant species (Wright et al., 2001).

1.3 Leaf life span in high latitude environments

Osborne and Beerling (2002) used extant conifers to simulate the growth of trees at high latitudes in a warm CO_2-rich climate. They were able to fit a model to the observed amount of carbon, nitrogen, and water fluxes in a conifer forest based on LLS and its related attributes (Osborne and Beerling, 2002). One issue associated with plants growing at high paleolatitudes is the penalty of respiration during the dark winter versus the loss of carbon in a deciduous habit. By measuring the metabolism of conifers in growth rooms simulating light in a high latitude environment with a high atmospheric CO_2 concentration, it has been demonstrated that the carbon lost by dropping leaves for the winter could be regained by 10 to 20 days of photosynthesis in the summer (Osborne and Beerling, 2003). Further research into conifer growth at high latitudes used mathematical models to simulate carbon loss in the deciduous habit versus respiration in the evergreen habit (Osborne et al., 2004b). These authors reached the conclusion that the evergreen habit at high latitudes was less costly in terms of carbon loss than a deciduous habit, despite the fact that deciduous trees flourished in high paleolatitude environments. More recent work on plants grown experimentally under continuous light conditions suggests that plants with a deciduous habit and indeterminate growth (e.g., *Metasequoia glyptostroboides*) are much better adapted for continuous light than plants with a

deciduous habit and determinate growth or a plant with an evergreen habit (e.g., *Sequoia sempervirens*) (Jagels and Day, 2004; Equiza et al., 2006a, 2006b, 2007). Fossil plants provide an opportunity to study this phenomenon in plants that were naturally growing at these extreme limits.

1.4 C_3, C_4, and CAM photosynthetic pathways

A generalized relationship between plant form and function that has been studied in detail is the relationship between leaf anatomy and photosynthetic pathway. Dengler et al. (1994) quantified the anatomical differences between C_3 and C_4 grasses, finding that interveinal distance in C_4 grasses is significantly shorter than in C_3 grasses. They also determined that C_4 plants have a lower proportion of primary carbon assimilation (PCA) tissue per vein and a higher proportion of photosynthetic carbon reduction (PCR) tissue per vein than C_3 plants. Furthermore, it was noted that the proportion of intercellular space within the mesophyll tissue is significantly lower in C_4 plants, as is the mean cross-sectional area of vascular tissue per vein (Dengler et al., 1994). In 2003, Ogle expanded the scope of this research and formulated a relationship between interveinal distance and the quantum yield of photosynthesis in C_4 grasses. When the relationship is plotted over a variety of interveinal distances, the data suggest that there is a theoretical threshold in a given environment where the photosynthetic competitive advantage can switch between C_3 and C_4 plants (Ogle, 2003).

Research into quantifying these relationships also expanded to C_3 and C_4 eudicots (Muhaidat et al., 2007). It was discovered that C_4 plants have a significantly lower proportion of PCA tissue to PCR tissue than C_3 plants. Muhaidat et al. (2007) also reported a significantly lower ratio of intercellular space to the total leaf cross sectional area in C_4 plants compared to C_3 plants. A lower ratio of PCR external perimeter to tissue area and a greater proportion of leaf

cross-sectional area were also found in C_4 plants.

Compared to extant plants, there has been little research into the physiology of fossil plants. This may be due in large part to the relative dearth of anatomically preserved fossils. In spite of this fact, some paleophysiological data have been produced; below is a brief summary of some of the recent work into plant paleophysiology.

2. Studies in fossil plant physiology

2.1 Fossil hydraulics, vasculature, and models of photosynthesis

John A. Raven has done several studies where he attempted to elucidate physiological characteristics of extinct plants, although many of these studies did not involve the direct study of fossil plants. Raven (1977) used published descriptions of early vascular land plants (e.g., rhyniophytes) and knowledge of water and gas exchange in extant plants to infer how these transport processes may have occurred in the Devonian. He concluded that all of the defining characteristics of extant homoiohydric land plants could be found in the early plant fossil record (Raven, 1977). A similar line of thought was used to hypothesize the biochemical and structural 'pre-adaptations' that may have occurred in the precursors to the land plants (Raven, 1984). Later studies incorporated a quantitative analysis of photosynthesis in a hypothetical early land plant (Raven, 1993). Raven (1994a,1994b) also used a comparative anatomy approach to hypothesize how the differences in tissue organization between extant land plants and early land plants affected plant physiology. It was concluded that the early land plants were less efficient with respect to water and solute transport (Raven, 1994a; Raven, 1994b). Raven (1991) examined the ability of extant plants to photosynthesize in O_2 levels many times higher than those found today. It was found that extant plants could withstand O_2 concentrations higher than those modeled for the Phanerozoic (Berner and Canfield, 1989; Raven, 1991).

Cichan (1986) used the Hagen-Poiseuille relationship to calculate water conductance in the wood of several Carboniferous ferns and gymnosperms. The highest conductance values were found in *Sphenophyllum plurifoliatum*, *Medullosa noei*, and *Paralycopodites brevifolius*; values were roughly equivalent to the middle range of conductance in vessel-containing angiosperms. These are overestimates, however, as the Hagen-Poiseuille relationship assumes that the tracheids are perfect capillaries and does not take into account the 'leaky' nature of tracheids (Cichan, 1986). Wilson et al. (2008) expanded on this work by refining the conductance model to include the resistance to flow from the cell lumen, pits, and pit membranes. In addition, the petiole and leaf size were considered in addition to the stem tracheids. The fluid flow in *Medullosa* was again found to be comparable to that in angiosperms (Wilson et al., 2008). The same techniques were applied to the early land plant *Asteroxylon mackei*. Their results suggest that *Asteroxylon* had evolved mechanisms of rapid water transport without also developing safety mechanisms that would limit damage caused by excessive evapotranspiration (Wilson and Fischer, 2011). Cavitation in *Archaeopteris* has been studied and it was concluded that the hydraulics of this progymnosperm were similar to those of conifers (Pittermann, 2010).

In a study of fossil leaves from the Cretaceous, research demonstrated that the number of angiosperm species with high leaf vein densities increased throughout that geologic period (Feild et al., 2011a). In another study of Early Cretaceous angiosperm leaves, it was concluded through the use of fossil leaf modeling that the earliest angiosperms had lower gas exchange capacities than their modern counterparts (Feild et al., 2011b). It has also been demonstrated that the increased hydraulic conductance of the angiosperms relative to other fossil groups played a role in the rise of the angiosperms during the Cretaceous (Boyce et al., 2009).

Beerling and Woodward (1997) modeled changes in plant photosynthetic output and water use efficiency (WUE) over the Phanerozoic. Their model predicts that WUE was at its peak early after the evolution of leaves and dropped to its lowest levels approximately 300 Ma, before recovering to about half its initial level shortly afterward. Photosynthetic output, on the other hand, appears to have had a more sinusoidal pattern through time. The model was based on models of photosynthesis derived from extant plants and incorporated stomatal data and changes in atmospheric CO_2 concentrations, atmospheric O_2 concentrations, and temperature through time (Beerling and Woodward, 1997). The model was validated by comparing predicted carbon isotope ratios to those found in the studied fossils.

A complex model of transpiration and assimilation was developed by Konrad et al. (2000) and applied to *Aglaophyton major*, an early land plant from the Early Devonian Rhynie Chert. The values for assimilation and transpiration for *Aglaophyton* were found to be similar to those modeled by Beerling and Woodward (1997) for all plants during the same time period. Modeled values of transpiration (47 μmol m^{-2} s^{-1}) and assimilation (3.1 μmol m^{-2} s^{-1}) are considerably low when compared to extant plants (Konrad et al., 2000). The WUE for *Aglaophyton* is much higher than in extant plants, but this is mainly due to its much lower modeled transpiration rate (Konrad et al., 2000).

Raven (1994a) analyzed the maximum distance between photosynthetic cells and vascular tissue in several extant and fossil groups. The maximum distance was consistently larger in the fossil plants, which were all Paleozoic. Due to the increased amount of time it would take for photosynthates to reach transport tissues, it was concluded that the photosynthetic rates of early land plants were likely lower than those of plants today (Raven, 1994a).

Roth-Nebelsick et al. (2000) performed a morphometric analysis of stems of the early

land plants *Rhynia gwynne-vaughanii* and *Asteroxylon mackiei* to determine the functional aspects of their xylem. The authors discovered that the ratio of cross-sectional area of the xylem to the xylem perimeter was constant during ontogenetic development for *Asteroxylon*. The ratio was shown to play a major role in water transport performance and was twice as large in *Asteroxylon* as it was in *Rhynia*. Contrary to their predictions, the relatively large distance from the xylem to the transpirational surface in these plants was not a limiting factor for water transport in these axes (Roth-Nebelsick et al., 2000).

Franks and Beerling (2009) developed a model driven by atmospheric CO_2 concentration that studies the long-term environmental influences on stomatal size, stomatal density, and the maximum Rubisco carboxylation rate. The model showed that those three parameters changed in response to changing atmospheric CO_2 concentration in a way that minimized the energetic costs and nitrogen requirements for CO_2 assimilation. The authors also documented a calculated rise in stomatal conductance over the Phanerozoic that parallels the evolutionary trend in plants towards increased hydraulic capacity (Franks and Beerling, 2009).

The sporophytes of early land plants were exceedingly small. Most of these early plants had stem diameters less than 10 mm (Boyce, 2008). Such small sizes have led some to wonder if these sporophytes were dependent upon gametophyte generations that are rarely preserved in the fossil record. Boyce (2008) looked at the diameter of many of these fossils and after accounting for thicknesses of support tissues, desiccation resistance tissues, and transport tissues, discovered that many of the earliest land plants would not have a large enough diameter to also contain photosynthetic tissues.

2.2 Leaf development

Osborne et al. (2004a) performed a morphometric analysis of 300 fossil plants to examine

the effects of high atmospheric CO_2 concentration on the size of leaves shortly after their evolution. During this time, biophysical constraints on leaf size (mainly overheating) are hypothesized to have kept megaphylls relatively small. As the CO_2 concentration decreased and resulted in increased stomatal density, there was a 25-fold increase in leaf size in two phylogenetically independent lineages (Osborne et al., 2004a). The 5-fold increase in stomatal density that resulted from the falling atmospheric CO_2 concentration provided leaves with an adequate cooling mechanism, allowing them to reach greater sizes.

2.3 Fossil leaf economics

Royer et al. (2007) examined the relationship between LMA and petiole width (PW). Due to the biomechanical role that the petiole plays in support of a leaf of a given size, a generalized relationship was documented between LMA and PW. Since there is no strong relationship between phylogeny and LMA (Ackerly and Reich, 1999), these relationships can be directly applied to the fossil record and paleoecosystems. Royer et al. (2007) then applied the principles of leaf economics to Eocene fossil plants. Analysis of leaves from three different fossil localities demonstrated a range of ecological structuring among the localities. The Republic, Washington locality was dominated by deciduous plants, and the Bonanza, Utah locality by evergreen plants although it also contained a substantial portion of deciduous plants. The authors were also able to successfully correlate LMA and LLS with insect herbivory; leaves with the highest LMA and LLS were less likely to show evidence of insect herbivory. Based on the LMA values, the Republic locality was shown to have more rapid gas exchange and faster litter decomposition than the Bonanza site. Since the litter decomposition rate influences the nutrient turnover and regional biogeochemical cycling rates, it was definitively shown that the nutrient cycle at the Republic locality was much faster than at the Bonanza locality (Royer et al., 2007).

Leaves are not the only plant organ used to determe LLS. Falcon-Lang (2000a, 2000b) has utilized methods of wood growth ring analysis to determine LLS. This technique involves measuring successive tracheids in transverse section across growth rings and calculating the cumulative algebraic sum of each cell's deviation from the mean. Plotting a curve of these sums can indicate the leaf habit (Falcon-Lang, 2000a, 2000b). Taylor and Ryberg (2007) applied these techniques to fossil wood from the Permian and Triassic of Antarctica; these fossil plants were subjected to high polar latitude light regimes while they were living. Although the paleoclimate reconstructions of the two localities were different, the plants exhibited similar responses to the extreme light regimes (Taylor and Ryberg, 2007). Growth rings from the two sights contained very small amounts of late-wood, indicating that the transition to dormancy was relatively fast, likely in response to the high paleolatitude light regime.

2.4 Hormones

Rothwell and Lev-Yadun (2005) have demonstrated that polar auxin flow occurred as early as the Late Devonian. Wood of the progymnosperm *Archaeopteris* contains areas of distorted tracheary elements above branches. Similar structures can be found in extant plants where barriers to auxin flow, such as branches, cause 'auxin whirlpools.' The auxin causes the tracheary elements to differentiate in unusual ways within the secondary xylem (Rothwell and Lev-Yadun, 2005).

3. Paleogeographic research focus

Although plant fossils from nearly any locality could be analyzed in a physiological context, it is perhaps more interesting to place their physiological characteristics in a broader framework. In order to accomplish this, one needs to pick a study area from which multiple questions can be asked and for which a large amount of material is available. The KU Natural History Museum Division of Paleobotany has a large collection of Permian and Triassic plant

fossils from Antarctica and is the official NSF repository for Antarctic fossil plants. The collection includes >3000 Permian compression/impression fossils; most specimens bear several leaves. These specimens come from 64 different fossil localities, including fossils from other Gondwanan localities such as Australia, Argentina, South Africa, India, and Zimbabwe. These localities cover a wide range of paleolatitudes and extend from the Early to Late Permian; the majority of specimens are Late Permian. The collection also contains >700 permineralized blocks that each contains hundreds of anatomically preserved *Glossopteris* leaves. Most of these come from a single Upper Permian locality (Skaar Ridge), but some come from other localities. Over 1500 compression/impression fossils containing *Dicroidium* leaves are housed in the KU collection. The fossils come from several localities in Antarctica and are dated Middle and a Upper Triassic. Most of the *Dicroidium* fossils are from Antarctica; <60 specimens come from other locations (Australia, South Africa). More than 500 permineralized blocks with abundant leaves in each are housed in the collection. Most of these specimens are from a lower Middle Triassic locality (Fremouw Peak) and others are from a Late Triassic locality (Mt. Falla), both in Antarctica. Fossils plants from these localities in Antarctica are ideal for several reasons. The fossil plants from this region are preserved in a variety of modes which allows for different physiological studies. The plants lived in a warm, high paleolatitude environment for which there is no modern analogue, and the climate during the Permian and Triassic was fluctuating in a way that may have had a large impact on plant physiology.

Fossil plants from Permian and Triassic localities in Antarctica are preserved as compression/impression fossils and as permineralizations; compression/impression fossils are much more abundant than permineralizations. While compression/impression fossils are useful for many aspects of paleobotany, including fossil plant physiology, they contain little or no

internal preservation. Permineralized fossils, on the other hand, are anatomically preserved and provide information on the cells and tissues of the fossil plant. This preservation provides a greater opportunity to study physiology due to relationships that exist between the anatomy of the organ and physiology. Permineralized plants form when tissue systems become immersed in water containing dissolved minerals. Water and minerals permeate into the cells, where the minerals precipitate to embed the plant tissue in rock. Once collected, permineralized plants can be serially sectioned so that anatomy can be studied.

3.1 High latitude environments

Fossil plants from the Transantarctic Mountains localities allow for the study of continuous light and continuous dark conditions in a natural setting. Plants from Skaar Ridge and Fremouw Peak grew under conditions for which there are no modern analogues: a warm, high latitude environment. High latitude organisms are subjected to months of continuous light in the summer and months of continuous darkness in the winter (Figure 1). While these conditions would be difficult for any organism, they are especially stressful for those that rely on photosynthesis for energy. When the amount of photosynthetically available radiation (PAR) is calculated for the entire year, it is considerably less than the PAR for lower latitudes that never have extended periods of continuous light (Campbell and Aarup, 1989). Changes in PAR can not only affect the maximum photosynthetic rate of a plant, but also play a role in biomass allocation (Poorter et al., 2012). Under conditions of low light, plants will invest more biomass in leaves, while more biomass is invested in roots under high light conditions (Poorter et al., 2012). Equiza et al. (2006a) have shown that under continuous light conditions, some extant gymnosperms show a lower photosynthetic rate than those grown under diurnal light. This rate decrease is likely protects the photosystems from over stimulation caused by excess photon absorbtion.

Despite the lower photosynthetic rate, these gymnosperms produced more biomass. Most of this biomass was allocated to the leaves, but the plants were apparently not grown to reproductive age (Equiza et al., 2006a). Fossil plants growing in periods of continuous dark are assumed to be deciduous based on the carbon loss hypothesis (Spicer and Chapman, 1990; Falcon-Lang and Cantrill, 2001). According to this idea, the carbon cost of dropping leaves for the period of winter darkness is less than the cost of carbon lost to respiration in the leaves during that same time. An experiment with extant plants (*Metasequoia glyptostroboides*, *Taxodium distichum*, *Sequoia sempervirens, Nothofagus cunninghamii,* and *Ginkgo biloba*) grown under continuous light conditions suggests that the deciduous nature is more costly up to latitudes of 83° (Royer et al., 2003). However, the conditions these modern plants were growing in may not be completely analogous to those in the past and the fossil plants may vary greatly from the modern gymnosperms studied. In a more detailed study, the authors found that deciduous plants have larger rates of carbon uptake in the late summer and early autumn, which may offset any carbon losses from dropping leaves (Royer et al., 2005a). Investigating the anatomy of fossils growing under these conditions may provide some valuable physiological insights.

3.2 Permian and Triassic climate

The climatic factors at play during the Permian and Triassic periods also make for an interesting backdrop with which to study fossil plant physiology. Throughout the Permian and into the beginning of the Triassic there was a rapid increase in both atmospheric CO_2 concentration (Figure 2) and temperature (Figure 3). The environmental factors under which the fossil plants from this time were growing are somewhat analogous to what extant plants are presently experiencing.

Atmospheric CO_2 concentrations at the beginning of the Permian (approximately 299 Ma)

are believed to have been at the lowest levels reached since plants evolved onto terrestrial environments (Berner, 2006; Osborne and Beerling, 2006). Towards the end of the Permian (ca. 251 Ma) the atmospheric CO_2 concentration began to rise rapidly, making the late Paleozoic an excellent model system for studying the effects of rapid changes in atmospheric CO_2 concentration on land plants (Osborne and Beerling, 2006). By the Middle Triassic, the atmospheric CO_2 levels evened out and remained relatively constant for the remainder of the Triassic (Berner, 2006).

3.3 The Glossopteris *leaf morphotype*

Permian Gondwana floras are composed mainly of glossopterid seed ferns, an enigmatic group with diverse reproductive structures. *Glossopteris* leaves (Figure 4A) are found on Gondwana through a range of paleolatitudes. The midrib of the leaf is composed of several vascular strands that extend out to the leaf tip. The lateral veins repeatedly dichotomize and anastomose, forming a reticulate venation pattern lacking in hierarchy (Trivett and Pigg, 1996). Up until the Permian, leaves with anastomosing venation patterns were quite rare; such patterns have been linked with declines in atmospheric CO_2 concentrations (Roth-Nebelsick et al., 2001). *Glossopteris* leaves were present by the early Permian at the latest, when CO_2 concentrations were still low. CO_2 concentrations continued to rise into the Triassic, where evidence indicates that the climate was hot and dry (Dickins, 1993).

Another interesting aspect of the glossopterids and the Permian climate is that the environmental factors present at that time are the same ones thought to have shaped the evolution of the C_4 photosynthetic pathway (Osborne and Beerling, 2006). The C_4 pathway is thought to have evolved in several independent lineages of angiosperms as a response to aridity and the low CO_2 levels of 25 Ma (Sage, 2004; Sage et al., 2012). Generalized photosynthesis models of C_3

plants in this type of climate show a 60% to 80% decrease in photosynthetic rate (Beerling, 2005). Without a CO_2-concentrating mechanism, the growth rates of Permian plants would have dropped significantly. It is conceivable, therefore, that the low atmospheric CO_2 concentrations of the Permian could have also caused the evolution of a C_4 carbon pathway over 200 million years earlier than typically believed. Once developed, however, the pathway could have been a disadvantage as the atmospheric CO_2 concentration continued to rise through the Permian into the Triassic.

3.4 The Dicroidium *leaf morphotype*

The *Dicroidium* leaf morphotype (Figure 4B) is the most common leaf found in the Middle and Late Triassic floras of Antarctica. It does not dominate the landscape like the *Glossopteris* morphotype in the Permian (Cúneo, 1996), but is part of a more diverse assembledge of leaf morphotypes (Escapa et al., 2011). *Dicroidium* leaves are compound leaves characterized by a bifurcation of the rachis; the different species range from once pinnate to tripinnate (Taylor et al., 2009). The venation dichotomizes but never anastamoses.

Chapter 2

Methodology, Fossils, and Stratigraphy

1. Paleobotanical techniques

Specimens were prepared for physiological analysis using standard paleobotanical techniques. For analysis requiring fossil plant anatomy, permineralized fossil plants were used. Blocks permineralized by silica were sectioned into slabs using a geologic rock saw. The cut surfaces of the slabs were then hand-polished smooth using an aluminosilicate grit on a piece of glass. The smooth surfaces were then etched in a bath of 49% hydrofluoric acid for 1-5 minutes depending on the rock and strength on the acid. The slabs were then neutralized in a concentrated solution of aqueous sodium bicarbonate for approximately one hour. Slabs were then transferred to a warm water bath to remove any of the sodium bicarbonate that remained from the neutralizing phase. After drying, the etched surface of a slab was covered with acetone and a sheet of cellulose acetate was rolled onto this surface. The acetone was allowed to dissolve the cellulose acetate sheet, causing the sheet to surround the plant remains etched on the rock surface. After 15–20 minutes, the acetone had evaporated and the cellulose acetate sheet had hardened around the plant remains. The sheet was then removed from the rock for analysis in reflected light (Galtier and Phillips, 1999). Portions of the finished peel deemed worthy of further investigation were removed using a razor blade. The removed section of the peel was then mounted on a glass slide using Eukitt™ as a mounting medium; all slides with peels were mounted with a cover slip. Specimens are housed in the Paleobotany Division of the Natural History Museum and Biodiversity Institute, University of Kansas, Lawrence, KS. Peels and

slides were made from blocks 13688 D_{top}, 13752 A-1_{bot}, 13752 A-2_{bot}, 13752 A-5_{top}, 13752 B-1_{bot}, 13752 B-1_{top}, and 13752 B_{top}. Over 1800 compression/impression speciemens were used for this study (See Appendix I and II).

Slides were examined in greater detail using transmitted light microscopy. All specimens were photographed using a Leica DC500 digital camera attachment on a Leica DM 5000B compound microscope. Digital images of compression/impression fossils were originally obtained with a Fujifilm FinePix S1 Pro digital camera with a Nikon AF Micro Nikkor 60 mm 1:2.8 D lens under incandescent lighting. A polarizing filter was used with the lens as well as two stand alone sheets of polarizing filter placed in front of the lights, positioned on either side of the specimen. Other images were obtained with a Nikon D300S digital camera with a Nikon AF Micro Nikkor 60 mm 1:2.8 D lens under fluorescent lighting. A polarizing filter was used with the lens as well as built in polarizing filters for the light source. The camera was controlled with ControlMyNikon v3.0 software. Digital images were processed using Adobe® Photoshop® CS2 Version 9.0.2.

2. Stratigraphy

Fossils utilized in this study come from over 50 Permian (Figure 5, Table 1) and Triassic (Figure 6, Table 2) localities throughout Gondwana, most from Antarctica. The majority of these localities are from Permian rocks. Due to the difficulties of working in Antarctica, the ages of many fossils are only known in broad terms. As such, most of the data analyzed in this dissertation groups the localities by formation. Locality information for some sites is scarce; a portion of the collections at KU were collected decades ago by other paleobotanists who did not have the advantage of locating a site with modern GPS. For example, the earliest collected fossils used in this research were collected in 1934 as part of the Second Byrd Antarctic

Expedition; fossils were transported away from the locality on dog sleds. The positions of some localities have been inferred based on early maps of the region, original correspondence between the collectors, photographs of the area, field notes of the collectors, and discussions with Drs. David H. Elliot and James W. Collinson of The Ohio State University (correspondence, photographs, and field notes are housed at the University of Kansas).

2.1 Early Permian formations and localities of Antarctica

2.1.1 Weller Coal Measures

The Weller Coal Measures (Figure 7) are part of the Victoria Group within the Beacon Supergroup and are located in Southern Victoria Land. The base of this formation lies on the Pyramid erosion surface and is overlain by the Feather Conglomerate. The formation is composed of carbonaceous sandstones, siltstones, conglomerate lenses, and seams of coal of bituminous to anthracite rank (Collinson et al., 1994; Faure and Mensing, 2010).

The Allan Hills locality contains fossil plants found within the Weller Coal Measures. This site is located at 76º 43' 00" S, 159º 40' 00" E in the Victoria Land Basin. In older references, this locality is sometimes referred to as Allan Nunatak. Fossils from this locality were collected in 1963, 1965, 1966, 1969, 1989, and 1993.

Fossils from Aztec Mountain (77º 48' 08" S, 160º 33' 08" E) were collected from the eastern side, 10 m below the summit. Specimens were collected in 1962, 1965, and 1988.

Kennar Valley (77º 45' 580" S, 160º 24' 34" E) fossils were collected from the median ridge of the valley during the 1988 field season.

Fossils from the Mt. Feather locality (77º 57' 40" S, 160º 21' 16" E) were obtained during the 1966-1967 field season. Compressions from this locality are preserved in a dark shale, making it difficult to photograph specimens and interpret results.

Mt. Fleming (77º 33' 03” S, 160º 05' 57” E) fossil were collected during 1967, 1988, and 1989 field seasons. Although the locality contains mostly compression and impression specimens, petrified wood has also been recovered from this locality.

Robison Peak fossils (77º 11' 32” S, 160º 15' 27” E) were collected during 1960, 1965, and 1966 field seasons. Fossils come from a unit of black shale approximately 400 ft above a Devonian disconformity.

2.1.2 Lower Buckley Formation

The Lower Buckley Formation (Figure 8) contains lower Permian rocks from the Buckley Formation, Victoria Group, Beacon Supergroup. The Lower Buckley overlies the Fairchild Formation. The Buckley Formation from the Central Transantarctic Mountains region is sometimes referred to in older literature as the Buckley Coal Measures. Coal seams from the Buckley Formation were first discovered by Frank Wild during Shackleton's Expedition to the South Pole (1907-1909). The Lower Buckley is comprised mainly of sandstones containing sparse and fragmented fossils (Plumstead, 1962; Grindley, 1963; Collinson et al., 1994; Faure and Mensing, 2010).

Cranfield Peak (83º 38' 00” S, 160º 54' 00” E) from the Queen Elizabeth Range was collected in 1968 by Peter Barrett. Leaf compressions occur in a sandy shale.

Fossils of McIntyre Promontory (84º 57' 00” S, 179º 40' 00” E) come from the Queen Alexandra Range and were collected in 1968. Leaf compressions occur in a blue-gray shale and are commonly associated with coalified plant remains.

Mt. Picciotto (83º 46' 00” S, 163º 00' 00” E) fossils were recovered in 1969, 1990, and 1991. Although the majority of fossils from this site are *Glossopteris* leaves, some *Paracalamites* specimens are also present.

2.1.3 Mackellar/Fairchild Formation

The Mackellar and Fairchild (Figure 8) are two distinct formations, but it is unclear to which formation leaves from two Antarctic sites belong. Both formations are considered to be Lower Permian, which leads to them being treated the same way with regards to the analyses in this study. The Mackellar Formation was deposited conformably on the Pagoda Formation and consists largely of carbonaceous shales interbedded with sandstones; it extends in the Queen Alexandra, Queen Elizabeth, Holland, and Holyoake Ranges, as well as into the Shackelton Glacier area. The Fairchild Formation overlies the Mackeller Formation, but the contact has been obscured by intrusions from the Ferrar Dolerite. The Buckley Formation lies conformably on the Fairchild (Collinson et al., 1994; Faure and Mensing, 2010).

McKay Cliffs (82º 19' 00" S, 156º 00' 00" E) is located in the Geologist's Range between the Lucy and Nimrod Glaciers. Fossils from this locality were obtained during the 1992-1993 field season. *Gangamopteris*, *Glossopteris*, and compressed ovules occur at this site in a black shale interpreted by the collector as a lacustrine environment (N.P. Rowe field notes).

Fossils collected at Mt. MacPherson (82º 29' 00" S, 155º 50' 00" E) were recovered in the Churchill Mountains in the Geologist's Range between the Byrd and Nimrod Glaciers. The association of plants and sedimentology is similar to that from the McKay Cliffs locality.

2.1.4 Takrouna Formation

The Takrouna Formation (Figure 9) of the Freyberg Mountains in northern Victoria Land is composed of sandstones, silty mudstones, and coal seams. It is considered to be equivalent to the Weller Coal Measures of southern Victoria Land. *Glossopteris*, *Gangamopteris*, *Vertebraria*, and *Paracalamites* are known to occur in this formation (Collinson et al., 1986,1994; Faure and Mensing, 2010).

Fossils from Mt. Baldwin (72º 15' 00” S, 163º 18' 00” E) were originally collected by James W. Collinson. *Glossopteris* leaves are preserved within the rocks.

2.1.5 Mt. Bastion Formation

The Mt. Bastion Formation (Figure 7) (sometimes referred to as the Mt. Bastion Coal Measures) occurs in the Victoria Valley and is thought to be correlated with the Weller Coal Measures. The Mt. Bastion Formation is composed largely of coal layers (Mulligan et al., 1963; Mirsky et al., 1965; Schopf, 1968; Faure and Mensing, 2010; Serbet et al., 2010).

Mt. Gran (76º 59' 00” S, 160º 58' 00” E) fossils occur in a highly metamorphosed black shale originally collected during the 1966-1967 field season. Along with *Glossopteris* leaves, these shales contain remains of the enigmatic coniferophyte Buriadia (Serbet et al., 2010). The locality is located in the Granite Harbor Area of the Prince Albert Mountains.

The Mt. Bastion locality (77º 19' 08” S, 160º 29' 37” E) contains fossil plants preserved within a dark shale. Specimens were collected during the 1965-1966 field season.

2.1.6 Pecora Formation

The Pecora Formation (Figure 9) is a lower Permian formation located in the Pensacola Mountains. It overlies the Gale Mudstone and is largely composed of graywackes and carbonaceous siltstones (Williams, 1969; Collinson et al., 1994).

The Pecora Nunatak localities (85º 45' 00” S, 69º 00' 00” W) are located in the Patuxent Range of the Pensacola Mountains. These fossils were originally collected in the 1965-1966 field season. The gray to dark gray shales contain numerous *Glosopteris* leaves and were collected from numerous sites in an area formerly known as Far South Arauco-Aztecs.

2.1.7 Weaver Formation

The Weaver Formation (Figure 9) is a thick sequence located in the Ohio and Wisconsin

Ranges of the Horlick Mountains. The lower portion of the formation consists of shales with animal traces and pebbles with glacial origins and overlies the Buckeye Tillite. The middle portion contains shales with animal traces alternating with siltstone layers. The upper portion of this formation consists of a large sandstone layer topped by a shale bed. *Glossopteris* leaves are found in the shale layer (Collinson et al., 1994; Faure and Mensing, 2010).

The Tillite Ridge locality is found at the top of the Weaver Formation of Mt. Howe (87º 22' 00" S, 149º 30' 00" W) in the Wisconsin Range of the Horlick Mountains. Fossil leaves are found in a fine-grained black shale with slightly irregular bedding patterns. Specimens were collected by Minshew and Teller during the 1964-1965 field season.

2.2 Early Permian formations and localities of Africa

2.2.1 Ecca Group

The Ecca Group (Figure 10) is a collection of mostly lower Permian formations in the Karoo Basin of south-central Africa. Ecca Group specimens used in this research were collected by J.M. Schopf in 1947 from the Waterberg coal field in Transvaal, South Africa. Details of the collection site are scarce, but based on the general location of where the fossils were collected and the distribution of rocks in the Karoo Basin, it is highly likely that these *Glossopteris* specimens are from the lower Permian portion of the Ecca Group (Catuneanu et al., 2005).

2.2.2 Wankie Sandstone

The Wankie Sandstone (Figure 10) is a lower Permian formation located in southern Africa. Specimens used in this study were collected at a clay pit near Wankie, Zimbabwe (South Rhodesia at time of collection) by Robert Broom at an unknown date. They were later donated to J.M. Schopf in 1947 by the Transvaal Museum (Catuneanu et al., 2005).

2.3 Lower Permian formations and localities of South America

2.3.1 Bonete Formation

The Bonete Formation (Figure 11) consists of a sequence of light green sandstones and dark green mudstones; it is approximately 400 m thick (Archangelsky and Cuneo, 1984; Lopez-Gamundi and Rossello, 1998; Tomezzoli and Vilas, 1999)

The Sierra de Pillahuinco locality can be found in the southern hills of Buenos Aires, Argentina. The fossil bed is approximately 480 mi southwest of Buenos Aires and 7.5 km east of Sierra de la Ventana. *Glossopteris* leaves from this locality were collected by D.L. Schmidt in 1967 as part of a field trip for a scientific meeting (Stop 5, Spec. Loc. 23).

2.4 Middle Permian formations and localities

2.4.1 Upper La Golondrina Formation

The Upper La Golondrina Formation is the only Middle Permian formation in this study. It is also one of the most thoroughly dated and reconstructed formations of all of those studied. The formation is dated Roadian to Wordian (272.5 - 265.0 Ma) based on its occurrence in an *Asterotheca singeri* zone. The formation contains numerous plant fossils: *Asterotheca* sp., *Glossopteris* sp. , *Dizeugotheca* sp., and *Sphenophyllum* sp. Paleocoordinates for the formation are estimated to be 57.2° S, 57.6° W (Archangelsky and Cuneo, 1984). Fossils from this formation were collected from Laguna Polina, Santa Cruz, Argentina.
Specimens used in this study were collected by Edith L. Taylor in 1986.

2.5 Upper Permian formations and localities from Antarctica

2.5.1 Upper Buckley Formation, Central Transantarctic Mountains

The Buckley Formation (Figure 8) is thought to be at least 745 m thick and composed of sandstone layers mixed with carbonaceous shales, coal layers, conglomerate lenses, and thin limestone beds. The uppermost portion of the Buckley Formation is composed mainly of shales,

many of which contain an abundance of *Glossopteris* leaves. Permineralized peat can also be found within the Upper Buckley. The formation is overlain unconformably by the Triassic Fremouw Formation (Grindley, 1963; Young and Ryburn, 1968; Barrett et al., 1986; Collinson et al., 1994; Collinson et al., 2006; Faure and Mensing, 2010, David Elliot, personal communications).

The Bowden Névé locality (83º 30' 00" S, 165º 00' 00" E) contains compression and impression fossils collected in 1962 by G.W. Grindley at an altitude of 7300 ft. The locality is in the Beardmore-Nimrod Glacier region.

Clarkson Peak (83º 19' 00" S, 160º 34' 00" E) *Glossopteris* leaves were collected by an unknown person at an unknown date.

Fossils of Coalsack Bluff (84º 14' 00" S, 162º 25' 00" E) were recovered during the 1969-1970 field season. The locality is in the Queen Alexandra Range of the Central Transantarctic Mountains.

Graphite Peak (85º 03' 00" S, 172º 45' 00" E) specimens used in this research were collected in 1967 by Peter Barrett, and during the 1969-1970 field season by J.W. Collinson. Graphite Peak is located in the southern part of the Hughes Range.

Mt. Achernar (84º 12' 00" S, 160º 56' 00" E) is located on the south side of Law Glacier and forms the northeast end of the MacAlpine Hills. In addition to numerous *Glossopteris* leaves, fossiliferous beds at this locality also contain the lycopsid *Collinsonites schopfii* and several glossopterid reproductive structures. Specimens were collected by Collinson and Schopf during the 1969-1970 field season, by T.N. Taylor and Ruben Cúneo during the 1990-1991 field season, and by Anne-Laure Decombeix, Rob Teasdale, Kim Lawton, Patricia Ryberg, and Rudolph Serbet during the 2010-2011 field season.

Fossils at the Mt. Ropar locality (83º 58' 00” S, 160º 29' 00” E) are found in a blue-gray calcareous shale that weathers to buff. Specimens were recovered in 1967 by P. Barrett.

Mt. Rosenwald (85º 04' 00” S, 179º 06' 00” E) specimens came from a fossiliferous bed 100 ft below the Fremouw Formation. *Glossopteris*-bearing shales were collected by J.W. Collinson in the 1969-1970 field season.

Mt. Sirius (84º 08' 00” S, 163º 15' 00” E) is located in the Colbert Hills, between Walcott Névé and Bowden Névé in the Beardmore-Nimrod Glacier area. Fossils from Mt. Sirius are found in mudstones collected during the 1969-1970 field season.

The Skaar Ridge locality (84º 49' 00” S, 163º 15' 00” E) is located in the Beardmore Glacier region of the Queen Alexandra Range and contains both compression/impression fossils and permineralized peat. Specimens from this locality were collected by J.M. Schopf in the 1969-1970 field season, T.N. Taylor and R. Cúneo during the 1990-1991 field season, T.N. Taylor, E. L. Taylor, Ruth A. Stockey, and Jerry Taylor in the1985 field season, E.L. Taylor, T.N. Taylor, N. Ruben Cúneo, Charles P. Daghlian, Pablo Puerta, Jeffery M. Osborn, David M. Buchanan, and Brennan Brunner during the 2003 field season, and by A.-L. Decombeix, Ignacio Escapa, E.L. Taylor, T.N. Taylor, P. Ryberg, R. Serbet, Brian Staite, Eric Gulbranson, and A.B. Schwendemann during the 2010-2011 field season. In some earlier references this locality is referred to as Mt. Augusta, a neighboring mountain.

The Mt. Wild (84º 48' 00” S, 162º 40' 00” E) locality is near Skaar Ridge and has similar compression/impression specimens. Fossils were recovered by G.W. Grindley in 1962.

Canopy Cliffs (84º 05' 00” S, 161º 00' 00” E) is located on the north side of the upper Law Glacier. Fossils were collected from the first Buckley section east of the plateau edge, from coal beds at 7400 ft. Specimens were collected by G.W. Grindley in 1961, before the cliffs were

given a formal name.

Mt. Bartlett (84º 56' 00” S, 164º 00' 00” E) fossils are found in a creamish to yellow claystone, possibly tuffaceous. Specimens were recovered by J.M. Schopf and J.F. Rigby during the 1965-1966 field season.

Specimens from Mt. Kinsey (84º 55' 00” S, 169º 18' 00” E) are preserved in a light blue-gray siltstone and were collected in 1968. Mt. Kinsey is located in the southern part of the Commonwealth Range on the east side of the Beardmore Glacier.

Sandford Cliffs (83º 54' 00” S, 159º 17' 00” E) fossils came from the top of the Buckley section, directly below the dolerite. Specimens were collected by G.W. Grindley in 1961.

2.5.2 Queen Maud Formation

The Queen Maud Formation (Figure 9) is composed of cyclic deposits of sandstone, shale, and coal and overlies the Weaver Formation. The top of the Queen Maud Formation is bounded by glacial till of the Sirius Group. *Glossopteris* leaves and petrified wood can be found in the Queen Maud (Minshew, 1966; Collinson et al., 1994; Collinson et al., 2006; Faure and Mensing, 2010).

Fossils at the Roaring Cliffs (78º 16' 00” S, 163º 03' 00” E) locality are found in light gray siltstones that weather light gray and reddish brown. Specimens were collected by W.E. Long in the 1963-1964 field season. This locality was originally referred to as Roaring Valley, but that name is officially assigned to another locality. The site where Long collected his fossils is now officially named Roaring Cliffs.

Mt. Howe (87º 22' 00” S, 149º 30' 00” W) and Mt. Weaver (86º 58' 00” S, 153º 50' 00” W) fossils of the Queen Maud Formation were recovered by Doumani, Minshew, and Skinner in the 1963-1964 field season. The localities are located in the Wisconsin Range of the Horlick

Mountains. Rubble Ridge (86º 58' 00" S, 153º 50' 00" W) is an informal name for a site at the base of Mt. Weaver. These specimens are thought to have originated from fossiliferous beds up higher on Mt. Weaver. Specimens from Rubble Ridge were collected by Quin A. Blackburn in 1934. Blackburn's letters note that many large specimens, including petrified wood, remain at the locality as they were too large to remove by dog sled. Several more specimens used in this study are only known to have been collected from the Horlick Mountains; no other locality information is available. These rocks, however, have the same lithology as other rocks from the Queen Maud Formation in the Horlick Mountains. These specimens have therefore been grouped with the rest of the Queen Maud Formation specimens.

Crack Bluff (86º 21' 00" S, 159º 00' 00" W) is located in the Thorvald Nilsen Mountains at the east side of Upper Amundsen Glacier, Queen Maud Range. The locality was not yet named at the time of collection and was described as being located: "About 29 miles up-glacier from small snow-covered peak at prominent bend of glacier; section at head of conspicuous debris-covered glacier (Porky Gulch) up the southern cirque to the highest peak, 390 ft above base of measurement, about 13 km south of section 7, 44 km S 100 E of Mount Helmer Hanssen". This corresponds to the present day locality officially named Crack Bluff.

2.5.3 Mt. Glossopteris Formation

The Mt. Glossopteris Formation (Figure 12) is restriced to the eastern portion of the Ohio Range and consists of cyclic deposits of sandstone, siltstone, shale, and coal beds. The formation is 700 m thick and only known to outcrop on two mountains, Mt. Glossopteris and Mt. Schopf. *Glossopteris*, *Gangamopteris*, petrified wood, and fossil conchostracans are abundant in this formation (Long, 1965; Collinson et al., 1994, 2006; Faure and Mensing, 2010).

Rocks from Mt. Glossopteris (84º 44' 00" S, 113º 43' 00" W) contain an abundance of

plant remains and coal. During the 1961-1962 field season, W.E. Long, G. Doumani, and J. Mercer collected specimens from 1350 ft to 300 ft below the diabase sill capping the mountain. During the same field season, J.M. Schopf collected Mt. Glossopteris specimens from a ledge of the northwest face of the mountain below the coal bed, officially termed Museum Ledge.

Mt. Schopf (84º 48' 00" S, 113 25' 00" W), named for the eponymous paleobotanist, is home to several distinct fossiliferous beds that have been given their own official locality names. Leaia Ledge fossils are found in a hard, light gray fissile shale; the locality is named after the conchostracan *Leaia*, which is abundant at the site. Fossils were collected by V. Minshew, Doumani, and Boucot during the1964-1965 field season and by J.M. Schopf during the 1967-1968 field season. Moraine Ridge is a locality 70 ft below Leaia Ledge on Mt. Schopf; fossils from this locality were collected during the 1960-1961 field season. Although referred to as Moraine Ridge by the collecters and some subsequent authors, this is not an official name for this locality. An official Moraine Ridge locality does exist in Antarctica, but the site is far from Mt. Schopf. Terrace Ridge fossils were collected by W.E. Long, G. Doumani, and J. Mercer during the 1960-1961 field season. During the subsequent field season, W.E. Long and J.M. Schopf collected *Glossopteris* leaves from a coaly shale at a locality termed Mine Ledge. Mine Ledge occurs on Terrace Ridge.

2.5.4 Upper Polarstar Formation

The Polarstar Formation (Figure 13) is a group of Permian rocks located in the Ellsworth Mountains and overlies the White Conglomerate. The upper portion of this formation is dated as upper Permian. Upper Permian sequences are composed of cycles of volcaniclastic sandstone, siltstone, and mudstone. The Upper Polarstar Formation formed from deltaic deposits (Collinson et al., 1994). Fossils from the Polarstar Peak (77º 32' 00" S, 86º 09' 00" W) locality were

recovered from the east ridge of the peak, located in the Sentinel Range of the Ellsworth Mountains. *Glossopteris* leaves, occuring in a dark gray siltstone, were collected by Campbell Craddock, Tom Bastien, and Bob Rutford during the 1963-1964 field season.

2.5.5 Erehwon Formation

The Erehwon Formation (Figure 9) occurs at Erehwon Nunatak (74º 31' 00" S, 76º 41' 00" W), located on the English Coast in Eastern Ellsworth Land. *Glossopteris* leaves from this locality are found in dark, fine-grained volcanogenic sedimentary rocks (Gee, 1989; Collinson et al., 1994).

2.6 Upper Permian formations and localities from Australia

2.6.1 Illawarra Coal Measures

The Illawarra Coal Measures (Figure 14) are an Upper Permian sequence from the foreland Sydney Basin. Fossils in the KU collections from this formation were collected in Cooyal, New South Wales, Australia (Herbert, 1995; Fielding et al., 2010).

2.7 Upper Permian formations and localities from South Africa

2.7.1 Normandien Formation

The Normandien Formation is a sequence of interbedded sandstones and mudstones in the northeastern portion of the Karoo Basin (Bamford, 2004; Catuneanu et al., 2005). *Glossopteris* leaves from the Free State province of South Africa (Orange Free State at time of collection) were collected on a farm near the city of Harrismith; these specimens were collected by J. J. Spies of the South African Geological Survey. Fossils from the KwaZulu-Natal province of South Africa were collected by J. G. Blignant ca. 9 miles east of Newcastle.

2.8 Upper Permian formations and localities from India

2.8.1 Kamthi Formation

The Kamthi Formation is a Upper Permian sequence from India. *Glossopteris* leaves from Bazargoan, Nagpur, India were recovered by D.V. Shukla (Chandra and Singh, 1992).

2.9 Middle Triassic formations and localities from Antarctica

2.9.1 Fremouw Formation

The Fremouw Formation (Figure 8) is composed of a cycle of sandstone and mudstone units that rest disconformably on the Permian Buckley Formation; it is overlain conformably by the Falla Formation. The lower portion of the Fremouw contains reptile and amphibian fossils, while the middle and upper parts of the formation contain plant fossils. No animal fossils have been found in the middle and upper portions of the Fremouw Formation to date. The basal portion of the formation is Lower Triassic, while the upper portion is Middle to Upper Triassic. These Triassic rocks can be found in the Queen Alexandra, Queen Elizabeth, Dominion, and Supporters Ranges, as well as a portion of the Queen Maud Mountains (Taylor et al., 1989; Collinson et al., 1994; Faure and Mensing, 2010; Escapa et al., 2011).

The Fremouw Peak locality (84º 17' 24.1" S, 164º 21' 24.2" E) is found in the Beardmore Glacier area of the Queen Alexandra Range in the central Transantarctic Mountains where the type section of the formation is found. This locality contains both compression/impression and permineralized specimens. Specimens used in this research were collected by J.M. Schopf and J.W. Collinson during the 1969-1970 field season, T.N. Taylor, E. L. Taylor, R. A. Stockey, and Jerry Taylor during the 1985 field season, T.N. Taylor and R. Cúneo during the 1990-1991 field season, T.N. Taylor, E. L. Taylor, C.P. Daghlian, and J. M. Osborn during the 2003 field season, and by A.-L. Decombeix, I. Escapa, E.L. Taylor, T.N. Taylor, P. Ryberg, R. Serbet, B. Staite, E. Gulbranson, and A.B. Schwendemann during the 2010-2011 field season. This site features a variety of seed ferns, gymnosperms, ferns, and sphenophytes.

Gordon Valley (84º 11' 10” S, 164º 54' 28” E) strata contain specimens of *Dicroidium* and *Neocalamites*. Specimens used in this research were collected by T.N. Taylor, E. L. Taylor, R. A. Stockey, and J. Taylor during the 1985 field season, and by T.N. Taylor and R. Cúneo during the 1990-1991 field season.

2.9 Upper Triassic formations and localities from Antarctica

2.9.1 Falla Formation

The Falla Formation (Figure 8) is an Upper Triassic unit composed of a sequence of sandstones and shales; it is overlain by the Jurassic Hanson Formation. The Falla is not as extensive as the Fremouw and is primarily found in the Queen Alexandra Range. Plant fossils from this formation are dated as Middle to Late Triassic based on palynological records (Kyle and Schopf, 1982; Collinson et al., 1994; Faure and Mensing, 2010; Escapa et al., 2011).

The Mt. Falla locality (84º 20' 50.1” S, 164º 39' 40.6” E) contains conifers, ginkgophytes, *Umkomasia*, *Dejerseya*, and numerous *Dicroidium* species. Specimens from this locality were recovered by D. Elliot during the 1966-1967 field season, J.M. Schopf during the 1969-1970 field season, T.N. Taylor, E. L. Taylor, R. A. Stockey, and Jerry Taylor during the 1985 field season, E. L. Taylor, C.P. Daghlian, and J. M. Osborn during the 2003 field season, and by A. Decombeix, Ignacio Escapa, E.L. Taylor, T.N. Taylor, P. Ryberg, R. Serbet, Brian Staite, Eric Gulbranson, and A.B. Schwendemann during the 2010-2011 field season

The Marshall Mountains locality (84º 37' 00” S, 164º 30' 00” E) is found on the west side of the Marshall Mountains, approximately 1.75 mi northwest of the summit of Frontz Peak. The fossil bed is located between sills of slope of a subsidiary peak, about 250 feet above the top of the Falla Formation at this location. The *Dicroidium* fossils from this locality are preserved in a dark shale and were collected by D. Elliot during the 1966-1967 field season.

2.9.2 Lashly Formation

The Lashly Formation (Figure 7) is found in southern Victoria Land and extends from the Middle Triassic to the Upper Triassic. It is composed of layers of sandstone, shale, and carbonaceous beds; it overlies the Triassic Feather Conglomerate.

Triassic plant fossils from the Allan Hills (76º 43' 00" S, 159º 40' 00" E) come from two separate members of the Lashly Formation. Fossils from Member A are dated Middle Triassic and those from Member C are dated Late Triassic. During the 1992-1993 field season, E.L. Taylor, T.N. Taylor, N. R. Cuneo, Lisa D. Boucher, J.M. Osborn, Brigitte Meyer-Berthaud, Georgina del Fueyo, Gar W. Rothwell, and D. Buchanan collected specimens. Other specimens were collected by J.M. Schopf in the 1965-1966 field season and by Schopf in the 1969 field season. Fossils occur in a dark shale that is thinly laminated and tends to break into thin flakes on weathered surfaces.

Shapeless Mountain (77º 25' 44.2" S, 160º 20' 48.2" E) is a southern Victoria Land locality with fossils from Member C of the Lashly Formation. Fossil-bearing rocks at this location are from section S4, Unit 12, approximately 66-76 m above ice level on the north side of the saddle in a southwest-trending ridge. Fossils from this locality were collected by E.L. Taylor, T.N. Taylor, G.W. Rothwell, and D. Buchanan during the 1997-1998 field season. In addition to compression fossils of corystosperms, gymnosperms, and sphenophytes, this locality also has permineralized wood.

2.10 Localities from Antarctica with uncertain stratigraphy

Fossils collected at the Alfie's Elbow (84º 23' 71" S, 174º 49' 91" W) site occur within the uppermost Fremouw or lower Falla Formations. Even without this information, the age of fossils from this locality is thought to be Late Triassic based on palynological data. Alfie's Elbow is

currently an unofficial name for the fossil locality located at the head of the Shackleton Glacier area, southeast of Schroeder Hill. The fossils analyzed in this study were collected during the 1996 field season by E.L. Taylor, T.N. Taylor, N. R. Cúneo, Ana Archangelsky, and Hans Kerp, and during the 2003-2004 field season by E.L. Taylor, T.N. Taylor, N. R. Cuneo, C.P. Daghlian, P. Puerta, and D. Buchanan.

The Mt. Wisting locality (86º 27' 00" S, 165º 30' 00" W) is oorly understood stratigraphically. Its location in the Queen Maud Range suggests that it may be more likely to be part of the Fremouw Formation, but there is no conclusive proof. Plant fossils at this locality include *Dicroidium*, *Neocalamites*, *Cladophlebis*, *Lepidopteris*, and *Heidiphyllum*. Similar to Alfie's Elbow, fossils at this site are considered Late Triassic. Plant fossils from this locality were recovered in 1971 by Helmut Ehrenspeck.

Fossil from the Mt. Bumstead locality (85º 39' 00" S, 174º 16' 00" E) are found in a moraine on the north side of Mt. Bumstead in the Grosvenor Mountains. Plant fossils from this locality were recovered by D. Elliot during the 1967-1968 field season. Although the exact age of these fossils is uncertain, they are definitely from the Triassic.

2.11 Upper Triassic formations and localities from South Africa

2.11.1 Molteno Formation

The Molteno Formation (Figure 10) forms the base of the Stronmberg Group, which is the uppermost division of the Karoo System. The Stromberg Group lies uncomformably on the Beaufort Group, which extends from the Permian into the Triassic. Evidence from plant fossils and vertebrates suggests that the Molteno Formation is Late Triassic (Carnian) in age. The formation consists of cycles of sandstone, gray shales, dark shales, and coal beds. Fossil plants are primarily found within the dark shales (Thomas, 1933; Lucas and Hancox, 2001).

Fossils from the Umkomaas Valley were collected by J.M. Schopf in 1947. The locality can be found in KwaZulu-Natal, South Africa. At the time of collection, the province was named Natal. Fossils from this locality were used to construct the corystosperms.

Fossils from Molteno, Eastern Cape, South Africa are similar to those collected at Umkomaas Valley. J.M. Schopf collected specimens from this locality in 1947 when Molteno was part of the Province of the Cape of Good Hope (commonly called Cape Province).

2.12 Upper Triassic formations and localities from Australia

2.12.1 Blackstone Formation

The Blackstone Formation is part of the Brassall Subgroup of the Ipswich Coal Measures. The formation outcrops mainly in Queensland, Australia. It has been assigned a Late Triassic (Carnian) age based on palynological evidence (de Jersey, 1975). *Dicroidium* fronds analyzed in this study were collected from a locality in Dinmore, Queensland.

Chapter 3

Leaf venation density and calculated hydraulic conductance of fossil leaves from the Permian and Triassic of Gondwana

1. Introduction

1.1 Leaf venation and fossil leaves

The diversity of fossil plants from the Permian and Triassic of Gondwana has been studied for decades. In that time, much has been discovered concerning the past diversity and evolution of plants (Oliver and Scott, 1905; Kidston and Lang, 1920; Beck, 1960; Eggert, 1961; Remy, 1982; Taylor et al., 2005). These pioneering studies make it possible to then view those fossil communities in a more detailed manner. For example, one can study community interactions, effects of mass extinction events, and even some physiological characteristics of fossils when enough material has been collected. Here, I examine some hydraulic and physiological characteristics of Permian and Triassic fossil plants using specimens collected from a wide geographic and temporal area in Antarctica and other Gondwanan continents. Using form/function relationships determined with extant plants, the hydraulic conductance of fossil plants is estimated from leaf venation density(Brodribb et al., 2004; Brodribb, 2009; Feild et al., 2011b). Using the data gathered on leaf hydraulic conductance in fossil plants, this study examines how the conductance is connected to taxonomy and environmental factors (e.g., CO_2 concentration, paleolatitudes) through deep time.

Leaf venation architecture, and therefore leaf venation density, have long played an important role in paleobotany. Plant fossils are rarely found with other organs attached. As a

result, it is common for the individual organs of the fossil plant to receive their own valid names. As more material is collected, organic connections between organs are often found or evidence from anatomy or distribution and co-occurrence allow the whole fossil plant to be reconstructed. Due to the nature of the discipline and the relative abundance of fossil leaves compared to other organs, many different leaf species have been described. They are frequently delimited by features such as leaf size, leaf shape, stomatal size and distribution, anatomy when available, and venation architecture. There have been numerous studies of leaf venation that attempt to study the evolution of a group using leaf characteristics (e.g., Melville, 1969; Alvin and Chaloner, 1970; Doyle and Hickey, 1976; Premoli, 1996; Uhl et al., 2002; Boyce et al., 2009).

1.2 Leaf venation and plant physiology

Venation architecture can function in a variety of ways, most notably in mechanical support and the transport of materials. Due to the strength of lignin found in xylem, as well as sclerified cells sometimes associated with vascular bundles, the venation architecture helps a leaf to retain its shape (Niklas, 1992). This mechanical strength exhibited by the leaf allows for more surface area to be exposed to sunlight. Successful strategies for increasing leaf mechanical stability are to decrease the leaf size, increase the *E*-modulus (description of an object's tendency to be temporarily deformed) of the leaf, and/or stabilize the leaf margin (Kull and Herbig, 1995). The venation architecture of some plants may, therefore, limit the size of the leaf. The transport of substances through the plant is just as important, if not more significant. Photosynthates produced in leaves are transported elsewhere through the phloem; xylem transports water, solutes, and some hormones throughout plants (Taiz and Zeiger, 2006). Water moving through a plant due to evapotranspiration can travel a great distance, with the leaf accounting for only a fraction of the route traveled. Water must first move from the soil to the roots, then through the

shoot before entering the leaf. Despite this, the pathway of water through the leaf accounts for approximately one-fourth of all the resistance to flow in the plant (Sack and Tyree, 2005). Furthermore, the leaf lamina hydraulic conductance can vary at least 30-fold across species, suggesting that this value has strong ecological importance (Becker et al., 1999; Nardini and Tyree, 1999; Nardini et al., 2000; Nardini and Salleo, 2000; Tsuda and Tyree, 2000; Sack and Tyree, 2005). Although important, leaf conductance does not directly determine the transpiration rate of a plant. In practice, the diffusion of water through the stomata and the supply of water in the soil have the greatest overall effect on day-to-day transpiration (Sack and Tyree, 2005). When conditions are ideal (i.e., well-watered soil and adequate energy for transpiration), however, the leaf conductance can be the limiting factor. Leaf hydraulic conductance describes the pathways of water movement through the leaf; it is linked to venation architecture, carbon economy, and drought tolerance. Leaf conductance can be used to estimate stomatal conductance, maximum photosynthetic capacity, and water use efficiency (Sack and Tyree, 2005). Venation density works well as an estimator of hydraulic conductance. This is simply because as venation density increases, there exists a larger number of paths for water to take through a leaf, thereby increasing the rate of conductance. Unfortunately, vein density is known to vary with several other parameters that cannot be adequately accounted for when using fossil leaves. Within a single plant, leaf venation density can increase with the height of the leaf on the plant (Roth-Nebelsick et al., 2001). Sun leaves will have a higher vein density (Esau, 1965; Roth-Nebelsick et al., 2001), and venation density will increase with a reduction in soil water availability and air humidity (Roth-Nebelsick et al., 2001). Given that fossil leaves are found dispersed from the canopy and the water conditions are difficult to determine, these factors have to be ignored when studying leaf hydraulics in fossil plants. It is assumed that if a large sample size of fossil leaves is

used it will contain leaves from a variety of canopy heights and exposure to light energy. Additionally, due to the diffuse nature of light at high polar latitudes (e.g., Antarctica), it is unlikely that a large difference exists between so-called sun and shade leaves.

1.3 Leaf venation and Glossopteris *leaves*

The Glossopteridales are an enigmatic group with easily identified leaves and a diverse assemblage of reproductive structures. Historically, the glossopterids have been grouped with cycads, gnetophytes, cordaites, angiosperms, and seed ferns; current thinking on the topic suggests an affinity with seed ferns. The glossopterids dominated Gondwana during the Permian and sometimes are the only plants found at localities throughout Antarctica; their domination continued until the Permian-Triassic mass extinction event. The most commonly found glossopterid organs are the leaves belonging to the genus *Glossopteris*. The *Glossopteris* leaf consists of a midvein composed of several independent veins and a network of lateral veins that dichotomize and anastomose to form a reticulate venation pattern; the overall leaf shape is lanceolate (Taylor et al., 2009). The ubiquity of glossopterids in the Permian strata of Antarctica, to the exclusion of much else, suggests that the group had some competitive advantage over other groups living at the time. One possibility for their dominance may be their unique reproductive structures, which are unlike most other structures of the time (Ryberg, 2009). Another possibility, explored throughout this dissertation, is that the glossopterids possessed some physiological advantage over other plants known in Gondwana. Leaves of the genus *Gangamopteris* are sometimes found in Permian strata of Gondwana, but they are generally confined to the Lower Permian. *Gangamopteris*, also a glossopterid leaf type, is similar to *Glossopteris* except that it lacks a distinct midvein. *Noeggerathiopsis*, in contrast, is a strap-shaped leaf with parallel venation; veins occasionally fuse together. The taxonomic position of

Noeggerathiopsis is unclear, but it is commonly treated as a cordaite (e.g., Taylor et al., 2009).

1.3.1 Leaf venation and Glossopteris *leaves in high latitude environments*

Utilizing fossils collected over a large geographic area allows for study of the effects of latitude on fossil plant physiology. The glossopterids and corystosperms are excellent candidates for this type of analysis due to their wide distribution and dominance during the Permian and Triassic, respectively. Fossil plants from these groups grew in a high paleolatitude environment with no modern analogue. The fossil plants closest to the poles would have been subjected to four months of continuous light conditions and four months of continuous dark (Figure 1); fossils from lower paleolatitudes grew in increasingly less extreme light regimes. Light conditions at lower latitudes eventually reach a more typical diurnal light pattern. Light at high latitudes is a low-angle, diffuse light of low to moderate irradiance (Pielou, 1995). Although this instantaneous flux density is much lower at high latitudes, it has been suggested that the integrated light flux would be similar to that found at the middle latitudes (Creber and Chaloner, 1984; Jagels and Day, 2004). Chabot et al. (1979) have demonstrated, at least in some angiosperms, that change in leaf anatomy and physiology is only detectable through changes in integrated light flux, not instantaneous light. However, the plants in this study were not subjected to full continuous light conditions (Chabot et al., 1979). This means that although the amount of intercepted light might be quantitatively similar to that of lower latitudes, the four months of continuous light conditions would change the nature of how the leaf utilizes the absorbed photons. This may actually be beneficial to the plants as the irradiance for most of the day is in the linear portion of the photosynthetic light response curve and it is within this area of the curve where photosynthesis reaches its maximum efficiency (Hikosaka and Terashima, 1995).

Based on fossils found at high paleolatitudes in Antarctica, it is known that the leaves

were as productive as those growing today at lower latitudes (Taylor and Ryberg, 2007). In a series of studies (e.g., Jagels and Equiza, 2005, 2007; Equiza et al., 2006a, 2006b, 2007) involving extant gymnosperms grown under continuous light conditions, it has been demonstrated that at least some genera show adaptive physiological responses to continuous light. Of the species studied (*Larix laricina*, *Metasequoia glyptostoboides*, *Sequoia sempervirens*, and *Taxodium distichum*), *M. glyptostoboides* demonstrated the greatest ability to adapt to continuous light conditions. A common problem exhibited by the other genera was the down regulation of photosynthetic activity. The feedback inhibition mechanism appears to function in response to photosynthetic end products (Jagels and Day, 2004). *Metasequoia. glyptostroboides* avoids this pitfall by having abundant carbon sinks associated with a strongly indeterminate growth habit (Equiza et al., 2006b). Specimens showed a lower accumulation of foliar starch and a higher allocation of resources to creating foliar and root biomass than the other gymnosperms studied (Equiza et al., 2006a; Equiza et al., 2006b). *Metasequoia* is known to produce new foliage throughout the growing season as new leaves on long shoots, through lateral shoots on short shoots, and from epicormic shoots (Jagels and Day, 2004). Epicormic shoots have been described in glossopterid wood from Antarctica (Decombeix et al., 2010) and short shoots are common in Antarctic corystosperms (Axsmith et al., 2000). With these potential adaptations to continuous light already found in other organs, the hydraulic parameters for the leaves were studied for potential adaptations.

1.3.1 Leaf venation and Glossopteris *leaves in different CO_2 concentrations*

Glossopterid leaves in the fossil collections at KU also come from a variety of localities that differ temporally. These fossils come from a wide range of geologic times where the environment no doubt differed drastically. Based on models incorporating geologic evidence, the

atmospheric CO_2 concentration (Figure 2) during the Late Carboniferous to the middle Permian was at its lowest level since the evolution of land plants (Berner, 2006). Moving from the middle to late Permian, there was a rapid increase in atmospheric [CO_2] (Berner, 2006). This rapid increase coincides with the end-Permian mass extinction event. After peaking in the Early Triassic, atmospheric [CO_2] began to decrease through the Middle Triassic and into the Late Triassic, where it began to rise once again (Berner, 2006). Within the fossil record, there is evidence of anastomosing venation patterns appearing when [CO_2] is low (Kull, 1999; Roth-Nebelsick et al., 2001). There are not, however, many instances in land plant evolution where [CO_2] has been extremely low. Research by Uhl and Mosbrugger (1999) suggests that leaf venation density is not affected by CO_2 concentration. They reach this conclusion by studying extant *Quercus petraea* grown at varying [CO_2] and by studying herbarium sheets of *Acer monspessulanum* and *Q. petraea* collected from 1890 to the present (Uhl and Mosbrugger, 1999). This study of *Glossopteris* leaves differs substantially from the former by having grown and evolved under the low [CO_2] conditions and differs from the latter by encompassing a time span of millions of years. This allows the opportunity to see a long term response to changing [CO_2].

2. Materials and methods

2.1 Calculation of leaf venation density and hydraulic characteristics

Leaf hydraulics and other physiological characteristics of the leaf are determined by first measuring leaf venation density. Using a set of regression equations developed by Brodribb et al. (2007), the leaf hydraulic conductance (K_{leaf}) can be calculated. From there, estimates of stomatal conductance (g_s), max photosynthetic capacity (P_c), and water use efficiency (WUE) can be calculated using regression equations or deterministic equations of photosynthesis.

Brodribb et al. (2007) demonstrated that K_{leaf} was proportional to the distance of the non-

vascular pathway from the leaf veins to the site of evaporation. This relationship can be described by the following equation:

$$K_{leaf} = 12670\ d_m^{-1.27}$$

The value d_m is defined as the distance water must travel from the leaf veins to the stomata and can be expressed in the following equation:

$$d_m = \pi/2\ (d_x^2 + d_y^2)^{1/2}$$

The variable d_y is defined as the distance from the vein terminal to the stomata. For permineralized specimens, this value can explicitly measured. For compression/impression fossils, a distance of 140 μm was used. This value is at the upper end of leaf vein thicknesses tested by Brodribb et al. (2007) and was chosen for this study to minimize any bias towards a high K_{leaf}. The variable d_x is the horizontal distance from the leaf vein to the stomata and can be calculated from the leaf vein density (D_v) using the following equation:

$$d_x = 650/D_v$$

D_v was measured directly from fossil leaves; high magnification images of the leaf surface showing the venation were taken with a Nikon D300S as previously described; the image was then analyzed using ImageJ (Rasband, 2012) software. One to four squares (5 mm by 5 mm for Permian leaves, 3 mm by 3 mm for the smaller Triassic leaves) were added to the image depending on the quality of the leaf preservation. The length of the veins within each of these squares was then measured (Figure 15) and the vein lengths of all squares was averaged to create a single vein density measurement for the leaf. The venation in the fossil leaves examined exhibit a fairly uniform pattern so there is little concern about the placement of the squares not being completely randomized. Density values were then used with the above equations to calculate K_{leaf}. From K_{leaf}, the g_s and P_c were calculated using the following equations:

$$g_s = (K_{leaf} \Delta\Psi_{leaf})/\upsilon$$

$$P_c = -0.0226*K_{leaf}^2 + 1.32*K_{leaf} - 0.26$$

The water potential gradient within the leaf ($\Delta\Psi_{leaf}$) and leaf-to-air vapor pressure deficit (υ) were estimated based on values from extant plants. Although it is unlikely that these values would be the same across all leaves sampled from such distant locations and times, there are currently no data to accurately measure these values for each site. A value of 2 kPa was used for υ and 0.4 MPa was used for $\Delta\Psi_{leaf}$ (Brodribb and Holbrook, 2003). The equation for P_c is a regression equation from Brodribb et al. (2007). The intrinsic WUE was calculated using the following equation:

$$WUE = P_c/g_s$$

Values derived from fossil leaves cannot be taken as being completely representative of their time due to the lack of critical parameters that cannot be directly measured and must instead be estimated based on living specimens.

2.2 Data set and analysis

For Permian specimens, over 42,000 vein segments were measured from 1375 leaves from 55 localities (Figure 5) located in Antarctica, Australia, India, South America, and Africa (See Appendix I for raw data). These localities (Figure 6) are spread out across 19 different geologic formations. For Triassic specimens, over 8,000 vein segments were measured from 359 leaves from 13 localities located in Antarctica and Australia (See Appendix I for raw data). These localities are spread out across 5 different geologic formations. In order to evaluate these data in a timely manner and reduce the potential for errors, a simple script was written in Python 2.7 to automate the process. Each leaf specimen has a spreadsheet file associated with each square superimposed onto the leaf. Each file includes the specimen number, locality, leaf species, and

other values used to differentiate leaves on the same slab and squares on the same leaf. The script takes the vein measurements from each file and averages to produce one vein density value per leaf. Those data are stored along with data related to the formation in which the fossil was found. The vein densities were then used in conjunction with the above equations to calculate the rest of the physiological attributes. Calculated values for each leaf were then outputed to spreadsheet files.

2.2 Determining the effects of CO_2 on leaf morphotypes

In order to investigate the effects of phylogeny on the leaves studied, they were grouped by genus and geologic period for statistical analysis. Likewise, leaves were grouped by genus and time for analysis with regards to change in atmospheric [CO_2]. For example, *Glossopteris* leaves would be separated out by whether they occurred in the early, middle, or late Permian, which roughly corresponds to atmospheric [CO_2]. The [CO_2]s of the early and middle Permian is nearly identical based on current models, but were separated to test for any differences that might arise. Investigating the effects of paleolatitude on fossil leaf physiology was more complex.

2.3 Determining the effects of latitude on leaf morphotypes

Although techniques exist to ascertain the paleolatitude at which sediments were deposited, there is little to no data concerning the examined localities in Antarctica. As such, current latitudes were used as a crude proxy. To test the effects of latitude, the localities from which fossils were examined were placed in bins intended to group localities that likely occurred at similar paleolatitudes as separate from those that likely occurred at disparate paleolatitudes. This is a simple solution to the problem and should work since the differences in paleolatitude are more important than the actual paleolatitude. Several groupings were tried in an attempt to limit the noise effects caused by tectonic activity while still retaining any signal of physiological

differences. The simplest grouping separated all of the Antarctic localities from those found elsewhere in Gondwana. A slightly more complex grouping separated the localities into three bins: non-Antarctic localities, localities currently located between 70º S and 79º S, and localities currently located at 80º S and higher. The finest grouping of latitudes grouped the fossils in bins of non-Antarctic leaves, those currently at 72º S, 73º S, 74º S, etc.

2.4 Methodology for statistical analysis

Data were statistically analyzed using R (R Core Team, 2012) to determine if there were any significant differences between the different groupings that would allow us to answer questions about how the environment affected their physiology on a broad scale. A factorial ANOVA with a Tukey HSD post-hoc test was used to evaluate the significance of the data. For comparisons among the different factors (genus, latitude, $[CO_2]$), D_v was used in the statistical analysis. Because all other hydraulic parameters are derived from D_v using deterministic equations, using D_v reduces the confounding factors in the analysis. A one-way ANOVA was used to test for significant differences in D_v between the genera, regardless of other factors. *Gangamopteris*, *Noeggerathiopsis*, and Triassic leaf morphotypes were not analyzed for changes due to latitude or $[CO_2]$ because of limited data. These other factors were analyzed for *Glossopteris* utilizing a 2x2 factorial ANOVA. Assumptions of normality and homogeneity of variance were tested and the data passed.

3. Results for Permian leaves

3.1 Differences among Permian genera

Results of the ANOVA indicate that there are significant differences ($p << 0.001$) in vein density among the genera analyzed (Figure 16). The post-hoc Tukey test indicates that there is a significant difference ($p << 0.001$) in vein density between *Glossopteris* and *Gangamopteris*.

Likewise, there is also a significant difference ($p << 0.001$) between the vein densities of *Noeggerathiopsis* and *Glossopteris*. The post-hoc test did not find a significant difference ($p = 0.118$) between the vein density values for *Noeggerathiopsis* and *Gangamopteris*.

3.2 Statistical results for Glossopteris

3.2.1 Glossopteris *and* CO_2

Results of the statistical analysis rely heavily on which grouping is used for the latitude. However, results of all analyses suggest that [CO_2] has a significant main effect on vein density (Figure 17). A significant main effect is also shown in the latitude groupings; however, there may be confounding factors that are discussed below.

3.2.2 Glossopteris *and latitude*

When latitudes are separated into two large bins (i.e., non-Antarctic vs. Antarctic), the [CO_2] is shown to have a significant main effect ($p << 0.001$) on the vein density of *Glossopteris* leaves (Figure 18). Whether the specimens were located in Antarctica or the non-Antarctic localities also shows a significant main effect ($p << 0.001$). With this data set, a significant interaction effect between [CO_2] and latitude was not found ($p = 0.755$).

When the latitudes were separated into three bins (i.e., non-Antarctic vs. localities from 70º S–79º S vs. localities from 80º S and higher), the [CO_2] is suggested to have a significant main effect ($p << 0.001$) and the changes in latitude are also shown to have a significant main effect ($p << 0.001$) (Figure 19). Unlike the previous analysis with only two groupings of latitudes, this analysis showed a significant interaction effect ($p << 0.001$) between latitude and [CO_2]. A Tukey post-hoc test showed significant interaction of factors for several pairings. Interactions existed between 80º S/early Permian and 70º S/early Permian, 70º S/late Permian and 70º S/early Permian, 80º S/late Permian and 70º S/early Permian, Non-Antarctic/late

Permian and 70º S/early Permian, non-Antarctic/early Permian and 80º S/early Permian, 70º S/late Permian and 80º S/early Permian, 80º S/late Permian and 80º S/early Permian, non-Antarctic/late Permian and 80º S/early Permian, non-Antarctic/late Permian and 70º S/late Permian, non-Antarctic/late Permian and 80º S/late Permian, and non-Antarctic/middle Permian and non-Antarctic/late Permian.

When latitudes were separated into several smaller bins (e.g., 71º S, 72º S, 73º S), the [CO_2] was shown to have a significant main effect ($p << 0.001$) on leaf venation density (Figure 20). The latitude was also shown to have a significant main effect ($p << 0.001$) on venation density. Additionally, a significant interaction effect ($p < 0.01$) was found between the factors. The post-hoc testing showed significant interaction effects between non-Antarctica/late Permian and 72º S/early Permian, 85º S/early Permian and 76º S/early Permian, 77º S/late Permian and 76º S/early Permian, 83º S/late Permian and 76º S/early Permian, 84º S/late Permian and 76º S/early Permian, 86º S/late Permian and 76º S/early Permian, non-Antarctica/late Permian and 76º S/early Permian, 85º S/early Permian and 77º S/early Permian, 83º S/late Permian and 77º S/early Permian, 84º S/late Permian and 77º S/early Permian, 86º S/late Permian and 77º S/early Permian, non-Antarctica/late Permian and 77º S/early Permian, 74º S/late Permian and 83º S/early Permian, 77º S/late Permian and 83º S/early Permian, 83º S/late Permian and 83º S/early Permian, 84º S/late Permian and 83º S/early Permian, 86º S/late Permian and 83º S/early Permian, 87º S/late Permian and 83º S/erly Permian, non-Antarctica/late Permian and 83º S/early Permian, 85º S/early Permian and 84º S/early Permian, 74º S/late Permian and 84º S/early Permian, 83º S/late Permian and 84º S/early Permian, 84º S/late Permian and 84º S/early Permian, 86º S/late Permian and 84º S/early Permian, 87º S/late Permian and 84º S/early Permian, non-Antarctic/late Permian and 84º S/early Permian, 87º S/early Permian and 85º

S/early Permian, non-Antarctic/early Permian and 85º S/early Permian, 74º S/late Permian and 85º S/early Permian, 77º S/late Permian and 85º S/early Permian, 78º S/late Permian and 85º S/early Permian, 83º S/late Permian and 85º S/early Permian, 84º S/late Permian and 85º S/early Permian, 85º S/late Permian and 85º S/early Permian, 86º S/late Permian and 85º S/early Permian, 87º S/late Permian and 85º S/early Permian, non-Antarctic/late Permian and 85º S/early Permian, non-Antarctic/late Permian and 87º S/early Permian, non-Antarctic/late Permian and 77º S/late Permian, non-Antarctic/late Permian and 84º S/late Permian, non-Antarctic/late Permian and 85º S/late Permian, and non-Antarctic/middle Permian and non-Antarctic/late Permian.

3.3 Physiological findings for Glossopteris

From all of the 1319 *Glossopteris* leaves examined at all localities (Table 3), the average vein density was 9.03 mm mm^{-2}. From the vein densities measured, K_{leaf} was found to be 11.43 mmol m^{-2} s^{-1} MPa^{-1}, stomatal conductance was found to be 231.7 mmol H_20 m^{-2} s^{-1}, max photosynthetic capacity was found to be 11.87 μmol CO_2 $m^{-2}s^{-1}$, and the intrinsic WUE was found to be 0.05 μmol CO_2/mmol H_2O.

3.3.1 Physiological findings for Glossopteris *by locality*

From the 57 *Glossopteris* leaves examined from the Allan Hills locality, the average vein density was 10.1 mm mm^{-2}. From the vein densities measured, K_{leaf} was found to be 11.84 mmol m^{-2} s^{-1} MPa^{-1}, stomatal conductance was found to be 240.0 mmol H_20 m^{-2} s^{-1}, max photosynthetic capacity was found to be 12.2 μmol CO_2 $m^{-2}s^{-1}$, and the intrinsic WUE was found to be 0.05 μmol CO_2/mmol H_2O.

From the 32 *Glossopteris* leaves examined from the Aztec Mountain locality, the average vein density was 9.68 mm mm^{-2}. From the vein densities measured, K_{leaf} was found to be 11.73

mmol m^{-2} s^{-1} MPa^{-1}, stomatal conductance was found to be 237.7 mmol H_20 m^{-2} s^{-1}, max photosynthetic capacity was found to be 12.11 μmol CO_2 $m^{-2}s^{-1}$, and the intrinsic WUE was found to be 0.05 μmol CO_2/mmol H_2O.

From the 3 *Glossopteris* leaves examined from the Bazargaon, India locality, the average vein density was 8.60 mm mm^{-2}. From the vein densities measured, K_{leaf} was found to be 11.01 mmol m^{-2} s^{-1} MPa^{-1}, stomatal conductance was found to be 223.0 mmol H_20 m^{-2} s^{-1}, max photosynthetic capacity was found to be 11.49 μmol CO_2 $m^{-2}s^{-1}$, and the intrinsic WUE was found to be 0.05 μmol CO_2/mmol H_2O.

From the 14 *Glossopteris* leaves examined from the Bowden Névé locality, the average vein density was 8.62 mm mm^{-2}. From the vein densities measured, K_{leaf} was found to be 11.31 mmol m^{-2} s^{-1} MPa^{-1}, stomatal conductance was found to be 229.1 mmol H_20 m^{-2} s^{-1}, max photosynthetic capacity was found to be 11.77 μmol CO_2 $m^{-2}s^{-1}$, and the intrinsic WUE was found to be 0.05 μmol CO_2/mmol H_2O.

From the 2 *Glossopteris* leaves examined from the Canopy Cliffs locality, the average vein density was 8.30 mm mm^{-2}. From the vein densities measured, K_{leaf} was found to be 11.05 mmol m^{-2} s^{-1} MPa^{-1}, stomatal conductance was found to be 223.9 mmol H_20 m^{-2} s^{-1}, max photosynthetic capacity was found to be 11.55 μmol CO_2 $m^{-2}s^{-1}$, and the intrinsic WUE was found to be 0.05 μmol CO_2/mmol H_2O.

From the 2 *Glossopteris* leaves examined from the Clarkson Peak locality, the average vein density was 9.34 mm mm^{-2}. From the vein densities measured, K_{leaf} was found to be 11.39 mmol m^{-2} s^{-1} MPa^{-1}, stomatal conductance was found to be 230.7 mmol H_20 m^{-2} s^{-1}, max photosynthetic capacity was found to be 11.82 μmol CO_2 $m^{-2}s^{-1}$, and the intrinsic WUE was found to be 0.05 μmol CO_2/mmol H_2O.

From the 57 *Glossopteris* leaves examined from the Coalsack Bluff locality, the average vein density was 8.47 mm mm^{-2}. From the vein densities measured, K_{leaf} was found to be 11.26 mmol m^{-2} s^{-1} MPa^{-1}, stomatal conductance was found to be 228.1 mmol H_20 m^{-2} s^{-1}, max photosynthetic capacity was found to be 11.72 μmol CO_2 $m^{-2}s^{-1}$, and the intrinsic WUE was found to be 0.05 μmol CO_2/mmol H_2O.

From the 25 *Glossopteris* leaves examined from the Crack Bluff locality, the average vein density was 8.96 mm mm^{-2}. From the vein densities measured, K_{leaf} was found to be 11.41 mmol m^{-2} s^{-1} MPa^{-1}, stomatal conductance was found to be 231.2 mmol H_20 m^{-2} s^{-1}, max photosynthetic capacity was found to be 11.85 μmol CO_2 $m^{-2}s^{-1}$, and the intrinsic WUE was found to be 0.05 μmol CO_2/mmol H_2O.

From the 6 *Glossopteris* leaves examined from the Cranfield Peak locality, the average vein density was 10.4 mm mm^{-2}. From the vein densities measured, K_{leaf} was found to be 11.89 mmol m^{-2} s^{-1} MPa^{-1}, stomatal conductance was found to be 240.9 mmol H_20 m^{-2} s^{-1}, max photosynthetic capacity was found to be 12.24 μmol CO_2 $m^{-2}s^{-1}$, and the intrinsic WUE was found to be 0.05 μmol CO_2/mmol H_2O.

From the 8 *Glossopteris* leaves examined from the Erehwon Nunatak locality, the average vein density was 8.04 mm mm^{-2}. From the vein densities measured, K_{leaf} was found to be 11.11 mmol m^{-2} s^{-1} MPa^{-1}, stomatal conductance was found to be 225.1 mmol H_20 m^{-2} s^{-1}, max photosynthetic capacity was found to be 11.61 μmol CO_2 $m^{-2}s^{-1}$, and the intrinsic WUE was found to be 0.05 μmol CO_2/mmol H_2O.

From the 7 *Glossopteris* leaves examined from the Graphite Peak locality, the average vein density was 10.13 mm mm^{-2}. From the vein densities measured, K_{leaf} was found to be 11.81 mmol m^{-2} s^{-1} MPa^{-1}, stomatal conductance was found to be 239.3 mmol H_20 m^{-2} s^{-1}, max

photosynthetic capacity was found to be 12.18 μmol CO_2 $m^{-2}s^{-1}$, and the intrinsic WUE was found to be 0.05 μmol CO_2/mmol H_2O.

From the 1 *Glossopteris* leaves examined from the Hampton Hill locality, the average vein density was 10.49 mm mm^{-2}. From the vein densities measured, K_{leaf} was found to be 11.99 mmol m^{-2} s^{-1} MPa^{-1}, stomatal conductance was found to be 242.9 mmol H_20 m^{-2} s^{-1}, max photosynthetic capacity was found to be 12.32 μmol CO_2 $m^{-2}s^{-1}$, and the intrinsic WUE was found to be 0.05 μmol CO_2/mmol H_2O.

From the 2 *Glossopteris* leaves examined from the Horlick Mts. locality, the average vein density was 10.43 mm mm^{-2}. From the vein densities measured, K_{leaf} was found to be 11.82 mmol m^{-2} s^{-1} MPa^{-1}, stomatal conductance was found to be 239.4 mmol H_20 m^{-2} s^{-1}, max photosynthetic capacity was found to be 12.17 μmol CO_2 $m^{-2}s^{-1}$, and the intrinsic WUE was found to be 0.05 μmol CO_2/mmol H_2O.

From the 26 *Glossopteris* leaves examined from the Illawarra Coal Measures, Australia, the average vein density was 7.25 mm mm^{-2}. From the vein densities measured, K_{leaf} was found to be 10.67 mmol m^{-2} s^{-1} MPa^{-1}, stomatal conductance was found to be 216.2 mmol H_20 m^{-2} s^{-1}, max photosynthetic capacity was found to be 11.24 μmol CO_2 $m^{-2}s^{-1}$, and the intrinsic WUE was found to be 0.05 μmol CO_2/mmol H_2O.

From the 3 *Glossopteris* leaves examined from the Kennar Valley locality, the average vein density was 9.83 mm mm^{-2}. From the vein densities measured, K_{leaf} was found to be 11.81 mmol m^{-2} s^{-1} MPa^{-1}, stomatal conductance was found to be 239.3 mmol H_20 m^{-2} s^{-1}, max photosynthetic capacity was found to be 12.18 μmol CO_2 $m^{-2}s^{-1}$, and the intrinsic WUE was found to be 0.05 μmol CO_2/mmol H_2O.

From the 4 *Glossopteris* leaves examined from the KwaZulu-Natal, South Africa locality,

the average vein density was 8.77 mm mm^{-2}. From the vein densities measured, K_{leaf} was found to be 11.05 mmol m^{-2} s^{-1} MPa^{-1}, stomatal conductance was found to be 223.9 mmol H_20 m^{-2} s^{-1}, max photosynthetic capacity was found to be 11.54 μmol CO_2 $m^{-2}s^{-1}$, and the intrinsic WUE was found to be 0.05 μmol CO_2/mmol H_2O.

From the 4 *Glossopteris* leaves examined from the Laguna Polina, Argentina locality, the average vein density was 10.74 mm mm^{-2}. From the vein densities measured, K_{leaf} was found to be 11.98 mmol m^{-2} s^{-1} MPa^{-1}, stomatal conductance was found to be 242.8 mmol H_20 m^{-2} s^{-1}, max photosynthetic capacity was found to be 12.31 μmol CO_2 $m^{-2}s^{-1}$, and the intrinsic WUE was found to be 0.05 μmol CO_2/mmol H_2O.

From the 13 *Glossopteris* leaves examined from the Leaia Ledge locality, the average vein density was 8.58 mm mm^{-2}. From the vein densities measured, K_{leaf} was found to be 11.32 mmol m^{-2} s^{-1} MPa^{-1}, stomatal conductance was found to be 229.4 mmol H_20 m^{-2} s^{-1}, max photosynthetic capacity was found to be 11.78 μmol CO_2 $m^{-2}s^{-1}$, and the intrinsic WUE was found to be 0.05 μmol CO_2/mmol H_2O.

From the 25 *Glossopteris* leaves examined from the McIntyre Promontory locality, the average vein density was 10.53 mm mm^{-2}. From the vein densities measured, K_{leaf} was found to be 11.87 mmol m^{-2} s^{-1} MPa^{-1}, stomatal conductance was found to be 240.5 mmol H_20 m^{-2} s^{-1}, max photosynthetic capacity was found to be 12.22 μmol CO_2 $m^{-2}s^{-1}$, and the intrinsic WUE was found to be 0.05 μmol CO_2/mmol H_2O.

From the 1 *Glossopteris* leaves examined from the McKay Cliffs locality, the average vein density was 7.86 mm mm^{-2}. From the vein densities measured, K_{leaf} was found to be 11.11 mmol m^{-2} s^{-1} MPa^{-1}, stomatal conductance was found to be 225.0 mmol H_20 m^{-2} s^{-1}, max photosynthetic capacity was found to be 11.61 μmol CO_2 $m^{-2}s^{-1}$, and the intrinsic WUE was

found to be 0.05 μmol CO_2/mmol H_2O.

From the 1 *Glossopteris* leaves examined from the Mill Glacier locality, the average vein density was 7.26 mm mm^{-2}. From the vein densities measured, K_{leaf} was found to be 10.8 mmol m^{-2} s^{-1} MPa^{-1}, stomatal conductance was found to be 218.9 mmol H_20 m^{-2} s^{-1}, max photosynthetic capacity was found to be 11.36 μmol CO_2 $m^{-2}s^{-1}$, and the intrinsic WUE was found to be 0.05 μmol CO_2/mmol H_2O.

From the 17 *Glossopteris* leaves examined from the Mine Ledge locality, the average vein density was 8.78 mm mm^{-2}. From the vein densities measured, K_{leaf} was found to be 11.44 mmol m^{-2} s^{-1} MPa^{-1}, stomatal conductance was found to be 231.8 mmol H_20 m^{-2} s^{-1}, max photosynthetic capacity was found to be 11.88 μmol CO_2 $m^{-2}s^{-1}$, and the intrinsic WUE was found to be 0.05 μmol CO_2/mmol H_2O.

From the 3 *Glossopteris* leaves examined from the Moraine Ridge locality, the average vein density was 11.09 mm mm^{-2}. From the vein densities measured, K_{leaf} was found to be 11.9 mmol m^{-2} s^{-1} MPa^{-1}, stomatal conductance was found to be 241.1 mmol H_20 m^{-2} s^{-1}, max photosynthetic capacity was found to be 12.23 μmol CO_2 $m^{-2}s^{-1}$, and the intrinsic WUE was found to be 0.05 μmol CO_2/mmol H_2O.

From the 205 *Glossopteris* leaves examined from the Mt. Achernar locality, the average vein density was 8.57 mm mm^{-2}. From the vein densities measured, K_{leaf} was found to be 11.28 mmol m^{-2} s^{-1} MPa^{-1}, stomatal conductance was found to be 228.6 mmol H_20 m^{-2} s^{-1}, max photosynthetic capacity was found to be 11.75 μmol CO_2 $m^{-2}s^{-1}$, and the intrinsic WUE was found to be 0.05 μmol CO_2/mmol H_2O.

From the 10 *Glossopteris* leaves examined from the Mt. Baldwin locality, the average vein density was 10.29 mm mm^{-2}. From the vein densities measured, K_{leaf} was found to be 11.88

mmol m^{-2} s^{-1} MPa^{-1}, stomatal conductance was found to be 240.6 mmol H_20 m^{-2} s^{-1}, max photosynthetic capacity was found to be 12.23 μmol CO_2 $m^{-2}s^{-1}$, and the intrinsic WUE was found to be 0.05 μmol CO_2/mmol H_2O.

From the 5 *Glossopteris* leaves examined from the Mt. Bartlett locality, the average vein density was 8.31 mm mm^{-2}. From the vein densities measured, K_{leaf} was found to be 10.94 mmol m^{-2} s^{-1} MPa^{-1}, stomatal conductance was found to be 221.6 mmol H_20 m^{-2} s^{-1}, max photosynthetic capacity was found to be 11.44 μmol CO_2 $m^{-2}s^{-1}$, and the intrinsic WUE was found to be 0.05 μmol CO_2/mmol H_2O.

From the 4 *Glossopteris* leaves examined from the Mt. Bastion locality, the average vein density was 11.08 mm mm^{-2}. From the vein densities measured, K_{leaf} was found to be 12.08 mmol m^{-2} s^{-1} MPa^{-1}, stomatal conductance was found to be 244.8 mmol H_20 m^{-2} s^{-1}, max photosynthetic capacity was found to be 12.39 μmol CO_2 $m^{-2}s^{-1}$, and the intrinsic WUE was found to be 0.05 μmol CO_2/mmol H_2O.

From the 9 *Glossopteris* leaves examined from the Mt. Feather locality, the average vein density was 11.75 mm mm^{-2}. From the vein densities measured, K_{leaf} was found to be 12.13 mmol m^{-2} s^{-1} MPa^{-1}, stomatal conductance was found to be 245.7 mmol H_20 m^{-2} s^{-1}, max photosynthetic capacity was found to be 12.42 μmol CO_2 $m^{-2}s^{-1}$, and the intrinsic WUE was found to be 0.05 μmol CO_2/mmol H_2O.

From the 7 *Glossopteris* leaves examined from the Mt. *Glossopteris* locality, the average vein density was 8.68 mm mm^{-2}. From the vein densities measured, K_{leaf} was found to be 11.27 mmol m^{-2} s^{-1} MPa^{-1}, stomatal conductance was found to be 228.3 mmol H_20 m^{-2} s^{-1}, max photosynthetic capacity was found to be 11.73 μmol CO_2 $m^{-2}s^{-1}$, and the intrinsic WUE was found to be 0.05 μmol CO_2/mmol H_2O.

From the 5 *Glossopteris* leaves examined from the Mt. Gran locality, the average vein density was 11.17 mm mm^{-2}. From the vein densities measured, K_{leaf} was found to be 12.13 mmol m^{-2} s^{-1} MPa^{-1}, stomatal conductance was found to be 245.8 mmol H_20 m^{-2} s^{-1}, max photosynthetic capacity was found to be 12.43 μmol CO_2 $m^{-2}s^{-1}$, and the intrinsic WUE was found to be 0.05 μmol CO_2/mmol H_2O.

From the 18 *Glossopteris* leaves examined from the Mt. Howe locality, the average vein density was 8.52 mm mm^{-2}. From the vein densities measured, K_{leaf} was found to be 11.27 mmol m^{-2} s^{-1} MPa^{-1}, stomatal conductance was found to be 228.3 mmol H_20 m^{-2} s^{-1}, max photosynthetic capacity was found to be 11.73 μmol CO_2 $m^{-2}s^{-1}$, and the intrinsic WUE was found to be 0.05 μmol CO_2/mmol H_2O.

From the 1 *Glossopteris* leaves examined from the Mt. Kinsey locality, the average vein density was 10.88 mm mm^{-2}. From the vein densities measured, K_{leaf} was found to be 12.08 mmol m^{-2} s^{-1} MPa^{-1}, stomatal conductance was found to be 244.7 mmol H_20 m^{-2} s^{-1}, max photosynthetic capacity was found to be 12.39 μmol CO_2 $m^{-2}s^{-1}$, and the intrinsic WUE was found to be 0.05 μmol CO_2/mmol H_2O.

From the 2 *Glossopteris* leaves examined from the Mt. MacPherson locality, the average vein density was 10.08 mm mm^{-2}. From the vein densities measured, K_{leaf} was found to be 11.89 mmol m^{-2} s^{-1} MPa^{-1}, stomatal conductance was found to be 240.8 mmol H_20 m^{-2} s^{-1}, max photosynthetic capacity was found to be 12.24 μmol CO_2 $m^{-2}s^{-1}$, and the intrinsic WUE was found to be 0.05 μmol CO_2/mmol H_2O.

From the 19 *Glossopteris* leaves examined from the Mt. Picciotto locality, the average vein density was 11.18 mm mm^{-2}. From the vein densities measured, K_{leaf} was found to be 12.04 mmol m^{-2} s^{-1} MPa^{-1}, stomatal conductance was found to be 243.9 mmol H_20 m^{-2} s^{-1}, max

photosynthetic capacity was found to be 12.35 μmol CO_2 $m^{-2}s^{-1}$, and the intrinsic WUE was found to be 0.05 μmol CO_2/mmol H_2O.

From the 5 *Glossopteris* leaves examined from the Mt. Ropar locality, the average vein density was 7.66 mm mm^{-2}. From the vein densities measured, K_{leaf} was found to be 10.95 mmol m^{-2} s^{-1} MPa^{-1}, stomatal conductance was found to be 221.9 mmol H_20 m^{-2} s^{-1}, max photosynthetic capacity was found to be 11.48 μmol CO_2 $m^{-2}s^{-1}$, and the intrinsic WUE was found to be 0.05 μmol CO_2/mmol H_2O.

From the 4 *Glossopteris* leaves examined from the Mt. Rosenwald locality, the average vein density was 8.25 mm mm^{-2}. From the vein densities measured, K_{leaf} was found to be 11.23 mmol m^{-2} s^{-1} MPa^{-1}, stomatal conductance was found to be 227.6 mmol H_20 m^{-2} s^{-1}, max photosynthetic capacity was found to be 11.71 μmol CO_2 $m^{-2}s^{-1}$, and the intrinsic WUE was found to be 0.05 μmol CO_2/mmol H_2O.

From the 2 *Glossopteris* leaves examined from the Mt. Schopf locality, the average vein density was 8.23 mm mm^{-2}. From the vein densities measured, K_{leaf} was found to be 11.25 mmol m^{-2} s^{-1} MPa^{-1}, stomatal conductance was found to be 227.9 mmol H_20 m^{-2} s^{-1}, max photosynthetic capacity was found to be 11.73 μmol CO_2 $m^{-2}s^{-1}$, and the intrinsic WUE was found to be 0.05 μmol CO_2/mmol H_2O.

From the 34 *Glossopteris* leaves examined from the Mt. Sirius locality, the average vein density was 9.18 mm mm^{-2}. From the vein densities measured, K_{leaf} was found to be 11.52 mmol m^{-2} s^{-1} MPa^{-1}, stomatal conductance was found to be 233.3 mmol H_20 m^{-2} s^{-1}, max photosynthetic capacity was found to be 11.94 μmol CO_2 $m^{-2}s^{-1}$, and the intrinsic WUE was found to be 0.05 μmol CO_2/mmol H_2O.

From the 6 *Glossopteris* leaves examined from the Mt. Weaver locality, the average vein

density was 7.64 mm mm^{-2}. From the vein densities measured, K_{leaf} was found to be 10.99 mmol m^{-2} s^{-1} MPa^{-1}, stomatal conductance was found to be 222.6 mmol H_20 m^{-2} s^{-1}, max photosynthetic capacity was found to be 11.51 μmol CO_2 $m^{-2}s^{-1}$, and the intrinsic WUE was found to be 0.05 μmol CO_2/mmol H_2O.

From the 6 *Glossopteris* leaves examined from the Mt. Wild locality, the average vein density was 10.48 mm mm^{-2}. From the vein densities measured, K_{leaf} was found to be 11.97 mmol m^{-2} s^{-1} MPa^{-1}, stomatal conductance was found to be 242.6 mmol H_20 m^{-2} s^{-1}, max photosynthetic capacity was found to be 12.3 μmol CO_2 $m^{-2}s^{-1}$, and the intrinsic WUE was found to be 0.05 μmol CO_2/mmol H_2O.

From the 1 *Glossopteris* leaves examined from the Mt. Wisting locality, the average vein density was 9.52 mm mm^{-2}. From the vein densities measured, K_{leaf} was found to be 11.73 mmol m^{-2} s^{-1} MPa^{-1}, stomatal conductance was found to be 237.6 mmol H_20 m^{-2} s^{-1}, max photosynthetic capacity was found to be 12.11 μmol CO_2 $m^{-2}s^{-1}$, and the intrinsic WUE was found to be 0.05 μmol CO_2/mmol H_2O.

From the 1 *Glossopteris* leaves examined from the Orange Free State locality, the average vein density was 6.01 mm mm^{-2}. From the vein densities measured, K_{leaf} was found to be 9.98 mmol m^{-2} s^{-1} MPa^{-1}, stomatal conductance was found to be 202.1 mmol H_20 m^{-2} s^{-1}, max photosynthetic capacity was found to be 10.66 μmol CO_2 $m^{-2}s^{-1}$, and the intrinsic WUE was found to be 0.05 μmol CO_2/mmol H_2O.

From the 39 *Glossopteris* leaves examined from the Pecora Nunatak locality, the average vein density was 12.08 mm mm^{-2}. From the vein densities measured, K_{leaf} was found to be 12.22 mmol m^{-2} s^{-1} MPa^{-1}, stomatal conductance was found to be 247.6 mmol H_20 m^{-2} s^{-1}, max photosynthetic capacity was found to be 12.49 μmol CO_2 $m^{-2}s^{-1}$, and the intrinsic WUE was

found to be 0.05 μmol CO_2/mmol H_2O.

From the 107 *Glossopteris* leaves examined from the Polarstar Peak locality, the average vein density was 9.2 mm mm^{-2}. From the vein densities measured, K_{leaf} was found to be 11.56 mmol m^{-2} s^{-1} MPa^{-1}, stomatal conductance was found to be 234.2 mmol H_20 m^{-2} s^{-1}, max photosynthetic capacity was found to be 11.98 μmol CO_2 $m^{-2}s^{-1}$, and the intrinsic WUE was found to be 0.05 μmol CO_2/mmol H_2O.

From the 8 *Glossopteris* leaves examined from the Roaring Cliffs locality, the average vein density was 8.78 mm mm^{-2}. From the vein densities measured, K_{leaf} was found to be 11.24 mmol m^{-2} s^{-1} MPa^{-1}, stomatal conductance was found to be 227.8 mmol H_20 m^{-2} s^{-1}, max photosynthetic capacity was found to be 11.71 μmol CO_2 $m^{-2}s^{-1}$, and the intrinsic WUE was found to be 0.05 μmol CO_2/mmol H_2O.

From the 4 *Glossopteris* leaves examined from the Robison Peak locality, the average vein density was 8.65 mm mm^{-2}. From the vein densities measured, K_{leaf} was found to be 11.42 mmol m^{-2} s^{-1} MPa^{-1}, stomatal conductance was found to be 231.3 mmol H_20 m^{-2} s^{-1}, max photosynthetic capacity was found to be 11.86 μmol CO_2 $m^{-2}s^{-1}$, and the intrinsic WUE was found to be 0.05 μmol CO_2/mmol H_2O.

From the 21 *Glossopteris* leaves examined from the Rubble Ridge locality, the average vein density was 8.35 mm mm^{-2}. From the vein densities measured, K_{leaf} was found to be 11.24 mmol m^{-2} s^{-1} MPa^{-1}, stomatal conductance was found to be 227.7 mmol H_20 m^{-2} s^{-1}, max photosynthetic capacity was found to be 11.72 μmol CO_2 $m^{-2}s^{-1}$, and the intrinsic WUE was found to be 0.05 μmol CO_2/mmol H_2O.

From the 4 *Glossopteris* leaves examined from the Sandford Cliffs locality, the average vein density was 7.99 mm mm^{-2}. From the vein densities measured, K_{leaf} was found to be 11.09

mmol m^{-2} s^{-1} MPa^{-1}, stomatal conductance was found to be 224.6 mmol H_20 m^{-2} s^{-1}, max photosynthetic capacity was found to be 11.59 μmol CO_2 $m^{-2}s^{-1}$, and the intrinsic WUE was found to be 0.05 μmol CO_2/mmol H_2O.

From the 2 *Glossopteris* leaves examined from the Sierra de Pillahuinco locality, the average vein density was 9.81 mm mm^{-2}. From the vein densities measured, K_{leaf} was found to be 11.67 mmol m^{-2} s^{-1} MPa^{-1}, stomatal conductance was found to be 236.4 mmol H_20 m^{-2} s^{-1}, max photosynthetic capacity was found to be 12.06 μmol CO_2 $m^{-2}s^{-1}$, and the intrinsic WUE was found to be 0.05 μmol CO_2/mmol H_2O.

From the 415 *Glossopteris* leaves examined from the Skaar Ridge locality, the average vein density was 8.67 mm mm^{-2}. From the vein densities measured, K_{leaf} was found to be 11.33 mmol m^{-2} s^{-1} MPa^{-1}, stomatal conductance was found to be 229.6 mmol H_20 m^{-2} s^{-1}, max photosynthetic capacity was found to be 11.79 μmol CO_2 $m^{-2}s^{-1}$, and the intrinsic WUE was found to be 0.05 μmol CO_2/mmol H_2O.

From the 46 *Glossopteris* leaves examined from the Terrace Ridge locality, the average vein density was 8.82 mm mm^{-2}. From the vein densities measured, K_{leaf} was found to be 11.36 mmol m^{-2} s^{-1} MPa^{-1}, stomatal conductance was found to be 230.2 mmol H_20 m^{-2} s^{-1}, max photosynthetic capacity was found to be 11.81 μmol CO_2 $m^{-2}s^{-1}$, and the intrinsic WUE was found to be 0.05 μmol CO_2/mmol H_2O.

From the 11 *Glossopteris* leaves examined from the Tillite Ridge locality, the average vein density was 10.0 mm mm^{-2}. From the vein densities measured, K_{leaf} was found to be 11.79 mmol m^{-2} s^{-1} MPa^{-1}, stomatal conductance was found to be 238.9 mmol H_20 m^{-2} s^{-1}, max photosynthetic capacity was found to be 12.16 μmol CO_2 $m^{-2}s^{-1}$, and the intrinsic WUE was found to be 0.05 μmol CO_2/mmol H_2O.

From the 3 *Glossopteris* leaves examined from the Waterberg Coal Field locality, the average vein density was 8.38 mm mm^{-2}. From the vein densities measured, K_{leaf} was found to be 11.29 mmol m^{-2} s^{-1} MPa^{-1}, stomatal conductance was found to be 228.7 mmol H_20 m^{-2} s^{-1}, max photosynthetic capacity was found to be 11.76 μmol CO_2 $m^{-2}s^{-1}$, and the intrinsic WUE was found to be 0.05 μmol CO_2/mmol H_2O.

From the 2 *Glossopteris* leaves examined from the Zimbabwe locality, the average vein density was 9.72 mm mm^{-2}. From the vein densities measured, K_{leaf} was found to be 11.71 mmol m^{-2} s^{-1} MPa^{-1}, stomatal conductance was found to be 237.3 mmol H_20 m^{-2} s^{-1}, max photosynthetic capacity was found to be 12.09 μmol CO_2 $m^{-2}s^{-1}$, and the intrinsic WUE was found to be 0.05 μmol CO_2/mmol H_2O.

3.3.2 Physiological findings for Glossopteris *by formation*

There were 8 *Glossopteris* leaves examined from the Erehwon beds Formation. The average vein density of the leaves is 8.04 mm mm^{-2}, the average K_{leaf} is 11.11 mmol m^{-2} s^{-1} MPa^{-1}, the stomatal conductance for these leaves averages 225.1 mmol H_20 m^{-2} s^{-1}, the maximum photosynthetic capacity is 11.6 μmol CO_2 $m^{-2}s^{-1}$, and the average intrinsic WUE is 0.05 μmol CO_2/mmol H_2O.

There were 4 *Glossopteris* leaves examined from the Upper La Golondrina Formation. The average vein density of the leaves is 10.74 mm mm^{-2}, the average K_{leaf} is 11.98 mmol m^{-2} s^{-1} MPa^{-1}, the stomatal conductance for these leaves averages 242.8 mmol H_20 m^{-2} s^{-1}, the maximum photosynthetic capacity is 12.31 μmol CO_2 $m^{-2}s^{-1}$, and the average intrinsic WUE is 0.05 μmol CO_2/mmol H_2O.

There were 26 *Glossopteris* leaves examined from the Illawarra Coal Measures Formation. The average vein density of the leaves is 7.25 mm mm^{-2}, the average K_{leaf} is 10.67

mmol m^{-2} s^{-1} MPa^{-1}, the stomatal conductance for these leaves averages 216.2 mmol H_20 m^{-2} s^{-1}, the maximum photosynthetic capacity is 11.24 μmol CO_2 $m^{-2}s^{-1}$, and the average intrinsic WUE is 0.05 μmol CO_2/mmol H_2O.

There were 10 *Glossopteris* leaves examined from the Takrouna Formation. The average vein density of the leaves is 10.29 mm mm^{-2}, the average K_{leaf} is 11.88 mmol m^{-2} s^{-1} MPa^{-1}, the stomatal conductance for these leaves averages 240.6 mmol H_20 m^{-2} s^{-1}, the maximum photosynthetic capacity is 12.23 μmol CO_2 $m^{-2}s^{-1}$, and the average intrinsic WUE is 0.05 μmol CO_2/mmol H_2O.

There were 5 *Glossopteris* leaves examined from the Normandien Formation. The average vein density of the leaves is 8.21 mm mm^{-2}, the average K_{leaf} is 10.84 mmol m^{-2} s^{-1} MPa^{-1}, the stomatal conductance for these leaves averages 219.6 mmol H_20 m^{-2} s^{-1}, the maximum photosynthetic capacity is 11.36 μmol CO_2 $m^{-2}s^{-1}$, and the average intrinsic WUE is 0.05 μmol CO_2/mmol H_2O.

There were 3 *Glossopteris* leaves examined from the Ecca Group Formation. The average vein density of the leaves is 8.38 mm mm^{-2}, the average K_{leaf} is 11.29 mmol m^{-2} s^{-1} MPa^{-1}, the stomatal conductance for these leaves averages 228.7 mmol H_20 m^{-2} s^{-1}, the maximum photosynthetic capacity is 11.76 μmol CO_2 $m^{-2}s^{-1}$, and the average intrinsic WUE is 0.05 μmol CO_2/mmol H_2O.

There were 105 *Glossopteris* leaves examined from the Weller Coal Measures Formation. The average vein density of the leaves is 10.05 mm mm^{-2}, the average K_{leaf} is 11.82 mmol m^{-2} s^{-1} MPa^{-1}, the stomatal conductance for these leaves averages 239.4 mmol H_20 m^{-2} s^{-1}, the maximum photosynthetic capacity is 12.18 μmol CO_2 $m^{-2}s^{-1}$, and the average intrinsic WUE is 0.05 μmol CO_2/mmol H_2O.

There were 39 *Glossopteris* leaves examined from the Pecora Formation. The average vein density of the leaves is 12.08 mm mm^{-2}, the average K_{leaf} is 12.22 mmol m^{-2} s^{-1} MPa^{-1}, the stomatal conductance for these leaves averages 247.6 mmol H_20 m^{-2} s^{-1}, the maximum photosynthetic capacity is 12.49 μmol CO_2 $m^{-2}s^{-1}$, and the average intrinsic WUE is 0.05 μmol CO_2/mmol H_2O.

There were 88 *Glossopteris* leaves examined from the Mt. Glossopteris Formation. The average vein density of the leaves is 8.83 mm mm^{-2}, the average K_{leaf} is 11.38 mmol m^{-2} s^{-1} MPa^{-1}, the stomatal conductance for these leaves averages 230.6 mmol H_20 m^{-2} s^{-1}, the maximum photosynthetic capacity is 11.83 μmol CO_2 $m^{-2}s^{-1}$, and the average intrinsic WUE is 0.05 μmol CO_2/mmol H_2O.

There were 11 *Glossopteris* leaves examined from the Weaver Formation. The average vein density of the leaves is 10.0 mm mm^{-2}, the average K_{leaf} is 11.79 mmol m^{-2} s^{-1} MPa^{-1}, the stomatal conductance for these leaves averages 238.9 mmol H_20 m^{-2} s^{-1}, the maximum photosynthetic capacity is 12.16 μmol CO_2 $m^{-2}s^{-1}$, and the average intrinsic WUE is 0.05 μmol CO_2/mmol H_2O.

There were 3 *Glossopteris* leaves examined from the Mackellar or Fairchild Formation. The average vein density of the leaves is 9.34 mm mm^{-2}, the average K_{leaf} is 11.63 mmol m^{-2} s^{-1} MPa^{-1}, the stomatal conductance for these leaves averages 235.5 mmol H_20 m^{-2} s^{-1}, the maximum photosynthetic capacity is 12.03 μmol CO_2 $m^{-2}s^{-1}$, and the average intrinsic WUE is 0.05 μmol CO_2/mmol H_2O.

There were 761 *Glossopteris* leaves examined from the Upper Buckley Formation. The average vein density of the leaves is 8.67 mm mm^{-2}, the average K_{leaf} is 11.32 mmol m^{-2} s^{-1} MPa^{-1}, the stomatal conductance for these leaves averages 229.4 mmol H_20 m^{-2} s^{-1}, the maximum

photosynthetic capacity is 11.78 μmol CO_2 $m^{-2}s^{-1}$, and the average intrinsic WUE is 0.05 μmol CO_2/mmol H_2O.

There were 107 *Glossopteris* leaves examined from the Polarstar Formation. The average vein density of the leaves is 9.2 mm mm^{-2}, the average K_{leaf} is 11.56 mmol m^{-2} s^{-1} MPa^{-1}, the stomatal conductance for these leaves averages 234.2 mmol H_20 m^{-2} s^{-1}, the maximum photosynthetic capacity is 11.98 μmol CO_2 $m^{-2}s^{-1}$, and the average intrinsic WUE is 0.05 μmol CO_2/mmol H_2O.

There were 2 *Glossopteris* leaves examined from the Wankie Sandstone Formation. The average vein density of the leaves is 9.72 mm mm^{-2}, the average K_{leaf} is 11.71 mmol m^{-2} s^{-1} MPa^{-1}, the stomatal conductance for these leaves averages 237.3 mmol H_20 m^{-2} s^{-1}, the maximum photosynthetic capacity is 12.09 μmol CO_2 $m^{-2}s^{-1}$, and the average intrinsic WUE is 0.05 μmol CO_2/mmol H_2O.

There were 2 *Glossopteris* leaves examined from the Bonete Formation. The average vein density of the leaves is 9.81 mm mm^{-2}, the average K_{leaf} is 11.67 mmol m^{-2} s^{-1} MPa^{-1}, the stomatal conductance for these leaves averages 236.4 mmol H_20 m^{-2} s^{-1}, the maximum photosynthetic capacity is 12.06 μmol CO_2 $m^{-2}s^{-1}$, and the average intrinsic WUE is 0.05 μmol CO_2/mmol H_2O.

There were 80 *Glossopteris* leaves examined from the Queen Maud Formation. The average vein density of the leaves is 8.62 mm mm^{-2}, the average K_{leaf} is 11.3 mmol m^{-2} s^{-1} MPa^{-1}, the stomatal conductance for these leaves averages 228.9 mmol H_20 m^{-2} s^{-1}, the maximum photosynthetic capacity is 11.76 μmol CO_2 $m^{-2}s^{-1}$, and the average intrinsic WUE is 0.05 μmol CO_2/mmol H_2O.

There were 9 *Glossopteris* leaves examined from the Mt. Bastion Formation. The average vein density of the leaves is 11.13 mm mm^{-2}, the average K_{leaf} is 12.11 mmol m^{-2} s^{-1} MPa^{-1}, the

stomatal conductance for these leaves averages 245.4 mmol H_20 m^{-2} s^{-1}, the maximum photosynthetic capacity is 12.41 μmol CO_2 $m^{-2}s^{-1}$, and the average intrinsic WUE is 0.05 μmol CO_2/mmol H_2O.

There were 50 *Glossopteris* leaves examined from the Lower Buckley Formation. The average vein density of the leaves is 10.76 mm mm^{-2}, the average K_{leaf} is 11.94 mmol m^{-2} s^{-1} MPa^{-1}, the stomatal conductance for these leaves averages 241.8 mmol H_20 m^{-2} s^{-1}, the maximum photosynthetic capacity is 12.27 μmol CO_2 $m^{-2}s^{-1}$, and the average intrinsic WUE is 0.05 μmol CO_2/mmol H_2O.

There were 3 *Glossopteris* leaves examined from the Kamthi Formation. The average vein density of the leaves is 8.6 mm mm^{-2}, the average K_{leaf} is 11.01 mmol m^{-2} s^{-1} MPa^{-1}, the stomatal conductance for these leaves averages 223.0 mmol H_20 m^{-2} s^{-1}, the maximum photosynthetic capacity is 11.49 μmol CO_2 $m^{-2}s^{-1}$, and the average intrinsic WUE is 0.05 μmol CO_2/mmol H_2O.

3.3.3 Physiological findings for Glossopteris *by time*

Glossopteris leaves from the early Permian (n = 234) have an average leaf venation density of 10.55 mm mm^{-2}, a K_{leaf} of 11.91 mmol m^{-2} s^{-1} MPa^{-1}, a stomatal conductance of 241.3 mmol H_20 m^{-2} s^{-1}, a maximum photosynthetic capacity of 12.25 μmol CO_2 $m^{-2}s^{-1}$, and an intrinsic WUE of 0.05 μmol CO_2/mmol H_2O. Middle Permian leaves (n = 4) have an average venation density of 10.74 mm mm^{-2}. The calculated K_{leaf} of these leaves is 11.98 mmol m^{-2} s^{-1} MPa^{-1}, a stomatal conductance of 242.8 mmol H_20 m^{-2} s^{-1}, a photosynthetic capacity of 12.31 μmol CO_2 $m^{-2}s^{-1}$, and an intrinsic WUE of 0.05 μmol CO_2/mmol H_2O. *Glossopteris* leaves from the late Permian (n = 1078) have an average leaf venation density of 8.69 mm mm^{-2}, a calculated K_{leaf} of 11.32 mmol m^{-2} s^{-1} MPa^{-1}, a stomatal conductance 229.5 mmol H_20 m^{-2} s^{-1}, a maximum

photosynthetic capacity of 11.78 μmol CO_2 $m^{-2}s^{-1}$, and an intrinsic WUE of 0.05 μmol CO_2/mmol H_2O.

3.4 Physiological findings for Gangamopteris

A total of 42 *Gangamopteris* leaves were analyzed for this study (Table 4). The average leaf venation density for all of these leaves 7.78 mm mm^{-2}. From this value, the K_{leaf} of *Gangamopteris* leaves was calculated to be 10.91 mmol m^{-2} s^{-1} MPa^{-1}, the stomatal conductance 221.06 mmol H_20 m^{-2} s^{-1}, the maximum photosynthetic capacity 11.44 μmol CO_2 $m^{-2}s^{-1}$, and the intrinsic WUE 0.05 μmol CO_2/mmol H_2O.

3.4.1 Physiological findings for Gangamopteris *by locality*

From the 5 *Gangamopteris* leaves examined from the Allan Hills locality, the average vein density was 7.62 mm mm^{-2}. From the vein densities measured, K_{leaf} was found to be 10.88 mmol m^{-2} s^{-1} MPa^{-1}, stomatal conductance was found to be 220.3 mmol H_20 m^{-2} s^{-1}, max photosynthetic capacity was found to be 11.41 μmol CO_2 $m^{-2}s^{-1}$, and the intrinsic WUE was found to be 0.05 μmol CO_2/mmol H_2O.

From the 15 *Gangamopteris* leaves examined from the Aztec Mt. locality, the average vein density was 7.91 mm mm^{-2}. From the vein densities measured, K_{leaf} was found to be 11.07 mmol m^{-2} s^{-1} MPa^{-1}, stomatal conductance was found to be 224.2 mmol H_20 m^{-2} s^{-1}, max photosynthetic capacity was found to be 11.58 μmol CO_2 $m^{-2}s^{-1}$, and the intrinsic WUE was found to be 0.05 μmol CO_2/mmol H_2O.

From the 2 *Gangamopteris* leaves examined from the Kennar Valley locality, the average vein density was 8.93 mm mm^{-2}. From the vein densities measured, K_{leaf} was found to be 11.53 mmol m^{-2} s^{-1} MPa^{-1}, stomatal conductance was found to be 233.5 mmol H_20 m^{-2} s^{-1}, max photosynthetic capacity was found to be 11.95 μmol CO_2 $m^{-2}s^{-1}$, and the intrinsic WUE was

found to be 0.05 μmol CO_2/mmol H_2O.

From the 1 *Gangamopteris* leaf examined from the Mt. Fleming locality, the vein density was 5.17 mm mm^{-2}. From the vein density measured, K_{leaf} was found to be 9.22 mmol m^{-2} s^{-1} MPa^{-1}, stomatal conductance was found to be 186.9 mmol H_20 m^{-2} s^{-1}, max photosynthetic capacity was found to be 9.99 μmol CO_2 $m^{-2}s^{-1}$, and the intrinsic WUE was found to be 0.05 μmol CO_2/mmol H_2O.

From the 9 *Gangamopteris* leaves examined from the Mt. Gran locality, the average vein density was 8.18 mm mm^{-2}. From the vein densities measured, K_{leaf} was found to be 11.11 mmol m^{-2} s^{-1} MPa^{-1}, stomatal conductance was found to be 225.2 mmol H_20 m^{-2} s^{-1}, max photosynthetic capacity was found to be 11.61 μmol CO_2 $m^{-2}s^{-1}$, and the intrinsic WUE was found to be 0.05 μmol CO_2/mmol H_2O.

From the 2 *Gangamopteris* leaves examined from the Pecora Nunatak locality, the average vein density was 9.24 mm mm^{-2}. From the vein densities measured, K_{leaf} was found to be 10.76 mmol m^{-2} s^{-1} MPa^{-1}, stomatal conductance was found to be 218.0 mmol H_20 m^{-2} s^{-1}, max photosynthetic capacity was found to be 11.26 μmol CO_2 $m^{-2}s^{-1}$, and the intrinsic WUE was found to be 0.05 μmol CO_2/mmol H_2O.

From the 8 *Gangamopteris* leaves examined from the Robison Peak locality, the average vein density was 6.86 mm mm^{-2}. From the vein densities measured, K_{leaf} was found to be 10.51 mmol m^{-2} s^{-1} MPa^{-1}, stomatal conductance was found to be 212.9 mmol H_20 m^{-2} s^{-1}, max photosynthetic capacity was found to be 11.11 μmol CO_2 $m^{-2}s^{-1}$, and the intrinsic WUE was found to be 0.05 μmol CO_2/mmol H_2O.

3.4.2 Physiological findings for Gangamopteris *by formation*

There were 31 *Gangamopteris* leaves examined from the Weller Coal Measures

Formation. The average vein density of the leaves is 7.57 mm mm^{-2}, the average K_{leaf} is 10.86 mmol m^{-2} s^{-1} MPa^{-1}, the stomatal conductance for these leaves averages 220.1 mmol H_20 m^{-2} s^{-1}, the maximum photosynthetic capacity is 11.4 μmol CO_2 $m^{-2}s^{-1}$, and the average intrinsic WUE is 0.05 μmol CO_2/mmol H_2O.

There were 2 *Gangamopteris* leaves examined from the Pecora Formation. The average vein density of the leaves is 9.24 mm mm^{-2}, the average K_{leaf} is 10.76 mmol m^{-2} s^{-1} MPa^{-1}, the stomatal conductance for these leaves averages 218.0 mmol H_20 m^{-2} s^{-1}, the maximum photosynthetic capacity is 11.26 μmol CO_2 $m^{-2}s^{-1}$, and the average intrinsic WUE is 0.05 μmol CO_2/mmol H_2O.

There were 9 *Gangamopteris* leaves examined from the Mt. Bastion Formation. The average vein density of the leaves is 8.18 mm mm^{-2}, the average K_{leaf} is 11.11 mmol m^{-2} s^{-1} MPa^{-1}, the stomatal conductance for these leaves averages 225.2 mmol H_20 m^{-2} s^{-1}, the maximum photosynthetic capacity is 11.61 μmol CO_2 $m^{-2}s^{-1}$, and the average intrinsic WUE is 0.05 μmol CO_2/mmol H_2O.

3.4.3 Physiological findings for Gangamopteris *by time*

All 42 leaves of *Gangamopteris* came from Lower Permian strata.

3.5 Physiological findings for Noeggerathiopsis

A total of 13 *Noeggerathiopsis* leaves were used in this analysis (Table 5). The average leaf venation density is 6.68 mm mm^{-2}. From these values, the K_{leaf} was calculated as 10.33 mmol m^{-2} s^{-1} MPa^{-1}, the stomatal conductance as 209.3 mmol H_20 m^{-2} s^{-1}, the photosynthetic capacity as 10.95 μmol CO_2 $m^{-2}s^{-1}$, and the intrinsic WUE as 0.05 μmol CO_2/mmol H_2O.

3.5.1 Physiological findings for Noeggerathiopsis *by locality*

From the 1 *Noeggerathiopsis* leaf examined from the Clarkson Peak locality, the vein

density was 7.79 mm mm^{-2}. From the vein density measured, K_{leaf} was found to be 11.08 mmol m^{-2} s^{-1} MPa^{-1}, stomatal conductance was found to be 224.4 mmol H_20 m^{-2} s^{-1}, max photosynthetic capacity was found to be 11.59 µmol CO_2 $m^{-2}s^{-1}$, and the intrinsic WUE was found to be 0.05 µmol CO_2/mmol H_2O.

From the 7 *Noeggerathiopsis* leaves examined from the Kennar Valley locality, the vein density was 6.06 mm mm^{-2}. From the vein density measured, K_{leaf} was found to be 9.98 mmol m^{-2} s^{-1} MPa^{-1}, stomatal conductance was found to be 202.1 mmol H_20 m^{-2} s^{-1}, max photosynthetic capacity was found to be 10.66 µmol CO_2 $m^{-2}s^{-1}$, and the intrinsic WUE was found to be 0.05 µmol CO_2/mmol H_2O.

From the 1 *Noeggerathiopsis* leaf examined from the Mt. Feather locality, the vein density was 8.55 mm mm^{-2}. From the vein density measured, K_{leaf} was found to be 11.4 mmol m^{-2} s^{-1} MPa^{-1}, stomatal conductance was found to be 230.9 mmol H_20 m^{-2} s^{-1}, max photosynthetic capacity was found to be 11.85 µmol CO_2 $m^{-2}s^{-1}$, and the intrinsic WUE was found to be 0.05 µmol CO_2/mmol H_2O.

From the 1 *Noeggerathiopsis* leaf examined from the Robison Peak locality, the vein density was 9.33 mm mm^{-2}. From the vein density measured, K_{leaf} was found to be 11.67 mmol m^{-2} s^{-1} MPa^{-1}, stomatal conductance was found to be 236.4 mmol H_20 m^{-2} s^{-1}, max photosynthetic capacity was found to be 12.07 µmol CO_2 $m^{-2}s^{-1}$, and the intrinsic WUE was found to be 0.05 µmol CO_2/mmol H_2O.

From the 1 *Noeggerathiopsis* leaf examined from the Terrace Ridge locality, the vein density was 6.62 mm mm^{-2}. From the vein density measured, K_{leaf} was found to be 10.42 mmol m^{-2} s^{-1} MPa^{-1}, stomatal conductance was found to be 211.1 mmol H_20 m^{-2} s^{-1}, max photosynthetic capacity was found to be 11.04 µmol CO_2 $m^{-2}s^{-1}$, and the intrinsic WUE was found to be 0.05

μmol CO_2/mmol H_2O.

From the 2 *Noeggerathiopsis* leaves examined from the Tillite Ridge locality, the average vein density was 6.03 mm mm^{-2}. From the vein densities measured, K_{leaf} was found to be 9.96 mmol m^{-2} s^{-1} MPa^{-1}, stomatal conductance was found to be 201.8 mmol H_20 m^{-2} s^{-1}, max photosynthetic capacity was found to be 10.64 μmol CO_2 $m^{-2}s^{-1}$, and the intrinsic WUE was found to be 0.05 μmol CO_2/mmol H_2O.

3.5.2 Physiological findings for Noeggerathiopsis *by formation*

There were 9 *Noeggerathiopsis* leaves examined from the Weller Coal Measures Formation. The average vein density of the leaves is 6.7 mm mm^{-2}, the average K_{leaf} is 10.32 mmol m^{-2} s^{-1} MPa^{-1}, the stomatal conductance for these leaves averages 209.1 mmol H_20 m^{-2} s^{-1}, the maximum photosynthetic capacity is 10.94 μmol CO_2 $m^{-2}s^{-1}$, and the average intrinsic WUE is 0.05 μmol CO_2/mmol H_2O.

There was 1 *Noeggerathiopsis* leaf examined from the Mt. Glossopteris Formation. The vein density of the leaf is 6.62 mm mm^{-2}, the K_{leaf} is 10.42 mmol m^{-2} s^{-1} MPa^{-1}, the stomatal conductance for this leaf is 211.1 mmol H_20 m^{-2} s^{-1}, the maximum photosynthetic capacity is 11.04 μmol CO_2 $m^{-2}s^{-1}$, and the intrinsic WUE is 0.05 μmol CO_2/mmol H_2O.

There were 2 *Noeggerathiopsis* leaves examined from the Weaver Formation. The average vein density of the leaves is 6.03 mm mm^{-2}, the average K_{leaf} is 9.96 mmol m^{-2} s^{-1} MPa^{-1}, the stomatal conductance for these leaves averages 201.8 mmol H_20 m^{-2} s^{-1}, the maximum photosynthetic capacity is 10.64 μmol CO_2 $m^{-2}s^{-1}$, and the average intrinsic WUE is 0.05 μmol CO_2/mmol H_2O.

There was 1 *Noeggerathiopsis* leaf examined from the Upper Buckley Formation. The vein density of the leaf is 7.79 mm mm^{-2}, the K_{leaf} is 11.08 mmol m^{-2} s^{-1} MPa^{-1}, the stomatal

conductance for this leaf is 224.4 mmol H_20 m^{-2} s^{-1}, the maximum photosynthetic capacity is 11.59 μmol CO_2 $m^{-2}s^{-1}$, and the average intrinsic WUE is 0.05 μmol CO_2/mmol H_2O.

3.5.3 Physiological findings for Noeggerathiopsis *by time*

Eleven leaves of Noeggerathiopsis were examined from the early Permian. The average leaf venation density of these specimens was 6.58 mm mm^{-2}, the K_{leaf} is 10.26 mmol m^{-2} s^{-1} MPa^{-1}, the stomatal conductance is 207.8 mmol H_20 m^{-2} s^{-1}, the photosynthetic capacity is 10.89 μmol CO_2 $m^{-2}s^{-1}$, and the intrinsic WUE is 0.05 μmol CO2/mmol H2O. Two leaves were examined from the late Permian. The average leaf venation density of these two specimens is 7.21 mm mm^{-2}. From these values, the K_{leaf} was calculated to be 10.75 mmol m^{-2} s^{-1} MPa^{-1}, the stomatal conductance 217.8 mmol H_20 m^{-2} s^{-1}, the photosynthetic capacity 11.3 μmol CO_2 $m^{-2}s^{-1}$, and the intrinsic WUE to be 0.05 μmol CO_2/mmol H_2O.

4. Results for Triassic leaves

4.1 Differences between genera

Results of the ANOVA on the Triassic genera show that there are significant differences ($p << 0.001$) in leaf venation density among the genera analyzed (Figure 21). The post-hoc Tukey test indicates that the only significant differences in leaf venation density occur between *Heidiphyllum* and all other genera (*Cladophlebis*: $p = 0.01$, *Dejerseya*: $p < 0.01$, *Dicroidium*: $p < 0.01$, *Osmunda*: $p < 0.01$, *Sphenobaiera*: $p < 0.01$, *Taeniopteris*: $p < 0.01$). Excluding *Heidiphyllum*, there are no statistically significant difference at a 95% confidence level between any other leaf type.

4.2 Physiological findings for Cladophlebis

From the two *Cladophlebis* leaves examined (Table 6), the average vein density was 4.8 mm mm^{-2}. From the vein densities measured, K_{leaf} was found to be 8.50 mmol m^{-2} s^{-1} MPa^{-1},

stomatal conductance was found to be 190.4 mmol H_20 m^{-2} s^{-1}, max photosynthetic capacity was found to be 9.23 μmol CO_2 $m^{-2}s^{-1}$, and the intrinsic WUE was found to be 0.05 μmol CO_2/mmol H_2O. Specimens of *Cladophlebis* came from a single formation and locality.

4.3 Physiological findings for Dejerseya

From the 8 *Dejerseya* leaves examined (Table 7), the average vein density was 4.9 mm mm^{-2}. From the vein densities measured, K_{leaf} was found to be 8.9 mmol m^{-2} s^{-1} MPa^{-1}, stomatal conductance was found to be 180.4 mmol H_20 m^{-2} s^{-1}, max photosynthetic capacity was found to be 9.69 μmol CO_2 m^{-2} s^{-1}, and the intrinsic WUE was found to be 0.05 μmol CO_2/mmol H_2O.

4.3.1 Physiological findings for Dejerseya *by locality*

From the 1 *Dejerseya* leaf examined from the Alfie's Elbow locality, thevein density was 4.53 mm mm^{-2}. From the vein density measured, K_{leaf} was found to be 8.51 mmol m^{-2} s^{-1} MPa^{-1}, stomatal conductance was found to be 172.4 mmol H_20 m^{-2} s^{-1}, max photosynthetic capacity was found to be 9.33 μmol CO_2 m^{-2} s^{-1}, and the intrinsic WUE was found to be 0.05 μmol CO_2/mmol H_2O.

From the 7 *Dejerseya* leaves examined from the Mt. Falla locality, the average vein density was 4.99 mm mm^{-2}. From the vein densities measured, K_{leaf} was found to be 8.96 mmol m^{-2} s^{-1} MPa^{-1}, stomatal conductance was found to be 181.5 mmol H_20 m^{-2} s^{-1}, max photosynthetic capacity was found to be 9.74 μmol CO_2 m^{-2} s^{-1}, and the intrinsic WUE was found to be 0.05 μmol CO_2/mmol H_2O. All 8 leaves were from the Falla formation.

4.4 Physiological findings for Dicroidium

From the 197 *Dicroidium* leaves examined, the average vein density was 4.84 mm mm^{-2}. From the vein densities measured, K_{leaf} was found to be 8.78 mmol m^{-2} s^{-1} MPa^{-1}, stomatal conductance was found to be 177.8 mmol H_20 m^{-2} s^{-1}, max photosynthetic capacity was found to

be 9.57 μmol CO_2 m^{-2} s^{-1}, and the intrinsic WUE was found to be 0.05 μmol CO_2/mmol H_2O.

4.4.1 Physiological findings for Dicroidium *by locality*

From the 59 *Dicroidium* leaves examined (Table 8) from the Alfie's Elbow locality, the average vein density was 4.72 mm mm^{-2}. From the vein densities measured, K_{leaf} was found to be 8.65 mmol m^{-2} s^{-1} MPa^{-1}, stomatal conductance was found to be 175.3 mmol H_20 m^{-2} s^{-1}, max photosynthetic capacity was found to be 9.45 μmol CO_2 m^{-2} s^{-1}, and the intrinsic WUE was found to be 0.05 μmol CO_2/mmol H_2O.

From the 59 *Dicroidium* leaves examined from the Allan Hills locality, the average vein density was 4.81 mm mm^{-2}. From the vein densities measured, K_{leaf} was found to be 8.73 mmol m^{-2} s^{-1} MPa^{-1}, stomatal conductance was found to be 176.9 mmol H_20 m^{-2} s^{-1}, max photosynthetic capacity was found to be 9.52 μmol CO_2 m^{-2} s^{-1}, and the intrinsic WUE was found to be 0.05 μmol CO_2/mmol H_2O.

From the 15 *Dicroidium* leaves examined from the Dinmore locality, the average vein density was 5.88 mm mm^{-2}. From the vein densities measured, K_{leaf} was found to be 9.84 mmol m^{-2} s^{-1} MPa^{-1}, stomatal conductance was found to be 199.4 mmol H_20 m^{-2} s^{-1}, max photosynthetic capacity was found to be 10.54 μmol CO_2 m^{-2} s^{-1}, and the intrinsic WUE was found to be 0.05 μmol CO_2/mmol H_2O.

From the 3 *Dicroidium* leaves examined from the Fremouw Peak locality, the average vein density was 4.75 mm mm^{-2}. From the vein densities measured, K_{leaf} was found to be 8.75 mmol m^{-2} s^{-1} MPa^{-1}, stomatal conductance was found to be 177.3 mmol H_20 m^{-2} s^{-1}, max photosynthetic capacity was found to be 9.56 μmol CO_2 m^{-2} s^{-1}, and the intrinsic WUE was found to be 0.05 μmol CO_2/mmol H_2O.

From the 7 *Dicroidium* leaves examined from the Gordon Valley locality, the average

vein density was 4.8 mm mm^{-2}. From the vein densities measured, K_{leaf} was found to be 8.76 mmol m^{-2} s^{-1} MPa^{-1}, stomatal conductance was found to be 177.5 mmol H_20 m^{-2} s^{-1}, max photosynthetic capacity was found to be 9.55 μmol CO_2 m^{-2} s^{-1}, and the intrinsic WUE was found to be 0.05 μmol CO_2/mmol H_2O.

From the 17 *Dicroidium* leaves examined from the Marshall Mountains locality, the average vein density was 5.1 mm mm^{-2}. From the vein densities measured, K_{leaf} was found to be 9.08 mmol m^{-2} s^{-1} MPa^{-1}, stomatal conductance was found to be 183.9 mmol H_20 m^{-2} s^{-1}, max photosynthetic capacity was found to be 9.85 μmol CO_2 m^{-2} s^{-1}, and the intrinsic WUE was found to be 0.05 μmol CO_2/mmol H_2O.

From the 1 *Dicroidium* leaf examined from the Molteno locality, the vein density was 4.23 mm mm^{-2}. From the vein density measured, K_{leaf} was found to be 8.13 mmol m^{-2} s^{-1} MPa^{-1}, stomatal conductance was found to be 164.7 mmol H_20 m^{-2} s^{-1}, max photosynthetic capacity was found to be 8.98 μmol CO_2 m^{-2} s^{-1}, and the intrinsic WUE was found to be 0.05 μmol CO_2/mmol H_2O.

From the 23 *Dicroidium* leaves examined from the Mt. Falla locality, the average vein density was 4.64 mm mm^{-2}. From the vein densities measured, K_{leaf} was found to be 8.55 mmol m^{-2} s^{-1} MPa^{-1}, stomatal conductance was found to be 173.2 mmol H_20 m^{-2} s^{-1}, max photosynthetic capacity was found to be 9.35 μmol CO_2 m^{-2} s^{-1}, and the intrinsic WUE was found to be 0.05 μmol CO_2/mmol H_2O.

From the 1 *Dicroidium* leaf examined from the Queen Alexandra Range locality, the vein density was 3.81 mm mm^{-2}. From the vein density measured, K_{leaf} was found to be 7.54 mmol m^{-2} s^{-1} MPa^{-1}, stomatal conductance was found to be 152.7 mmol H_20 m^{-2} s^{-1}, max photosynthetic capacity was found to be 8.4 μmol CO_2 m^{-2} s^{-1}, and the intrinsic WUE was found to be 0.06 μmol

CO_2/mmol H_2O.

From the 12 *Dicroidium* leaves examined from the Shapeless Mountain locality, the average vein density was 4.55 mm mm^{-2}. From the vein densities measured, K_{leaf} was found to be 8.48 mmol m^{-2} s^{-1} MPa^{-1}, stomatal conductance was found to be 171.8 mmol H_20 m^{-2} s^{-1}, max photosynthetic capacity was found to be 9.3 μmol CO_2 m^{-2} s^{-1}, and the intrinsic WUE was found to be 0.05 μmol CO_2/mmol H_2O.

4.4.5 Physiological findings for Dicroidium *by formation*

There was 1 *Dicroidium* leaf examined from the Molteno Formation. The vein density of the leaf is 4.23 mm mm^{-2}, the average K_{leaf} is 8.13 mmol m^{-2} s^{-1} MPa^{-1}, the stomatal conductance for the leaf is 164.7 mmol H_20 m^{-2} s^{-1}, the maximum photosynthetic capacity is 8.98 μmol CO_2 m^{-2} s^{-1}, and the intrinsic WUE is 0.05 μmol CO_2/mmol H_2O.

There were 15 *Dicroidium* leaves examined from the Blackstone Formation. The average vein density of the leaves is 5.88 mm mm^{-2}, the average K_{leaf} is 9.84 mmol m^{-2} s^{-1} MPa^{-1}, the stomatal conductance for these leaves averages 199.4 mmol H_20 m^{-2} s^{-1}, the maximum photosynthetic capacity is 10.54 μmol CO_2 m^{-2} s^{-1}, and the average intrinsic WUE is 0.05 μmol CO_2/mmol H_2O.

There were 59 *Dicroidium* leaves examined from localities that could be part of either the Fremouw or Falla formation. The average vein density of the leaves is 4.72 mm mm^{-2}, the average K_{leaf} is 8.65 mmol m^{-2} s^{-1} MPa^{-1}, the stomatal conductance for these leaves averages 175.3 mmol H_20 m^{-2} s^{-1}, the maximum photosynthetic capacity is 9.45 μmol CO_2 m^{-2} s^{-1}, and the average intrinsic WUE is 0.05 μmol CO_2/mmol H_2O.

There were 40 *Dicroidium* leaves examined from the Falla Formation. The average vein density of the leaves is 4.84 mm mm^{-2}, the average K_{leaf} is 8.77 mmol m^{-2} s^{-1} MPa^{-1}, the stomatal

conductance for these leaves averages 177.7 mmol H_20 m^{-2} s^{-1}, the maximum photosynthetic capacity is 9.56 μmol CO_2 m^{-2} s^{-1}, and the average intrinsic WUE is 0.05 μmol CO_2/mmol H_2O.

There were 71 *Dicroidium* leaves examined from the Lashly Formation. The average vein density of the leaves is 4.76 mm mm^{-2}, the average K_{leaf} is 8.69 mmol m^{-2} s^{-1} MPa^{-1}, the stomatal conductance for these leaves averages 176.0 mmol H_20 m^{-2} s^{-1}, the maximum photosynthetic capacity is 9.48 μmol CO_2 m^{-2} s^{-1}, and the average intrinsic WUE is 0.05 μmol CO_2/mmol H_2O.

There were 10 *Dicroidium* leaves examined from the Fremouw Formation. The average vein density of the leaves is 4.79 mm mm^{-2}, the average K_{leaf} is 8.76 mmol m^{-2} s^{-1} MPa^{-1}, the stomatal conductance for these leaves averages 177.4 mmol H_20 m^{-2} s^{-1}, the maximum photosynthetic capacity is 9.56 μmol CO_2 m^{-2} s^{-1}, and the average intrinsic WUE is 0.05 μmol CO_2/mmol H_2O.

4.5 Physiological findings for Heidiphyllum

From the 54 *Heidiphyllum* leaves examined (Table 9), the average vein density was 2.73 mm mm^{-2}. From the vein densities measured, K_{leaf} was found to be 5.60 mmol m^{-2} s^{-1} MPa^{-1}, stomatal conductance was found to be 113.4 mmol H_20 m^{-2} s^{-1}, max photosynthetic capacity was found to be 6.39 μmol CO_2 $m^{-2}s^{-1}$, and the intrinsic WUE was found to be 0.05 μmol CO_2/mmol H_2O.

4.5.1 Physiological findings for Heidiphyllum *by locality*

From the 18 *Heidiphyllum* leaves examined from the Alfie's Elbow locality, the average vein density was 2.57 mm mm^{-2}. From the vein densities measured, K_{leaf} was found to be 5.28 mmol m^{-2} s^{-1} MPa^{-1}, stomatal conductance was found to be 106.9 mmol H_20 m^{-2} s^{-1}, max photosynthetic capacity was found to be 6.05 μmol CO_2 m^{-2} s^{-1}, and the intrinsic WUE was found to be 0.06 μmol CO_2/mmol H_2O.

From the 13 *Heidiphyllum* leaves examined from the Allan Hills locality, the average vein

density was 2.96 mm mm^{-2}. From the vein densities measured, K_{leaf} was found to be 6.01 mmol m^{-2} s^{-1} MPa^{-1}, stomatal conductance was found to be 121.7 mmol H_20 m^{-2} s^{-1}, max photosynthetic capacity was found to be 6.82 μmol CO_2 m^{-2} s^{-1}, and the intrinsic WUE was found to be 0.06 μmol CO_2/mmol H_2O.

From the 7 *Heidiphyllum* leaves examined from the Molteno locality, the average vein density was 2.6 mm mm^{-2}. From the vein densities measured, K_{leaf} was found to be 5.36 mmol m^{-2} s^{-1} MPa^{-1}, stomatal conductance was found to be 108.5 mmol H_20 m^{-2} s^{-1}, max photosynthetic capacity was found to be 6.14 μmol CO_2 m^{-2} s^{-1}, and the intrinsic WUE was found to be 0.06 μmol CO_2/mmol H_2O.

From the 16 *Heidiphyllum* leaves examined from the Mt. Falla locality, the average vein density was 2.79 mm mm^{-2}. From the vein densities measured, K_{leaf} was found to be 5.74 mmol m^{-2} s^{-1} MPa^{-1}, stomatal conductance was found to be 116.2 mmol H_20 m^{-2} s^{-1}, max photosynthetic capacity was found to be 6.55 μmol CO_2 m^{-2} s^{-1}, and the intrinsic WUE was found to be 0.06 μmol CO_2/mmol H_2O.

4.5.2 Physiological findings for Heidiphyllum *by formation*

There were 7 *Heidiphyllum* leaves examined from the Molteno Formation. The average vein density of the leaves is 2.6 mm mm^{-2}, the average K_{leaf} is 5.36 mmol m^{-2} s^{-1} MPa^{-1}, the stomatal conductance for these leaves averages 108.5 mmol H_20 m^{-2} s^{-1}, the maximum photosynthetic capacity is 6.14 μmol CO_2 m^{-2} s^{-1}, and the average intrinsic WUE is 0.06 μmol CO_2/mmol H_2O.

There were 18 *Heidiphyllum* leaves examined from strata that could be a part of the Fremouw Formation or the Falla Formation. The average vein density of the leaves is 2.57 mm mm^{-2}, the average K_{leaf} is 5.28 mmol m^{-2} s^{-1} MPa^{-1}, the stomatal conductance for these leaves

averages 106.9 mmol H_20 m^{-2} s^{-1}, the maximum photosynthetic capacity is 6.05 μmol CO_2 m^{-2} s^{-1}, and the average intrinsic WUE is 0.06 μmol CO_2/mmol H_2O.

There were 16 *Heidiphyllum* leaves examined from the Falla Formation. The average vein density of the leaves is 2.79 mm mm^{-2}, the average K_{leaf} is 5.74 mmol m^{-2} s^{-1} MPa^{-1}, the stomatal conductance for these leaves averages 116.2 mmol H_20 m^{-2} s^{-1}, the maximum photosynthetic capacity is 6.55 μmol CO_2 m^{-2} s^{-1}, and the average intrinsic WUE is 0.06 μmol CO_2/mmol H_2O.

There were 13 *Heidiphyllum* leaves examined from the Lashly Formation. The average vein density of the leaves is 2.96 mm mm^{-2}, the average K_{leaf} is 6.01 mmol m^{-2} s^{-1} MPa^{-1}, the stomatal conductance for these leaves averages 121.7 mmol H_20 m^{-2} s^{-1}, the maximum photosynthetic capacity is 6.82 μmol CO_2 m^{-2} s^{-1}, and the average intrinsic WUE is 0.06 μmol CO_2/mmol H_2O.

4.6 Physiological findings for Osmunda

From the 10 *Osmunda* leaves examined (Table 10), the average vein density was 4.52 mm mm^{-2}. From the vein densities measured, K_{leaf} was found to be 8.48 mmol m^{-2} s^{-1} MPa^{-1}, stomatal conductance was found to be 171.9 mmol H_20 m^{-2} s^{-1}, max photosynthetic capacity was found to be 9.31 μmol CO_2 $m^{-2}s^{-1}$, and the intrinsic WUE was found to be 0.05 μmol CO_2/mmol H_2O. All specimens came from the Allan Hills locality of the Lashly Formation.

4.7 Physiological findings for Sphenobaiera

From the 4 *Sphenobaiera* leaves examined (Table 11), the average vein density was 4.39 mm mm^{-2}. From the vein densities measured, K_{leaf} was found to be 8.18 mmol m^{-2} s^{-1} MPa^{-1}, stomatal conductance was found to be 165.8 mmol H_20 m^{-2} s^{-1}, max photosynthetic capacity was found to be 9.00 μmol CO_2 $m^{-2}s^{-1}$, and the intrinsic WUE was found to be 0.05 μmol CO_2/mmol H_2O.

4.7.1 Physiological findings for Sphenobaiera *by locality*

From the 1 *Sphenobaiera* leaf examined from the Dinmore locality, the vein density was 6.01 mm mm^{-2}. From the vein density measured, K_{leaf} was found to be 9.98 mmol m^{-2} s^{-1} MPa^{-1}, stomatal conductance was found to be 202.2 mmol H_20 m^{-2} s^{-1}, max photosynthetic capacity was found to be 10.66 μmol CO_2 m^{-2} s^{-1}, and the intrinsic WUE was found to be 0.05 μmol CO_2/mmol H_2O.

From the 2 *Sphenobaiera* leaves examined from the Marshall Mountains locality, the average vein density was 3.76 mm mm^{-2}. From the vein densities measured, K_{leaf} was found to be 7.44 mmol m^{-2} s^{-1} MPa^{-1}, stomatal conductance was found to be 150.7 mmol H_20 m^{-2} s^{-1}, max photosynthetic capacity was found to be 8.31 μmol CO_2 m^{-2} s^{-1}, and the intrinsic WUE was found to be 0.06 μmol CO_2/mmol H_2O.

From the 1 *Sphenobaiera* leaf examined from the Mt. Falla locality, the vein density was 4.04 mm mm^{-2}. From the vein density measured, K_{leaf} was found to be 7.87 mmol m^{-2} s^{-1} MPa^{-1}, stomatal conductance was found to be 159.5 mmol H_20 m^{-2} s^{-1}, max photosynthetic capacity was found to be 8.73 μmol CO_2 m^{-2} s^{-1}, and the intrinsic WUE was found to be 0.05 μmol CO_2/mmol H_2O.

4.7.2 Physiological findings for Sphenobaiera *by formation*

There was 1 *Sphenobaiera* leaf examined from the Blackstone Formation. The vein density of the leavf is 6.01 mm mm^{-2}, the K_{leaf} is 9.98 mmol m^{-2} s^{-1} MPa^{-1}, the stomatal conductance for this leaf was 202.2 mmol H_20 m^{-2} s^{-1}, the maximum photosynthetic capacity is 10.66 μmol CO_2 m^{-2} s^{-1}, and the average intrinsic WUE is 0.05 μmol CO_2/mmol H_2O.

There were 3 *Sphenobaiera* leaves examined from the Falla Formation. The average vein density of the leaves is 3.85 mm mm^{-2}, the average K_{leaf} is 7.58 mmol m^{-2} s^{-1} MPa^{-1}, the stomatal

conductance for these leaves averages 153.6 mmol H_20 m^{-2} s^{-1}, the maximum photosynthetic capacity is 8.45 μmol CO_2 m^{-2} s^{-1}, and the average intrinsic WUE is 0.05 μmol CO_2/mmol H_2O.

4.8 Physiological findings for Taeniopteris

From the 21 *Taeniopteris* leaves examined (Table 12), the average vein density was 5.28 mm mm^{-2}. From the vein densities measured, K_{leaf} was found to be 9.01 mmol m^{-2} s^{-1} MPa^{-1}, stomatal conductance was found to be 182.6 mmol H_20 m^{-2} s^{-1}, max photosynthetic capacity was found to be 9.75 μmol CO_2 $m^{-2}s^{-1}$, and the intrinsic WUE was found to be 0.05 μmol CO_2/mmol H_2O.

4.8.1 Physiological findings for Taeniopteris *by location*

From the 3 *Taeniopteris* leaves examined from the Alfie's Elbow locality, the average vein density was 4.45 mm mm^{-2}. From the vein densities measured, K_{leaf} was found to be 8.21 mmol m^{-2} s^{-1} MPa^{-1}, stomatal conductance was found to be 166.3 mmol H_20 m^{-2} s^{-1}, max photosynthetic capacity was found to be 9.02 μmol CO_2 m^{-2} s^{-1}, and the intrinsic WUE was found to be 0.05 μmol CO_2/mmol H_2O.

From the 4 *Taeniopteris* leaves examined from the Allan Hills locality, the average vein density was 7.26 mm mm^{-2}. From the vein densities measured, K_{leaf} was found to be 10.74 mmol m^{-2} s^{-1} MPa^{-1}, stomatal conductance was found to be 217.5 mmol H_20 m^{-2} s^{-1}, max photosynthetic capacity was found to be 11.3 μmol CO_2 m^{-2} s^{-1}, and the intrinsic WUE was found to be 0.05 μmol CO_2/mmol H_2O.

From the 4 *Taeniopteris* leaves examined from the Dinmore locality, the average vein density was 5.39 mm mm^{-2}. From the vein densities measured, K_{leaf} was found to be 9.26 mmol m^{-2} s^{-1} MPa^{-1}, stomatal conductance was found to be 187.6 mmol H_20 m^{-2} s^{-1}, max photosynthetic capacity was found to be 10.0 μmol CO_2 m^{-2} s^{-1}, and the intrinsic WUE was found to be 0.05

μmol CO_2/mmol H_2O.

From the 3 *Taeniopteris* leaves examined from the Marshall Mountains locality, the average vein density was 5.8 mm mm^{-2}. From the vein densities measured, K_{leaf} was found to be 9.71 mmol m^{-2} s^{-1} MPa^{-1}, stomatal conductance was found to be 196.8 mmol H_20 m^{-2} s^{-1}, max photosynthetic capacity was found to be 10.41 μmol CO_2 m^{-2} s^{-1}, and the intrinsic WUE was found to be 0.05 μmol CO_2/mmol H_2O.

From the 1 *Taeniopteris* leaf examined from the Mt. Bumstead locality, the vein density was 6.54 mm mm^{-2}. From the vein density measured, K_{leaf} was found to be 10.37 mmol m^{-2} s^{-1} MPa^{-1}, stomatal conductance was found to be 210.0 mmol H_20 m^{-2} s^{-1}, max photosynthetic capacity was found to be 10.99 μmol CO_2 m^{-2} s^{-1}, and the intrinsic WUE was found to be 0.05 μmol CO_2/mmol H_2O.

From the 5 *Taeniopteris* leaves examined from the Mt. Falla locality, the average vein density was 3.73 mm mm^{-2}. From the vein densities measured, K_{leaf} was found to be 7.37 mmol m^{-2} s^{-1} MPa^{-1}, stomatal conductance was found to be 149.3 mmol H_20 m^{-2} s^{-1}, max photosynthetic capacity was found to be 8.23 μmol CO_2 m^{-2} s^{-1}, and the intrinsic WUE was found to be 0.06 μmol CO_2/mmol H_2O.

From the 1 *Taeniopteris* leavf examined from the Umkomaas Valley locality, the vein density was 4.35 mm mm^{-2}. From the vein density measured, K_{leaf} was found to be 8.29 mmol m^{-2} s^{-1} MPa^{-1}, stomatal conductance was found to be 167.9 mmol H_20 m^{-2} s^{-1}, max photosynthetic capacity was found to be 9.13 μmol CO_2 m^{-2} s^{-1}, and the intrinsic WUE was found to be 0.05 μmol CO_2/mmol H_2O.

4.8.2 Physiological findings for Taeniopteris *by formation*

There was 1 *Taeniopteris* leaf examined from the Molteno Formation. The vein density of

the leaf is 4.35 mm mm^{-2}, the K_{leaf} is 8.29 mmol m^{-2} s^{-1} MPa^{-1}, the stomatal conductance for this leaf is 167.9 mmol H_20 m^{-2} s^{-1}, the maximum photosynthetic capacity is 9.13 μmol CO_2 m^{-2} s^{-1}, and the intrinsic WUE is 0.05 μmol CO_2/mmol H_2O.

There were 4 *Taeniopteris* leaves examined from the Blackstone Formation. The average vein density of the leaves is 5.39 mm mm^{-2}, the average K_{leaf} is 9.26 mmol m^{-2} s^{-1} MPa^{-1}, the stomatal conductance for these leaves averages 187.6 mmol H_20 m^{-2} s^{-1}, the maximum photosynthetic capacity is 10.0 μmol CO_2 m^{-2} s^{-1}, and the average intrinsic WUE is 0.05 μmol CO_2/mmol H_2O.

There were 3 *Taeniopteris* leaves examined from localities that could belong to either the Fremouw or Falla Formations. The average vein density of the leaves is 4.45 mm mm^{-2}, the average K_{leaf} is 8.21 mmol m^{-2} s^{-1} MPa^{-1}, the stomatal conductance for these leaves averages 166.3 mmol H_20 m^{-2} s^{-1}, the maximum photosynthetic capacity is 9.02 μmol CO_2 m^{-2} s^{-1}, and the average intrinsic WUE is 0.05 μmol CO_2/mmol H_2O.

There were 8 *Taeniopteris* leaves examined from the Falla Formation. The average vein density of the leaves is 4.51 mm mm^{-2}, the average K_{leaf} is 8.25 mmol m^{-2} s^{-1} MPa^{-1}, the stomatal conductance for these leaves averages 167.1 mmol H_20 m^{-2} s^{-1}, the maximum photosynthetic capacity is 9.05 μmol CO_2 m^{-2} s^{-1}, and the average intrinsic WUE is 0.05 μmol CO_2/mmol H_2O.

There were 5 *Taeniopteris* leaves examined from the Lashly Formation. The average vein density of the leaves is 7.12 mm mm^{-2}, the average K_{leaf} is 10.66 mmol m^{-2} s^{-1} MPa^{-1}, the stomatal conductance for these leaves averages 216.0 mmol H_20 m^{-2} s^{-1}, the maximum photosynthetic capacity is 11.24 μmol CO_2 m^{-2} s^{-1}, and the average intrinsic WUE is 0.05 μmol CO_2/mmol H_2O.

5. Discussion

5.1 Hydraulic characteristics of Permian fossil leaves

Fossil leaves of the genus *Glossopteris* have been shown in this study to have a significantly higher leaf venation density than the *Gangamopteris* and *Noeggerathiopsis* leaves with which they co-occured (Figure 16). Based on the deterministic methods used in this study, the leaf hydraulic conductance, stomatal conductance, maximum photosynthetic capacity, and intrinsic WUE would all have been higher for *Glossopteris* leaves as well. There were significantly fewer leaves of *Gangamopteris* and *Noeggerathiopsis* to measure in comparison to *Glossopteris* and this might result in making the values for *Gangamopteris* and *Noeggerathiopsis* lower than they would have really been in the Permian. Given that *Glossopteris* leaves commonly outnumber other leaves in the matrix at so many different localities, this difference may be due to *Glossopteris* having a much larger biomass at those localities than other genera. The higher leaf hydraulic characteristics of *Glossopteris* provide some empirical evidence to the commonly held idea that *Glossopteris* plants were able to dominate the landscape, at least partially due to the physiological characteristics of their leaves.

An alternative hypothesis would be that *Glossopteris* plants only dominated areas where preservation was more common, as opposed to dominating most of Gondwana. This might explain why fewer leaves of other species are found preserved with glossopterids. It could be that the distinctive *Vertebraria* roots of the glossopterids allowed them to dominate areas where fossilization was common (i.e., environments close to water). If this were indeed true, however, one might expect to find more specimens of *Gangamopteris* since these leaves are also members of the glossopterids.

In either scenario, it seems unlikely that the hydraulic characteristics of *Glossopteris* leaves alone can account for the prominence of the glossopterids in the Permian of Gondwana. The higher leaf venation densities allow the *Glossopteris* leaves to reach more desirable levels of

the hydraulic characteristics studied. As *Glossopteris* leaves persist through the Permian, however, there is a significant decrease in leaf venation density and therefore the other hydraulic characteristics. If lower venation densities played a large role in the dominance of this leaf type, one might have expected *Gangamopteris* and *Noeggerathiopsis*, both of which have lower vein densities, to show a marked increase in population through the Permian. *Gangamopteris* is typically only known from the early Permian, however, and may not have survived long enough under high levels of CO_2. Another possibility is that *Glossopteris* leaves could have had a higher degree of plasticity than other genera and were more able to adapt to the changing environment. Unfortunately, most of these hypotheses are untestable with our current knowledge of both these groups and the environments in which they lived. It is clear that the *Glossopteris* leaf type had a statistically significant advantage over many other leaf types of the time, regardless of the extent to which the higher venation density gave them an advantage.

5.2 Statistical issues and interpretations

In the statistical analysis of leaf venation density in different [CO_2] and living at different paleolatitudes, the 2x2 factorial ANOVA showed statistically significant main effects of [CO_2] and paleolatitude on leaf venation density in *Glossopteris*. Additionally, the ANOVA found a statistically significant interaction effect between [CO_2] and paleolatitudes. This means that the combination of [CO_2] and paleolatitude are the factors that affect leaf venation density. When a statistically significant interaction effect is found, interpretation of the main effects should be avoided because the interaction effect could lead to erroneous conclusions (Sokal and Rohlf, 1995; Logan, 2010). If the results are interpreted in this manner, it means that we cannot conclude that *Glossopteris* leaf venation changed in response to [CO_2]. Rather, one could only conclude that both [CO_2] and paleolatitude affected vein density in cases where the post-hoc

Tukey test showed a significant interaction. However, when the paleolatitude data is examined more closely, it appears that the apparent changes in venation density may only be due to bias of the fossil collections and geologic processes.

If the paleolatitude does have a significant effect on how the leaves of *Glossopteris* develop, it should be safe to assume that the effect would be of a continuous nature and not fall into discrete sections. Moving from the equator to the poles, the amount of light that reaches the latitudes and the angle at which the light intercepts the earth changes in a predictable and continuous manner; there is no alternation of light levels from latitude to latitude. The different methods of grouping localities into latitude bins demonstrates that the changes in vein density are not continuous as one would expect.

In the simplest grouping in bins of non-Antarctic specimens and Antarctic (Figure 18), higher leaf venation density is found in the Antarctic specimens. This is the opposite of what I hypothesized based on the diffuse nature of light at the higher latitudes. Obviously, the rejection of a hypothesis is not a valid reason to reject a statistical analysis. When interpreted along with the data from the other groupings, however, it becomes apparent that something is confounding the analysis.

When the data are grouped into three latitude bins (i.e., 80° S and higher, 70° S–79° S, non-Antarctic; Figure 19), there is no continuous relationship in leaf venation density changes. Again, the non-Antarctic localities have the lowest leaf venation density. However, it is the middle grouping of latitudes that has the highest leaf venation density and the grouping of 80° S and higher latitudes that has leaf venation densities between the others.

When the data were grouped into twelve latitude bins (i.e., non-Antarctic, 72° S, 74° S, 76° S, 77° S, 78° S, 82° S, 83° S, 84° S, 85° S, 86° S, 87° S; Figure 20), the lack of a continuous

pattern is even more apparent. In order of highest venation density to lowest venation density, the groupings are 85° S, 72° S, 76° S, 82° S, 83° S, 77° S, 78° S, 87° S, 84° S, 86° S, 74° S, and non-Antarctic. The lack of the expected continuous pattern suggests that paleolatitude is not having a significant effect on leaf venation density, but that the interaction effect is only appearing significant due to confounding factors.

One potential confounding factor that is readily apparent is that we lack accurate paleolatitude data for the majority of the localities studied. Tectonic activities could have moved these localities in a manner that put the localities out of a continuous order. Without accurate paleolatitude data, it is nearly impossible to get accurate results in any study that attempts to use paleolatitude as an independent variable. This may prove to be less of a problem in geologically younger strata or in areas where the tectonic activity has been minimal since the deposition of the rocks.

Another potential confounding factor in this analysis is that the distribution of localities through the paleolatitudes is not completely independent of geologic time. Vein densities at the various latitudes appear to depend more on the strata found at that locality. There are few areas in Antarctica where both lower and upper Permian strata are preserved, and this makes it more difficult to compare vein densities across latitudes. Although fossils from numerous geologic formations were used in this study, most of the lower and upper Permian formations do not occur in the same area. With this in mind, it may be that larger sections of strata are needed to adequately study the effects of paleolatitude on leaf venation density.

5.3 Effects of CO_2 concentration on leaf venation density in Glossopteris

Although significant main effects generally should not be analyzed in the presence of significant interaction effects, I feel that the above section demonstrates that the interaction

effects are largely the result of geologic processes. Therefore, the effects of [CO_2] on leaf venation density will be discussed here.

The statistical analysis did not show a significant difference between vein densities of leaves living during the early and middle Permian (Figure 17). There are two likely reasons for this. Firstly, there are very few middle Permian specimens available for study. These specimens were limited to non-Antarctic localities. Secondly, there is not a very large difference in modeled [CO_2] between these two time periods (Berner, 2006); the difference may not have been large enough to force changes in venation density. A significant difference was found, however, between venation density in early/middle Permian and late Permian specimens (Figure 17). The lower leaf venation density in leaves of the late Permian fits with the hypothesis that the density would decrease without a strong selective pressure to keep it lower.

The changes in leaf venation density as a response to changes in [CO_2] may be explained in the context of costs and benefits. The maximum photosynthetic rate of a plant is often limited by its hydraulic capacity (Brodribb et al., 2007); which is strongly affected by venation architecture and, therefore, venation density. From this it is clear that leaf venation density plays a large role in the maximum photosynthetic rate of a plant (Noblin et al., 2008; McKown et al., 2010). There is a limit to the positive effects that leaf venation density can have on a plant. This limit is caused both by the finite amount of space within a leaf and by the metabolic costs of producing dense venation patterns. This cost is amplified in deciduous species that annually reinvest in xylem tissues. The production of xylem costs the plant 6.5 mmol glucose g^{-1} of cellulose and 11.8 mmol glucose g^{-1} of lignin (Lambers and Poorter, 1992). If the energy investment does not yield an increase in photosynthesis, it is possible that glossopterid leaves with lower leaf venation patterns would be favored. In theory, these plants would be able to

invest the energy saved from reduced construction costs into new productive biomass or for reproduction. The costs of increased venation would be more pronounced in the glossopterids than in the angiosperms, as the venation network of angiosperm leaves is built with progressively smaller veins which are less costly metabolically. *Glossopteris* leaves, in contrast, only have veins of similar diameter, equivalent to the larger vein orders in angiosperms. Although leaf venation pattern also plays a role in the structural support of leaves, the thickness of midveins plays the most important role in leaf structural support (Niinemets et al., 2007).

5.4 Glossopteris *leaves and the effects of paleolatitudes*

The data from this study appear to indicate that it is difficult to examine the effects of latitude in a fossil group. In order to adequately study the effects of high paleolatitudes of fossil plants, more time-synchronous localities need to be discovered and paleolatitudes need to be accurately determined. The latter aspect will likely be especially difficult due to volcanic activity during the Jurassic that altered much of the younger strata on the Antarctic continent.

The difficulty in studying the effects of paleolatitude may also lie in the study of leaf venation itself. There are many factors that affect leaf venation density and the role of paleolatitude may be lost in developmental responses to other phenomena. It is known that increases in leaf insertion height can increase venation density for grasses, herbs, and some temperate and tropical trees (Roth-Nebelsick et al., 2001 and citations therein). Some plants, however, (e.g., *Populus, Hedera helix*, *Mahonia grandiflora,* and *Prunus tenella*) show a decrease in venation with increasing height above ground (Critchfield, 1960; Uhl and Mosbrugger, 1999). Leaves of some species can show an increase or decrease in leaf venation relative to the size of the leaf (Gupta, 1961). Other effectors of leaf venation density include sun vs. shade leaves, temperature, soil moisture, humidity, and nutrient deficiency (Uhl and

Mosbrugger, 1999).

5.5 Hydraulic characteristics of Triassic fossil leaves

Dicroidium leaves are the most common leaf morphotype of Middle and Late Triassic ecosystems of Antarctica and other areas of Gondwana. Contrary to the Permian, however, they are just a large component of a much more diverse assemblege of plants (Escapa et al., 2011). With the exception of *Heidiphyllum*, the leaf venation density of *Dicroidium* is not statistically different from any other contemporaneous leaf types (e.g., *Cladophlebis*, *Dejerseya*, *Heidiphyllum*, *Osmunda*, and *Taeniopteris*; Figure 21). Although it is the most common leaf type, *Dicroidium* does not appear to have any hydraulic advantage over co-occurring leaves (with the exception of *Heidiphyllum*). This suggests that the *Dicroidium* morphotype is not the reason for the dominance of the corystosperms during the Middle and Late Triassic of Antarctica. The low venation density of *Heidiphyllum* leaves relative to all other taxa suggests that these leaves would be at a significant disadvantage with respect to leaf hydraulics. The potential competative disadvantage of the low leaf hydraulic conductance values of *Heidiphyllum* could have been offset by other characteristics of the plant. *Heidiphyllum* leaves are attached to the voltzialean conifer *Telemachus*, which is the earliest plant known to posses mycorrhizal root nodules (Schwendemann et al., 2011).

5.6 Comparison of hydraulic characteristics across time

Although leaf venation density is easily compared across the time intervals studied here, it is much more difficult to measure stomatal conductance, maximum photosynthetic capacity, and intrinsic WUE. Calculations of stomatal conductance rely on the calculated K_{leaf}, as well as an assumed vapor pressure deficit and water potential of the leaf. These latter two parameters are likely to vary by locality and could give very different values due to the different growing

conditions among the plants. With current knowledge and techniques, there is no method to accurately determine what the water potential and vapor deficit were for a given locality. The maximum photosynthetic capacity was calculated from a regression equation developed using extant plants grown under current levels of CO_2 (Brodribb et al., 2007). This method may overestimate photosynthetic capacity for early Permian plants and underestimate the capacity of late Permian and Triassic plants. Ideally, a method that allows one to calculate the photosynthetic capacity at different levels of CO_2 would be used. Photosynthesis equations (e.g., Farquhar et al., 1980) would make this possible, but the introduction of more unknown variables makes it impractical at this time. This makes it difficult to interpret WUE since it is calculated using the maximum photosynthetic capacity and stomatal conductance. Interestingly, the intrinsic WUE is calculated to be approximately 0.05 μmol CO_2/mmol H_2O for nearly all leaves examined.

Chapter 4

Investigations into the photosynthetic pathway of Permian *Glossopteris* leaves

1. Introduction

1.1 C_4 photosynthesis in modern plants

The C_4 photosynthetic pathway can be described as a series of anatomical and biochemical modifications that result in a higher concentration of CO_2 in the presence of the carboxylating enzyme Ribulose-1,5-bisphosphate carboxylase oxygenase (Rubisco). This increases photosynthetic efficiency in conditions that promote high rates of photorespiration, such as low CO_2 and low water availability. There are numerous C_4 subtypes with variations in the reactions that occur. In all subtypes, however, the initial step is the fixation of inorganic carbon by Phosphoenolpyruvate carboxylase (PEP carboxylase), followed by the movement of the resulting four-carbon acids to an interior compartment where Rubisco is located. In this tissue, CO_2 is released by the decarboxylation of the four-carbon acid. As a result, the [CO_2] rises to a level that nearly saturates the Rubisco active site. The decarboxylation reaction also produces a three-carbon acid that diffuses back to the tissue where PEP carboxylase is located. The three-carbon acid can then undergo a series of steps that regenerate PEP. In addition to the above biochemical modifications, the C_4 pathway requires anatomical modifications of the C_3 leaf to concentrate Rubisco and CO_2 in the same region. Although some C_4 plants lack significant anatomical modifications (Voznesenskaya et al., 2001), the majority have a wreath-like layer of cells, the bundle sheath cells (BSC), surrounding the vascular tissue. This anatomical modification (Figure 22A), termed Kranz anatomy, is the tissue where Rubisco is concentrated.

In a leaf with the typical Kranz anatomy, the outer ring of cells is derived from the leaf mesophyll and the inner layer is derived from any cell layers that are near or within the vascular bundle . PEP carboxylase is located in the outer layer of cells. This is the site of the initial carboxylation step and has been termed the photosynthetic carbon assimilation (PCA) tissue. The inner ring of tissue, sometimes called the bundle sheath, is the site of Rubisco and many of the enzymes associated with the Calvin cycle. This layer has therefore been termed the photosynthetic carbon reduction (PCR) tissue (Sage, 2004; Taiz and Zeiger, 2006).

In all photosynthetic organisms that exist today, Rubisco is the enzyme that catalyzes the fixation of CO_2 into molecules that store energy. Rubisco and the C_3 photosynthetic pathway are thought to have evolved early and remained immensely successful and relatively unchanged to the present (Hayes, 1994). At the time it is thought to have originated, CO_2 levels in the atmosphere are interpreted as being quite high (Berner, 2006). It is at high CO_2 levels that Rubisco is the most efficient (Sage, 2004). Although less common than carboxylation, it is possible for Rubisco to facilitate the oxygenation of Ribulose-1,5-bisphosphate (RuBP). This process, termed photorespiration, results in the production of one molecule of PGA and one molecule of phosphogylcolate (PG), which can be toxic if it accumulates within the cell (Ogren, 1984; Andrews and Lorimer, 1987). The PG is metabolically useless and must therefore be converted into a non-toxic compound through a process that requires more energy (Ogren, 1984; Douce and Heldt, 2004). Although metabolically costly because the plant uses light reaction products without producing glucose, photorespiration can be beneficial. Under stressful conditions where CO_2 may not be readily available (e.g., closed stomata due to dry conditions), the light reactions will continue and Adenosine-5'-triphosphate (ATP) and Nicotinamide adenine dinucleotide phosphate (NADPH) will continue to be formed without being able to be used in the

carbon reduction reactions. Photorespiration allows the Calvin cycle to continue in the absence of CO_2. The products of the light reactions can then be used and Adenosine diphosphate (ADP) and $NADP^+$ are regenerated for use in the light reactions; this helps to protect the photosynthetic apparatus, but at a high metabolic cost.

The C_4 photosynthetic pathway can operate under stress without undergoing photorespiration. In general, the C_4 pathway requires more energy from the light reactions to produce a molecule of glucose; this is due to the energy required to concentrate the CO_2 in the presence of Rubisco. Under more stressful condition (e.g., low CO_2, high temperature), however, the C_4 pathway has a higher quantum yield (Figure 23) than a C_3 plant in the same conditions (Ehleringer and Björkman, 1977; Taiz and Zeiger, 2006). Under current environmental conditions, the quantum yield of well-watered C_3 and C_4 plants is nearly identical for a temperature range of 22–30° C (Ehleringer et al., 1997). At temperatures above this level, the quantum yield for C_3 plants decreases (Figure 23) while the yield of plants with the C_4 pathway remains the same (Ehleringer et al., 1997). As temperature rises, Rubisco's affinity for binding to O_2 increases; additionally, CO_2 becomes less soluble than O_2 as temperature increases (Jordan and Ogren, 1984). However, when temperatures fall below the above range, the quantum yield of C_3 plants rises while that of C_4 plants remains the same (Figure 23). Likewise, low [CO_2] would also result in a lower quantum yield for C_3 plants relative to C_4 plants, while a high [CO_2] would increase the quantum yield of C_3 plants relative to C_4 plants (Ehleringer et al., 1991).

1.2 Origin of the C_4 pathway

Among extant plants, the C_4 photosynthetic pathway is believed to have evolved multiple times across numerous families (Sage, 2004). To date, there are over 45 instances of the independent evolution of the C_4 pathway in 19 different angiosperm families. Within the dicots

alone, there are 30 separate lineages in which the C_4 pathway has evolved. In terms of species richness, C_4 plants are mostly found within the grasses, then the sedges, with dicots having the fewest species with C_4 photosynthesis (Sage, 1999, 2004; Sage et al., 2012). Grasses and sedges that exhibit the C_4 pathway dominate grasslands in the tropics, subtropics, and warm temperate zones; C_4 grasses are also commonly found in arid landscapes (Archibold, 1995; Sage, 1999). The earliest undisputed C_4 plant fossil is *Tomlinsonia thomassonii*, a permineralized grass from the Miocene Ricardo Formation, California (Tidwell and Nambudiri, 1989). This coincides with an isotopic shift in some soils and herbivores during the Miocene that suggests the expansion of plants with C_4 photosynthesis (Kingston et al., 1994; Morgan et al., 1994; Fox and Koch, 2003). Molecular clock analysis of grasses suggests an Oligocene origin for the C_4 photosynthetic pathway in angiosperms (Kellogg, 1999).

Geologic modeling, isotope analysis, and cuticular analysis all suggest that CO_2 levels during the Oligocene (Figure 2) were relatively low compared to the Cretaceous (Zachos et al., 2001; Pagani, 2002; Retallack, 2002; Berner, 2006). Evidence from oxygen isotopes suggests that the climate was cooling (Zachos et al., 2001) during the Oligocene. Although a warm climate is more favorable to C_4 plants because such conditions stimulate photorespiration (Brooks and Farquhar, 1985; Sharkey, 1988), global cooling can cause more arid growing conditions and cause precipitation to become more seasonal (Prothero, 1994; Farrera et al., 1999). Such dry conditions may have favored a C_4 pathway by promoting closure of the stomata. This closure reduces the concentration of intercellular CO_2 and can then cause photorespiration (Guy et al., 1980). The distribution of C_4 plants and C_3-C_4 intermediates in dry and saline conditions also suggests that such conditions may be key in promoting the evolution of the C_4 pathway (Osborne and Beerling, 2006). Given that the origin of the C_4 pathway in the Oligocene

corresponds with environmental conditions that are favorable to the success of the pathway (e.g., low CO_2, arid), it is worth investigating older occurrences of such conditions in the geologic record to see if they mimic responses in more recent times (Osborne and Beerling, 2006).

There are few times in the Earth's history where conditions for the origin of the C_4 pathway would have been present (Figure 2). The atmospheric conditions prior to 400 mya were ones with CO_2 levels much higher than current levels and O_2 concentrations that were lower (Berner and Kothavala, 2001; Berner, 2006; Osborne and Beerling, 2006). During the Late Carboniferous and early Permian, however, the conditions were such that photorespiration was likely a significant factor in plant productivity. Based on calculated models of geologic carbon and oxygen cycles (Berner, 2005) consistent with isotope and fossil data (Royer et al., 2005b; Royer, 2006), the late Paleozoic shows a marked decline in atmospheric CO_2 and a rise in O_2 (Figure 2). Osborne and Beerling (2006) assessed the likelihood of the C_4 pathway evolving during this time by modeling the quantum yield of hypothetical C_3 and C_4 plants living under these conditions (Figure 24). The quantum yield of the C_4 plant is assumed to remain constant while that of the C_3 plant changes in response to fluctuating CO_2 and O_2 levels. The model also incorporated estimates of global mean temperature based on a planetary energy balance model and tropical temperatures. These data were obtained from general circulation model (GCM) simulations of past climates. This methodology allowed Osborne and Beerling (2006) to assess whether the Late Paleozoic would have been an opportune time for the origin of the C_4 pathway in a non-angiosperm group. Their modeling suggests that C_4 plants growing in a tropical climate have a greater quantum yield than C_3 plants growing in the same area.

To further test their hypothesis, Osborne and Beerling (2006) constructed global dynamic vegetation models using two GCMs to identify regions that would be most likely to support

plants with a C_4 photosynthetic pathway. The GCMs used were the UK Universities Global Atmospheric Modelling Programme (UGAMP) and the National Center for Atmospheric Reseach (NCAR) GCM. These simulations work by assuming that C_4 plants had already evolved and they then predict the regions most likely to be dominated by C_4 plants. The vegetation model based on the UGAMP GCM indicates that plants exhibiting the C_4 pathway would be expected to dominate the high latitudes (Osborne and Beerling, 2006). Osborne and Beerling (2006) tested their hypothesis further by conducting an isotopic survey Late Carboniferous and early Permian plants from the tropics and high southern latitudes, including *Glossopteris* leaves and wood from Antarctica. All of the plants examined had carbon isotope discrimination values typical of those found in C_3 plants.

Although tissue from glossopterid plants was examined, the dominance of the group during this time warrants a closer inspection. The carbon isotope discrimination values reported by Osborne and Beerling (2006) are consistent with C_3 plants, but those values are also consistent with those found in some C_3-C_4 intermediates (von Caemmerer, 1992). These intermediates may contain many of the adaptations that are found in C_4 plants (e.g., anatomical modifications, some biochemical modifications). The intermediates would not have a C_4 isotopic signature unless PEP carboxylase had evolved to fill the same role as in extant C_4 plants. Sage (2004) suggests that there are several intermediate steps leading from a C_3 plant to a C_4 plant. The first steps are anatomical modifications that help to concentrate CO_2 around Rubisco. The remaining steps are mostly biochemical modifications, including enhancement of PEP carboxylase activity.

The purpose of this study is to investigate Permian *Glossopteris* leaves for adaptations consistent with the evolution of the C_4 photosynthetic pathway. Anatomically preserved leaves

from Skaar Ridge, the permineralized peat deposit in the Central Transantarctic Mountains, are ideal for this analysis because they are structurally preserved.

2. Materials and methods

2.1 Analysis of potential anatomical adaptations

To test for possible anatomical adaptations to the C_4 photosynthetic pathway, the methodology of Muhaidat et al. (2007) was applied to permineralized *Glossopteris* leaves. Muhaidat et al. (2007) discovered five sets of measurements that could accurately distinguish C_3 plants from C_4 plants based on anatomy. Additionally, the methodology allowed the authors to distinguish between several of the C_4 subtypes. The five measurements deal with the perimeter and area of various tissues: (1) the ratio of PCA tissue area to PCR tissue area, (2) the percentage of intercellular space in a leaf cross section, (3) the ratio of the perimeter of PCR tissue to the area of PCR tissue, (4) the amount of PCR perimeter exposed to the intercellular space, and (5) the percentage of the leaf area in cross section that is comprised of epidermal tissue (Muhaidat et al., 2007). Of these five metrics, only three can be accurately applied to permineralized *Glossopteris* leaves: PCA:PCR area, PCR perimeter:PCR area, and the percentage of epidermal area. Although cells of the *Glossopteris* leaves have been preserved, some degradation of the tissue has occurred. As a result, it is impossible to accurately measure the amount of intercellular space in the leaf cross section. It should be noted that Muhaidat et al. (2007) use slightly different terminology in their paper. What is referred to here as perimeter and area, they refer to as area and volume, respectively. I feel that my terminology is more accurate because it correctly references the number of dimensions used in the measurements.

Due to the need for well-preserved leaves showing PCR, PCA, and epidermal tissues, coupled with the relatively poor preservation of leaves at the locality, a sample size of 24 leaves

was used for analysis of PCA:PCR area and PCR perimeter:PCR area; a sample size of only two leaves was used to measure the percentage of epidermal area. The measurements were made from digital images using the software ImageJ (Rasband, 2012). Images were captured from prepared slides of acetate peels. The permineralized *Glossopteris* leaves come from the late Permian Skaar Ridge locality.

The averages of all measurements were compared to those measured by Muhaidat et al. (2007) using Student's t-test. The complete data set of Muhaidat et al. (2007) that was used for the comparison can be found in the supplemental material of the aforementioned paper. Statistical analysis was done using R (R Core Team, 2012).

2.2 Analysis of potential biochemical adaptations

Permian leaves from Antarctica were also used for stable carbon isotope analysis. The purpose of this analysis was to determine if the *Glossopteris* fossils housed at the University of Kansas have a different isotopic signature than those measured by others, as well as to obtain isotopic measurements of the fossils used in anatomical analysis. Samples for isotopic analysis were obtained from specimens from five different localities. Two samples came from permineralized *Glossopteris* leaf mats from the late Permian Skaar Ridge locality. The sample was obtained by macerating the leaf mat in HF until completely dissolved. The sample then underwent a series of water changes until a neutral pH was obtained. The water was then allowed to evaporate until only a dry powder remained. The dry powder was then used in the analysis.

The remaining samples came from compression specimens. For these specimens, the carbon film of the leaf compression was scraped from the surface and used in the analysis. Prior to removal of the film, the specimen was gently cleaned in 95% ethanol. The compression samples came from Kennar Valley (early Permian; Weller Coal Measures), Aztec Mountain

(early Permian; Weller Coal Measures), Robison Peak (early Permian; Weller Coal Measures), Mt. Achernar (late Permian; Upper Buckley), and Prebble Glacier (late Permian; Upper Buckley). The sample from Prebble Glacier was *Schizoneura*; all other specimens were *Glossopteris*. *Schizoneura* was used for comparison to *Glossopteris* leaves because there is no reason to believe that *Schizoneura* was a C_4 or C_4-like plant, due to the low venation density and affinities with the sphenopterids. To account for differences in atmospheric CO_2 for the various specimens, the isotope ratios were converted to discrimination values using data from Straus and Peter-Kottig (2003). Isotopes were analyzed at the Keck Paleoenvironmental & Environmental Stable Isotope Laboratory at the University of Kansas. The analysis was done using a Costech 4010 elemental analyzer in conjunction with a ThermoFinnigan MAT 253 IRMS (ThermoFinnigan, Germany). All carbon isotope ratios are measured against a Vienna Pee Dee Belemnite (VPDB) standard.

3. Results

3.1 Anatomical analysis

The average PCA:PCR tissue area ratio for *Glossopteris* leaves from Skaar Ridge (Table 13, Figure 25A) is 5.5 ± 1.74 (n = 24). The average ratio of PCR perimeter to PCR area for *Glossopteris* leaves (Table 13, Figure 25B) is 0.045 ± 0.014 (n = 24). The average percentage of epidermal tissue in cross section for *Glossopteris* (Table 13, Figure 25C) is 22.3% ± 3.1 (n = 2).

From Muhaidat et al., (2007), the average PCA:PCR tissue area ratio for C_3 plants was 10.4 ± 4.87 (n = 22) and for C_4 plants was 3.57 ± 1.82 (n = 33). The average ratio of PCR perimeter to PCR area for C_3 leaves was 0.089 ± 0.037 (n = 20) and for C_4 leaves was 0.055 ± 0.014 (n = 33). The average percentage of epidermal tissue in cross section for C_3 leaves was 13.74% ± 3.19 (n = 19) and for C_4 leaves was 19.82% ± 6.66 (n = 30) (Figure 25).

Statistical analysis showed that for PCA:PCR tissue and PCR perimeter:PCR area, the values for *Glossopteris* leaves were significantly different from values for extant C_3 leaves ($p < 0.01$) but were not significantly different from the values for extant C_4 leaves. The small sample size for the percentage of epidermal tissue made meaningful statistical comparison to the Muhaidat et al. (2007) values impossible.

3.2 Stable carbon isotope analysis

All Permian samples showed similar ranges of isotopic discrimination and enrichment (Table 14). The four samples from late Permian permineralized leaves had $\delta^{13}C$ of –27.86‰, –28.93‰, –26.69‰, and –27.2 ‰. The range of $\Delta^{13}C$ for these specimens is 22.7 to 26.9‰. The *Glossopteris* leaf compression from Kennar Valley had a $\delta^{13}C$ of –24.17‰ and a $\Delta^{13}C$ of 20.1 to 22.4‰. The two *Schizoneura* specimens examined had $\delta^{13}C$ of –25.52‰ and –25.01‰; the range of $\Delta^{13}C$ for these specimens is 20.9 to 23.3‰. The specimen from Mt. Achernar had a $\delta^{13}C$ of –23.68‰ and a $\Delta^{13}C$ range of 19.5 to 21.4‰. The *Glossopteris* leaf from Robison Peak has a $\delta^{13}C$ of –22.26‰ and a range of 18.1 to 20.4‰ for $\Delta^{13}C$. The sample from Aztec Mountain has a $\delta^{13}C$ of –22.44‰ and a $\Delta^{13}C$ ranging from 18.2 to 20.6‰.

4. Discussion

4.1 Photosynthetic pathways in Glossopteris

Taken separately, the anatomical and isotopic data provide evidence that points to two different conclusions; when taken together, the evidence points to a third conclusion. The stable carbon isotope data (Table 14) are consistent with discrimination values typically found in C_3 plants and are substantially different from those associated with C_4 plants (Dawson et al., 2002). The results of the anatomical data (Table 13, Figure 25), however, are consistent with the values Muhaidat et al. (2007) gives for C_4 plants. These two techniques taken together allow for a

different conclusion—that *Glossopteris* leaves are on the continuum of C_3-C_4 intermediates. C_3-C_4 intermediates typically have at least some anatomical adaptations seen in C_4 photosynthesis but do not possess all of the biochemical pathways found in the C_4 condition. In some C_3-C_4 intermediates, the anatomical characteristics may even be more similar to C_3 plants than to C_4 plants (Brown and Hattersley, 1989). Given the large number of independent origins of C_4 photosynthesis in the angiosperms, it is not especially surprising that the groundwork to evolve some of the characteristics of the pathway may have existed long ago. Recent phylogenetic research suggests that the genes involved in the release of CO_2 around Rubisco in bundle sheath cells have existed for at least 180 million years (Brown et al., 2011).

Despite this, C_3-C_4 intermediates are thought to be relatively rare today. Most C_3-C_4 intermediates today tend to live in environments where the potential for photorespiration is high (Christin et al., 2010, 2011). It has been demonstrated that C_3-C_4 intermediates have CO_2 compensation points and photosynthetic water-use efficiencies between C_3 plants and C_4 plants (Vogan et al., 2007), but these plants still exhibit $\delta^{13}C$ values within the normal range for C_3 plants. There are two types of C_3-C_4 intermediacy, termed type I and type II (Edwards and Ku, 1987). In type I intermediates, CO_2 is concentrated in the bundle sheath by limiting glycine decarboxylation to the bundle sheath, thereby increasing the CO_2 in the presence of Rubisco (Edwards and Ku, 1987; Monson and Rawsthorne, 2000). Type II intermediates posses the features of type I as well as a limited portion of the C_4 cycle (Edwards and Ku, 1987). With our current knowledge and technology, it is impossible to determine which type is present in *Glossopteris*.

Increased protection against photorespiration in an environment that promotes this metabolic process could have played a large factor in the dominance of *Glossopteris* throughout

the Permian, particularly at polar latitudes. When subjected to continuous light conditions at the high polar latitudes, photorespiration was likely a substantial concern. Although the tmperature during the Early Permian is thought to be cool, the climate has been modeled as quite warm during the Late Permian and Triassic (Osborne and Beerling, 2006). With CO_2 levels already low at the start of the Permian, any additional stress placed on the plant may have been a catalyst for photorespiration. Although the frequent preservation of fossil *Glossopteris* leaves suggests that many of the species did not live in dry conditions, it is unlikely that water was available in quantities large enough to keep the stomata open during four months of continuous light. During times of stomatal closure, the intercellular CO_2 level would have dropped while the light reactions continued. Over time, the opportunities for photorespiration to occur could have had a major impact on the productivity of the glossopterids and any other plants living at those latitudes. A plant with a photosynthetic pathway that could limit photorespiration would have great advantage over competitors. Although the factors leading to the end-Permian mass extinction are complicated, and apparently caused fewer extinctions in terrestrial plant life, the disappearance of the glossopterids around the boundary suggests that as the CO_2 levels rose, the competitive advantage of its C_3-C_4 intermediate pathway may have lessened. Once into the Triassic, the diversity of plant life found at high latitudes in Antarctica is greatly increased relative to the Permian (e.g., Escapa et al., 2011).

4.2 Potential methodological issues

There are several factors which could pose problems for the interpretation of *Glossopteris* as a C_3-C_4 intermediate. Comparing isotopic values across geologic time can be difficult due to the fluctuation of atmospheric $\delta^{13}C$. The methodology in this study attempts to avoid the problem by converting $\delta^{13}C$ VPDB to isotope discrimination values. This poses its own

problem as it requires knowledge of atmospheric $\delta^{13}C$ to calculate $\Delta^{13}C$. Values of atmospheric $\delta^{13}C$ were taken from the literature (Strauss and Peters-Kottig, 2003). Atmospheric $\delta^{13}C$ is rarely preserved, however, so a proxy must be used. To calculate past atmospheric $\delta^{13}C$, the oceanic $\delta^{13}C$ is measured and a known offset between atmospheric and oceanic $\delta^{13}C$ is used. For samples from the early Permian, this is not likely to cause a problem because the difference between atmospheric and oceanic $\delta^{13}C$ normally remains constant. Around mass extinction events, however, the offset becomes less reliable due to rapid fluctuations in $\delta^{13}C$ often found associated with mass extinction events. This could pose a problem for the late Permian isotope samples, as they existed closer to the extinction boundary. Given that the $\Delta^{13}C$ values for late Permian and early Permian samples were similar, this is not likely to be a large concern.

Another concern for the isotope analysis is that two samples produced a voltage below the voltage of the lowest weighted DORM-2 standard. This occurred with the Robison Peak sample and one of the two samples of *Schizoneura* from Prebble Glacier. The two samples of *Schizoneura* had nearly identical values and the sample from Robison Peak was within the range of all other samples. With this in mind, the low voltages are not a great concern.

The possibility exists that the samples were thermally altered due to the volcanic activity during the Jurassic. Evidence from other studies indicates that thermally altered carbon will produce an increase in $\delta^{13}C$ (Des Marais, 1997). Had the analyzed specimens been thermally altered, their unaltered $\delta^{13}C$ would be even further into the range of C_3 plants, thereby having no effect on the interpretation of the results. Additionally, the samples examined come from different localities, times, formation, and modes of preservation, yet all posses $\delta^{13}C$ values that converge in the C_3 range.

A potential issue with the anatomical analysis concerns the number of measurements of

Muhaidat et al. (2007) that can be used with permineralized *Glossopteris* leaves. With the extant plants, five different measurements were shown that could differentiate between C_3 and C_4 photosynthetic pathways. Due to issues of tissue preservation, however, only three of those measurements could be used in this research; of those three, only two have samples sizes large enough to be statistically powerful. Theoretically, the other measurements could have given values more in the range of C_3 plants, which would give less power to the interpretation of *Glossopteris* as a C_3-C_4 intermediate. This could be rectified by finding *Glossopteris* leaves with better anatomical preservation and by increasing the sample size. Additionally, the permineralized leaves studied here are from the late Permian. The greatest threat caused by photorespiration was likely to occur in the early Permian. Investigation of anatomically preserved fossils from this time period may yield different results. Other Permian plants with dense venation patterns, such as *Gigantopteris*, would be ideal for this analysis. The results of this study are an excellent example of the importance of utilizing multiple approaches to test a hypothesis.

Chapter 5

A leaf economics analysis of high latitude *Glossopteris* leaves using a technique to estimate leaf mass per area

1. Introduction

Growth strategies can be difficult to determine for fossil plants, but the rate of plant resource use can be estimated using leaf mass per area analysis. Leaf mass per area (LMA) is a measure of leaf economics that, at its most basic, attempts to analyze the leaf level cost of light interception (Gutschick and Wiegel, 1988). It is typically expressed in units of g m^{-2}. The difference between leaves with a high LMA and a low LMA mainly deals with the rate of resource acquisition and growth of the plant (Westoby et al., 2002). Plants with leaves at the high end of the LMA spectrum tend to grow more slowly and have less turnover of plant organs. Plants at the lower end of the spectrum grow more quickly and do not invest as many resources in their leaves. Low LMA plants therefore have a higher photosynthetic rate, a higher concentration of protein, and are more susceptible to attacks by herbivores (Wright and Westoby, 2002).

LMA can be used as a proxy for a variety of environmental conditions. This is largely a result of the many factors that affect LMA (Poorter et al., 2009). Unfortunately, this can also lead to difficulties when attempting to determine why a leaf has a particular LMA. Although the structure of a leaf is relatively simple, the distribution and volume of the tissue components can change the LMA of a leaf in a variety of ways. For example, some leaves may have more fibers for rigidity or to deter herbivores. Succulent leaves have larger mesophyll cells used for storage,

and a complex vascular architecture can also add considerable mass to a leaf. So although light interception is an important component of LMA, the thickness of the leaf can have a large effect on the mass, and therefore on the LMA.

1.1 Relationship of LMA to plant functional groups and habitats

LMA measurements can vary greatly by and within species and can be caused by numerous factors. This provides a fertile area to investigate the environmental conditions of fossil plants, provided that some of the varible factors can be determined. One factor that can often be analyzed using LMA is a determination of which plant functional group the specimen represents. Plant functional groups can be described as a grouping of plants or organisms that have functional traits in common and can be relatively similar in response to changes in a particular environment (Raunkiaer, 1934; Smith et al., 1997a; Poorter and Navas, 2003). Similar responses to the environment could imply that the plants have a similar life history, similar growth form, or similar physiological characteristics that elicit similar responses to factors such as CO_2. In general, the LMA of aquatic plants is different from that of a fern, which is different from deciduous plants, which is different from evergreen plants (Sobrado, 1991; Villar and Merino, 2001), which is also different from succulents (Poorter et al., 2009). Similarly, LMA can also help to distinguish between different habitats. For example, plants growing in aquatic environments have lower LMA than plants growing in forests and these plants have an LMA lower than plants found in dessert environments (Poorter et al., 2009). This should not be too surprising since the functional group of most leaves will be a product of the environment in which they live. Indeed, leaves of many species seem to show a remarkable plasticity with regard to their LMA. When *Glycine max* (L.) Merr. and *Alocasia macrorrhizos* (L.) G. Don were grown in a high-light environment and subsequently moved to a low-light environment, the leaves

showed a substantial decrease in LMA within a few days (Sims and Pearcy, 1992; Pons and Pearcy, 1994). Although LMA can be used in many cases to differentiate between habitats and functional groups, LMA can significantly overlap in multiple groups (Castro-Díez et al., 2000; Wright et al., 2005). Attempts to differentiate plants with different photosynthetic pathways using LMA has had mixed results. CAM plants have been shown to have LMAs much larger than C_3 or C_4 plants, which is not surprising given that many CAM plants are succulent. Comparisons between C_3 and C_4 plants have met with mixed results (Da Matta et al., 2001; Reich et al., 2003).

The main causes for the differences in LMA for evergreen and deciduous plants is based on the volume of the mesophyll and the composition of the cells. Evergreen taxa typically have significantly more mesophyll tissue (Castro-Díez et al., 2000) with thicker cell walls (Terashima et al., 2006). Evergreen leaves typically posses a higher proportion of lignified tissue and secondary metabolites that often play a role in limiting herbivory.

The amount of light intercepted by leaves also plays a large role in determining LMA. Current research indicates that the daily integrated photon flux (DPI) is what affects LMA the most and not instantaneous peak irradiance (Chabot et al., 1979; Niinemets et al., 2004). Currently, no research has been reported with respect to the effects of a continuous light environment on LMA. Poorter et al. (2009) have demonstrated that the effect is more pronounced at low light levels and the response increases more slowly above a DPI of 20 mol m^{-2} d^{-1}. With a variety of plants growing in a variety of habitats, LMA increases with increases in DPI. At higher DPI, the changes in LMA are largely a product of an increase in palisade mesophyll thickness, while the thickness of the epidermis remains constant (Onoda et al., 2008). The decrease in LMA of leaves in low-light conditions is largely driven by an increase in leaf surface area while the mass of the leaf remains the same. The LMA is also increased in high light

conditions due to an increased production of in carbohydrates in the plant (Niinemets et al., 1998). Plants in different environments, or leaves in different portions of the canopy, can experience vastly different qualities of light. This is due to the more shaded leaves intercepting light with a lower red to far-red ratio. Interestingly, the quality of light has been shown to have little effect of LMA (Poorter et al., 2009).

Atmospheric CO_2 concentrations play a significant role in determining LMA. Experimental evidence indicates that plants exposed to CO_2 levels above the current ambient concentration will have an increase in LMA (Radoglou and Jarvis, 1990; Sims et al., 1998). Likewise, those grown in lower CO_2 concentrations developed leaves with a lower LMA (Radoglou and Jarvis, 1990; Sims et al., 1998). Increases in LMA are not associated with an increase in the number of mesophyll layers of the leaf, but the leaves do show an increase in thickness. This is mainly due to an increase in mesophyll cell size along with an increase in starch content (Radoglou and Jarvis, 1990; Sims et al., 1998). Increased CO_2 levels cause little increase in leaf structural biomass, making the changes in LMA reversible if the stored carbohydrates are used or moved (Allen et al., 1998; Roumet et al., 1999).

Temperature has also been shown to have a significant effect on LMA, although the response is non-linear (Poorter et al., 2009). Leaves of plants grown at low temperatures have a higher LMA than those grown in high temperatures. Low temperatures cause the cell layers of leaves to grow at a slower rate. Smaller cells increase the amount of cell wall in a given volume of leaf, increasing the mass (Atkin et al., 2006). Plants native to different habitats will also have different LMA responses to changes in temperature. Plants native to the tropics show a greater sensitivity to temperature change than those native to other areas (Poorter et al., 2009).

These environmental effects on LMA can be summarized more succinctly. In conditions

where light is readily available and CO_2 is not limiting, LMA will increase due to faster rates of photosynthesis. The trend can be reversed in conditions where nutrients or temperaturs are low due to the lower demands of carbohydrates for growth (Poorter et al., 2009).

1.2 Within-plant and within-leaf variations in LMA

There are many confounding factors when analyzing LMA due to within-plant variation. Variations in available light and air temperature within a canopy and reduced water availability in the taller portions of trees can have significant effects on LMA (Anten and Hirose, 1999; Baldocchi et al., 2002; Niinemets, 2007). Such factors can make analyses with fossils leaves more difficult since it is impossible to determine their position in the canopy with accuracy. Attempts have been made to construct a methodology for determining canopy position with leaves from extant *Ginkgo* and it was determined that trends in venation patterns and morphology could be quantified within a single tree (Boyce, 2009). However, it is unlikely that the fossil leaves being examined at any one locality came from a single tree. Additionally, the characteristics used to differentiate between species of fossil leaves could also be due to variations in venation due to canopy differences. Attempting to assescanopy position of leaves from the fossil record, particularly in plants grown in a high latitude diffusive-light environment, would likely raise more problems that it could solve. The LMA of an individual leaf can also vary throughout the growing season, making the time of leaf deposition an important factor when analyzing the LMA of fossil leaves. LMA is high after bud break and then drops during leaf expansion. After expansion, LMA will increase again as the number of chloroplasts increase and cell walls thicken (Jurik, 1986). LMA will then remain constant, assuming environmental factors remain constant, until the beginning of leaf senescence (Poorter et al., 2009). In cases where younger leaves shade older leaves, it can be difficult to tease apart the effects of age and light

interception (Brooks et al., 1994).

The age of a tree can also influence the LMA of the leaves it produces. Although evergreen leaves do not show much variation in LMA throughout their lives (Wright et al., 2006), leaves developed on older trees will have a higher LMA throughout the life of the leaf (Niinemets et al., 2009a, 2009b, 2009c). Fluctuation in LMA can even occur throughout the course of the day (Tardieu et al., 1999); the changes are due to the build up of carbohydrates in the leaf throughout the day.

2. Materials and methods

2.1 Calculation of LMA

LMA of fossil leaves can be calculated using a regression equation developed by Royer et al. (2007). The regression equation was developed to find a scaling relationship between petiole width and leaf mass normalized by the surface area of the leaf. The data set consisted of 667 species of leaves from 65 Eocene sites from Washington and Utah (Royer et al., 2007). This data set was later supplemented with 93 species of broad-leaved gymnosperms and 58 species of herbaceous angiosperms from Early Cretaceous strata of North America (Royer et al., 2010). The revised power law between petiole width and leaf mass from Royer et al. (2010) was used in the present study:

$$\log(\mathrm{LMA}) = 0.3076 \times \log(\mathrm{PW}^2/\mathrm{A}) + 3.015$$

where PW is the width of the petiole and A is the surface area of the leaf. The power law works due to the biomechanical relationship between the cross-sectional area of the petiole and the mass of the leaf (Niklas, 1991a, 1991b). Since the cross-sectional area of the petiole cannot be measured in compression/impression specimens, the width of the petiole at its closest to the base of the lamina was used (Royer et al., 2007). This portion of the petiole was used as it is more

likely to be preserved in the fossil record. Due to the type of leaves used in the calibration data set and the nature of the Triassic leaves found in Antarctica, this technique will not work for Triassic specimens at this time.

Measurements of petiole width and leaf surface area of *Glossopteris* leaves (Figure 26) were taken from digital images of compression/impression fossils using the software ImageJ (Rasband, 2012); digital images were taken with a Nikon D300S as previously described. Petiole width was measured at the point closest to the blade of the leaf. Measurements of the leaf surface area were taken by completely outlining the blade of the leaf and calculating the area in ImageJ. These measurements, along with one other for unit conversion, were saved as spreadsheets. A simple script was written in Python 2.7 to automate the process of calculating LMA and the accompanying statistics. Each leaf specimen has a spreadsheet file that includes the specimen number, locality, leaf species, and other values used to differentiate leaves on the same slab. Calculated values for each leaf were then outputted to spreadsheet files.

2.2 Fossil leaves and localities

For LMA analysis, 191 Permian *Glossopteris* leaves were selected (See Appendix II for data). This sample size is much smaller than that for leaf hydraulics analysis because the LMA analysis has stricter requirements for the type of fossil leaf that can be measured. For this study, leaves missing a portion of the blade or without a petiole could not be used. This limited the sites from which samples could be taken. In some cases this was the result of an energetic depositional environment that did not allow for the preservation of whole leaves. In other cases, the slabs collected from some localities were not large enough to contain a whole leaf.

Usable specimens were analyzed from 14 different fossil localities; the only non-Antarctic locality was located in Bazargaon, India. Of the 13 fossil localities from Antarctica,

four localities are found in the Weller Coal Measures, five in the Upper Buckley Formation, two in the Mt. Glossopteris Formation, one in the Queen Maud Formation, and one in the Polarstar Formation. Five of the Antarctic localities are between 70° S and 79° S, and eight are found at 80° S and higher. Of the 191 leaves, only 33 were from early Permian localities.

2.3 Statistical analysis

A 95% prediction interval (PI) was calculated around the average value found at each locality. A prediction interval differs from a confidence interval; a confidence interval describes how well the mean has been calculated and tells you a likely range for the true location of the population mean. A prediction interval describes a range around which you can expect to find the next data point sampled. Prediction intervals are commonly used to evaluate regression analyses (Sokal and Rohlf, 1995). Prediction intervals were calculated with the following equation:

$$\log PI = \left\{ \log LMA \pm \sqrt{s_{Y \cdot X^2} \left[\frac{1}{k} + \frac{1}{n} + \frac{(X_i - X_m)^2}{\sum x^2} \right]} \right\} \times t_{0.05[n-2]}$$

where s_{YX}^2 = unexplained mean square, k = size of unknown sample, n = sample size of calibration data, X_i = mean log(PW^2 / A) of unknown sample, X_m = mean log(PW^2 / A) of calibration data, $\sum x^2$ = sum of squares of calibration data, and $t_{0.05[n-2]}$ = critical value of Student's distribution for (n-2) degrees of freedom. In order to calculate a prediction interval, the data used in creating the original regression equation are required. The variables needed from Royer et al. (2010) are s_{YX}^2 = 0.0231325, n = 95, X_m = -2.473, $\sum x^2$ = 17.76, and $t_{0.05[n-2]}$ = 1.986. The prediction interval was calculated within the Python script.

3. Results

Prediction intervals for LMA varied by locality and sample size for the *Glossopteris* leaves measured (Table 15).

3.1 Allan Hills LMA

For the 22 leaves analyzed from Allan Hills, the average LMA is 120.8 g m^{-2} with a prediction interval of 99.8 to 146.1 g m^{-2}.

3.2 Aztec Mountain LMA

There were 9 specimens measured from the Aztec Mountain locality. The prediction interval for this locality is 87.2 to 148.5 g m^{-2} with an average LMA of 113.8 g m^{-2}.

3.3 Bazargaon LMA

A single *Glossopteris* leaf was measured from this locality. The single leaf had an LMA of 116.0 g m^{-2} with a prediction interval of 57.2 to 235.1 g m^{-2}.

3.4 Coalsack Bluff LMA

One *Glossopteris* leaf was examined from this locality. The LMA for this leaf was 114.1 g m^{-2} with a prediction interval of 56.2 to 231.3 g m^{-2}.

3.5 Leaia Ledge LMA

One *Glossopteris* leaf was analyzed at this locality. This leaf has an LMA of 114.3 g m^{-2} with a prediction interval of 56.4 to 231.9 g m^{-2}.

3.6 Mt. Achernar LMA

A single *Glossopteris* leaf was examined from this locality. The single leaf has an LMA of 108.5 g m^{-2} and a prediction interval of 53.3 to 220.4 g m^{-2}.

3.7 Mt. Feather LMA

One *Glossopteris* leaf was analyzed from Mt. Feather; the LMA of this leaf was 97.5 g m^{-2} with a prediction interval of 47.8 to 199.0 g m^{-2}.

3.8 Mt. Fleming LMA

One *Glossopteris* leaf was examined from Mt. Fleming. The single leaf has an LMA of

111.8 g m^{-2} with a prediction interval of 55.1 to 226.9 g m^{-2}.

3.9 Mt. Ropar LMA

One *Glossopteris* leaf was examined at this locality. The leaf has an LMA of 105.5 g m^{-2} with a prediction interval of 51.9 to 214.6 g m^{-2}.

3.10 Mt. Weaver LMA

A single leaf of *Glossopteris* was analyzed from Mt. Weaver. The leaf has a prediction interval of 50.8 to 210.5 g m^{-2} and an LMA of 103.4 g m^{-2}.

3.11 Mt. Wild LMA

One leaf was analyzed from Mt. Wild. The *Glossopteris* leaf has an LMA of 95.8 g m^{-2} and a prediction interval of 46.9 to 195.7 g m^{-2}.

3.12 Polarstar Peak LMA

There were 4 leaves examined from Polarstar Peak. The average LMA of these leaves is 111.9 g m^{-2} with a prediction interval of 77.1 to 162.2 g m^{-2}.

3.13 Skaar Ridge LMA

Skaar Ridge provided the largest sample size of leaves in this analysis. The average LMA of the 132 *Glossopteris* leaves analyzed was 111.8 g m^{-2} with a prediction interval of 96.6 to 129.4 g m^{-2}.

3.14 Terrace Ridge LMA

There were 8 *Glossopteris* leaves examined at this locality. The average LMA for these leaves were 106.3 g m^{-2} with a prediction interval of 80.0 to 141.2 g m^{-2}.

4. Discussion

4.1 Differences in prediction intervals across localities

The prediction interval (PI) for the majority of the Permian localities analyzed is rather

large (Table 15). This suggests that the regression equation has little predictive power at these localities. Since the PI is so much smaller at Skaar Ridge compared to localities like Allan Hills and Terrace Ridge, the sample size of *Glossopteris* leaves at this locality appear to be the limiting factor. If the problem were more closely related to the regression equation itself or the sample size used in the initial data set, all of the predictive intervals would be large. The Skaar Ridge locality, where 132 *Glossopteris* leaves were analyzed, had the smallest PI with a range of 96.6 to 129.4 g m^{-2}. The fossil leaves used for this analysis were collected during a recent (2010-2011) Antarctic field season and are preserved in large slabs. These large slabs proved to be integral to this type of analysis and underscore the importance of putting in extra effort to retrieve the largest intact specimens possible.

4.2 Possible functional groups and habitats based on LMA analysis

The predictive interval (PI) of leaves from the Allan Hills ranges from 99.8 to 146.1 g m^{-2}. The LMA values in this range straddle several different functional groups. Most values fall heavily into the range for evergreen trees. At the extreme lower end of the PI for Allan Hills are LMA values typically associated with deciduous plants and graminoids (Poorter et al., 2009). For habitat, the LMA of leaves at this locality fall mostly into the range of plants from woodlands, shrublands, and deserts. At the lower end of the PI for leaves at Allan Hills are LMA values associated with tropical and temperate forests, as well as tundra (Poorter et al., 2009).

The PI for the Aztec Mountain locality is much larger and ranges from 87.2 to 148.5 g m^{-2}. Despite the PI, the LMA values at this locality are associated with the same functional groups and habitats as leaves from the Allan Hills. Leaves analyzed from Polarstar Peak (PI = 77.1 to 162.2 g m^{-2}) and Terrace Ridge (80.0 to 141.2 g m^{-2}) also fall within the same groupings.

The Bazargaon locality in India has *Glossopteris* leaves with an LMA falling in the range

of 57.2 to 235.1 g m^{-2}. This is a much broader range of LMA that covers more functional groups and habitats. In addition to the groups mentioned for the previous localities, leaves at the Bazargaon locality fall within the herb and succulent functional groups as well as the grassland and marine habitats (Poorter et al., 2009). The leaves examined from Coalsack Bluff (PI = 56.2 to 231.3 g m^{-2}), Leaia Ledge (PI = 56.4 to 231.9 g m^{-2}), Mt. Weaver (PI = 50.8 to 210.5 g m^{-2}), Mt. Wild (PI = 46.9 to 195.7 g m^{-2}), Mt. Feather (PI = 47.8 to 199.0 g m^{-2}), Mt. Ropar (PI = 51.9 to 214.6 g m^{-2}), Mt. Achernar (PI = 53.4 to 220.4 g m^{-2}), and Mt. Fleming (PI = 55.1 to 226.9 g m^{-2}) falls within the same groupings as those from Bazargaon.

The PI for LMA at Skaar Ridge is the smallest of all localities studied because of the larger sample size. The PI for his locality (96.6 to 129.4 g m^{-2}) falls mainly in the range of evergreen trees. At the lower end of the PI for Skaar Ridge are plants that are deciduous (Poorter et al., 2009). For habitats, leaves from this locality fall mainly into the ranges of plants located in woodlands and forests. At the lower end of the PI, the LMA for *Glossopteris* leaves at Skaar Ridge fall into the range for plants growing in the tundra (Poorter et al., 2009).

The PI for the LMA of *Glossopteris* leaves growing at these Permian localities contains a variety of functional groups and habitats that clearly do not fit with what we currently know about the glossopterids and the depositional environments in which they are found. This is either a reflection of the small sample sizes from these localities or the overlapping ranges of LMA found in nature. It seems likely that this discrepancy is due to sample sizes, as localities with similar sample sizes produced similar prediction intervals. This underscores the importance of increasing the sample sizes of leaves available for this type of analysis. *Glossopteris* is definitely not an herb, graminoid-like, or succulent as it displays none of the characteristics of these plants. The glossopterids being studied did not live in deserts, marine habitats, grasslands, or tundras.

Not only would the leaves be unlikely to be preserved in a desert environment, but all of the localities studied are thought to have had an abundance of water. These plants were deposited in a terrestrial environment and grasslands did not exist during the Permian. A tundra environment seems unlikely as well. Evidence from tree ring analysis of glossopterids from Antarctica (Taylor and Ryberg, 2007) demonstrates that the growing seasons in Antarctica were not shortened and were not likely to be inhibited by temperature or water availability. As for the difference between forest and woodlands, Poorter et al., (2009) describe woodlands as an area of open vegetation with trees. Based on our current knowledge of these ecosystems, it is not clear in which of the groups the glossopterids lived.

4.3 Deciduous vs. evergreen habit in Glossopteris

Several arguments have been made in favor of a deciduous habit for *Glossopteris* as well as for an evergreen habit in Antarctica. The crux of the argument centers around whether or not the loss of carbohydrate stores due to respiration during four months of continuous darkness in the cold would be greater than the loss of carbon due to shedding leaves. Royer et al. (2003) produced a study that tested the carbon-loss hypothesis by combining plant growth experiments in simulated high-latitude environments with numerical modeling simulations of conifer forests. Plants grown in the simulated conditions include three deciduous gymnosperms (*Metasequoia glyptostroboides*, *Taxodium distichum*, and *Ginkgo biloba*) and two evergreen plants (*Sequoia sempervirens* and *Nothofagus cunninghamii*). One-year-old saplings of each species were grown in chambers for three years with a relatively high latitude photoperiod (69° N; 6 weeks of continuous light/dark at the extremes) and atmospheric CO_2 in concentrations above current levels (Royer et al., 2003). Although all trees survived each growing season and produced and maintained new biomass in a normal rhythm, the loss of carbon from dropping leaves each

winter was found to be an order of magnitude higher than the carbon loss experienced by the evergreen trees (14–25% loss of annual net primary productivity vs 1–3% loss of annual net primary productivity). When these data for individual trees are scaled up to encompass groups of trees living together, a large difference remains but the gap is smaller. The cost of respiration for an evergreen canopy in the winter scales with canopy size. Even when this factor is taken into account, the carbon cost of producing a deciduous canopy of leaves is twice the cost of winter respiration, depending on the winter temperature. This growth experiment was based on photoperiods from a single latitude, but using these data and a model of forest biogeochemistry, Royer et al. (2003) calculated the carbon cost for latitudes up to 83° N. Although respiration in darkness increased in evergreen trees as the latitude increased, it did not increase by enough to close the carbon loss gap with deciduous plants. Royer et al. (2005a) revisited these experiments with a focus on measuring the carbon gain during the summer months for trees growing in light conditions found at 69° N. They found that the deciduous trees had enhanced carbon uptake during the late summer and early autumn months relative to evergreen taxa. The enhanced carbon uptake canceled out the losses incurred by leaf drop and gave the deciduous trees an annual carbon budget similar to those of evergreens. The authors suggested that evergreens would still become favored at higher latitudes (Royer et al., 2005a).

The evidence for a deciduous nature of the glossopterids is based on depositional characteristics. It is not uncommon for *Glossopteris* leaves to appear in varved strata (i.e., layers of strata deposited in a single year). Within the varved strata, *Glossopteris* leaves appear only in the fall/winter portion of the deposits (Plumstead, 1958; Retallack, 1980). Based on field observations during the 2010-2011 field season, the leaves analyzed from Skaar Ridge are deposited in the same manner. Additionally, permineralized *Glossopteris* leaves from Skaar

Ridge are preserved in thick leaf mats that suggest a mass leaf fall. In one of the rare cases of a permineralized *Glossopteris* leaf being attached to a stem, the stem was still quite young and lacked any growth rings (Pigg and Taylor, 1993). The question of the deciduous or evergreen nature of *Glossopteris* leaves was also studied by Taylor and Ryberg (2007) using the ring analysis technique of Falcon-Lang (2000a). Interestingly, the results of their study were inconclusive as the analysis of the tree rings spanned the ranges for deciduous and evergreen. Although Taylor and Ryberg (2007) concluded that thier were problems with the technique of Falcon-Lang (2000a), the LMA analysis of this study achieved similar results, suggesting that the confounding issues in both analyses may be the result of physiological changes induced by a high latitude environment.

If depositional evidence suggests that *Glossopteris* leaves were deciduous and two types of analysis suggest that these leaves could be deciduous or evergreen, might other phenomena be responsible for erroneously suggesting an evergreen habit? For the tree ring analysis it is more difficult to determine. Although Falcon-Lang (2000a) found a strong relationship between deciduousness and the evergreen habit in his tree ring analysis with extant plants, the biological mechanism that forms the basis of this relationship is not known. Therefore, there is a less compelling argument as to why it might not work on the wood from polar latitudes. The most obvious candidates to be confounding factors are the continuous light environment and the higher levels of CO_2 found in the late Permian, where the permineralized wood samples originated. If the basis of the relationship in the tree ring analysis is rooted in a source-sink connection, changes in light pattern can modify source-sink relationships (Equiza et al., 2007). The woods analyzed by Falcon-Lang (2000a) grew at current CO_2 levels and under diurnal light conditions.

There are several environmental factors that could have caused an increase in LMA relative to the functional groups and habitats of extant plants. For this discussion, only the compression/impression leaves from Skaar Ridge will be considered because this locality has the largest sample size and smallest PI. During the late Permian when these *Glossopteris* leaves were growing, the CO_2 levels were much higher than at present and the plants were subjected to unusual photoperiods. Although the instantaneous photon irradiance would be lower for high latitude plants, the integrated irradiance should be equivalent to that of middle latitudes. The lengthy period of continuous light may have a large effect on LMA by altering the source-sink relationship. LMA can vary throughout the course of the day due to build up of photosynthates and a subsequent decrease in photosynthates as the products move to sinks at night. Under continuous light conditions, the leaves would not have such downtime and if the photosynthates were allowed to accumulate, down regulation of photosynthesis would result (Equiza et al., 2006a). Since the regression equation used for this LMA analysis uses the scaling relationship between petiole width and leaf mass, the thicker petiole that would develop to support the mass of more photosynthates could give this analysis a bias toward higher LMA levels.

Evidence from extant plants grown at high latitudes suggests that the glossopterids may not have undergone photosynthetic down regulation, as seen in some extant plants grown in continuous light. The extant plant *M. glyptostroboides* was able to avoid down regulation of photosynthesis because it could utilize indeterminate growth. *Metasequoia glyptostroboides* grown in continuous light had leaves that were much higher in biomass than those grown in diurnal conditions, and it continued to produce new biomass throughout the growing season by continuing to produce new leaves from long shoots, short shoots, and through production of epicormic shoots (Jagels and Day, 2004; Equiza et al., 2006b). Epicormic shoots have been

described in glossopterids from Skaar Ridge (Decombeix et al., 2010) and several authors have suggested that the glossopterids produced long and short shoots (Plumstead, 1958; Pant and Singh, 1974; Gould and Delevoryas, 1977; Retallack and Dilcher, 1988). The higher predicted LMA of *Glossopteris* leaves suggest that the leaves acquired more biomass due to the continuous light conditions of high latitudes.

Additionally, increases in CO_2 are also correlated with an increase in LMA. The *Glossopteris* leaves were growing in environments of CO_2 higher than those used to determine the evergreen and deciduous LMA ranges in extant plants (Poorter et al., 2009). Given the depositional evidence for a deciduous habit and the similar responses of *Glossopteris* to continuous light to those seen in *M. glyptostroboides*, it is reasonable to conclude that high latitude glossopterids were indeed deciduous and that the uncertainty in previous analysis by Taylor and Ryberg (2007) was the result of a continuous light environment. This once again underscores the importance of using multiple approaches and data sets to tackle complex problems.

Chapter 6

Conclusions

This is the first study to investigate the large scale physiological effects of light regime and climate on Permian and Triassic fossil plants from Antarctica. This research adds another component to some well studied floras and provides empirical evidence of plant adaptations in an environment with no modern analogue. The insights gained through this investigation would not have been possible without multiple approaches to the problems and the large data sets available from decades of fossil collecting. Having fossils plants available for study from both sides of the Permian-Triassic boundary also make it possible to track large scale changes in community physiology that occur on either side of extinction boundaries.

1. Leaf Hydraulics

Glossopteris has long been known to be the dominant leaf type in the Permian of Antarctica and throughout Gondwana. In many localities in Antarctica it is the only leaf type found and is found in abundance. When the leaf venation density of *Glossopteris* leaves was compared to the co-occurring genera *Gangamopteris* and *Noeggerathiopsis*, it was determined that *Glossopteris* leaves had a venation density significantly higher (Figure 16). Since venation density is closely related to physiological characteristics such as leaf hydraulic conductance, maximum photosynthetic capacity, stomatal conductance, and water use efficiency, it is likely that *Glossopteris* leaves also excelled in these other characteristics when compared to plants inhabiting the same environments. The venation density advantage of *Glossopteris* leaves is probably due to the more frequent anastomosing of veins (thus making the venation more dense),

thus forming a reticulum, than in the other taxa. Interestingly, all three Permian genera studied had veins that anastomose, although very infrequently in the case of *Noeggerathiopsis*.

Leaf hydraulic analysis of *Glossopteris* leaves from Antarctica suggest that this leaf type demonstrates a strong reaction to the environment. As the Permian world moved from an icehouse to a greenhouse state, *Glossopteris* leaves showed a marked change in leaf venation density (Figures 2 and 3). *Glossopteris* leaves from the early and middle Permian showed no significant difference between venation density. Venation density of leaves from the late Permian, however, were significantly different from those growing the early and middle Permian (Figure 17). Leaf venation and maximum photosynthetic capacity are closely related, as is CO_2 concentration (Brodribb et al., 2007). Dense venation patterns come with higher construction costs (Lambers and Poorter, 1992). If the denser venation patterns of *Glossopteris* leaves were less beneficial under high CO_2 levels, it is entirely possible that the venation density could decrease over the course of millions of years.

Glossopteris leaf venation density did not show an interpretable response to changes in latitude (Figures 18–20). Analysis of the data shows that the leaves did not have a continuous response to changes in latitude, as one would expect from the continuous change in light conditions. Instead, *Glossopteris* leaves from the various localities showed continued increases and decreases in leaf venation density as the latitudes changed. There are several possible reasons for these results. For one, it is entirely possible the leaf venation density in *Glossopteris* leaves does not change in response to changes in latitude or that other, unknown environmental effects masked any changes potentially caused by differences in latitude. Another possibility that could confound analysis is the method used to combine latitudes into different groupings. It could be that combining the latitudes into artificial bins obscures any signal of changes in leaf

venation density. The grouping itself seems unlikely to be the main problem, however, as several different groupings produced confounding results. Perhaps the factor most likely to interfere with any signal of changing venation density is the tectonic activity that may have moved the fossil localities into different positions relative to where they were originally deposited. The extent of the effects of tectonic activity cannot be fully examined until better paleolatitude data are available for these localities.

Although *Dicroidium* leaves are the most common element of Middle and Late Triassic ecosystems in Antarctica, they are part of a much more diverse assemblage of plants relative to the Permian flora of Antarctica. When compared to the other leaf genera present in the same deposits (e.g., *Cladophlebis*, *Dejerseya*, *Heidiphyllum*, *Osmunda*, and *Taeniopteris*), *Dicroidium* has a vein density that is only statistically different from *Heidiphyllum* (Figure 21). In contrast to the Permian leaves, there are no leaf types that appear to have a distinct advantage in leaf hydraulic conductance, stomatal conductance, maximum photosynthetic capacity, or water use efficiency. If anything, the *Heidiphyllum* leaf type appears to be at a distinct disadvantage from a leaf hydraulics standpoint. Based on the comparison of vein densities to co-occurring leaf genera, it appears that the ubiquitous nature of *Dicroidium* leaves at Middle and Late Triassic localities is not related to any potential competitive advantage from leaf hydraulic conductance.

The differences in venation density and leaf hydraulic conductance values from either side of the Permian-Triassic boundary are fairly large. In the Triassic, no leaf type has a venation density over 5 mm mm^{-2}. The Permian genera, however, have average venation densities above 8 mm mm^{-2}. It is also interesting that there is little differentiation in leaf venation displayed by the Triassic genera studied. The fern genera have similar values to gymnosperms and the lowest venation density (*Heidiphyllum*) occurs in a conifer (Escapa et al., 2010). It is somewhat counter

intuative that leaf venation density would be so much lower in a warmer climate. Leaf venation density typically increases with temperature (Uhl and Mosbrugger, 1999) due to increased transpirational demand. In this case the change may have less to do with the importance of leaf hydraulic conductance and more to do with leaf size. Smaller, more dissected leaf types like the many compound leaves analyzed from the Triassic localities (*Cladophlebis*, *Dicroidium*, and *Osmunda*) are commonly found in high temperature environments because they more readily dissipate heat (Nobel, 1983; Nicotra et al., 2008).

2. Permian photosynthetic pathways

Analysis of the potential photosynthetic pathways of *Glossopteris* leaves provided anatomical and biochemical evidence that initially appear to be in conflict. Results of stable carbon isotope analysis (Table 14) indicate that the photosynthetic pathway of *Glossopteris* leaves falls into the range of isotope values for C_3 plants. The anatomical evidence (Table 13, Figure 25), however, indicates that permineralized *Glossopteris* leaves from Skaar Ridge have leaf tissues distributed in ways similar to those of extant plants with C_3-C_4 intermediate photosynthetic pathways. In a climate thought to promote photorespiration (Figures 2, 3, 24), a pathway intermediate between C_3 and C_4 plants would be beneficial; some C_3-C_4 intermediates are able to easily recapture the CO_2 lost during photorespiration by only decarboxylating glycine in the presence of Rubisco, instead of in the mitochondria (Edwards and Ku, 1987; Monson and Rawsthorne, 2000). Recovering the CO_2 used for photorespiration limits the main problem caused by photorespiration. As long as photorespiration stops before all energy stores are used, it allows leaves to use excess light energy and reduce the possibility of damage to the photosynthetic apparatus (Foyer et al., 2009). When light is constant and the potential for stomatal closure exists due to low CO_2 or dry conditions, the chances of photorespiration

occurring are much higher. As such, the evolution of a C_3-C_4 intermediate pathway in *Glossopteris* leaves at Skaar Ridge may represent an adaptation to continuous light as well as an adaptation to low CO_2. Leaves used in this analysis are from the late Permian and would have lived under higher CO_2 levels than *Glossopteris* leaves from the early and middle Permian.

3. Leaf economics

An analysis of the leaf mass per area (LMA) of Permian leaves from Antarctica (Table 15), particularly those from Skaar Ridge, gives several insights into how *Glossopteris* leaves fit into functional groups and habitats compared to extant plants. The predictive intervals for *Glossopteris* LMA from some localities were rather large due to small data sets. These predictive intervals spanned a large enough range of functional groups and habitats that unbiased interpretation is impossible. The data set of *Glossopteris* leaves from Skaar Ridge was the largest by far in this analysis and provided the most useful predictive interval for analysis. The predictive interval spanned the range of LMAs associated with both deciduous and evergreen leaves (PI: 96.6–129.4 g m^{-2}), similar to the tree ring analysis by Taylor and Ryberg (2007). The possibility of deciduous or evergreen plants growing in warm, high-latitude environments has become controversial of late (Royer et al., 2003, 2005a; Osborne et al., 2004b). Although an initial examination of this data may suggest that the technique failed to resolve any questions, the LMA range from these localities may very well extend into the range for evergreen plants due to the effects of CO_2 and high latitude light conditions. Since LMA increases with CO_2 concentration and light (Poorter et al., 2009), the LMA of late Permian *Glossopteris* leaves was likely larger do to these factors. Since the range of LMA for certain functional groups in extant plants was determined under ambient CO_2 and a normal diurnal light pattern, the LMA of *Glossopteris* leaves exposed to elevated CO_2 (Figure 2) and continuous light conditions (Figure

1) would appear high relative to extant leaves. Additionally, if *Glossopteris* leaves are able to avoid downregulation of photosynthesis under continuous light, the LMA could increase due to an increase in photosynthates similar to that seen in *Metasequoia glyptostroboides* grown under experimental continuous light conditions (Equiza et al., 2006b). *Metasequoia glyptostroboides* avoided downregulation of photosynthesis when other gymnosperms could not due to its utilization of carbon sinks (Jagels and Day, 2004; Equiza et al., 2006b). It produced larger leaves than *M. glyptostroboides* grown under diurnal light conditions and continued to produce new biomass through leaves on long shoots, short shoots, and epicormic shoots; these are all characteristics found in the glossopterids (Plumstead, 1958; Pant and Singh, 1974; Gould and Delevoryas, 1977; Retallack and Dilcher, 1988; Decombeix et al., 2010). This suggests that the glossopterids living in high latitudes had deciduous leaves and adaptations that allowed them to thrive in a continuous light environment. Such an adaptation to continuous light conditions provides further reasoning for the dominance of the glossopterids during the late Permian, particularly at high latitudes.

4. Future directions

The research described herein provides a foundation for several new areas of investigation. Although the data sets used in this study are significant, analysis and interpretations will continuously be improved by increasingly larger data sets. From Permian localities, a larger sample of *Noeggerathiopsis* and *Gangamopteris* leaves may make comparisons to *Glossopteris* more meaningful. With more of these leaf types, other Permian genera can be studied for changes in physiological characteristics associated with latitude and CO_2 levels. This will not be especially easy since the reduced number of these leaf morphotypes, even in the fossil collection at KU, is not due to a collection bias, but rather because they

represent a smaller component of the biodiversity in time and space. An increase in specimens from non-Antarctic Gondwanan localities should also improve the ability to examine the effects of latitude. Paleolatitude estimates for Permian fossil localities would also greatly benefit this study. This will also be difficult due to the lack of unaltered rocks for gathering paleomagnetic data.

The analysis of leaf morphotypes from the Middle and Late Triassic of Antarctica will also benefit from an increased data set. There were fewer Triassic samples with the appropriate preservation that could be used in this research. Additionally, the samples came from fewer localities and formations than the Permian specimens. The lack of adequate specimens from localities at a variety of latitudes made it impossible to carry out any analysis of latitude. It will be interesting to see if the analyses of Triassic leaf types demonstrate the same sort of issues concerning latitude that became apparent with the Permian analysis. The nature of the *Dicroidium* leaf morphotype also made it impossible to study the LMA of the Triassic. The regression equations of Royer et al. (2007, 2010) do not work with fern-like compound leaves. A new scaling relationship that would work with *Dicroidium*-type leaves is currently being developed by others (Royer, personal communication). It seems likely that there would be large differences in the LMA of leaves from the Permian and Triassic localities studied here. The temperature of the Middle and Late Triassic appears to have favored smaller, more dissected leaves that should have a substantially different LMA from *Glossopteris* leaves.

These techniques can also be used to study other geographic areas and geologic times. The fluctuations of the Earth's climate provides numerous opportunities to study the effects of climate change on past plant life. Other high latitude fossils can be examined to determine if the findings in this dissertation have a narrow or broader applications to other fossil groups and

environments. We are witnessing a major paradigm shift in many areas of paleobiology relative to discussions of deep time climate and the effects of these environments on the biology and evolution of the biota. Because of the large amount of biomass produced by plants and their relative ease of preservation in a large number of differing environments, the proxy records of climate stability and shift will increasingly become more important. Exploring questions that link deep time environment and plant growth can now be addressed with greater levels of resolution and confidence. Finally, the integration of such data as presented here can now make it possible to effectively trace parameters such as the physiology of the plant and adaptations to increasing global warming.

Table 1. List of Permian Localities and Genera Analyzed at Each Locality

Locality	*Gangamopteris*	*Glossopteris*	*Noeggerathiopsis*
Allan Hills	●	●	
Aztec Mt.	●	●	
Bazargaon, India		●	
Bowden Neve		●	
Canopy Cliffs		●	
Clarkson Peak		●	●
Coalsack Bluff		●	
Crack Bluff		●	
Cranfield Peak		●	
Erehwon Nunatak		●	
Graphite Peak		●	
Horlick Mts.		●	
Illawarra Coal Measures, Australia		●	
Kennar Valley	●	●	●
KwaZulu-Natal, South Africa		●	
Laguna Polina, Argentina		●	
Leaia Ledge		●	
McIntyre Promontory		●	
McKay Cliffs		●	
Mine Ledge		●	
Moraine Ridge		●	
Mt. Achernar		●	
Mt. Baldwin		●	
Mt. Bartlett		●	
Mt. Bastion		●	
Mt. Feather		●	●
Mt. Fleming	●	●	
Mt. Glossopteris		●	
Mt. Gran	●	●	
Mt. Howe		●	
Mt. Kinsey		●	
Mt. MacPherson		●	
Mt. Picciotto		●	
Mt. Ropar		●	
Mt. Rosenwald		●	
Mt. Schopf		●	
Mt. Sirius		●	
Mt. Weaver		●	
Mt. Wild		●	
Orange Free State, South Africa		●	
Pecora Nunatak	●	●	
Polarstar Peak		●	
Roaring Cliffs		●	
Robison Peak	●	●	●
Rubble Ridge		●	

Table 1. Continued

Locality	*Gangamopteris*	*Glossopteris*	*Noeggerathiopsis*
Sandford Cliffs		●	
Sierra de Pillahuinco, Argentina		●	
Skaar Ridge		●	
Terrace Ridge		●	●
Tillite Ridge		●	●
Waterberg Coal Field, South Africa		●	
Zimbabwe		●	

Table 2. List of Triassic Localities and Genera Analyzed at Each Locality

Locality	*Cladophlebis*	*Dejerseya*	*Dicroidium*	*Hediphyllum*	*Osmunda*	*Sphenobaiera*	*Taeniopteris*
Alfie's Elbow		•	•	•			•
Allan Hills			•	•	•		•
Dinmore, Australia			•			•	•
Fremouw Peak			•				
Gordon Valley			•				
Marshall Mountains			•			•	•
Molteno, South Africa			•	•			
Mt. Bumstead							•
Mt. Falla		•	•	•		•	•
Mt. Wisting	•						
Shapeless Mountain			•				
Umkomaas Valley, South Africa							•

Table 3. Summary of *Glossopteris* hydraulic characteristics by locality. K_{leaf} = leaf hydraulic conductance, gs = stomatal conductance, Pc = maximum photosynthetic capacity, and WUE = water use efficiency

Locality	Sample Size	Venation density	K_{leaf}	g_s	P_c	WUE
Allan Hills	57	10.1	11.84	239.9	12.2	0.05
Aztec Mt.	32	9.68	11.73	237.7	12.11	0.05
Bazargaon, India	3	8.6	11.01	223	11.49	0.05
Bowden Neve	14	8.62	11.31	229.1	11.77	0.05
Canopy Cliffs	2	8.3	11.05	223.9	11.55	0.05
Clarkson Peak	2	9.34	11.39	230.7	11.82	0.05
Coalsack Bluff	57	8.47	11.26	228.1	11.72	0.05
Crack Bluff	25	8.96	11.41	231.2	11.85	0.05
Cranfield Peak	6	10.4	11.89	240.9	12.24	0.05
Erehwon Nunatak	8	8.04	11.11	225.1	11.61	0.05
Graphite Peak	7	10.13	11.81	239.3	12.18	0.05
Hampton Hill	1	10.49	11.99	242.9	12.32	0.05
Horlick Mts.	2	10.43	11.82	239.4	12.17	0.05
Illawarra Coal Measures, Australia	26	7.25	10.67	216.2	11.24	0.05
Kennar Valley	3	9.83	11.81	239.3	12.18	0.05
KwaZulu-Natal, South Africa	4	8.77	11.05	223.9	11.54	0.05
Laguna Polina, Argentina	4	10.74	11.98	242.8	12.31	0.05
Leaia Ledge	13	8.58	11.32	229.4	11.78	0.05
McIntyre Promontory	25	10.53	11.87	240.5	12.22	0.05
McKay Cliffs	1	7.86	11.11	225	11.61	0.05
Mill Glacier	1	7.26	10.8	218.9	11.36	0.05
Mine Ledge	17	8.78	11.44	231.8	11.88	0.05
Moraine Ridge	3	11.09	11.9	241.1	12.23	0.05
Mt. Achernar	205	8.57	11.28	228.6	11.75	0.05
Mt. Baldwin	10	10.29	11.88	240.6	12.23	0.05
Mt. Bartlett	5	8.31	10.94	221.6	11.44	0.05
Mt. Bastion	4	11.08	12.08	244.8	12.39	0.05
Mt. Feather	9	11.75	12.13	245.7	12.42	0.05
Mt. Glossopteris	7	8.68	11.27	228.3	11.73	0.05
Mt. Gran	5	11.17	12.13	245.8	12.43	0.05
Mt. Howe	18	8.52	11.27	228.3	11.73	0.05
Mt. Kinsey	1	10.88	12.08	244.7	12.39	0.05
Mt. MacPherson	2	10.08	11.89	240.8	12.24	0.05
Mt. Picciotto	19	11.18	12.04	243.9	12.35	0.05
Mt. Ropar	5	7.66	10.95	221.9	11.48	0.05
Mt. Rosenwald	4	8.25	11.23	227.6	11.71	0.05
Mt. Schopf	2	8.23	11.25	227.9	11.73	0.05
Mt. Sirius	34	9.18	11.52	233.3	11.94	0.05
Mt. Weaver	6	7.64	10.99	222.6	11.51	0.05
Mt. Wild	6	10.48	11.97	242.6	12.3	0.05
Mt. Wisting	1	9.52	11.73	237.6	12.11	0.05

Table 3. Continued

Locality	Sample Size	Venation density	K_{leaf}	g_s	P_c	WUE
Orange Free State, South Africa	1	6.01	9.98	202.1	10.66	0.05
Pecora Nunatak	39	12.08	12.22	247.6	12.49	0.05
Polarstar Peak	107	9.2	11.56	234.2	11.98	0.05
Roaring Cliffs	8	8.78	11.24	227.8	11.71	0.05
Robison Peak	4	8.65	11.42	231.3	11.86	0.05
Rubble Ridge	21	8.35	11.24	227.7	11.72	0.05
Sandford Cliffs	4	7.99	11.09	224.6	11.59	0.05
Sierra de Pillahuinco, Argentina	2	9.81	11.67	236.4	12.06	0.05
Skaar Ridge	415	8.67	11.33	229.6	11.79	0.05
Terrace Ridge	46	8.82	11.36	230.2	11.81	0.05
Tillite Ridge	11	10	11.79	238.9	12.16	0.05
Waterberg Coal Field, South Africa	3	8.38	11.29	228.7	11.76	0.05
Zimbabwe	2	9.72	11.71	237.3	12.09	0.05

Table 4. Summary of *Gangamopteris* hydraulic characteristics by locality. K_{leaf} = leaf hydraulic conductance, gs = stomatal conductance, Pc = maximum photosynthetic capacity, and WUE = water use efficiency

Locality	Sample Size	Venation density	K_{leaf}	g_s	P_c	Intrinsic WUE
Allan Hills	5	7.62	10.88	220.3	11.41	0.05
Aztec Mt.	15	7.91	11.07	224.2	11.58	0.05
Kennar Valley	2	8.93	11.53	233.5	11.95	0.05
Mt. Fleming	1	5.17	9.22	186.9	9.99	0.05
Mt. Gran	9	8.18	11.11	225.2	11.61	0.05
Pecora Nunatak	2	9.24	10.76	218	11.26	0.05
Robison Peak	8	6.86	10.51	212.9	11.11	0.05

Table 5. Summary of *Noeggerathiopsis* hydraulic characteristics by locality. K_{leaf} = leaf hydraulic conductance, gs = stomatal conductance, Pc = maximum photosynthetic capacity, and WUE = water use efficiency

Locality	Sample Size	Venation density	K_{leaf}	g_s	P_c	Intrinsic WUE
Clarkson Peak	1	7.79	11.08	224.4	11.59	0.05
Kennar Valley	7	6.06	9.98	202.1	10.66	0.05
Mt. Feather	1	8.55	11.4	230.9	11.85	0.05
Robison Peak	1	9.33	11.67	236.4	12.07	0.05
Terrace Ridge	1	6.62	10.42	211.1	11.04	0.05
Tillite Ridge	2	6.03	9.96	201.8	10.64	0.05

Table 6. Summary of *Cladophlebis* hydraulic characteristics by locality. K_{leaf} = leaf hydraulic conductance, gs = stomatal conductance, Pc = maximum photosynthetic capacity, and WUE = water use efficiency

Locality	Sample Size	Venation density	K_{leaf}	g_s	P_c	Intrinsic WUE
Mt. Wisting	2	4.8	8.5	190.4	9.23	0.05

Table 7. Summary of *Dejerseya* hydraulic characteristics by locality. K_{leaf} = leaf hydraulic conductance, gs = stomatal conductance, Pc = maximum photosynthetic capacity, and WUE = water use efficiency

Locality	Sample Size	Venation density	K_{leaf}	g_s	P_c	Intrinsic WUE
Alfie's Elbow	1	4.53	8.51	172.4	9.33	0.05
Mt. Falla	7	4.99	8.96	181.5	9.74	0.05

Table 8. Summary of *Dicroidium* hydraulic characteristics by locality. K_{leaf} = leaf hydraulic conductance, gs = stomatal conductance, Pc = maximum photosynthetic capacity, and WUE = water use efficiency

Locality	Sample Size	Venation density	K_{leaf}	g_s	P_c	Intrinsic WUE
Alfie's Elbow	59	4.72	8.65	175.3	9.45	0.05
Allan Hills	59	4.81	8.73	176.9	9.52	0.05
Dinmore, Australia	15	5.88	9.84	199.4	10.54	0.05
Fremouw Peak	3	4.75	8.75	177.3	9.56	0.05
Gordon Valley	7	4.8	8.76	177.5	9.55	0.05
Marshall Mountains	17	5.1	9.08	183.9	9.85	0.05
Molteno, South Africa	1	4.23	8.13	164.7	8.98	0.05
Mt. Falla	23	4.64	8.55	173.2	9.35	0.05
Shapeless Mountain	12	4.55	8.48	171.8	9.3	0.05

Table 9. Summary of *Heidiphylum* hydraulic characteristics by locality. K_{leaf} = leaf hydraulic conductance, gs = stomatal conductance, Pc = maximum photosynthetic capacity, and WUE = water use efficiency

Locality	Sample Size	Venation density	K_{leaf}	g_s	P_c	Intrinsic WUE
Alfie's Elbow	18	2.57	5.28	106.9	6.05	0.05
Allan Hills	13	2.96	6.01	121.7	6.82	0.05
Molteno, South Africa	7	2.6	5.36	108.5	6.14	0.05
Mt. Falla	16	2.79	5.74	116.2	6.55	0.05

Table 10. Summary of *Osmunda* hydraulic characteristics by locality. K_{leaf} = leaf hydraulic conductance, gs = stomatal conductance, Pc = maximum photosynthetic capacity, and WUE = water use efficiency

Locality	Sample Size	Venation density	K_{leaf}	g_s	P_c	Intrinsic WUE
Alfie's Elbow	1	4.44	8.41	170.3	9.24	0.05
Allan Hills	9	4.53	8.49	172	9.32	0.05

Table 11. Summary of *Sphenobaiera* hydraulic characteristics by locality. K_{leaf} = leaf hydraulic conductance, gs = stomatal conductance, Pc = maximum photosynthetic capacity, and WUE = water use efficiency

Locality	Sample Size	Venation density	K_{leaf}	g_s	P_c	Intrinsic WUE
Dinmore, Australia	1	6.01	9.98	202.2	10.66	0.05
Marshall Mountains	2	3.76	7.44	150.7	8.31	0.05
Mt. Falla	1	4.04	7.87	159.5	8.73	0.05

Table 12. Summary of *Taeniopteris* hydraulic characteristics by locality. K_{leaf} = leaf hydraulic conductance, gs = stomatal conductance, Pc = maximum photosynthetic capacity, and WUE = water use efficiency

Locality	Sample Size	Venation density	K_{leaf}	g_s	P_c	Intrinsic WUE
Alfie's Elbow	3	4.45	8.21	166.3	9.02	0.05
Allan Hills	4	7.26	10.74	217.5	11.3	0.05
Dinmore, Australia	4	5.39	9.26	187.6	10	0.05
Marshall Mountains	3	5.8	9.71	196.8	10.41	0.05
Mt. Bumstead	1	6.54	10.37	210	10.99	0.05
Mt. Falla	5	3.73	7.37	149.3	8.23	0.06
Umkomaas Valley, South Africa	1	4.35	8.29	167.9	9.13	0.05

Table 13. Measurements of permineralized *Glossopteris* leaf tissue from Skaar Ridge, Antarctica. PCA = Photosynthetic carbon assimilation tissue, PCR = Photosynthetic carbon reduction tissue. Measurement technique from Muhaidat et al. (2007).

Specimen	PCA:PCR area	PCA perimeter:PCR area	Epidermis Percentage
13688 D top #2	6.46	0.052	
13752 A-1 bot #3 Leaf A	3.21	0.041	
13752 A-1 bot #3 Leaf C	5.46	0.038	
13752 A-1 bot #3 Leaf D	4.1	0.029	
13752 A-1 bot #3 Leaf E	5.37	0.064	20.1
13752 A-1 bot #3 Leaf F	4.13	0.035	
13752 A-2 bot #1 Leaf A	4.42	0.057	
13752 A-2 bot #1 Leaf B	3.12	0.042	
13752 A-2 bot #3 Leaf A	8.13	0.037	
13752 A-5 top #2 Leaf A	10.5	0.039	
13752 A-5 top #2 Leaf B	4.88	0.068	
13752 A-5 top #2 Leaf C	5.84	0.049	
13752 A-5 top #2 Leaf D	4.98	0.058	
13752 A-5 top #2 Leaf E	8.28	0.068	
13752 B-1 bot #2 Leaf A	5.83	0.041	25.6
13752 B-1 bot #2 Leaf B	4.05	0.037	
13752 B-1 bot #2 Leaf C	6.66	0.039	
13752 B-1 bot #2 Leaf D	4.31	0.029	
13752 B-1 top #2 Leaf A	5.8	0.047	
13752 B-1 top #2 Leaf B	4.94	0.038	
13752 B-1 top #2 Leaf C	5.02	0.054	
13752 B-1 top #2 Leaf D	3.8	0.036	
13752 B top #3 beta Leaf A	7.53	0.056	
13752 B top #10 Leaf A	5.26	0.032	

Table 14. Stable Carbon Isotope Data for Permian Leaves. All leaves are *Glossopteris*, except for two *Schizoneura* samples (Pm 2552). VPDB = Vienna Pee Dee Belemnite.

Specimens	Carbon isotope enrichment ($\delta^{13}C$ VPDB)	Carbon isotope discrimination (Δ)
13702 B-1	-27.86	23.9 to 25.8
13702 B-2	-28.93	25.1 to 26.9
70-1-42-A	-26.69	22.7 to 24.5
70-1-42-B	-27.20	23.2 to 25.1
PM 171b	-24.17	20.1 to 22.4
PM 3002	-23.68	19.5 to 21.4
PM 4067	-22.26	18.1 to 20.4
PM 72b	-22.44	18.2 to 20.6
PM 2552 Sample 1	-25.52	21.5 to 23.3
PM 2552 Sample 2	-25.01	20.9 to 22.8

Table 15. Leaf mass per area predictive intervals for *Glossopteris* leaves by locality

Locality	Sample Size	LMA Predictive Interval (g m^{-2})	Average LMA (g m^{-2})
Allan Hills	22	99.8 to 146.1	120.8
Aztec Mountain	9	87.2 to 148.5	113.8
Bazargaon, India	1	57.2 to 235.1	116.0
Coalsack Bluff	1	56.2 to 231.3	114.1
Leaia Ledge	1	56.4 to 231.9	114.3
Mt. Achernar	1	53.4 to 220.4	108.5
Mt. Feather	1	47.8 to 199.0	97.5
Mt. Fleming	1	55.1 to 226.9	111.8
Mt. Ropar	1	51.9 to 214.6	105.5
Mt. Weaver	1	50.8 to 210.5	103.4
Mt. Wild	1	46.9 to 195.7	95.8
Polarstar Peak	4	77.1 to 162.2	111.9
Skaar Ridge	132	96.6 to 129.4	111.8
Terrace Ridge	8	78.0 to 141.2	106.3

Page left intentionally blank.

Figure 1. A contour plot of the hours of daylight as a function of latitude and day of the year. This is a public domain image from Wikimedia Commons.

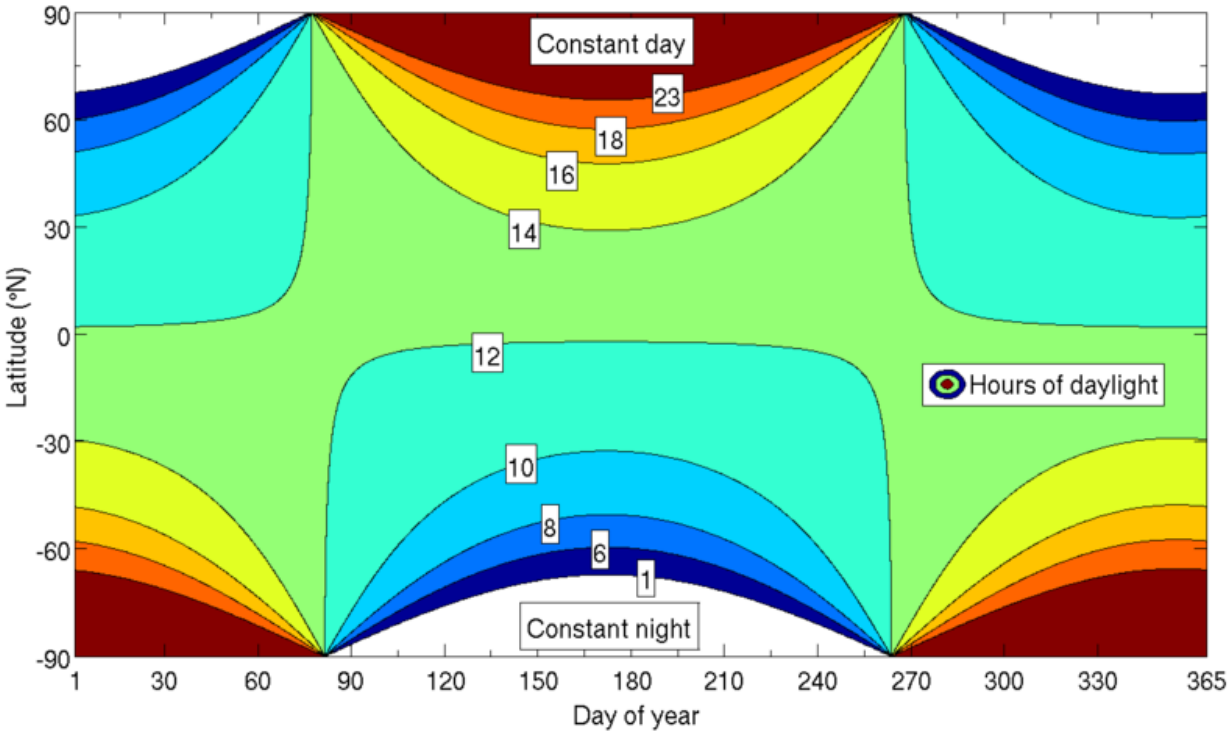
Constant day
23
18
16
14
12
10
8
6
1
Constant night
Hours of daylight
Latitude (°N)
Day of year
90
60
30
0
-30
-60
-90
1
30
60
90
120
150
180
210
240
270
300
330
365

Figure 2. A plot of the partial pressure of atmospheric CO_2 and O_2 from 500 Ma to the present. The blue portion of the graph marks the Permian, the green portion the Triassic, and the yellow portion the Oligocene. The data are based on geochemical models of Earth's atmospheric evolution (Berner, 2005). The image is modified from Osborne and Beerling (2006).

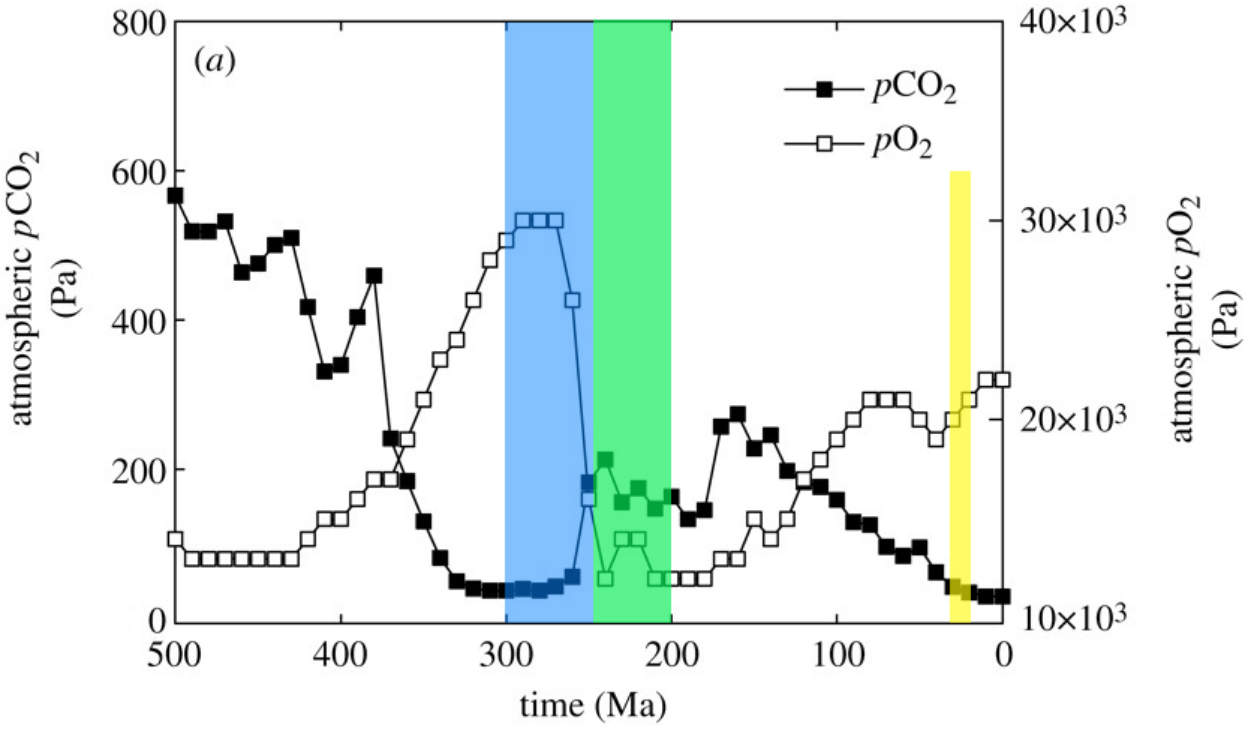
(a)
pCO_2
pO_2
atmospheric pCO_2 (Pa)
atmospheric pO_2 (Pa)
800
600
400
200
0
40×10³
30×10³
20×10³
10×10³
500
400
300
200
100
0
time (Ma)

Figure 3. Calculated changes in global mean surface temperature from 500 Ma to the present. Calculated temperatures are based on a model of planetary energy balance that reduces latitude, altitude, and longitude into a single global mean temperature for a given atmospheric CO_2 concentration. The solar forcing data attempt to account for changes in the Sun's output through time. The blue portion of the graph marks the Permian, the green portionthe Triassic, and the yellow portion the Oligocene. The image is modified from Osborne and Beerling (2006).

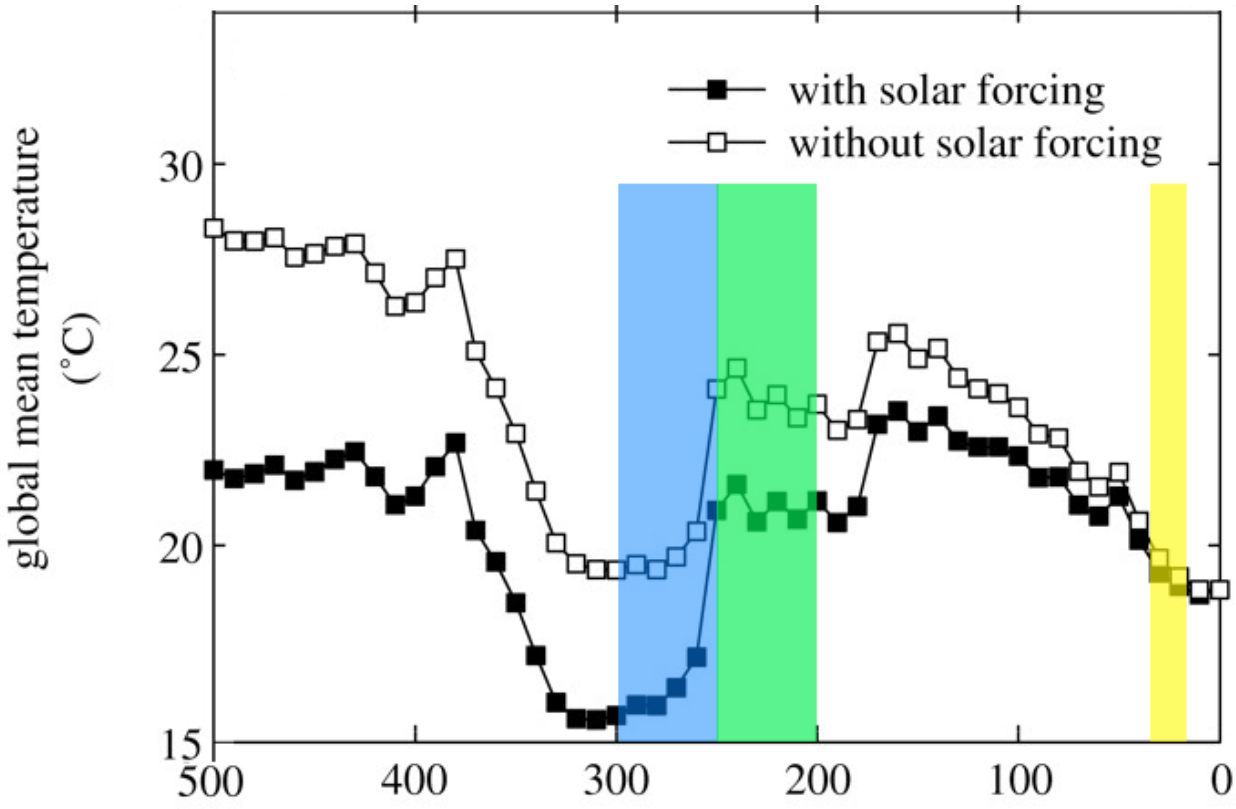
with solar forcing
without solar forcing
global mean temperature
(°C)
30
25
20
15
500
400
300
200
100
0

Figure 4. Compression fossils of dominant leaf morphotypes (A) *Glossopteris* and (B) *Dicroidium*. Scale bars = 2 cm.


A
B

Figure 5. Map of Permian fossil localities from Antarctica.

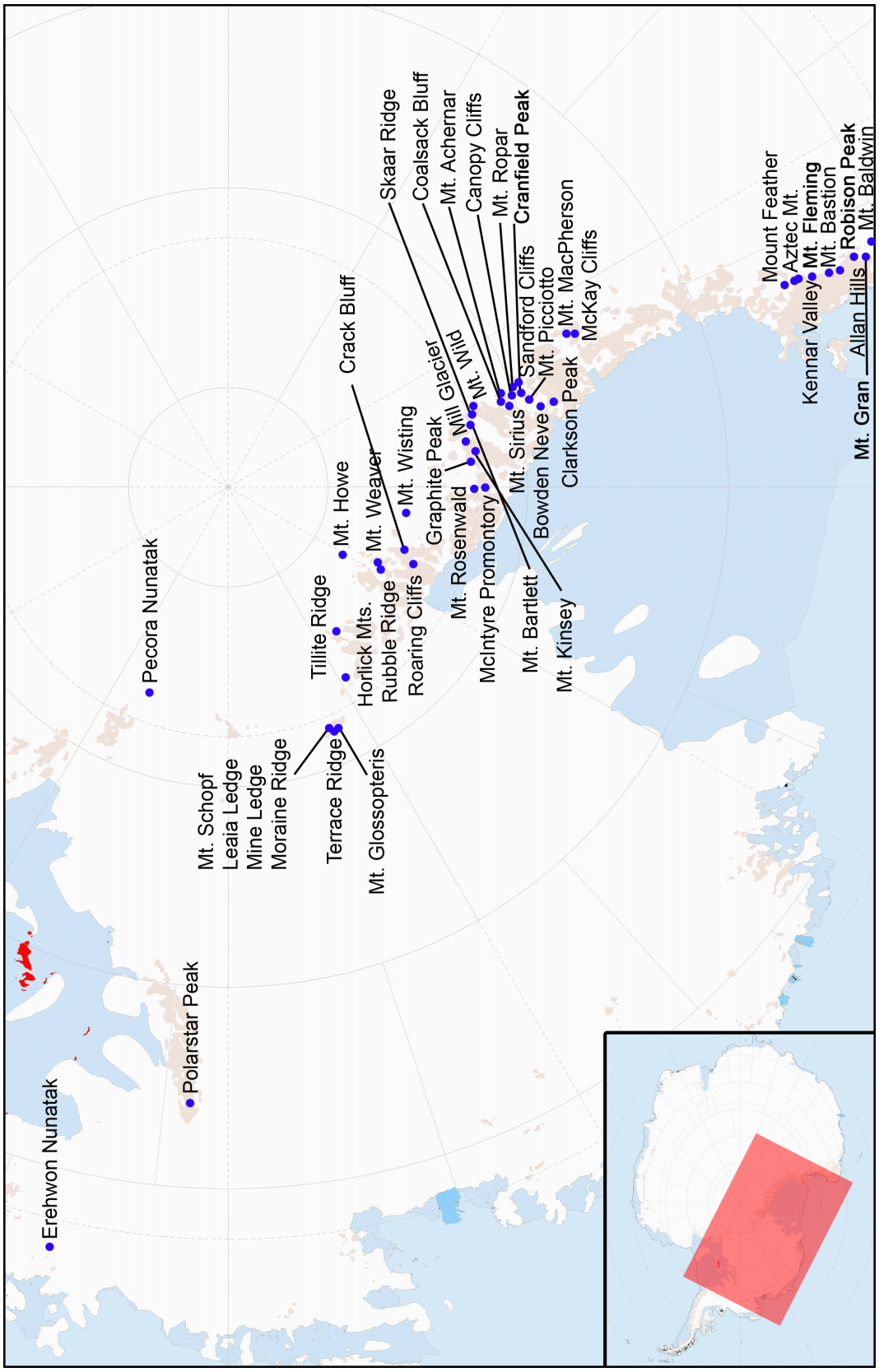
Erehwon Nunatak
Polarstar Peak
Pecora Nunatak
Mt. Schopf
Leaia Ledge
Mine Ledge
Moraine Ridge
Terrace Ridge
Mt. Glossopteris
Tillite Ridge
Horlick Mts.
Rubble Ridge
Roaring Cliffs
Mt. Howe
Crack Bluff
Mt. Weaver
Mt. Wisting
Graphite Peak
Mt. Rosenwald
McIntyre Promontory
Mill Glacier
Mt. Wild
Mt. Bartlett
Mt. Sirius
Skaar Ridge
Coalsack Bluff
Mt. Achernar
Canopy Cliffs
Mt. Ropar
Cranfield Peak
Sandford Cliffs
Mt. Picciotto
Bowden Neve
Mt. Kinsey
Clarkson Peak
Mt. MacPherson
McKay Cliffs
Mount Feather
Aztec Mt.
Kennar Valley
Mt. Fleming
Mt. Bastion
Robison Peak
Mt. Baldwin
Mt. Gran
Allan Hills

Figure 6. Map of Triassic fossil localities from Antarctica.

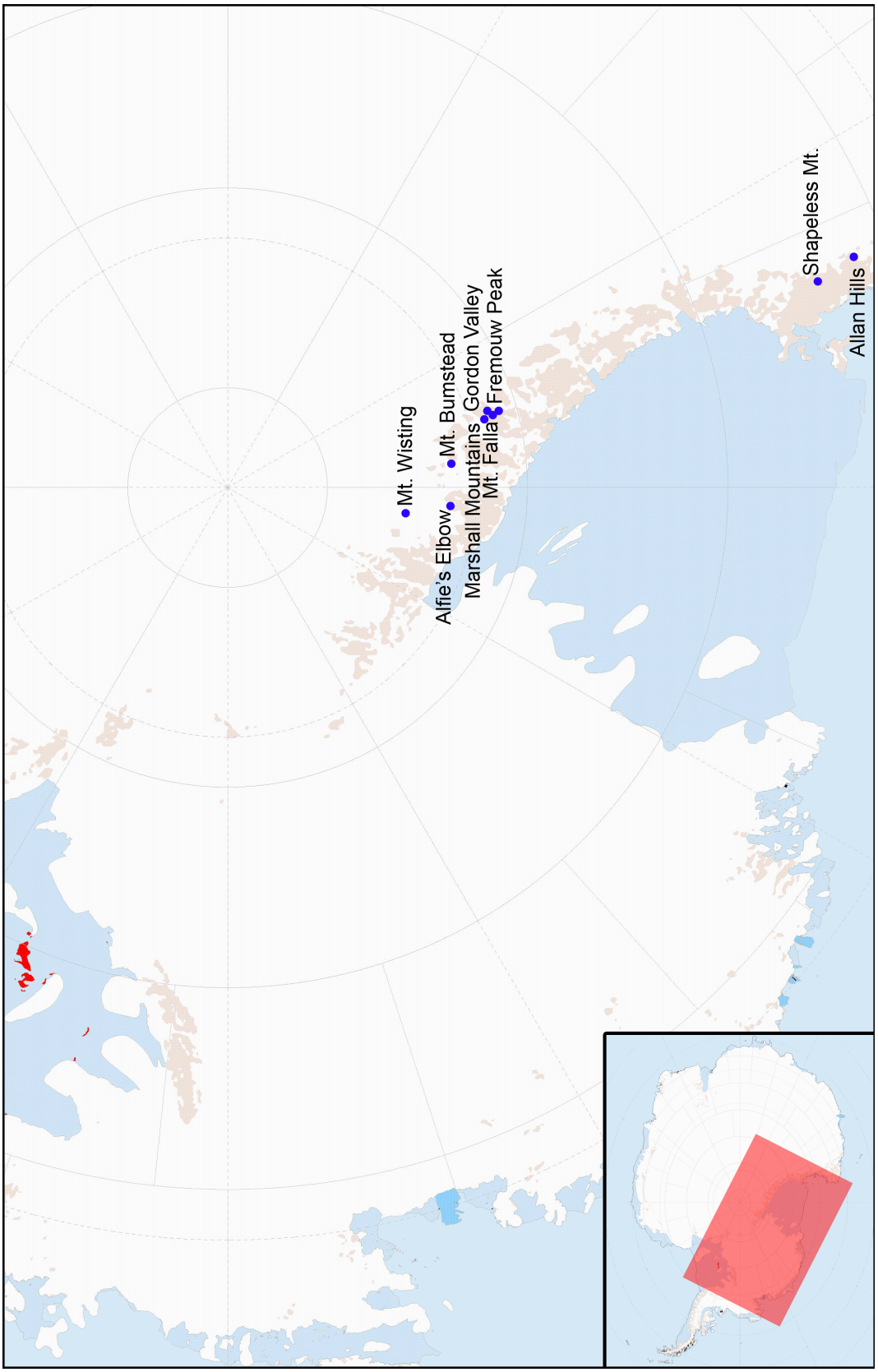
Mt. Wisting
Mt. Bumstead
Alfie's Elbow
Marshall Mountains
Gordon Valley
Mt. Falla
Fremouw Peak
Shapeless Mt.
Allan Hills

Figure 7. Generalized stratigraphic section of southern Victoria Land. 1. Allan Hills, 2. Aztec Mt., 3. Kennar Valley, 4. Mt. Feather, 5. Mt. Fleming, 6. Robison Peak, 7. Allan Hills, 8. Shapeless Mountain, 9. Mt. Bumstead. Modified from Collinson et al. (1994).

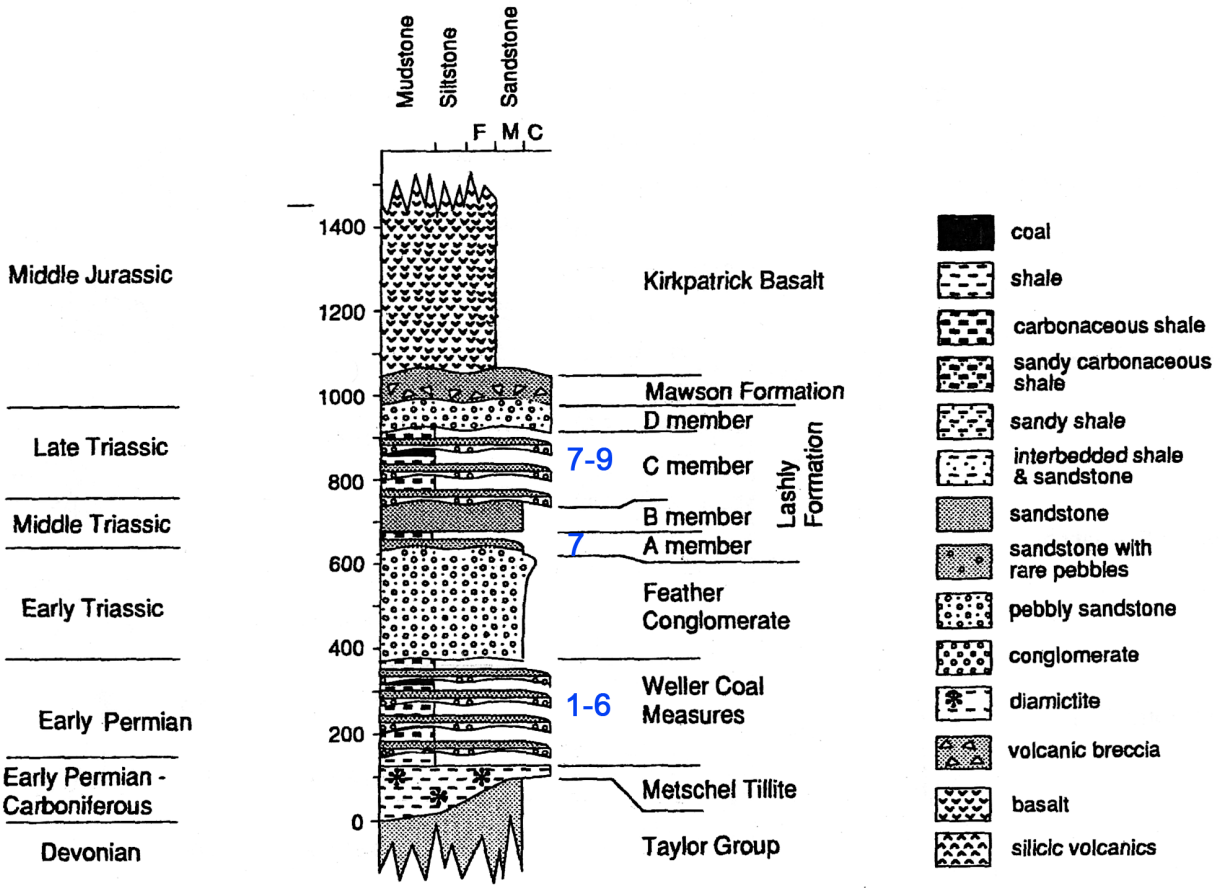
Mudstone
Siltstone
Sandstone
F M C
1400
1200
1000
800
600
400
200
0
Middle Jurassic
Late Triassic
Middle Triassic
Early Triassic
Early Permian
Early Permian - Carboniferous
Devonian
Kirkpatrick Basalt
Mawson Formation
D member
7-9
C member
B member
7
A member
Lashly Formation
Feather Conglomerate
1-6
Weller Coal Measures
Metschel Tillite
Taylor Group
coal
shale
carbonaceous shale
sandy carbonaceous shale
sandy shale
interbedded shale & sandstone
sandstone
sandstone with rare pebbles
pebbly sandstone
conglomerate
diamictite
volcanic breccia
basalt
silicic volcanics

Figure 8. Generalized stratigraphic section of the Beardmore Glacier Region. 1. Cranfield Peak, 2. McIntyre Promontory, 3. Mt. Picciotto, 4. McKay Cliffs, 5. Mt. MacPherson. 6. Bowden Neve, 7. Clarkson Peak, 8. Coalsack Bluff, 9. Graphite Peak, 10. Mt. Achernar, 11. Mt. Ropar, 12. Mt. Rosenwald, 13. Mt. Sirius, 14. Skaar Ridge, 15. Mt. Wild, 16. Canopy Cliffs, 17. Mt. Bartlett, 18. Mt. Kinsey, 19. Sandford Cliffs, 20. Fremouw Peak, 21. Gordan Valley, 22. Mt. Falla, 23. Marshall Mountains. Symbols in Figure 5. Modified from Collinson et al. (1994).

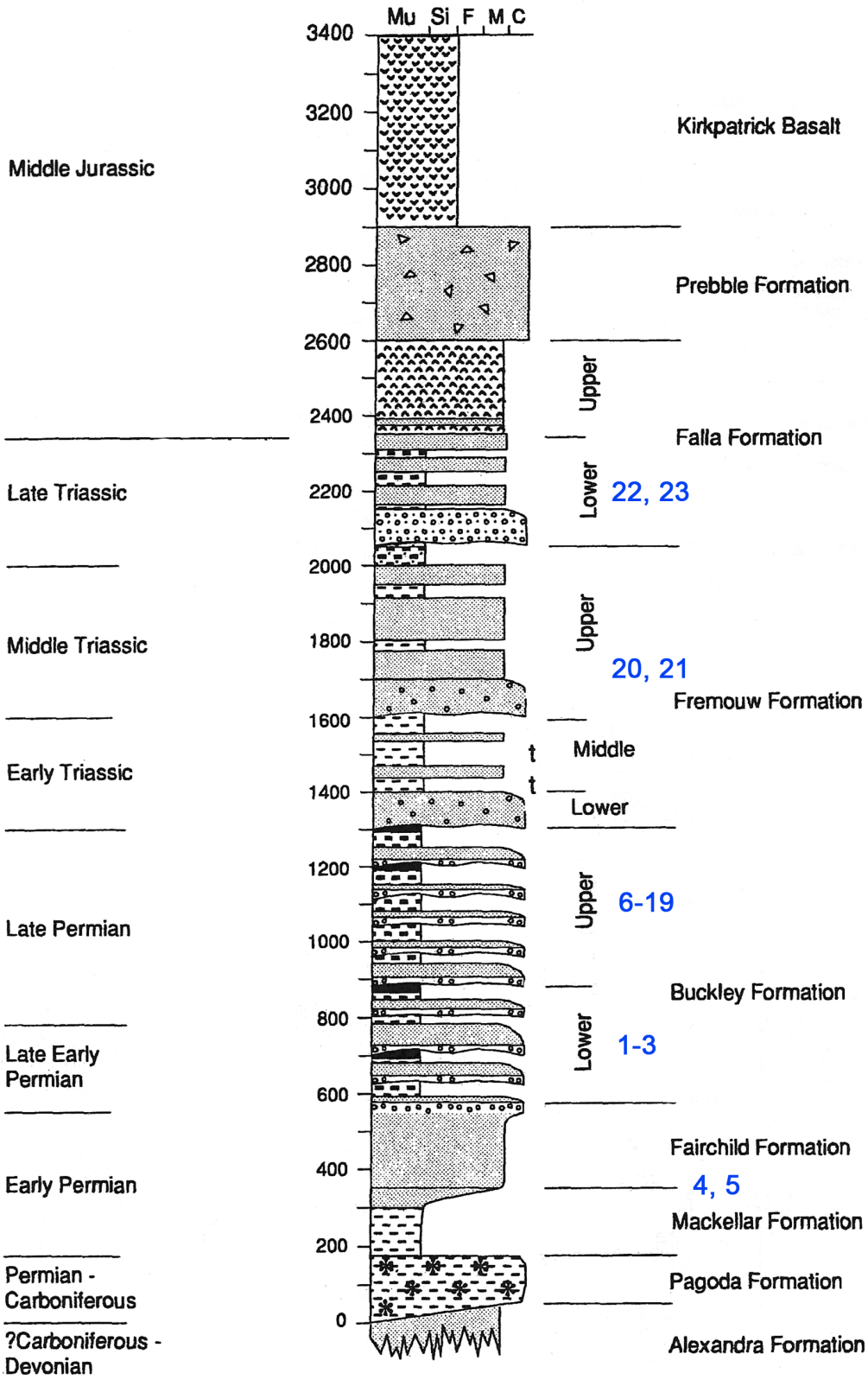
Mu Si F M C
3400
3200
3000
2800
2600
2400
2200
2000
1800
1600
1400
1200
1000
800
600
400
200
0
Middle Jurassic
Late Triassic
Middle Triassic
Early Triassic
Late Permian
Late Early Permian
Early Permian
Permian - Carboniferous
?Carboniferous - Devonian
Kirkpatrick Basalt
Prebble Formation
Upper
Falla Formation
Lower
22, 23
Upper
20, 21
Fremouw Formation
t
Middle
t
Lower
Upper
6-19
Buckley Formation
Lower
1-3
Fairchild Formation
4, 5
Mackellar Formation
Pagoda Formation
Alexandra Formation

Figure 9. Correlation chart of Antarctic strata. 1. Mt. Baldwin, 2. Mt. Gran (Member of Mt. Bastion Formation, but correlated with the Weller Coal Measures), 3. Mt. Bastion (same as Mt. Gran), 4. Pecora Nunatak, 5. Tillite Ridge, 6. Roaring Cliffs, 7. Mt. Howe, 8. Crack Bluff, 9. Erehwon Nunatak. Modified from Collinson et al. (1994).

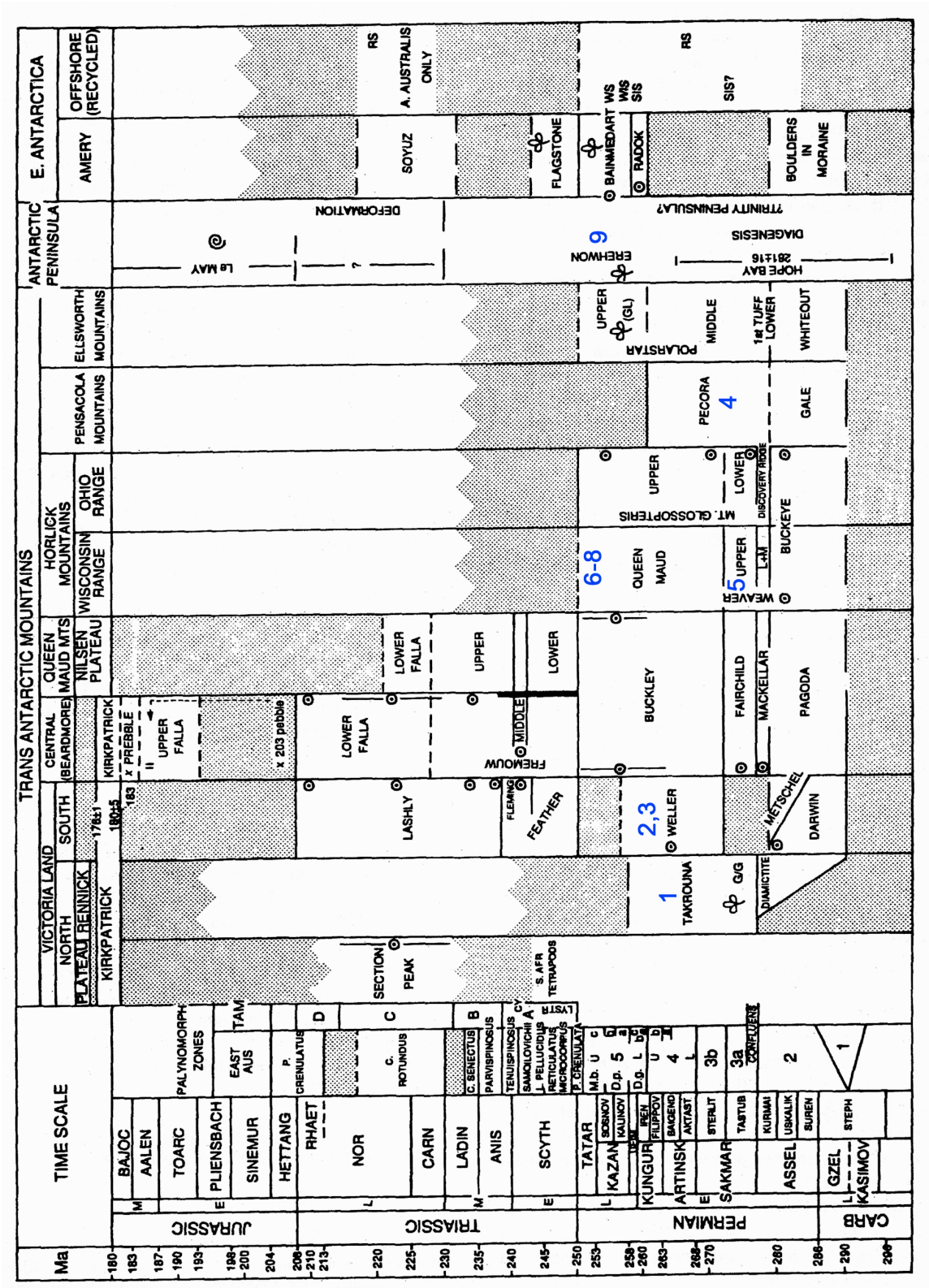
TRANS ANTARCTIC MOUNTAINS
ANTARCTIC PENINSULA
E. ANTARCTICA
TIME SCALE
Ma
VICTORIA LAND
NORTH
SOUTH
CENTRAL (BEARDMORE)
QUEEN MAUD MTS
HORLICK MOUNTAINS
PENSACOLA MOUNTAINS
ELLSWORTH MOUNTAINS
AMERY
OFFSHORE (RECYCLED)
PLATEAU
RENNICK
KIRKPATRICK
NILSEN PLATEAU
WISCONSIN RANGE
OHIO RANGE
PALYNOMORPH ZONES
EAST AUS
TAM
JURASSIC
TRIASSIC
PERMIAN
CARB
BAJOC
AALEN
TOARC
PLIENSBACH
SINEMUR
HETTANG
RHAET
NOR
CARN
LADIN
ANIS
SCYTH
TATAR
KAZAN
KUNGUR
ARTINSK
SAKMAR
ASSEL
GZEL
KASIMOV
P. CRENULATUS
C. ROTUNDUS
C. SENECTUS
PARVISPINOSUS
TENUISPINOSUS
SAMOILOVICHI
L. PELLUCIDUS
RETICULATUS
MICROCORNUS
P. CRENULATA
S. AFR TETRAPODS
SECTION
PEAK
LYSTR
SOSNOV
KAZANOV
IREN
FILIPPOV
BAIGEND
ARTAST
STERLIT
TASTUB
KURMAI
USKALIK
BURER
STEPH
M.b. U c
D.p. 5 c b a
D.g. L b a
U 4 L
3b
3a CONFLUENT
2
1
D
C
B
A
CY
LYSTR
x 203 pebble
x PREBBLE
UPPER FALLA
LOWER FALLA
UPPER
LOWER
MIDDLE
FREMOUW
FLEMING
FEATHER
LASHLY
BUCKLEY
FAIRCHILD
MACKELLAR
PAGODA
WEAVER
QUEEN MAUD
BUCKEYE
DISCOVERY RIDGE
MT. GLOSSOPTERIS
PECORA
GALE
1st TUFF
WHITEOUT
POLARSTAR
HOPE BAY 281416
DIAGENESIS
ERENHOW
TRINITY PENINSULA?
DEFORMATION
LE MAY
FLAGSTONE
BAINMEDART
RADOK
SOYUZ
BOULDERS IN MORAINE
A. AUSTRALIS ONLY
RS
SIS?
WS
WS/S
SIS
DIAMICTITE
G/G
METSCHEL
DARWIN
TAKROUNA
WELLER
1
2,3
4
5
6-8
9

Figure 10. Generalized stratagraphic section of the major lithostratigraphic subdivisions of the Karoo Supergroup in the main Karoo Basin of South Africa. 1. Waterberg Coal Field, 2. Wankie Sandstone (not part of the Ecca Group, but correlated with its lower Permian strata), 3. Free State, 4. Bazargoan, Nagpur, India (Not the Kamthi Formation, but it correlates with the Balfour Formation), 5. Umkomaas Valley, 6. Molteno, Eastern Cape. Modified from Catuneanu et al. (2005).

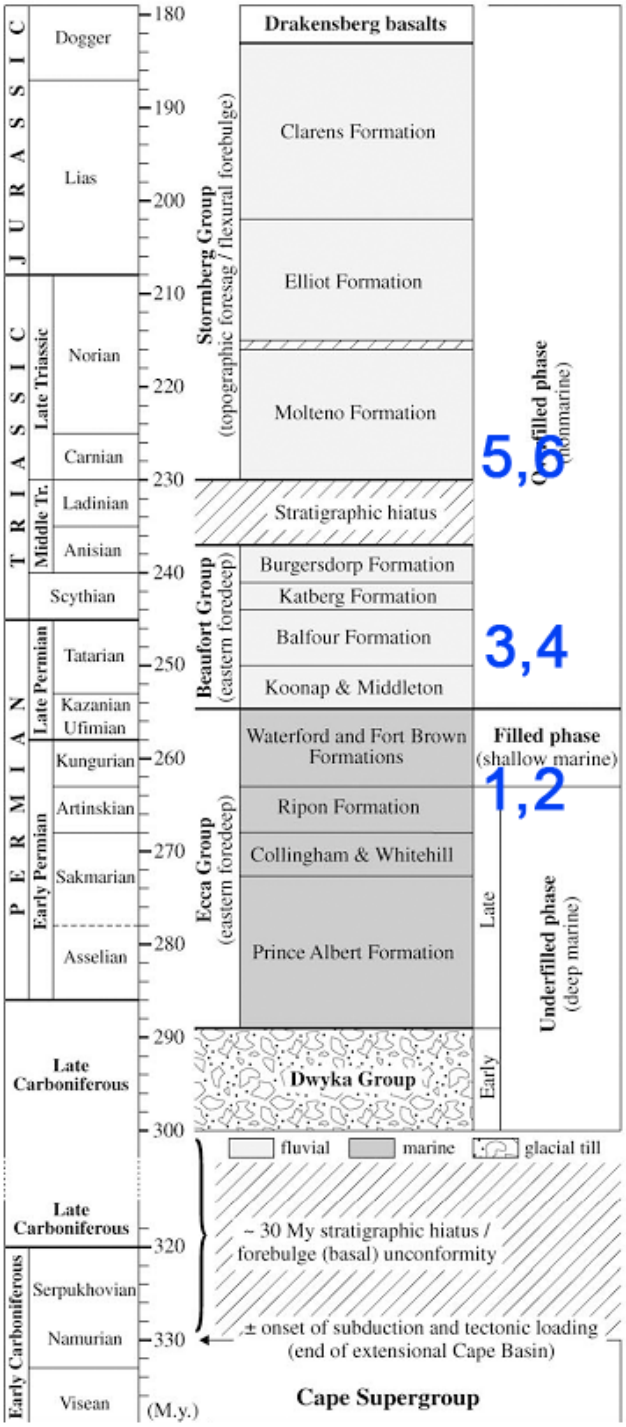
Drakensberg basalts
Clarens Formation
Elliot Formation
Molteno Formation
Stormberg Group
(topographic foresag / flexural forebulge)
Overfilled phase
(continental)
5,6
Stratigraphic hiatus
Burgersdorp Formation
Katberg Formation
Balfour Formation
Koonap & Middleton
Beaufort Group
(eastern foredeep)
3,4
Filled phase
(shallow marine)
Waterford and Fort Brown Formations
Ripon Formation
Collingham & Whitehill
Prince Albert Formation
Ecca Group
(eastern foredeep)
1,2
Underfilled phase
(deep marine)
Late
Early
Dwyka Group
fluvial
marine
glacial till
~ 30 My stratigraphic hiatus /
forebulge (basal) unconformity
± onset of subduction and tectonic loading
(end of extensional Cape Basin)
Cape Supergroup
JURASSIC
Dogger
Lias
TRIASSIC
Late Triassic
Norian
Carnian
Middle Tr.
Ladinian
Anisian
Scythian
PERMIAN
Late Permian
Tatarian
Kazanian
Ufimian
Early Permian
Kungurian
Artinskian
Sakmarian
Asselian
Late Carboniferous
Late Carboniferous
Early Carboniferous
Serpukhovian
Namurian
Visean
180
190
200
210
220
230
240
250
260
270
280
290
300
320
330
(M.y.)

Figure 11. Generalized stratigraphic section of Grande and Karoo basins, Falkland Islands, and Parana basin for the late Paleozoic. 1. Sierra de Pillahuinco. Modified from Gamundi and Rossello (1998).

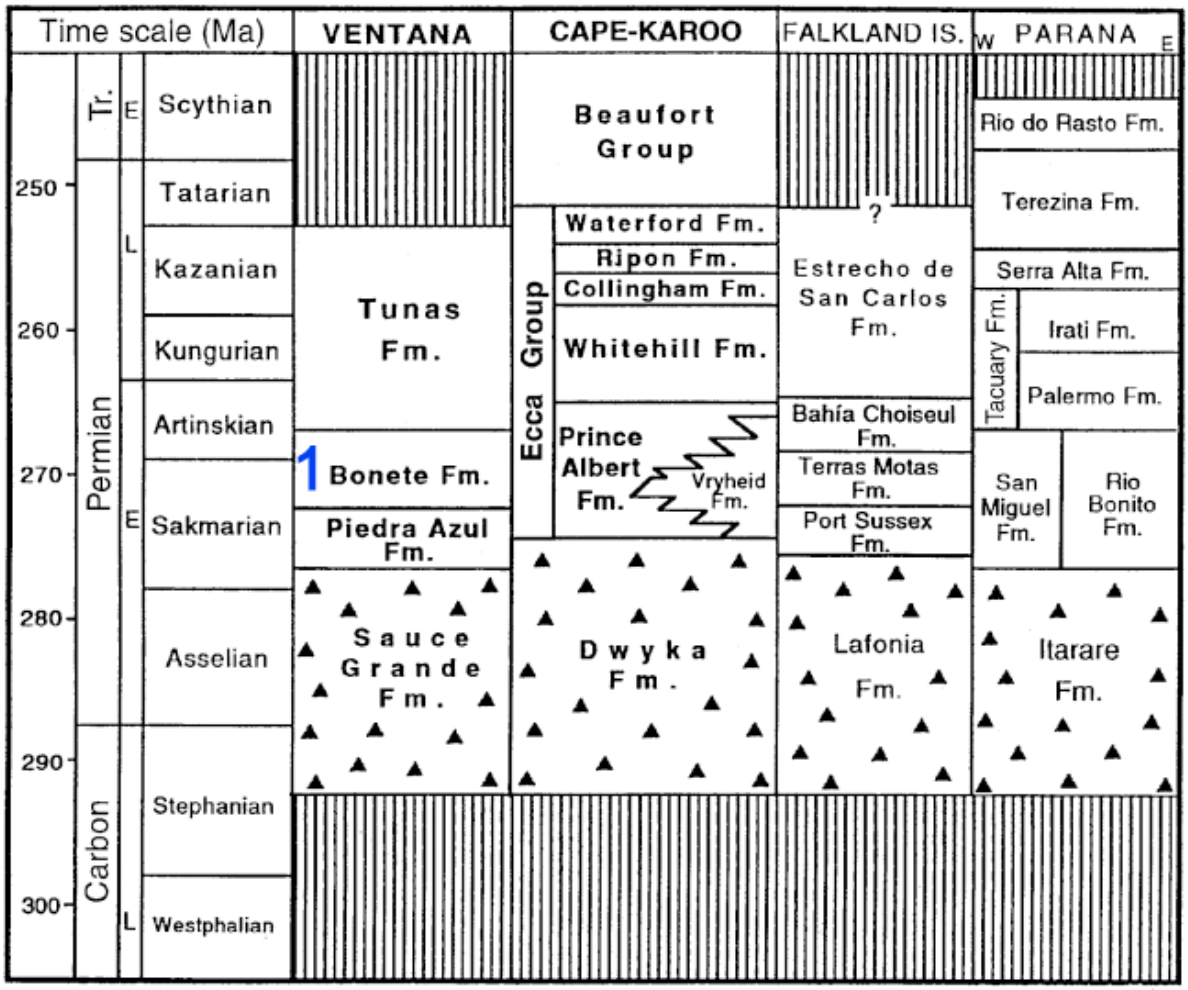
Time scale (Ma)
VENTANA
CAPE-KAROO
FALKLAND IS.
W PARANA E
Tr.
E
Scythian
Tatarian
L
Kazanian
Kungurian
Permian
E
Artinskian
Sakmarian
Asselian
Carbon
L
Stephanian
Westphalian
250
260
270
280
290
300
Tunas Fm.
1 Bonete Fm.
Piedra Azul Fm.
Sauce Grande Fm.
Beaufort Group
Ecca Group
Waterford Fm.
Ripon Fm.
Collingham Fm.
Whitehill Fm.
Prince Albert Fm.
Vryheid Fm.
Dwyka Fm.
?
Estrecho de San Carlos Fm.
Bahía Choiseul Fm.
Terras Motas Fm.
Port Sussex Fm.
Lafonia Fm.
Rio do Rasto Fm.
Terezina Fm.
Serra Alta Fm.
Tacuary Fm.
Irati Fm.
Palermo Fm.
San Miguel Fm.
Rio Bonito Fm.
Itarare Fm.

Figure 12. Generalized stratigraphic section from the Ohio Range of Antarctica. 1. Mt. Glossopteris, 2. Mt. Schopf. Symbols in Figure 5. Modified from Collinson et al. (1994).

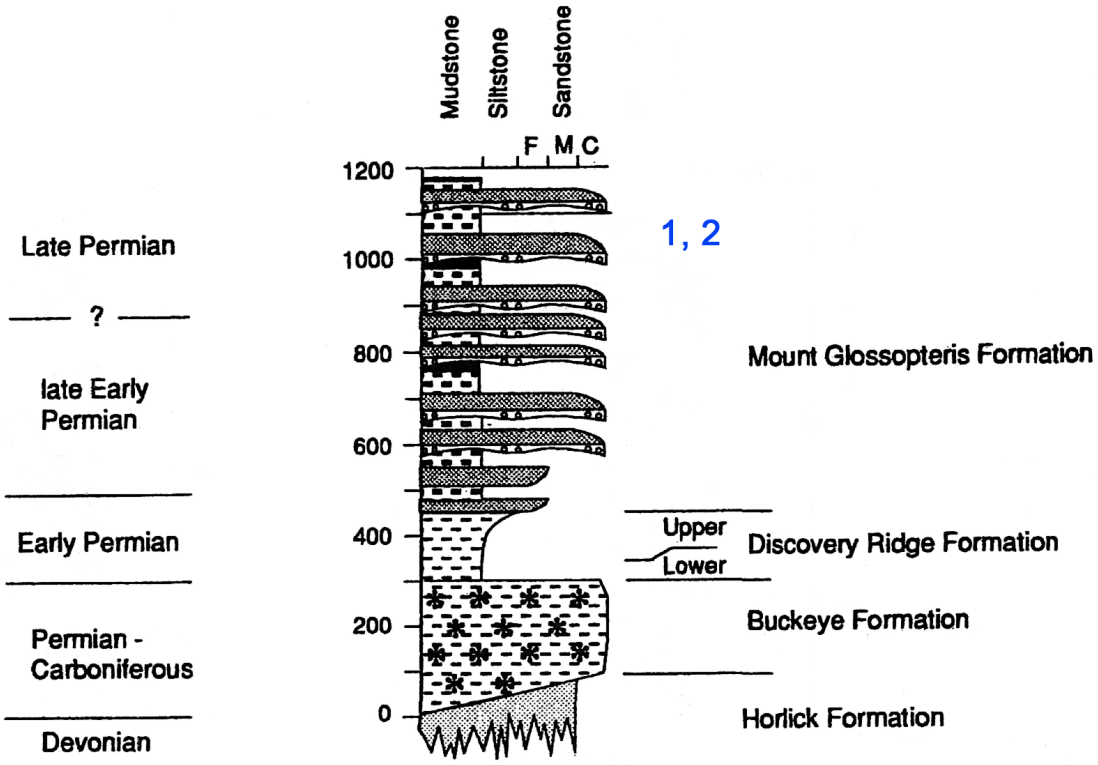
Mudstone
Siltstone
Sandstone
F M C
1200
1000
800
600
400
200
0
1, 2
Late Permian
?
late Early Permian
Early Permian
Permian - Carboniferous
Devonian
Mount Glossopteris Formation
Upper
Lower
Discovery Ridge Formation
Buckeye Formation
Horlick Formation

Figure 13. Generalized stratigraphic section from the Ellsworth Mountains of Antarctica. 1. Polarstar Peak. Symbols in Figure 5. Modified from Collinson et al. (1994).

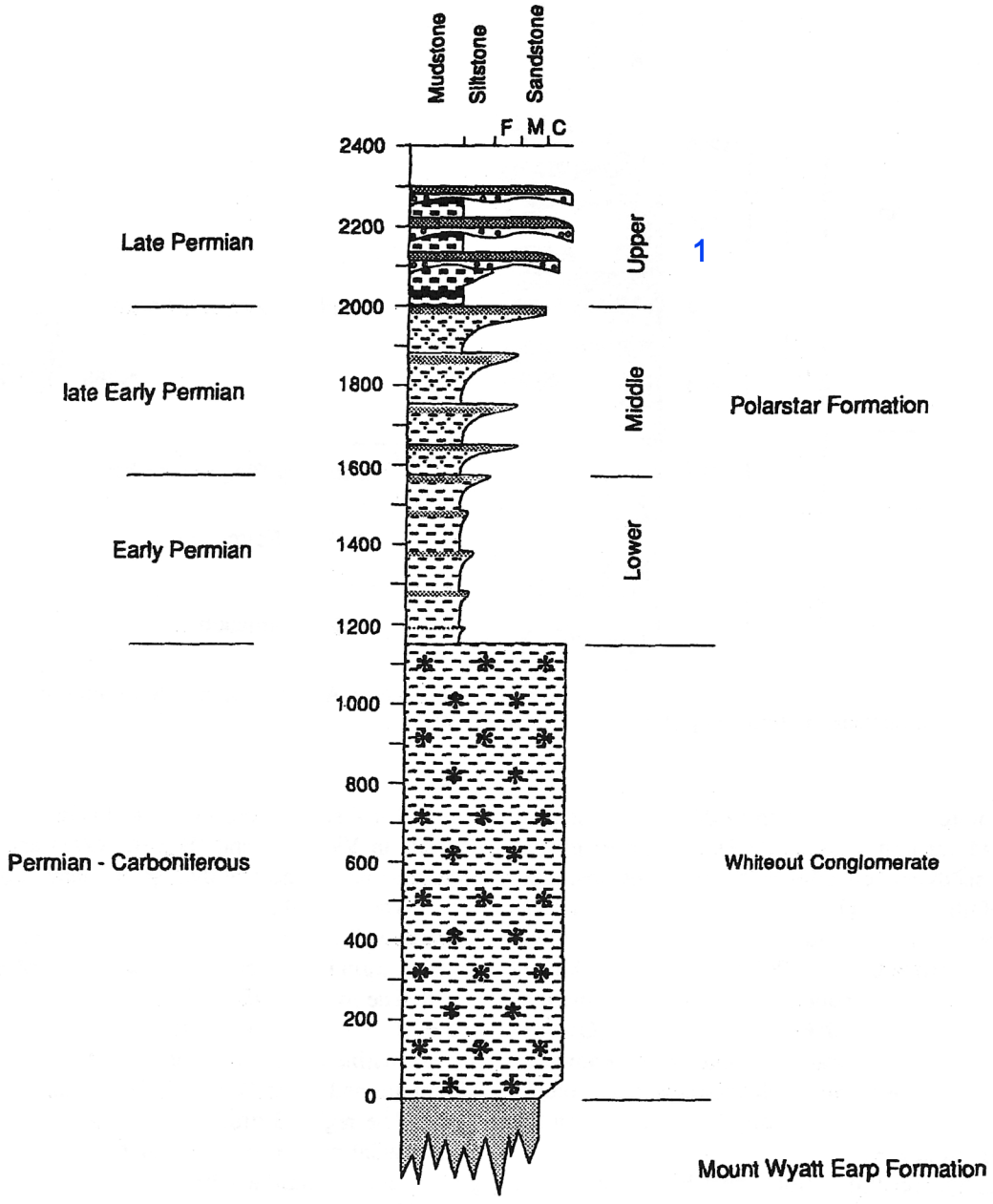
Mudstone
Siltstone
Sandstone
F M C
2400
2200
2000
1800
1600
1400
1200
1000
800
600
400
200
0
Late Permian
late Early Permian
Early Permian
Permian - Carboniferous
Upper
Middle
Lower
1
Polarstar Formation
Whiteout Conglomerate
Mount Wyatt Earp Formation

Figure 14. Generalized stratigraphic section of the Sydney Basin. 1. Cooyal, New South Wales. Modified from Fielding et al. (2010).

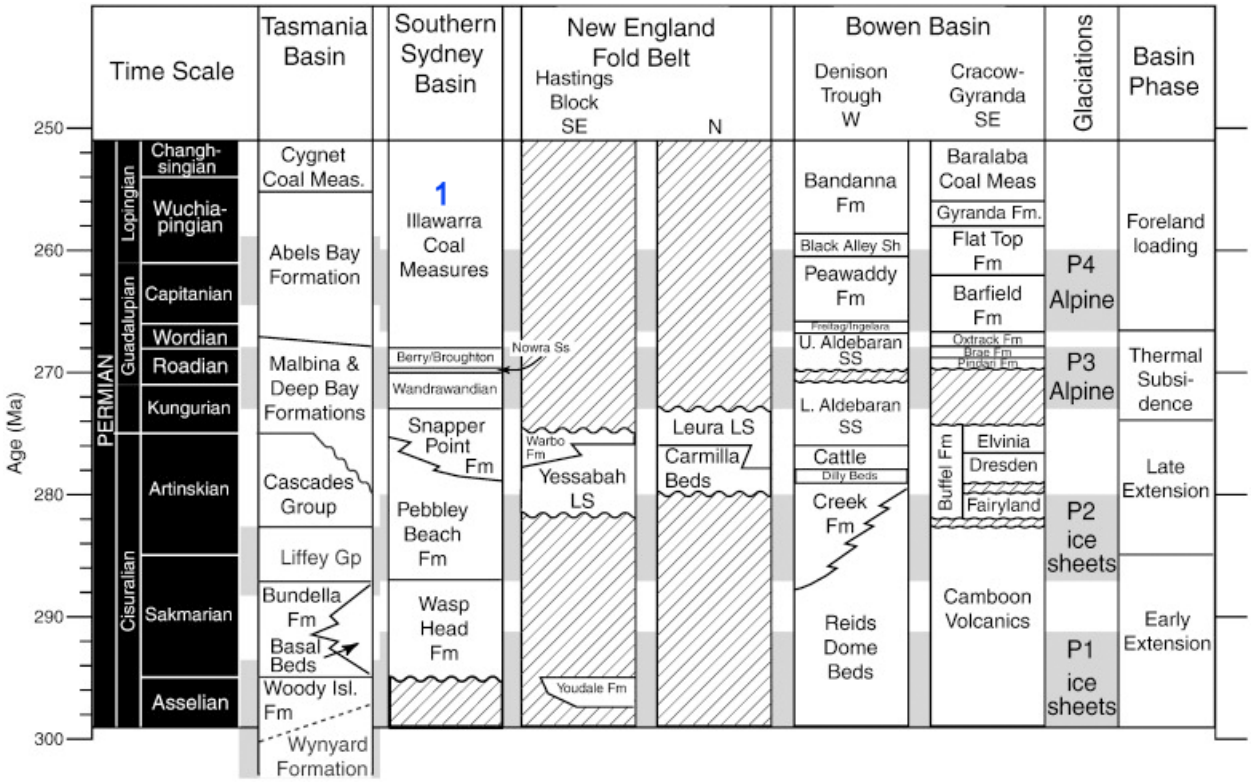
Time Scale
Tasmania Basin
Southern Sydney Basin
New England Fold Belt
Hastings Block
SE
N
Bowen Basin
Denison Trough W
Cracow-Gyranda SE
Glaciations
Basin Phase
Age (Ma)
250
260
270
280
290
300
PERMIAN
Lopingian
Guadalupian
Cisuralian
Changh-singian
Wuchia-pingian
Capitanian
Wordian
Roadian
Kungurian
Artinskian
Sakmarian
Asselian
Cygnet Coal Meas.
Abels Bay Formation
Malbina & Deep Bay Formations
Cascades Group
Liffey Gp
Bundella Fm
Basal Beds
Woody Isl. Fm
Wynyard Formation
1
Illawarra Coal Measures
Berry/Broughton
Wandrawandian
Snapper Point Fm
Pebbley Beach Fm
Wasp Head Fm
Nowra Ss
Warbo Fm
Yessabah LS
Youdale Fm
Leura LS
Carmilla Beds
Bandanna Fm
Black Alley Sh
Peawaddy Fm
Freitag/Ingelara
U. Aldebaran SS
L. Aldebaran SS
Cattle
Dilly Beds
Creek Fm
Reids Dome Beds
Baralaba Coal Meas
Gyranda Fm.
Flat Top Fm
Barfield Fm
Oxtrack Fm
Brain Fm
Pindari Fm
Buffel Fm
Elvinia
Dresden
Fairyland
Camboon Volcanics
P4 Alpine
P3 Alpine
P2 ice sheets
P1 ice sheets
Foreland loading
Thermal Subsi-dence
Late Extension
Early Extension

Figure 15. Example of vein measurements on a *Glossopteris* leaf. Each box measures 5 by 5 mm.


ety for Sedimentary Geology

Figure 16. Box plot of venation density in Permian leaf morphotypes.

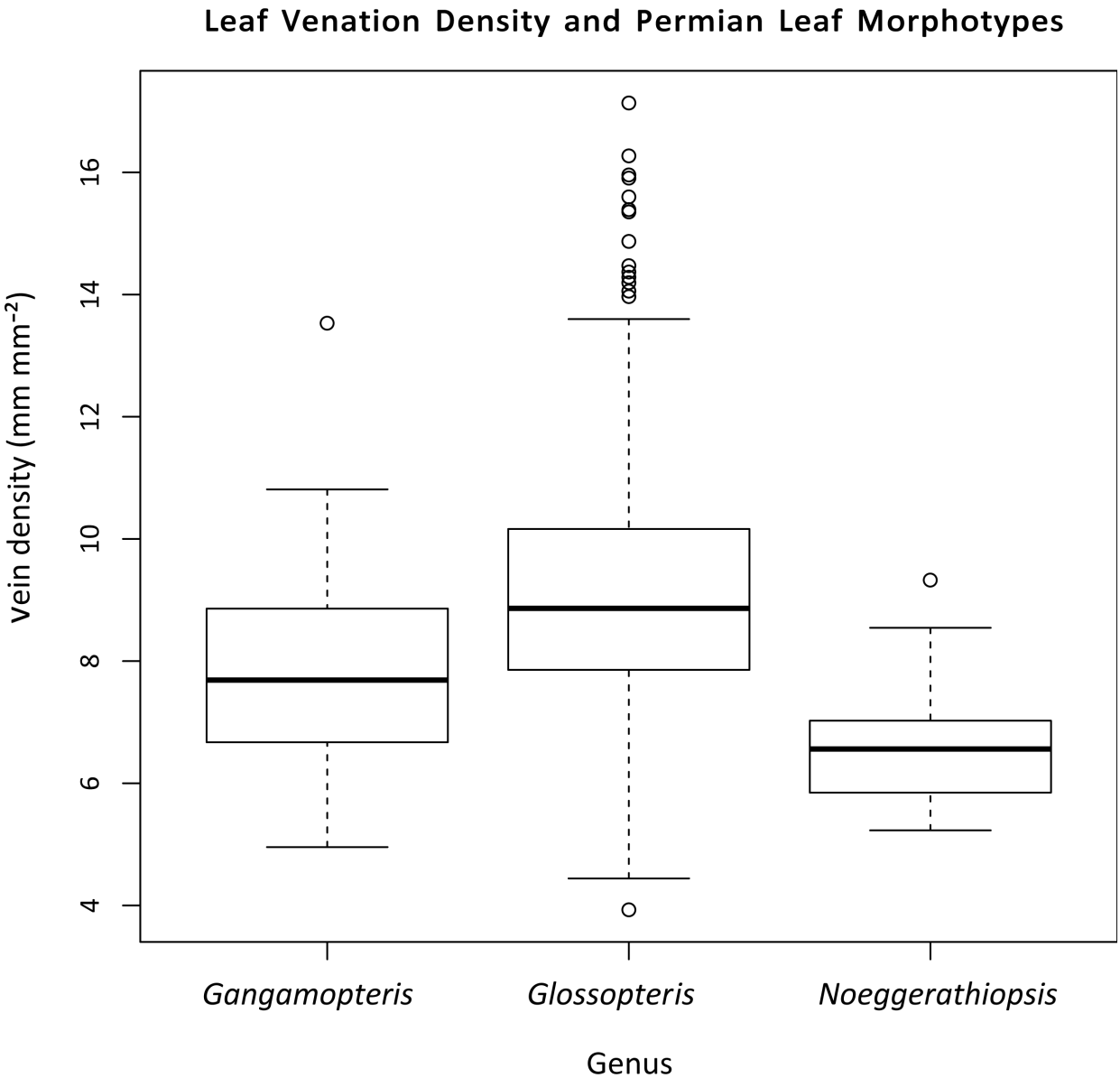
Leaf Venation Density and Permian Leaf Morphotypes
Vein density (mm mm^{-2})
4
6
8
10
12
14
16
Gangamopteris
Glossopteris
Noeggerathiopsis
Genus

Figure 17. Box plot of venation density in *Glossopteris* through the Permian. CO_2 levels were low in the early and middle Permian before rising rapidly to the late Permian.

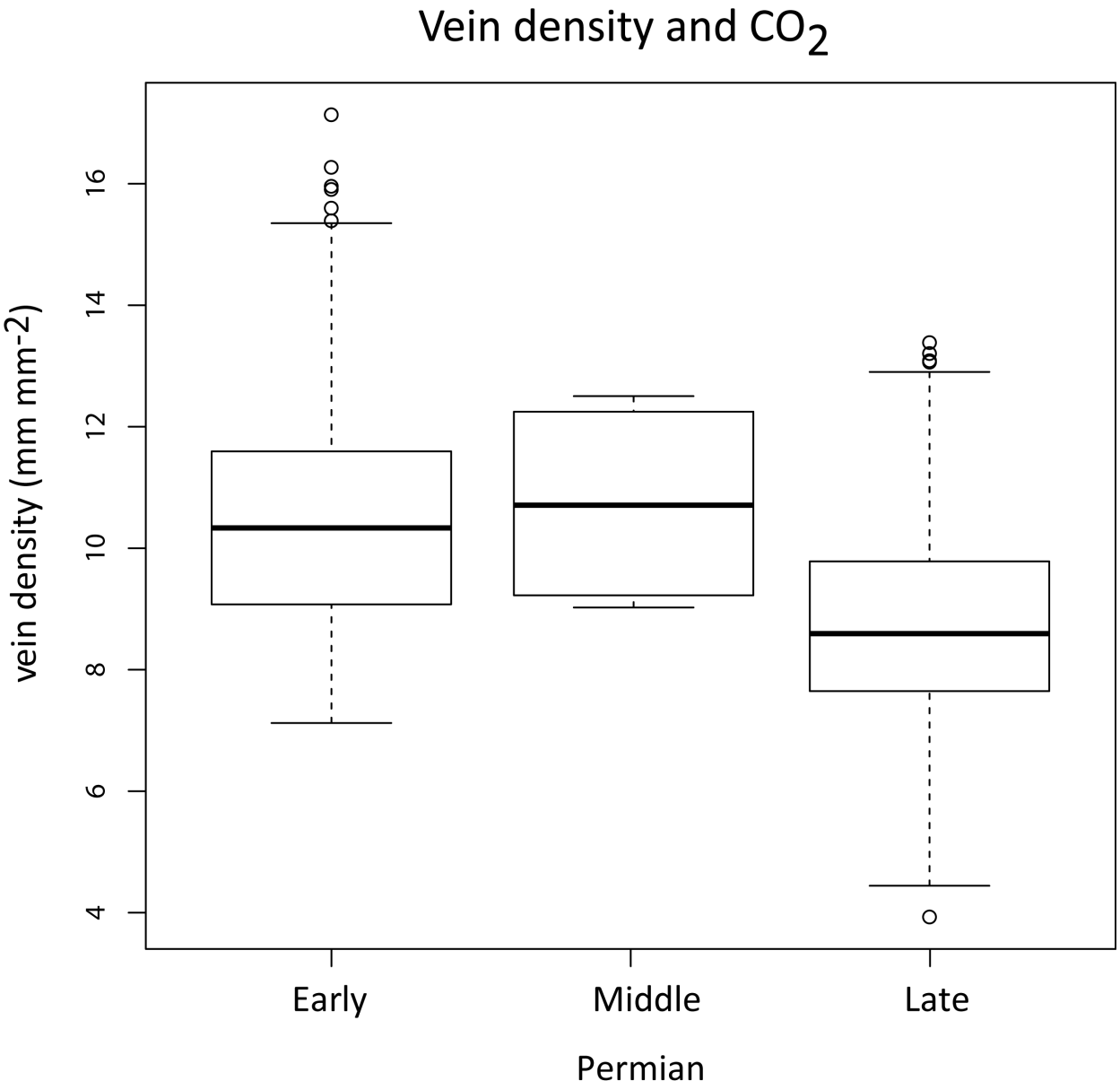
Vein density and CO_2
vein density (mm mm^{-2})
4
6
8
10
12
14
16
Early
Middle
Late
Permian

Figure 18. Box plot of venation density in *Glossopteris* across a latitudinal gradient. In this case, the latitudes are split into two groups, Antarctic and non-Antarctic.

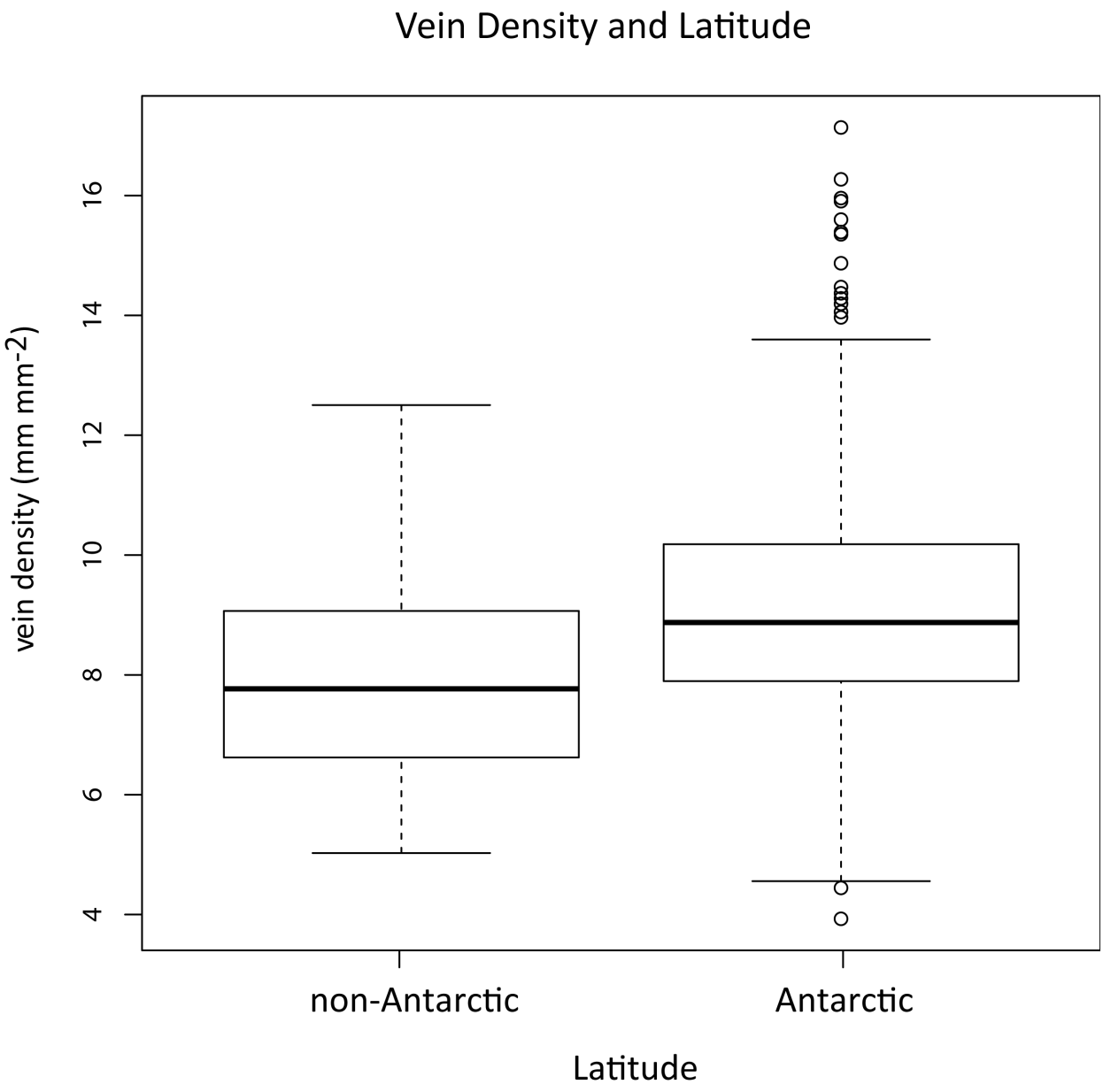
Vein Density and Latitude
vein density (mm mm-2)
4
6
8
10
12
14
16
non-Antarctic
Antarctic
Latitude

Figure 19. Box plot of venation density in *Glossopteris* across a latitudinal gradient. In this case, the latitudes are split into three groups: non-Antarctic, 70º S to 79º S, and 80º S and higher.

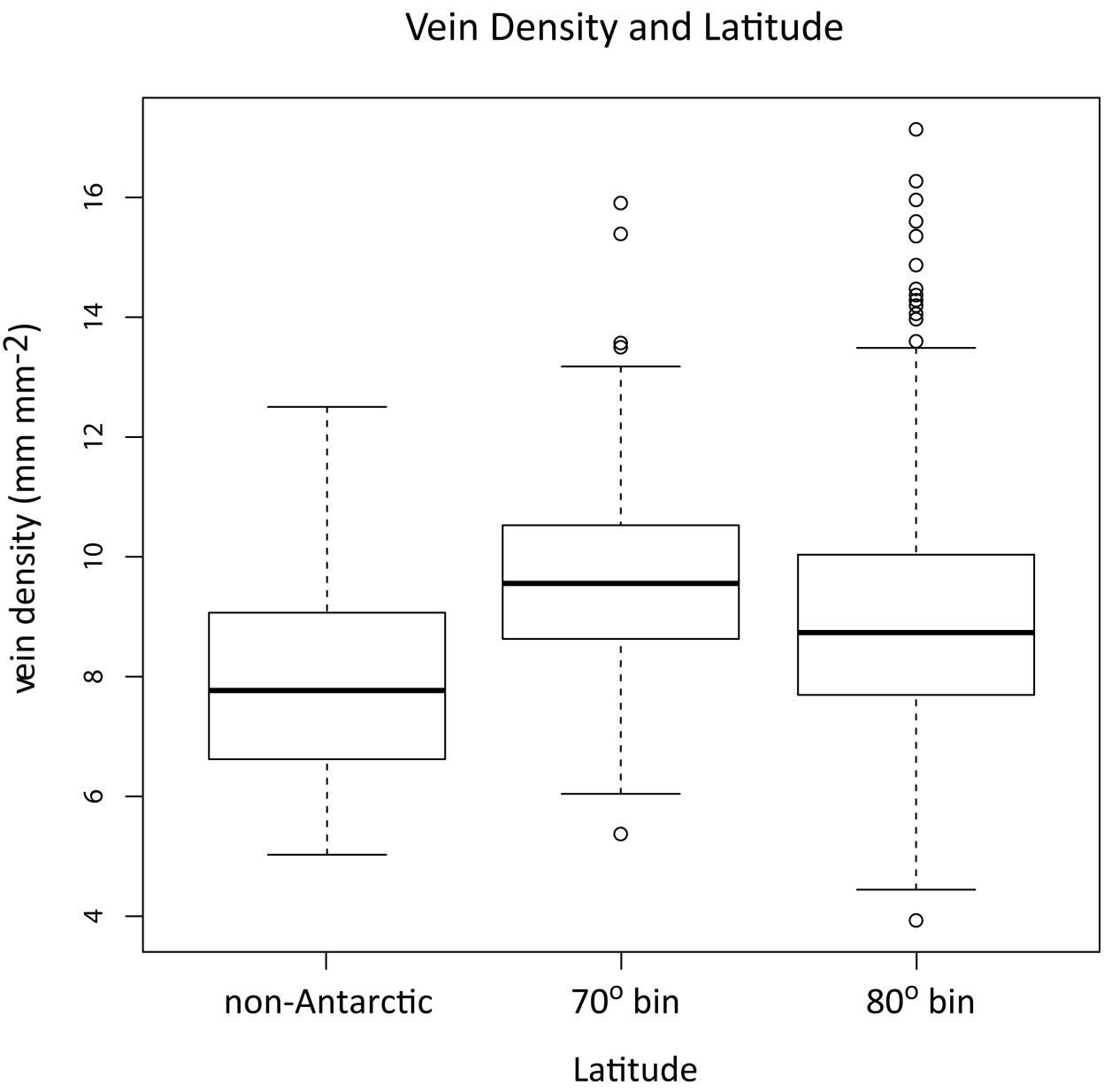
Vein Density and Latitude
vein density (mm mm-2)
4
6
8
10
12
14
16
non-Antarctic
70o bin
80o bin
Latitude

Figure 20. Box plot of venation density in *Glossopteris* across a latitudinal gradient. In this case, the latitudes are split into several groups: non-Antarctic and the others were separated to the nearest whole degree.

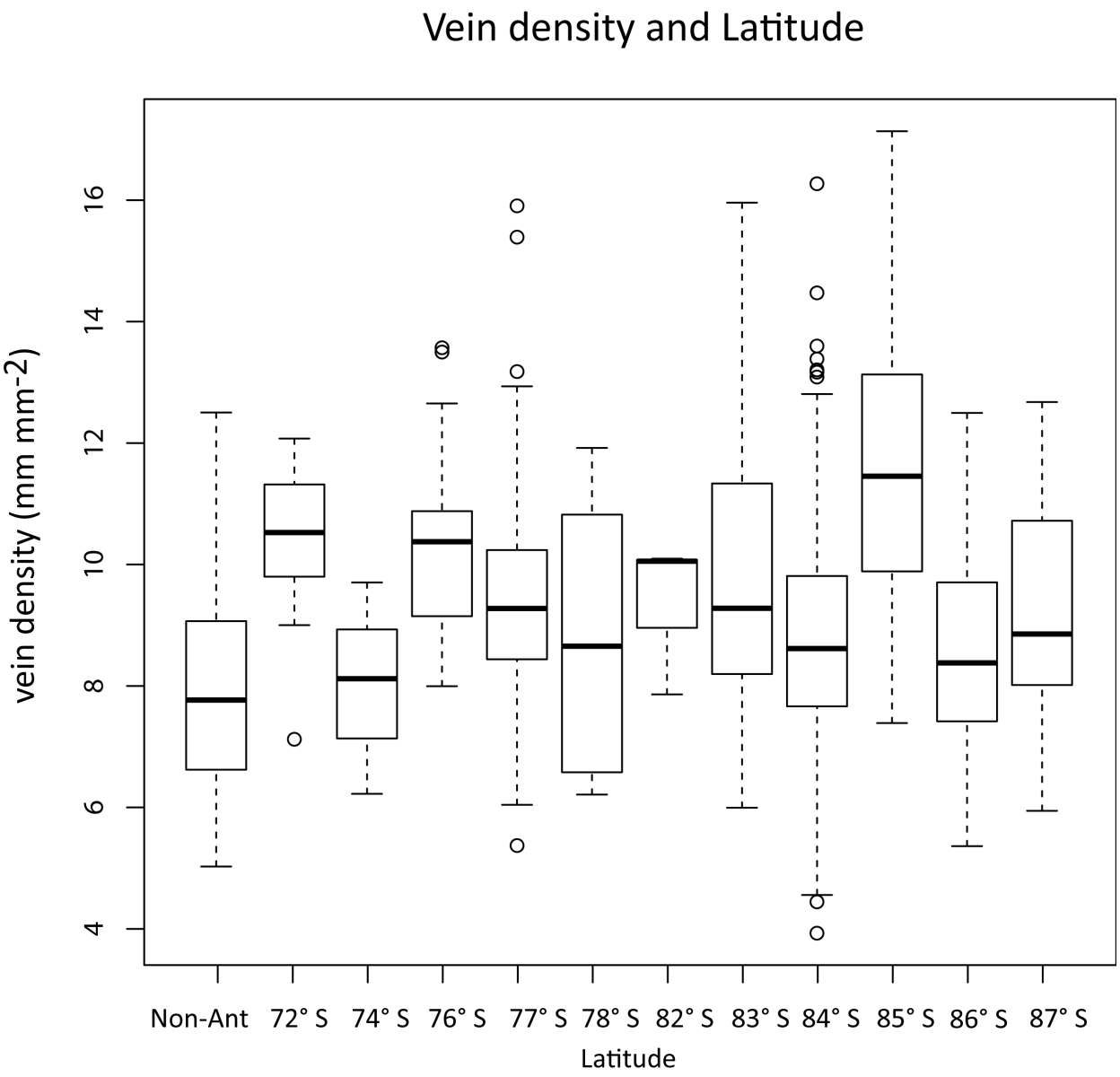
Vein density and Latitude
vein density (mm mm-2)
4
6
8
10
12
14
16
Non-Ant
72° S
74° S
76° S
77° S
78° S
82° S
83° S
84° S
85° S
86° S
87° S
Latitude

Figure 21. Box plot of venation density in Triassic leaf morphotypes.

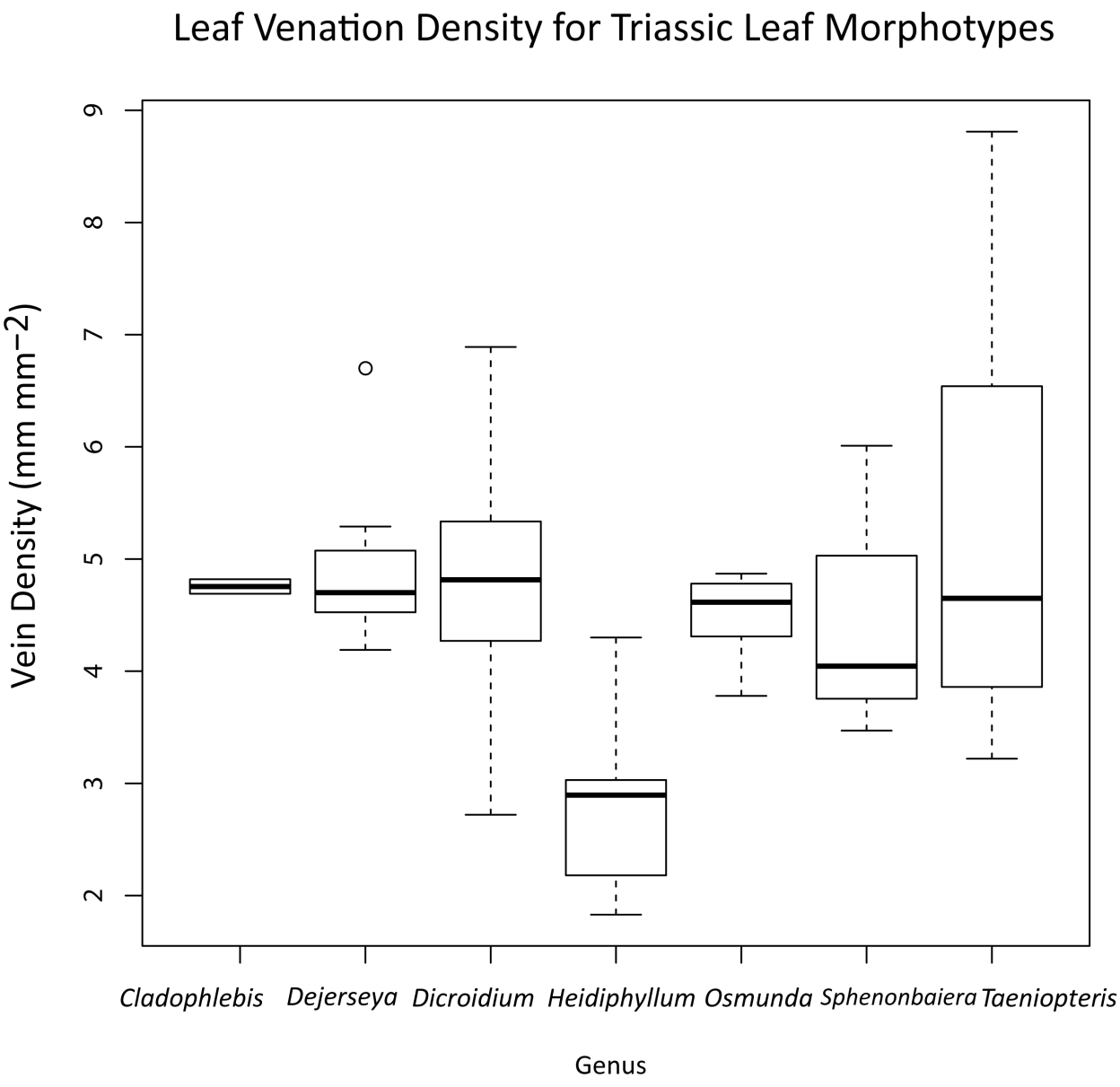
Leaf Venation Density for Triassic Leaf Morphotypes
Vein Density (mm mm−2)
2
3
4
5
6
7
8
9
Cladophlebis
Dejerseya
Dicroidium
Heidiphyllum
Osmunda
Sphenonbaiera
Taeniopteris
Genus

Figure 22. Leaf cross sections of (A) extant C_4 plant *Pennisetum villosum* and (B) permineralized *Glossopteris* leaf from the late Permian of Skaar Ridge. BSC = bundle sheath cells, or photosynthetic carbon reduction (PCR) tissue. MC = mesophyll cell, or photosynthetic carbon assimilation (PCA) tissue. (A) is modified from Christin et al. (2010).

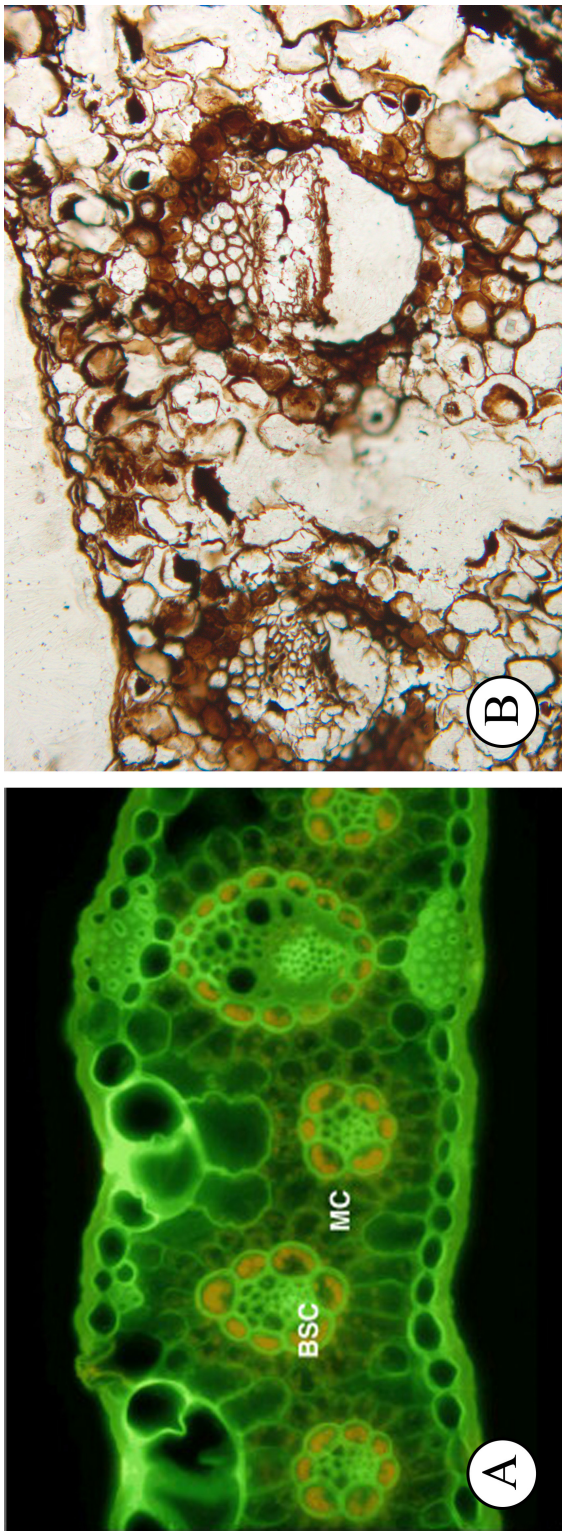
B
A
BSC
MC

Figure 23. Modeled effects of temperature and CO_2 on the quantum yield of photosynthesis in C_3 and C_4 plants. Image is modified from Osborne and Beerling (2006).

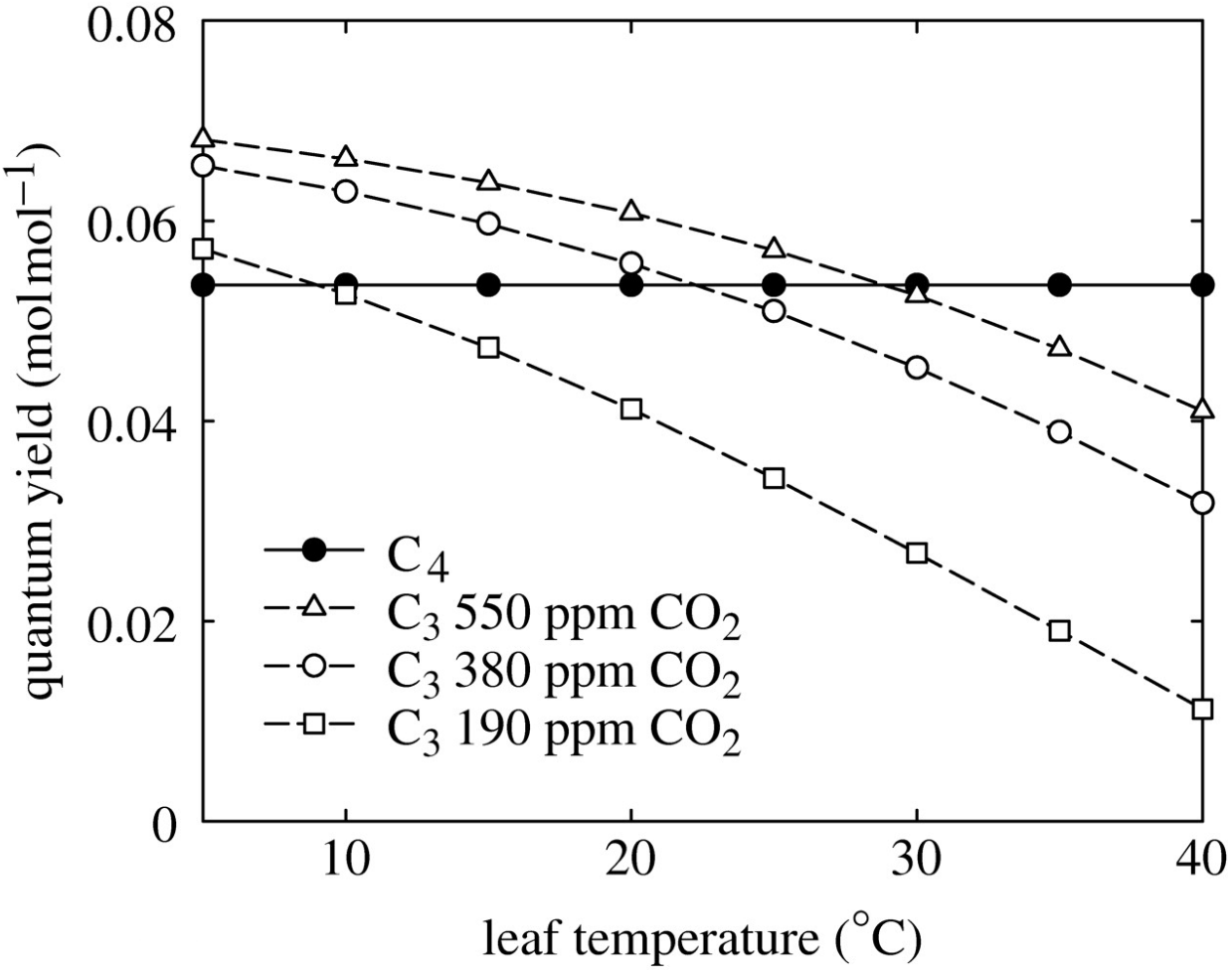
0.08
0.06
0.04
0.02
0
quantum yield (mol mol^{-1})
10
20
30
40
leaf temperature (°C)
C$_4$
C$_3$ 550 ppm CO$_2$
C$_3$ 380 ppm CO$_2$
C$_3$ 190 ppm CO$_2$

Figure 24. The combined effects of CO_2 and climate on the quantum yield of photosynthesis in C_3 and C_4 plants. Solid squares represent a tropical climate and atmospheric CO_2 and open squares represent the global mean temperature and atmospheric CO_2. The blue portion of the graph marks the Permian. Image is modified from Osborne and Beerling (2006).

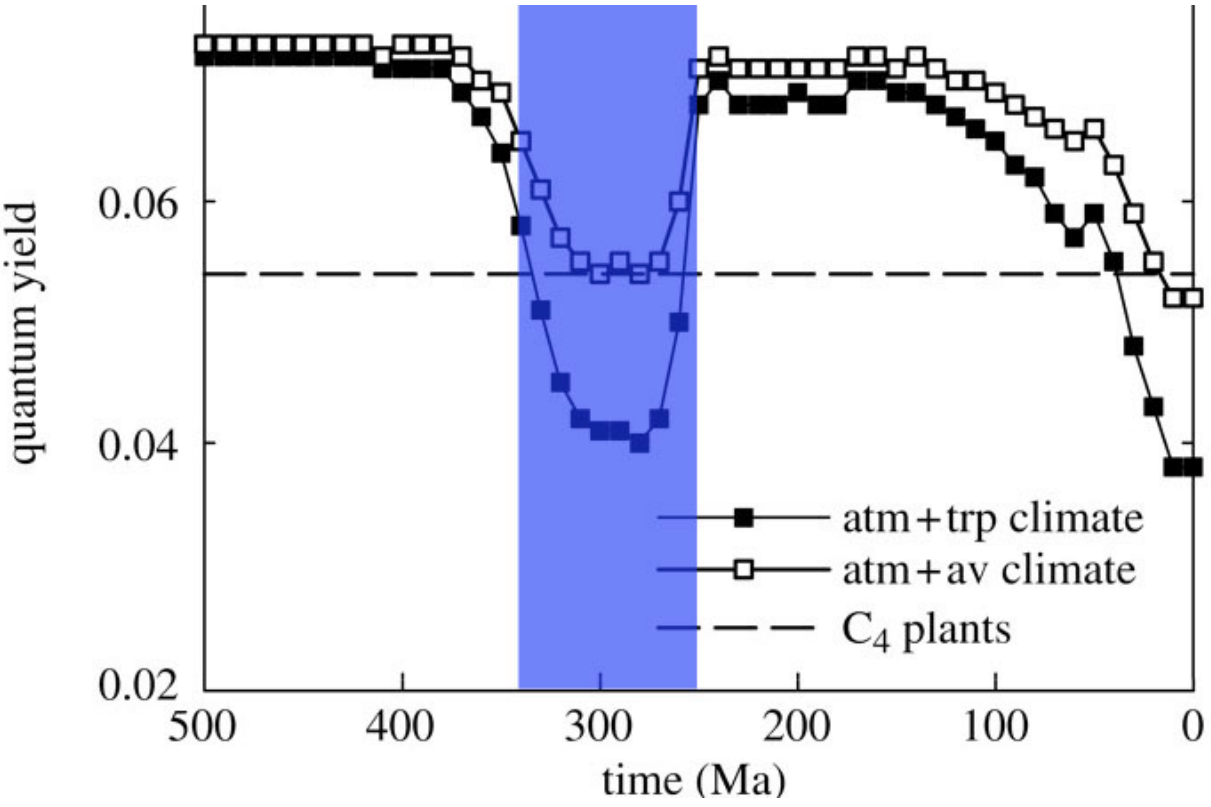
quantum yield
0.06
0.04
0.02
500
400
300
200
100
0
time (Ma)
atm+trp climate
atm+av climate
C4 plants

Figure 25. Plots of anatomical measurements of extant C_3 and C_4 plants compared with fossil *Glossopteris* leaves. The red line in each figure represents the average measurements of permineralized *Glossopteris* leaves. (A) Ratio of PCA: PCR tissues. (B) Ratio of PCR perimeter to PCR volume. (C) Percentage of a leaf cross section that is epidermis. Plots are modified from Muhaidat et al. (2007).

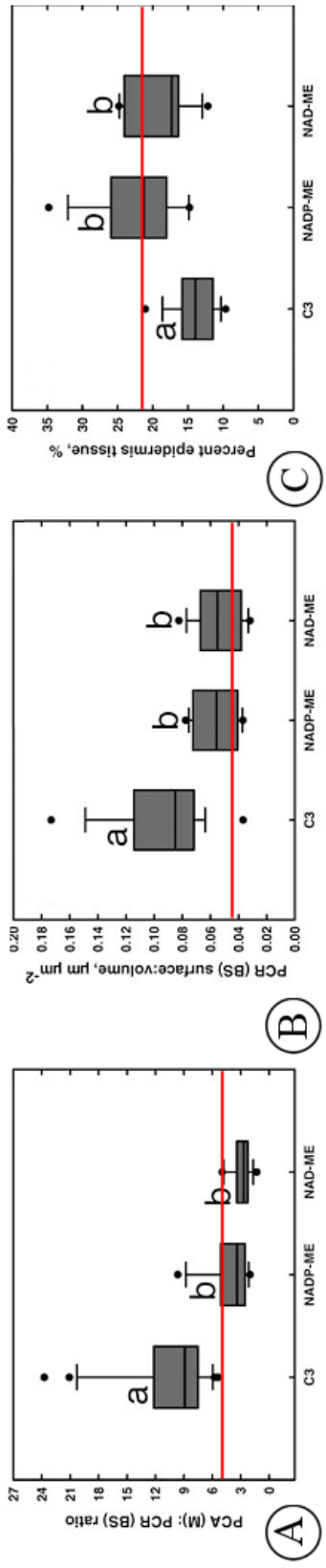
A
PCA (M): PCR (BS) ratio
27
24
21
18
15
12
9
6
3
0
a
b
b
C3
NADP-ME
NAD-ME
B
PCR (BS) surface:volume, μm μm-2
0.20
0.18
0.16
0.14
0.12
0.10
0.08
0.06
0.04
0.02
0.00
a
b
b
C3
NADP-ME
NAD-ME
C
Percent epidermis tissue, %
40
35
30
25
20
15
10
5
0
a
b
b
C3
NADP-ME
NAD-ME

Figure 26. *Glossopteris* leaf used in leaf mass per area analysis with a red line indicating the position where the petiole width measurement was taken. The area of the leaf blade was measured as well.

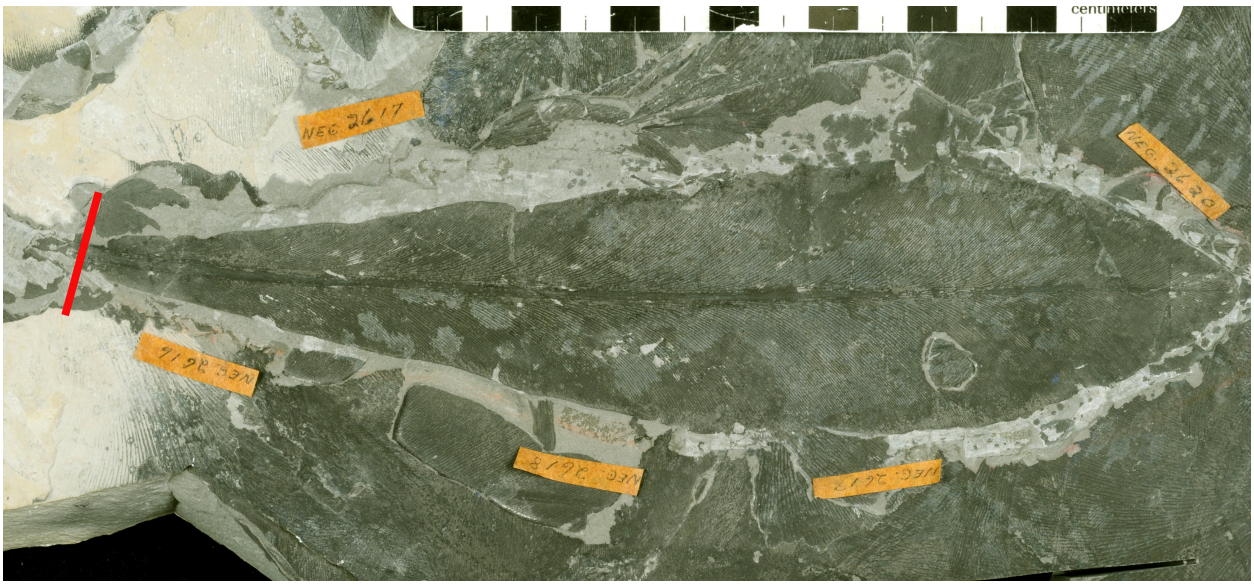
centimeters
NEG. 26 17

Literature Cited

Ackerly, D. D., Reich, P. B., 1999. Convergence and correlations among leaf size and function in seed plants: a comparative test using independent contrasts. American Journal of Botany 86, 1272–1281.

Allen, L. H., Bisbal, E. C., Boote, K. J., 1998. Nonstructural carbohydrates of soybean plants grown in subambient and superambient levels of CO2. Photosynthesis research 56, 143–155.

Alvin, K., Chaloner, W. G., 1970. Parallel Evolution in Leaf Venation: an Alternative View of Angiosperm Origins. Nature 226, 662–663.

Andrews, T. J., Lorimer, G. H., 1987. Rubisco: structure, mechanisms, and prospects for improvement. In: Hatch, M. D., Boardman, N. K. (Eds.), The Biochemistry of plants : a comprehensive treatise. Academic Press, San Diego, pp. 131–218.

Anten, N. P. R., Hirose, T., 1999. Interspecific differences in above-ground growth patterns result in spatial and temporal partitioning of light among species in a tall-grass meadow. Journal of ecology 87, 583–597.

Archangelsky, S., Cuneo, N. R., 1984. Zonación del Pérmico continental de Argentina sobre la base de sus plantas fosiles. 3 Congreso Latinoamericano de Paleontología, Memoria 1984, 143–153.

Archibold, O. W., 1995. Ecology of world vegetation. Chapman and Hall, London.

Atkin, O. K., Loveys, B. R., Atkinson, L. J., Pons, T. L., 2006. Phenotypic plasticity and growth temperature: understanding interspecific variability. Journal of Experimental Botany 57, 267–281.

Axsmith, B. J., Taylor, E. L., Taylor, T. N., Cúneo, N. R., 2000. New perspectives on the Mesozoic seed fern order Corystospermales based on attached organs from the Triassic of Antarctica. American Journal of Botany 87, 757–768.

Baldocchi, D. D., Wilson, K. B., Gu, L., 2002. How the environment, canopy structure and canopy physiological functioning influence carbon, water and energy fluxes of a temperate broad-leaved deciduous forest—an assessment with the biophysical model CANOAK. Tree Physiology 22, 1065–1077.

Bamford, M. K., 2004. Diversity of the woody vegetation of Gondwanan southern Africa. Gondwana Research 7, 153–164.

Barrett, P. J., Elliot, D. H., Lindsay, J. F., 1986. The Beacon Supergroup (Devonian-Triassic) and Ferrar Group (Jurassic) in the Beardmore Glacier Area, Antarctica. In: Turner, M. D., Splettstoesser, J. D. (Eds.), Geology of the Central Transantarctic Mountains. Antarctic Research Series. American Geophysical Union, Washington, D.C., pp. 339–428.

Beck, C. B., 1960. Connection between *Archaeopteris* and *Callixylon*. Science 131, 1524–1525.

Becker, P., Tyree, M. T., Tsuda, M., 1999. Hydraulic conductances of angiosperms versus conifers: similar transport sufficiency at the whole-plant level. Tree Physiology 19, 445–452.

Beerling, D. J., 2005. Evolutionary Responses of Land Plants to Atmospheric CO_2. In: Baldwin, I. T., Caldwell, M. M., Heldmaier, G., Jackson, R. B., Lange, O. L., Mooney, H. A., Schulze, E.-D., Sommer, U., Ehleringer, J. R., Denise Dearing, M., Cerling, T. E. (Eds.), A History of Atmospheric CO_2 and Its Effects on Plants, Animals, and Ecosystems. Springer-Verlag, New York, pp. 114–132.

Beerling, D., Woodward, F., 1997. Changes in land plant function over the Phanerozoic: Reconstructions based on the fossil record. Botanical Journal of the Linnean Society 124, 137–153.

Berner, R. A., 2005. The Phanerozoic Carbon Cycle: CO_2 and O_2. Oxford University Press.

Berner, R. A., 2006. GEOCARBSULF: A combined model for Phanerozoic atmospheric O_2 and CO_2. Geochimica et Cosmochimica Acta 70, 5653–5664.

Berner, R. A., Canfield, D. E., 1989. A new model for atmospheric oxygen over Phanerozoic time. American Journal of Science 289, 333–361.

Berner, R. A., Kothavala, Z., 2001. Geocarb III: A Revised Model of Atmospheric CO_2 over Phanerozoic Time. American Journal of Science 301, 182–204.

Bohn, S., Magnasco, M., 2007. Structure, scaling, and phase tansition in the optimal transport network. Physical Review Letters 98.

Boyce, C. K., 2008. How green was *Cooksonia*? The importance of size in understanding the early evolution of physiology in the vascular plant lineage. Paleobiology 34, 179–194.

Boyce, C. K., 2009. Seeing the forest with the leaves - clues to canopy placement from leaf fossil size and venation characteristics. Geobiology 7, 192–199.

Boyce, C. K., Brodribb, T. J., Feild, T. S., Zwieniecki, M. A., 2009. Angiosperm leaf vein evolution was physiologically and environmentally transformative. Proceedings of the Royal Society B: Biological Sciences 276, 1771–1776.

Brodribb, T., Hill, R. S., 1997. Imbricacy and stomatal wax plugs reduce maximum leaf conductance in southern hemisphere conifers. Aust. J. Bot. 45, 657–668.

Brodribb, T. J., Holbrook, N. M., 2003. Changes in leaf hydraulic conductance during leaf shedding in seasonally dry tropical forest. New Phytologist 158, 295–303.

Brodribb, T. J., Feild, T. S., Jordan, G. J., 2007. Leaf Maximum Photosynthetic Rate and

Venation Are Linked by Hydraulics. Plant Physiology 144, 1890 –1898.

Brodribb, T. J., Holbrook, N. M., Zwieniecki, M. A., Palma, B., 2004. Leaf hydraulic capacity in ferns, conifers and angiosperms: impacts on photosynthetic maxima. New Phytologist 165, 839–846.

Brooks, A., Farquhar, G., 1985. Effect of temperature on the CO_2/O_2 specificity of ribulose- 1,5-bisphosphate carboxylase/0xygenase and the rate of respiration in the light. Planta 165, 397–406.

Brooks, J. R., Hinckley, T. M., Sprugel, D. G., 1994. Acclimation responses of mature *Abies amabilis* sun foliage to shading. Oecologia 100, 316–324.

Brown, N. J., Newell, C. A., Stanley, S., Chen, J. E., Perrin, A. J., Kajala, K., Hibberd, J. M., 2011. Independent and parallel recruitment of preexisting mechanisms underlying C_4 photosynthesis. Science 331, 1436–1439.

Brown, R. H., Hattersley, P. W., 1989. Leaf anatomy of C_3-C_4 species as related to evolution of C_4 photosynthesis 1. Plant Physiology 91, 1543–1550.

Caemmerer, S. von, 1992. Carbon isotope discrimination in C_3-C_4 intermediates. Plant, cell and environment 15, 1063–1072.

Campbell, J. W., Aarup, T., 1989. Photosynthetically available radiation at high latitudes. Limnology and Oceanography 34, 1490–1499.

Canny, M. J., 1993. The transpiration stream in the leaf apoplast: water and solutes. Philosophical Transactions of the Royal Society of London. Series B: Biological Sciences 341, 87–100.

Castro-Díez, P., Puyravaud, J. P., Cornelissen, J. H. C., 2000. Leaf structure and anatomy as related to leaf mass per area variation in seedlings of a wide range of woody plant species and types. Oecologia 124, 476–486.

Catuneanu, O., Wopfner, H., Eriksson, P. G., Cairncross, B., Rubidge, B. S., Smith, R. M. H., Hancox, P. J., 2005. The Karoo basins of south-central Africa. Journal of African Earth Sciences 43, 211–253.

Chabot, B. F., Jurik, T. W., Chabot, J. F., 1979. Influence of instantaneous and integrated light-flux density on leaf anatomy and photosynthesis. American Journal of Botany 66, 940–945.

Chandra, S., Singh, K. J., 1992. The genus *Glossopteris* from the Late Permian beds of Handapa, Orissa, India. Review of Palaeobotany and Palynology 75, 183–218.

Christin, P.-A., Freckleton, R. P., Osborne, C. P., 2010. Can phylogenetics identify C_4 origins and reversals? Trends in Ecology & Evolution 25, 403–409.

Christin, P.-A., Sage, T. L., Edwards, E. J., Ogburn, R. M., Khoshravesh, R., Sage, R. F., 2011. Complex evolutionary transitions and the significance of C_3-C_4 intermediate forms of photosynthesis in Molluginaceae. Evolution 65, 643–660.

Cichan, M. A., 1986. Conductance in the wood of selected Carboniferous plants. Paleobiology 12, 302–310.

Collinson, J. W., Pennington, D. C., Kemp, N. R., 1986. Stratigraphy and petrology of Permian and Triassic fluvial deposits in northern Victoria Land, Antarctica. In: Stump, E. (Ed.), Geological Investigations in Northern Victoria Land. Antarctic Research Series. American Geophysical Union, Washington, D.C., pp. 211–242.

Collinson, J. W., Isbell, J. L., Elliot, D. H., Miller, M. F., Miller, J. M. G., Veevers, J. J., 1994. Permian-Triassic Transantarctic basin. Geological Society of America Memoir 184, 173–222.

Collinson, J. W., Hammer, W. R., Askin, R. A., Elliot, D. H., 2006. Permian-Triassic boundary in the central Transantarctic Mountains, Antarctica. Geological Society of America Bulletin 118, 747–763.

Creber, G. T., Chaloner, W. G., 1984. Influence of environmental factors on the wood structure of living and fossil trees. The Botanical Review 50, 357–448.

Critchfield, W. B., 1960. Leaf Dimorphism in *Populus trichocarpa*. American Journal of Botany 47, 699.

Cúneo, N. R., 1996. Permian phytogeography in Gondwana. Palaeogeography, Palaeoclimatology, Palaeoecology 125, 75–104.

Dauzat, J., Rapidel, B., Berger, A., 2001. Simulation of leaf transpiration and sap flow in virtual plants: model description and application to a coffee plantation in Costa Rica. Agricultural and Forest Meteorology 109, 143–160.

Dawson, T. E., Mambelli, S., Plamboeck, A. H., Templer, P. H., Tu, K. P., 2002. Stable isotopes in plant ecology. Annual Review of Ecology and Systematics 33, 507–559.

Decombeix, A., Taylor, E. L., Taylor, T. N., 2010. Epicormic shoots in a Permian gymnosperm from Antarctica. International Journal of Plant Sciences 171, 772–782.

Dengler, N. G., Dengler, R. E., Donnelly, P. M., Hattersley, P. W., 1994. Quantitative leaf anatomy of C_3 and C_4 grasses (Poaceae): bundle sheath and mesophyll surface area relationships. Annals of Botany 73, 241–255.

Dickins, J. M., 1993. Climate of the Late Devonian to Triassic. Palaeogeography, Palaeoclimatology, Palaeoecology 100, 89–94.

Diemer, M., 1998. Life span and dynamics of leaves of herbaceous perennials in high-elevation

environments: news from the elephant's leg. Functional Ecology 12, 413–425.

Douce, R., Heldt, H.-W., 2004. Photorespiration. In: Leegood, R. C., Sharkey, T. D., Caemmerer, S. (Eds.), Photosynthesis: Advances in photosynthesis and respiration. Kluwer Academic Publishers, Dordrecht, pp. 115–136.

Doyle, J. A., Hickey, L. J., 1976. Pollen and leaves from the mid-Cretaceous Potomac Group and their bearing on early angiosperm evolution. In: Beck, C. B. (Ed.), Origin and Early Evolution of Angiosperms. Columbia University Press, New York, NY, pp. 139–206.

Durand, M., 2006. Architecture of optimal transport networks. Physical Review E 73, .

Edwards, G. E., Ku, M. S. B., 1987. Biochemistry of C_3–C_4 intermediates. In: Hatch, M. D., Boardman, N. K. (Eds.), The Biochemistry of plants : a comprehensive treatise. Academic Press, San Diego, pp. 275–325.

Eggert, D. A., 1961. The ontogeny of Carboniferous arborescent Lycopsida. Palaeontographica Abteilung B 108, 43–92.

Ehleringer, J., Björkman, O., 1977. Quantum yields for CO_2 Uptake in C_3 and C_4 Plants. Plant Physiology 59, 86–90.

Ehleringer, J. R., Cerling, T. E., Helliker, B. R., 1997. C_4 photosynthesis, atmospheric CO_2, and climate. Oecologia 112, 285–299.

Ehleringer, J. R., Sage, R. F., Flanagan, L. B., Pearcy, R. W., 1991. Climate change and the evolution of C_4 photosynthesis. Trends in Ecology & Evolution 6, 95–99.

Equiza, M. A., Day, M. E., Jagels, R., 2006a. Physiological responses of three deciduous conifers (*Metasequoia glyptostroboides*, *Taxodium distichum* and *Larix laricina*) to continuous light: adaptive implications for the early Tertiary polar summer. Tree Physiology 26, 353 –364.

Equiza, M. A., Day, M. E., Jagels, R., Li, X., 2006b. Photosynthetic downregulation in the conifer *Metasequoia glyptostroboides* growing under continuous light: the significance of carbohydrate sinks and paleoecophysiological implications. Canadian Journal of Botany 84, 1453–1461.

Equiza, M. A., Jagels, R., Cirelli, D., 2007. Differential Carbon Allocation in *Metasequoia glyptostroboides*, *Taxodium distichum* and *Sequoia sempervirens* growing under continuous light. Bulletin of the Peabody Museum of Natural History 48, 269–280.

Esau, K., 1965. Plant Anatomy. Wiley.

Escapa, I. H., Decombeix, A., Taylor, E. L., Taylor, T. N., 2010. Evolution and relationships of the conifer seed cone *Telemachus*: evidence from the Triassic of Antarctica. International Journal of Plant Sciences 171, 560–573.

Escapa, I., Taylor, E. L., Cuneo, N. R., Bomfleur, B., Bergene, J., Serbet, R., Taylor, T. N., 2011. Triassic floras of Antarctica: plant diversity and distribution in high paleolatitude communities. PALAIOS 26, 522–544.

Falcon-Lang, H. J., 2000a. The relationship between leaf longevity and growth ring markedness in modern conifer woods and its implications for palaeoclimatic studies. Palaeogeography, Palaeoclimatology, Palaeoecology 160, 317–328.

Falcon-Lang, H. J., 2000b. A method to distinguish between woods produced by evergreen and deciduous coniferopsids on the basis of growth ring anatomy: a new palaeoecological tool. Palaeontology 43, 785–793.

Falcon-Lang, H. J., Cantrill, D. J., 2001. Leaf phenology of some mid-Cretaceous polar forests, Alexander Island, Antarctica. Geological Magazine 138, 39–52.

Farquhar, G. D., Caemmerer, S., Berry, J. A., 1980. A biochemical model of photosynthetic CO_2 assimilation in leaves of C_3 species. Planta 149, 78–90.

Farrera, I., Harrison, S. P., Prentice, I. C., Ramstein, G., Guiot, J., Bartlein, P. J., Bonnefille, R., Bush, M., Cramer, W., Grafenstein, U. von, Holmgren, K., Hooghiemstra, H., Hope, G., Jolly, D., Lauritzen, S.-E., Ono, Y., Pinot, S., Stute, M., Yu, G., 1999. Tropical climates at the last glacial maximum: a new synthesis of terrestrial palaeoclimate data. I. Vegetation, lake-levels and geochemistry. Climate Dynamics 15, 823–856.

Faure, G., Mensing, T. M., 2010. The Transantarctic Mountains: Rocks, Ice, Meteorites and Water. Springer.

Feild, T. S., Brodribb, T. J., Iglesias, A., Chatelet, D. S., Baresch, A., Upchurch, G. R., Gomez, B., Mohr, B. A. R., Coiffard, C., Kvacek, J., Jaramillo, C., 2011a. Fossil evidence for Cretaceous escalation in angiosperm leaf vein evolution. Proceedings of the National Academy of Sciences 108, 8363–8366.

Feild, T. S., Upchurch, G. R., Chatelet, D. S., Brodribb, T. J., Grubbs, K. C., Samain, M.-S., Wanke, S., 2011b. Fossil evidence for low gas exchange capacities for Early Cretaceous angiosperm leaves. Paleobiology 37, 195–213.

Fielding, C. R., Frank, T. D., Isbell, J. L., Henry, L. C., Domack, E. W., 2010. Stratigraphic signature of the late Palaeozoic Ice Age in the Parmeener Supergroup of Tasmania, SE Australia, and inter-regional comparisons. Palaeogeography, Palaeoclimatology, Palaeoecology 298, 70–90.

Fox, D. L., Koch, P. L., 2003. Tertiary history of C_4 biomass in the Great Plains, USA. Geology 31, 809–812.

Foyer, C. H., Bloom, A. J., Queval, G., Noctor, G., 2009. Photorespiratory metabolism: genes, mutants, energetics, and redox signaling. Annual Review of Plant Biology 60, 455–484.

Franks, P. J., Beerling, D. J., 2009. Maximum leaf conductance driven by CO_2 effects on stomatal size and density over geologic time. Proceedings of the National Academy of Sciences 106, 10343–10347.

Galtier, J., Phillips, T., 1999. The acetate peel technique. In: Jones, T. P., Rowe, N. (Eds.), Fossil plants and spores: modern techniques. Geological Society, London, UK, pp. 67–70.

Gee, C. T., 1989. Permian *Glossopteris* and *Elatocladus* megafossil floras from the English Coast, Eastern Ellsworth Land, Antarctica. Antarctic Science 1, 35–44.

Gould, R. E., Delevoryas, T., 1977. The biology of *Glossopteris*: evidence from petrified seed-bearing and pollen-bearing organs. Alcheringa: An Australasian Journal of Palaeontology 1, 387–399.

Grindley, G. W., 1963. The Geology of the Queen Alexandra Range, Beardmore Glacier, Ross dependency, Antarctica;; with notes on the correlation of Gondwana sequences. New Zealand Journal of Geology and Geophysics 6, 307–347.

Grubb, P. J., 1998. A reassessment of the strategies of plants which cope with shortages of resources. Perspectives in Plant Ecology, Evolution and Systematics 1, 3–31.

Gupta, B., 1961. Correlation of tissues in leaves. Annals of Botany 25, 65–70.

Gutschick, V. P., Wiegel, F. W., 1988. Optimizing the canopy photosynthetic rate by patterns of investment in specific leaf mass. The American naturalist 132, 67–86.

Guy, R. D., Reid, D. M., Krouse, H. R., 1980. Shifts in carbon isotope ratios of two C_3 halophytes under natural and artificial conditions. Oecologia 44, 241–247.

Hacke, U. G., Sperry, J. S., Pittermann, J., 2005. Efficiency vs. safety trade-offs for water conduction in angiosperm vessels vs. gymnosperm tracheids. In: Holbrook, N. M., Zwieniecki, M. A. (Eds.), Vascular transport in plants. Elsevier, Boston, Massachusettes, USA, pp. 333–353.

Hacke, U. G., Sperry, J. S., Wheeler, J. K., Castro, L., 2006. Scaling of angiosperm xylem structure with safety and efficiency. Tree Physiology 26, 689–701.

Harley, P. C., Sharkey, T. D., 1991. An improved model of C_3 photosynthesis at high CO_2 : reversed O_2 sensitivity explained by lack of glycerate reentry into the chloroplast. Photosynthesis research 27, 169–178.

Hayes, J. M., 1994. Global methanothophy at the Archean-Proterozoic transition. In: Bengtson, S. (Ed.), Early life on Earth. Columbia University Press, New York, NY, USA, pp. 220–236.

Herbert, C., 1995. Sequence stratigraphy of the Late Permian Coal Measures in the Sydney Basin. Australian Journal of Earth Sciences 42, 391–405.

Hikosaka, K., Terashima, I., 1995. A model of the acclimation of photosynthesis in the leaves of C_3 plants to sun and shade with respect to nitrogen use. Plant, Cell and Environment 18, 605–618.

Jagels, R., Day, M. E., 2004. The adaptive physiology of Metasequoia to Eocene high-latitude environments. In: Hemsley, A., Poole, I. (Eds.), Evolution of Plant Physiology. Elsevier Academic Press, Boston, pp. 401–425.

Jagels, R., Equiza, M. A., 2005. Competitive advantages of *Metasequoia* in warm high latitudes. In: LePage, B. A., Williams, C. J., Yang, H. (Eds.), The Geobiology and Ecology of *Metasequoia*. Springer-Verlag, Berlin/Heidelberg, pp. 335–349.

Jagels, R., Equiza, M. A., 2007. Why did *Metasequoia* disappear from North America but not from China. Bulletin of the Peabody Museum of Natural History 48, 281–290.

Jersey, N. J. de, 1975. Miospore zones in the lower Mesozoic of southeastern Queensland. In: Campbell, K. S. W. (Ed.), Gondwana Geology. Australian National University Press, Canberra, Australia, pp. 159–172.

Jordan, D. B., Ogren, W. L., 1984. The CO_2/O_2 specificity of ribulose 1,5-bisphosphate carboxylase/oxygenase. Planta 161, 308–313.

Jurik, T. W., 1986. Temporal and spatial patterns of specific leaf weight in successional northern hardwood tree species. American Journal of Botany 73, 1088–1092.

Kellogg, E. A., 1999. Phylogenetic aspects of the evolution of C_4 photosynthesis. In: Sage, R. F., Monson, R. K. (Eds.), C_4 Plant Biology. Academic Press, San Diego, pp. 411–444.

Kidston, R., Lang, W. H., 1920. On Old Red Sandstone plants showing structure, from the Rhynie Chert Bed, Aberdeenshire. Part II. Additional notes on *Rhynia gwynne-vaughani*, Kidston and Lang; with descriptions of *Rhynia major*, n.sp., and *Hornea lignieri*, n.g. n.sp. Transactions of the Royal Society of Edinburgh 52 Part 3, 603–627.

Kingston, J. D., Hill, A., Marino, B. D., 1994. Isotopic evidence for Neogene hominid paleoenvironments in the Kenya Rift Valley. Science 264, 955–959.

Kirschbaum, M., Farquhar, G., 1984. Temperature dependence of whole-leaf photosynthesis in *Eucalyptus pauciflora* Sieb. Ex Spreng. Functional Plant Biol. 11, 519–538.

Konrad, W., Roth-Nebelsick, A., Kerp, H., Hass, H., 2000. Transpiration and assimilation of early Devonian land plants with axially symmetric telomes - Simulations on the tissue level. Journal of Theoretical Biology 206, 91–107.

Kull, U., 1999. Zur evolution der adernetze von blattern, insbesondere der Angiospermen. Profil 16, 35–48.

Kull, U., Herbig, A., 1995. The leaf vein system of angiosperms: form and evolution.

Naturwissenschaften 82, 441–451.

Kyle, R. A., Schopf, J. M., 1982. Permian and Triassic palynostratigraphy of the Victoria Group, Transantarctic Mountains. In: Craddock, C. (Ed.), Antarctic Geoscience. University of Wisconsin Press, Madison, WI, pp. 649–659.

LaBarbera, M., 1990. Principles of design of fluid transport systems in zoology. Science 249, 992–1000.

Lambers, H., Poorter, H., 1992. Inherent variation in growth-rate between higher-plants - a search for physiological causes andecological consequences. Advances In Ecological Research 23, 187–261.

Logan, D. M., 2010. Biostatistical Design and Analysis Using R: A Practical Guide. John Wiley & Sons.

Long, W. E., 1965. Stratigraphy of the Ohio Range, Antarctica. In: Hadley, J. B. (Ed.), Geology and Paleontology of the Antarctic. American Geophysical Union, Washington, D.C., pp. 71–116.

Lopez-Gamundi, O. R., Rossello, E. A., 1998. Basin fill evolution and paleotectonic patterns along the Samfrau geosyncline: the Sauce Grande basin-Ventana foldbelt (Argentina) and Karoo basin-Cape foldbelt (South Africa) revisited. Geologische Rundschau 86, 819–834.

Lucas, S. G., Hancox, P. J., 2001. Tetrapod-based correlation of the nonmarine Upper Triassic of southern Africa. Albertina 25, 5–9.

Marais, D. J. Des, 1997. Isotopic evolution of the biogeochemical carbon cycle during the Proterozoic Eon. Organic Geochemistry 27, 185–193.

Matta, F. M. Da, Loos, R. A., Rodrigues, R., Barros, R. S., 2001. Actual and potential photosynthetic rates of tropical crop species. Revista Brasileira de Fisiologia Vegetal 13, 24–32.

McCulloh, K. A., Sperry, J. S., 2005. Patterns in hydraulic architecture and their implications for transport efficiency. Tree Physiology 25, 257–267.

McCulloh, K. A., Sperry, J. S., Adler, F. R., 2003. Water transport in plants obeys Murray's law. Nature 421, 939–942.

McKown, A. D., Cochard, H., Sack, L., 2010. Decoding leaf hydraulics with a spatially explicit model: principles of venation architecture and implications for its evolution. The American Naturalist 175, 447–460.

Melville, R., 1969. Leaf venation patterns and the origin of the angiosperms. Nature 224, 121–125.

Mirsky, A., Treves, S. B., Calkin, P. E., 1965. Stratigraphy and petrography, Mount Gran area, southern Victoria Land, Antarctica. In: Hadley, J. B. (Ed.), Geology and Paleontology of the Antarctic. American Geophysical Union, Washington, D.C., pp. 145–175.

Monson, R. K., Rawsthorne, S., 2000. CO_2 assimilation in C_3–C_4 intermediate plants. In: Leegood, R. C., Sharkey, T. D., Caemmerer, S. C. von (Eds.), Photosynthesis: Physiology and Metabolism. Kluwer Academic, Dordrecht, the Netherlands, pp. 533–550.

Morgan, M. E., Kingston, J. D., Marino, B. D., 1994. Carbon isotopic evidence for the emergence of C_4 plants in the Neogene from Pakistan and Kenya. Nature 367, 162–165.

Muhaidat, R., Sage, R. F., Dengler, N. G., 2007. Diversity of Kranz anatomy and biochemistry in C_4 eudicots. American Journal of Botany 94, 362–381.

Mulligan, J. J., Parks, B. C., Hess, H. D., Schopf, J. M., 1963. Mount Gran coal deposits, Victoria Land, Antarctica. United States Bureau of Mines Report and Investigations 621, 1–66.

Nardini, A., Salleo, S., 2000. Limitation of stomatal conductance by hydraulic traits: sensing or preventing xylem cavitation? Trees 15, 14–24.

Nardini, A., Salleo, S., Gullo, M. A. L., Pitt, F., 2000. Different responses to drought and freeze stress of *Quercus ilex* L. growing along a latitudinal gradient. Plant Ecology 148, 139–147.

Nardini, A., Tyree, M. T., 1999. Root and shoot hydraulic conductance of seven *Quercus* species. Annals of Forest Science 56, 371–377.

Nicotra, A. B., Cosgrove, M. J., Cowling, A., Schlichting, C. D., Jones, C. S., 2008. Leaf shape linked to photosynthetic rates and temperature optima in South African *Pelargonium* species. Oecologia 154, 625–635.

Niinemets, U, 2007. Photosynthesis and resource distribution through plant canopies. Plant, Cell & Environment 30, 1052–1071.

Niinemets, U., Portsmuth, A., Tobias, M., 2007. Leaf shape and venation pattern alter the support investments within leaf lamina in temperate species: a neglected source of leaf physiological differentiation? Functional Ecology 21, .

Niinemets, U., Diaz-Espejo, A., Flexas, J., Galmes, J., Warren, C. R., 2009a. Importance of mesophyll diffusion conductance in estimation of plant photosynthesis in the field. Journal of Experimental Botany 60, 2271–2282.

Niinemets, U., Diaz-Espejo, A., Flexas, J., Galmes, J., Warren, C. R., 2009b. Role of mesophyll diffusion conductance in constraining potential photosynthetic productivity in the field. Journal of Experimental Botany 60, 2249–2270.

Niinemets, U., Kull, O., Tenhunen, J. D., 2004. Within-canopy variation in the rate of development of photosynthetic capacity is proportional to integrated quantum flux density in temperate deciduous trees. Plant, cell and environment 27, 293–313.

Niinemets, U., Kull, O., Tenhunen, J. D., 1998. An analysis of light effects on foliar morphology, physiology, and light interception in temperate deciduous woody species of contrasting shade tolerance. Tree Physiology 18, 681–696.

Niinemets, U., Wright, I. J., Evans, J. R., 2009c. Leaf mesophyll diffusion conductance in 35 Australian sclerophylls covering a broad range of foliage structural and physiological variation. Journal of Experimental Botany 60, 2433–2449.

Niklas, K. J., 1991a. Flexural stiffness allometries of angiosperm and fern petioles and rachises: evidence for biomechanical convergence. Evolution 45, 734–750.

Niklas, K. J., 1991b. The elastic moduli and mechanics of *Populus tremuloides* (Salicaceae) petioles in bending and torsion. American Journal of Botany 78, 989–996.

Niklas, K. J., 1992. Plant Biomechanics: An Engineering Approach to Plant Form and Function. University of Chicago Press.

Nobel, P. S., 1983. Biophysical Plant Physiology and Ecology. W.H. Freeman.

Noblin, X., Mahadevan, L., Coomaraswamy, I. A., Weitz, D. A., Holbrook, N. M., Zwieniecki, M. A., 2008. Optimal vein density in artificial and real leaves. Proceedings of the National Academy of Sciences 105, 9140–9144.

Ogle, K., 2003. Implications of interveinal distance for quantum yield in C_4 grasses: a modeling and meta-analysis. Oecologia 136, 532–542.

Ogren, W. L., 1984. Photorespiration: pathways, regulation, and modification. Annual Review of Plant Physiology 35, 415–442.

Oliver, F. W., Scott, D. H., 1905. On the structure of the palaeozoic seed *Lagenostoma lomaxi*, with a statement of the evidence upon which it is referred to Lyginodendron. Philosophical Transactions of the Royal Society of London. Series B, Containing Papers of a Biological Character 197, 193–247.

Onoda, Y., Schieving, F., Anten, N. P. R., 2008. Effects of light and nutrient availability on leaf mechanical properties of *Plantago major*: a conceptual approach. Annals of Botany 101, 727–736.

Osborne, C. P., Beerling, D. J., 2002. A process-based model of conifer forest structure and function with special emphasis on leaf lifespan. Global Biogeochemical Cycles 16, 23 PP.

Osborne, C. P., Beerling, D. J., 2003. The penalty of a long, hot summer. Photosynthetic acclimation to high CO_2 and continuous light in “living fossil” conifers. Plant Physiology

133, 803 –812.

Osborne, C. P., Beerling, D. J., 2006. Nature's green revolution: the remarkable evolutionary rise of C_4 plants. Philosophical Transactions of the Royal Society B: Biological Sciences 361, 173–194.

Osborne, C. P., Beerling, D. J., Lomax, B. H., Chaloner, W. G., 2004a. Biophysical constraints on the origin of leaves inferred from the fossil record. Proceedings of the National Academy of Sciences of the United States of America 101, 10360–10362.

Osborne, C. P., Royer, D. L., Berling, D. J., 2004b. Adaptive role of leaf habit in extinct polar forests. International Forestry Review 6, 181–186.

Pagani, M., 2002. The alkenone-CO_2 proxy and ancient atmospheric carbon dioxide. Philosophical Transactions of the Royal Society of London. Series A: Mathematical, Physical and Engineering Sciences 360, 609–632.

Pant, D. D., Singh, R. S., 1974. On the stem and attachment of *Glossopteris* and *Gangamopteris* leaves. Part II --- Structural features. Palaeontographica Abteilung B 147, 42–73.

Parkhurst, D. F., 1994. Diffusion of CO_2 and other gases inside leaves. New Phytologist 126, 449–479.

Parlange, J.-Y., Waggoner, P. E., 1970. Stomatal dimensions and resistance to diffusion. Plant Physiology 46, 337–342.

Pielou, E. C., 1995. A Naturalist's Guide to the Arctic. University of Chicago Press.

Pigg, K. B., Taylor, T. N., 1993. Anatomically preserved *Glossopteris* stems with attached leaves from the Central Transantarctic Mountains, Antarctica. American Journal of Botany 80, 500–516.

Pittermann, J., 2010. The evolution of water transport in plants: an integrated approach. Geobiology 8, 112–139.

Plumstead, E. P., 1958. The habit of growth of Glossopteridae. Transactions of the Geological Society of South Africa 61, 81–96.

Plumstead, E. P., 1962. Fossil floras of Antarctica. Trans-Antarctic Expedition 1955-1958, Scientific Reports 9 (Geology), 1–132.

Pons, T. L., Pearcy, R. W., 1994. Nitrogen reallocation and photosynthetic acclimation in response to partial shading in soybean plants. Physiologia Plantarum 92, 636–644.

Poorter, H., Navas, M.-L., 2003. Plant growth and competition at elevated CO_2: on winners, losers and functional groups. New Phytologist 157, 175–198.

Poorter, H., Niinemets, U., Poorter, L., Wright, I. J., Villar, R., 2009. Causes and consequences of variation in leaf mass per area (LMA): a meta-analysis. New Phytologist 182, 565–588.

Poorter, H., Niklas, K. J., Reich, P. B., Oleksyn, J., Poot, P., Mommer, L., 2012. Biomass allocation to leaves, stems and roots: meta-analyses of interspecific variation and environmental control. The New Phytologist 193, 30–50.

Premoli, A. C., 1996. Leaf architecture of South American *Nothofagu*s (Nothofagaceae) using traditional and new methods in morphometrics. Botanical Journal of the Linnean Society 121, 25–40.

Prothero, D. R., 1994. The Eocene-Oligocene Transition: Paradise Lost. Columbia University Press.

R Core Team, 2012. R: a language and environment for statistical computing. R Foundation for Statistical Computing, Vienna, Austria.

Radoglou, K. M., Jarvis, P. G., 1990. Effects of CO_2 enrichment on four *Poplar* clones. II. Leaf surface properties. Annals of Botany 65, 627–632.

Rasband, W.S., 2012. ImageJ, U. S. National Institutes of Health, Bethesda, Maryland, USA.

Raunkiaer, C., 1934. Life forms of plants and statistical plant geography. Arno Press.

Raven, J. A., 1977. The evolution of vascular land plants in relation to supracellular transport processes. Advances in Botanical Research Volume 5, 153–219.

Raven, J. A., 1984. Physiological correlates of the morphology of early vascular plants. Botanical Journal of the Linnean Society 88, 105–126.

Raven, J. A., 1991. Plant responses to high O_2 concentrations: relevance to previous high O_2 episodes. Global and Planetary Change 5, 19–38.

Raven, J. A., 1993. The evolution of vascular plants in relation to quantitative functioning of dead water-conducting cells and stomata. Biological Reviews 68, 337–363.

Raven, J. A., 1994a. The significance of the distance from photosynthesizing cells to vascular tissue in extant and early vascular plants. Botanical Journal of Scotland 47, 65–81.

Raven, J. A., 1994b. Physiological analyses of aspects of the functioning of vascular tissue in early plants. Botanical Journal of Scotland 47, 49–64.

Reich, P. B., Buschena, C., Tjoelker, M. G., Wrage, K., Knops, J., Tilman, D., Machado, J. L., 2003. Variation in growth rate and ecophysiology among 34 grassland and savanna species under contrasting N supply: a test of functional group differences. New Phytologist 157, 617–631.

Reich, P. B., Walters, M. B., Ellsworth, D. S., 1997. From tropics to tundra: global convergence in plant functioning. Proceedings of the National Academy of Sciences 94, 13730–13734.

Remy, W., 1982. Lower Devonian gametophytes: relation to the phylogeny of land plants. Science 215, 1625–1627.

Retallack, G. J., 1980. Late Carboniferous to Middle Triassic megafossil floras from the Sydney Basin. In: Herbert, C., Helby, R. J. (Eds.), A Guide to the Sydney Basin. Geological Survey of New South Wales Bulletin, NSW, pp. 384–430.

Retallack, G. J., 2002. Carbon dioxide and climate over the past 300 Myr. Philosophical Transactions of the Royal Society of London. Series A: Mathematical, Physical and Engineering Sciences 360, 659–673.

Retallack, G. J., Dilcher, D. L., 1988. Reconstructions of selected seed ferns. Annals of the Missouri Botanical Garden 75, 1010.

Roth-Nebelsick, A., Grimm, G., Mosbrugger, V., Hass, H., Kerp, H., 2000. Morphometric analysis of *Rhynia* and *Asteroxylon*: testing functional aspects of early land plant evolution. Paleobiology 26, 405–418.

Roth-Nebelsick, A., Uhl, D., Mosbrugger, V., Kerp, H., 2001. Evolution and function of leaf venation architecture: A review. Annals of Botany 87, 553–566.

Rothwell, G. W., Lev-Yadun, S., 2005. Evidence of polar auxin flow in 375 million-year-old fossil wood. American Journal of Botany 92, 903–906.

Roumet, C., Laurent, G., Roy, J., 1999. Leaf structure and chemical composition as affected by elevated CO_2: genotypic responses of two perennial grasses. New Phytologist 143, 73–81.

Royer, D. L., 2006. CO_2-forced climate thresholds during the Phanerozoic. Geochimica et Cosmochimica Acta 70, 5665–5675.

Royer, D. L., Miller, I. M., Peppe, D. J., Hickey, L. J., 2010. Leaf economic traits from fossils support a weedy habit for early angiosperms. American Journal of Botany 97, 438–445.

Royer, D. L., Osborne, C. P., Beerling, D. J., 2003. Carbon loss by deciduous trees in a CO_2-rich ancient polar environment. Nature 424, 60–62.

Royer, D. L., Osborne, C. P., Beerling, D. J., 2005a. Contrasting seasonal patterns of carbon gain in evergreen and deciduous trees of ancient polar forests. Paleobiology 31, 141–150.

Royer, D. L., Sack, L., Wilf, P., Lusk, C. H., Jordan, G. J., Niinemets, Ü., Wright, I. J., Westoby, M., Cariglino, B., Coley, P. D., Cutter, A. D., Johnson, K. R., Labandeira, C. C., Moles, A. T., Palmer, M. B., Valladares, F., 2007. Fossil leaf economics quantified: calibration, Eocene case study, and implications. Paleobiology 33, 574–589.

Royer, D. L., Wilf, P., Janesko, D. A., Kowalski, E. A., Dilcher, D. L., 2005b. Correlations of climate and plant ecology to leaf size and shape: potential proxies for the fossil record. American Journal of Botany 92, 1141 –1151.

Ryberg, P. E., 2009. Reproductive diversity of Antarctic glossopterid seed-ferns. Review of Palaeobotany and Palynology 158, 167–179.

Ryser, P., Urbas, P., 2000. Ecological significance of leaf life span among Central European grass species. Oikos 91, 41–50.

Sack, L., Holbrook, N. M., 2006. Leaf hydraulics. Annual Review of Plant Biology 57, 361–381.

Sack, L., Tyree, M. T., 2005. Leaf hydraulics and its implications in plant structure and function. In: Holbrook, N. M., Zwieniecki, M. A. (Eds.), Vascular transport in plants. Academic Press.

Sage, R. F., 1999. Why C_4 photosynthesis? In: Sage, R. F., Monson, R. K. (Eds.), C_4 Plant Biology. Academic Press, San Diego, pp. 3–16.

Sage, R. F., 2004. The evolution of C_4 photosynthesis. New phytologist 161, 341–370.

Sage, R. F., Sage, T. L., Kocacinar, F., 2012. Photorespiration and the evolution of C_4 photosynthesis. Annual Review of Plant Biology 63, 19–47.

Schopf, J. M., 1968. Studies in Antarctic paleobotany. Antarctic Journal of the United States 3, 176–177.

Schwendemann, A. B., Decombeix, A.-L., Taylor, T. N., Taylor, E. L., Krings, M., 2011. Morphological and functional stasis in mycorrhizal root nodules as exhibited by a Triassic conifer. Proceedings of the National Academy of Sciences 108, 13630–13634.

Serbet, R., Escapa, I., Taylor, T. N., Taylor, E. L., Cúneo, N. R., 2010. Additional observations on the enigmatic Permian plant *Buriadia* and implications on early coniferophyte evolution. Review of Palaeobotany and Palynology 161, 168–178.

Sharkey, T. D., 1988. Estimating the rate of photorespiration in leaves. Physiologia Plantarum 73, 147–152.

Sherman, T. F., 1981. On connecting large vessels to small. The meaning of Murray's law. The Journal of General Physiology 78, 431–453.

Sims, D. A., Pearcy, R. W., 1992. Response of leaf anatomy and photosynthetic capacity in *Alocasia macrorrhiza* (Araceae) to a transfer from low to high light. American journal of botany 79, 449–455.

Sims, D. A., Seemann, J. R., Luo, Y., 1998. Elevated CO_2 concentration has independent effects on expansion rates and thickness of soybean leaves across light and nitrogen gradients.

Journal of Experimental Botany 49, 583–591.

Smith, T. M., Shugart, H. H., Woodward, F. I., 1997a. Plant functional types: their relevance to ecosystem properties and global change. Cambridge University Press.

Smith, W. K., Vogelmann, T. C., DeLucia, E. H., Bell, D. T., Shepherd, K. A., 1997b. Leaf form and photosynthesis. Bioscience 47, 785–793.

Sobrado, M. A., 1991. Cost-benefit relationships in deciduous and evergreen leaves of tropical dry forest species. Functional Ecology 5, 608.

Sokal, R. R., Rohlf, F. J., 1995. Biometry: The Principles and Practice of Statistics in Biological Research. Macmillan.

Spicer, R. A., Chapman, J. L., 1990. Climate change and the evolution of high-latitude terrestrial vegetation and floras. Trends in Ecology & Evolution 5, 279–284.

Strauss, H., Peters-Kottig, W., 2003. The Paleozoic to Mesozoic carbon cycle revisited: The carbon isotopic composition of terrestrial organic matter. Geochemistry Geophysics Geosystems 4, 1–15.

Taiz, L., Zeiger, E., 2006. Plant Physiology. Sinauer Associates, Inc.

Tardieu, F., Granier, C., Muller, B., 1999. Modelling leaf expansion in a fluctuating environment: are changes in specific leaf area a consequence of changes in expansion rate? New Phytologist 143, 33–43.

Taylor, E. L., Ryberg, P. E., 2007. Tree growth at polar latitudes based on fossil tree ring analysis. Palaeogeography Palaeoclimatology Palaeoecology 225, 246–264.

Taylor, E. L., Taylor, T. N., Collinson, J. W., 1989. Depositional setting and paleobotany of Permian and Triassic permineralized peat from the central Transantarctic Mountains, Antarctica. International Journal of Coal Geology 12, 657–679.

Taylor, T. N., Kerp, H., Hass, H., 2005. Life history biology of early land plants: Deciphering the gametophyte phase. Proceedings of the National Academy of Sciences of the United States of America 102, 5892–5897.

Taylor, T. N., Taylor, E. L., Krings, M., 2009. Paleobotany: The Biology and Evolution of Fossil Plants. Academic Press.

Terashima, I., Hanba, Y. T., Tazoe, Y., Vyas, P., Yano, S., 2006. Irradiance and phenotype: comparative eco-development of sun and shade leaves in relation to photosynthetic CO_2 diffusion. Journal of Experimental Botany 57, 343–354.

Terashima, I., Miyazawa, S., Hanba, Y., 2001. Why Are Sun Leaves Thicker Than Shade Leaves? Consideration Based on Analyses of CO_2 Diffusion in the Leaf. J Plant Res 114, 93–105.

Thomas, H. H., 1933. On some pteridospermous plants from the mesozoic rocks of south africa. Philosophical Transactions of the Royal Society of London. Series B, Containing Papers of a Biological Character 222, 193–265.

Tidwell, W. D., Nambudiri, E. M. V., 1989. *Tomlisonia thomassonii*, gen. et sp. nov., a permineralized grass from the upper miocene Ricardo Formation, California. Review of Palaeobotany and Palynology 60, 165–177.

Timothy J., B., 2009. Xylem hydraulic physiology: the functional backbone of terrestrial plant productivity. Plant Science 177, 245–251.

Tomezzoli, R. N., Vilas, J. F., 1999. Palaeomagnetic constraints on the age of deformation of the Sierras Australes thrust and fold belt, Argentina. Geophysical Journal International 138, 857–870.

Trivett, M. L., Pigg, K. B., 1996. A survey of reticulate venation among fossil and living land plants. In: Taylor, D. W., Hickey, L. J. (Eds.), Flowering Plant Origin, Evolution & Phylogeny. Springer US, Boston, MA, pp. 8–31.

Tsuda, M., Tyree, M. T., 2000. Plant hydraulic conductance measured by the high pressure flow meter in crop plants. Journal of Experimental Botany 51, 823–828.

Uhl, D., Mosbrugger, V., 1999. Leaf venation density as a climate and environmental proxy: a critical review and new data. Palaeogeography, Palaeoclimatology, Palaeoecology 149, 15–26.

Uhl, D., Walther, H., Mosbrugger, V., 2002. Leaf venation density in angiosperm leaves as related to climatic and environmental conditions - problems and potential for palaeoclimatology. Neues Jahrbuch für Geologie und Paläontologie Abhandlungen 224, 49–95.

Velon H. Minshew, 1966. Stratigraphy of the Wisconsin Range, Horlick Mountains, Antarctica. Science 152, 637–638.

Villar, R., Merino, J., 2001. Comparison of leaf construction costs in woody species with differing leaf life-spans in contrasting ecosystems. New Phytologist 151, 213–226.

Vogan, P. J., Frohlich, M. W., Sage, R. F., 2007. The functional significance of C_3–C_4 intermediate traits in Heliotropium L. (Boraginaceae): gas exchange perspectives. Plant, Cell & Environment 30, 1337–1345.

Voznesenskaya, E. V., Franceschi, V. R., Kiirats, O., Freitag, H., Edwards, G. E., 2001. Kranz anatomy is not essential for terrestrial C_4 plant photosynthesis. Nature 414, 543–546.

Westoby, M., Falster, D. S., Moles, A. T., Vesk, P. A., Wright, I. J., 2002. Plant ecological strategies: some leading dimensions of variation between species. Annual Review of Ecology and Systematics 33, 125–159.

Williams, P. L., 1969. Petrology of upper Precambrian and Paleozoic sandstones in the Pensacola mountains, Antarctica. Journal of Sedimentary Research 39, 1455–1465.

Wilson, J. P., Fischer, W. W., 2011. Hydraulics of *Asteroxylon mackei*, an early Devonian vascular plant, and the early evolution of water transport tissue in terrestrial plants. Geobiology 9, 121–130.

Wilson, J. P., Knoll, A. H., Holbrook, N. M., Marshall, C. R., 2008. Modeling fluid flow in *Medullosa*, an anatomically unusual Carboniferous seed plant. Paleobiology 34, 472–493.

Wright, I. J., Westoby, M., 2002. Leaves at low versus high rainfall: coordination of structure, lifespan and physiology. New Phytologist 155, 403–416.

Wright, I., Reich, P. B., Westoby, M., 2001. Strategy shifts in leaf physiology, structure and nutrient content between species of high- and low-rainfall and high- and low-nutrient habitats. Functional ecology. 15, 423.

Wright, I. J., Reich, P. B., Westoby, M., Ackerly, D. D., Baruch, Z., Bongers, F., Cavender-Bares, J., Chapin, T., Cornelissen, J. H. C., Diemer, M., Flexas, J., Garnier, E., Groom, P. K., Gulias, J., Hikosaka, K., Lamont, B. B., Lee, T., Lee, W., Lusk, C., Midgley, J. J., Navas, M.-L., Niinemets, U., Oleksyn, J., Osada, N., Poorter, H., Poot, P., Prior, L., Pyankov, V. I., Roumet, C., Thomas, S. C., Tjoelker, M. G., Veneklaas, E. J., Villar, R., 2004. The worldwide leaf economics spectrum. Nature 428, 821–827.

Wright, I. J., Reich, P. B., Cornelissen, J. H. C., Falster, D. S., Groom, P. K., Hikosaka, K., Lee, W., Lusk, C. H., Niinemets, U., Oleksyn, J., Osada, N., Poorter, H., Warton, D. I., Westoby, M., 2005. Modulation of leaf economic traits and trait relationships by climate. Global Ecology and Biogeography 14, 411–421.

Wright, I. J., Leishman, M. R., Read, C., Westoby, M., 2006. Gradients of light availability and leaf traits with leaf age and canopy position in 28 Australian shrubs and trees. Funct. Plant Biol. 33, 407–419.

Young, D. J., Ryburn, R. J., 1968. The geology of Buckley and Darwin Nunataks, Beardmore Glacier, Ross Dependency, Antarctica. New Zealand Journal of Geology and Geophysics 11, 922–939.

Zachos, J. C., Shackleton, N. J., Revenaugh, J. S., Pälike, H., Flower, B. P., 2001. Climate response to orbital forcing across the oligocene-miocene boundary. Science 292, 274–278.

Zwieniecki, M. A., Stone, H. A., Leigh, A., Boyce, C. K., Holbrook, N. M., 2006. Hydraulic design of pine needles: one-dimensional optimization for single-vein leaves. Plant, Cell & Environment 29, 803–809.

Appendix I: Leaf hydraulics data

Appendix I. Table I. Leaf Venation Density for Permian Leaves Analyzed

Specimen Number	Venation Density (mm mm-2)	Genus	Locality	Formation
Pm 342	5.68	*Gangamopteris*	Allan Hills	Weller Coal Measures
Pm 400a	7.68	*Gangamopteris*	Allan Hills	Weller Coal Measures
Pm 410	6.96	*Gangamopteris*	Allan Hills	Weller Coal Measures
Pm 410	8.29	*Gangamopteris*	Allan Hills	Weller Coal Measures
Pm 5173	9.5	*Gangamopteris*	Allan Hills	Weller Coal Measures
Pm 100	7.7	*Gangamopteris*	Aztec Mt.	Weller Coal Measures
Pm 111	6.39	*Gangamopteris*	Aztec Mt.	Weller Coal Measures
Pm 111	9.54	*Gangamopteris*	Aztec Mt.	Weller Coal Measures
Pm 121	7.19	*Gangamopteris*	Aztec Mt.	Weller Coal Measures
Pm 124	6.67	*Gangamopteris*	Aztec Mt.	Weller Coal Measures
Pm 136a	7.24	*Gangamopteris*	Aztec Mt.	Weller Coal Measures
Pm 35	7.45	*Gangamopteris*	Aztec Mt.	Weller Coal Measures
Pm 37	8.35	*Gangamopteris*	Aztec Mt.	Weller Coal Measures
Pm 50	9.32	*Gangamopteris*	Aztec Mt.	Weller Coal Measures
Pm 5105	7.19	*Gangamopteris*	Aztec Mt.	Weller Coal Measures
Pm 5111	6.83	*Gangamopteris*	Aztec Mt.	Weller Coal Measures
Pm 5117	9.31	*Gangamopteris*	Aztec Mt.	Weller Coal Measures
Pm 63a	7.84	*Gangamopteris*	Aztec Mt.	Weller Coal Measures
Pm 67	8.86	*Gangamopteris*	Aztec Mt.	Weller Coal Measures
Pm 89	8.84	*Gangamopteris*	Aztec Mt.	Weller Coal Measures

Pm 210	9.46	*Gangamopteris*	Kennar Valley	Weller Coal Measures
Pm 230	8.4	*Gangamopteris*	Kennar Valley	Weller Coal Measures
Pm327a	5.17	*Gangamopteris*	Mt. Fleming	Weller Coal Measures
Pm 5463	6.25	*Gangamopteris*	Mt. Gran	Mt. Bastion
Pm 5464	6.5	*Gangamopteris*	Mt. Gran	Mt. Bastion
Pm 5468	6.13	*Gangamopteris*	Mt. Gran	Mt. Bastion
Pm 5470	8.29	*Gangamopteris*	Mt. Gran	Mt. Bastion
Pm 5471	8.96	*Gangamopteris*	Mt. Gran	Mt. Bastion
Pm 5472	9.32	*Gangamopteris*	Mt. Gran	Mt. Bastion
Pm 5474	8.4	*Gangamopteris*	Mt. Gran	Mt. Bastion
Pm 5475	8.94	*Gangamopteris*	Mt. Gran	Mt. Bastion
Pm 5476	10.81	*Gangamopteris*	Mt. Gran	Mt. Bastion
Pm 4211	13.53	*Gangamopteris*	Pecora Nunatak	Pecora
Pm 607	4.96	*Gangamopteris*	Pecora Nunatak	Pecora
Pm 4066	8.1	*Gangamopteris*	Robison Peak	Weller Coal Measures
Pm 4076	7.9	*Gangamopteris*	Robison Peak	Weller Coal Measures
Pm 4084	6.89	*Gangamopteris*	Robison Peak	Weller Coal Measures
Pm 4085	6.48	*Gangamopteris*	Robison Peak	Weller Coal Measures
Pm 860	6.79	*Gangamopteris*	Robison Peak	Weller Coal Measures
Pm 860	5.55	*Gangamopteris*	Robison Peak	Weller Coal Measures
Pm 860	5.9	*Gangamopteris*	Robison Peak	Weller Coal Measures
Pm 861	7.26	*Gangamopteris*	Robison Peak	Weller Coal Measures
Pm 342	9.17	*Glossopteris*	Allan Hills	Weller Coal Measures
Pm 342	8.96	*Glossopteris*	Allan Hills	Weller Coal Measures
Pm 342	8.38	*Glossopteris*	Allan Hills	Weller Coal Measures
Pm 342	9.15	*Glossopteris*	Allan Hills	Weller Coal Measures
Pm 342	12.15	*Glossopteris*	Allan Hills	Weller Coal Measures
Pm 342	8.73	*Glossopteris*	Allan Hills	Weller Coal Measures
Pm 363	8.56	*Glossopteris*	Allan Hills	Weller Coal Measures
Pm 374	8.18	*Glossopteris*	Allan Hills	Weller Coal Measures

Pm 374	10.08	*Glossopteris*	Allan Hills	Weller Coal Measures
Pm 374	8.82	*Glossopteris*	Allan Hills	Weller Coal Measures
Pm 389	10.52	*Glossopteris*	Allan Hills	Weller Coal Measures
Pm 389	10.88	*Glossopteris*	Allan Hills	Weller Coal Measures
Pm 389	8	*Glossopteris*	Allan Hills	Weller Coal Measures
Pm 389	10.72	*Glossopteris*	Allan Hills	Weller Coal Measures
Pm 393a	9.42	*Glossopteris*	Allan Hills	Weller Coal Measures
Pm 393b	8	*Glossopteris*	Allan Hills	Weller Coal Measures
Pm 400a	8.42	*Glossopteris*	Allan Hills	Weller Coal Measures
Pm 4052	9.02	*Glossopteris*	Allan Hills	Weller Coal Measures
Pm 410	9.02	*Glossopteris*	Allan Hills	Weller Coal Measures
Pm 4892b	11.07	*Glossopteris*	Allan Hills	Weller Coal Measures
Pm 4893a	10.26	*Glossopteris*	Allan Hills	Weller Coal Measures
Pm 4895	13.57	*Glossopteris*	Allan Hills	Weller Coal Measures
Pm 4895	10.76	*Glossopteris*	Allan Hills	Weller Coal Measures
Pm 4898b	9.68	*Glossopteris*	Allan Hills	Weller Coal Measures
Pm 4934	10.6	*Glossopteris*	Allan Hills	Weller Coal Measures
Pm 4936	10.99	*Glossopteris*	Allan Hills	Weller Coal Measures
Pm 4937	10.88	*Glossopteris*	Allan Hills	Weller Coal Measures
Pm 4942	10.34	*Glossopteris*	Allan Hills	Weller Coal Measures
Pm 4942	11.55	*Glossopteris*	Allan Hills	Weller Coal Measures
Pm 4943	10.62	*Glossopteris*	Allan Hills	Weller Coal Measures
Pm 4943	9.72	*Glossopteris*	Allan Hills	Weller Coal Measures
Pm 4947	10.61	*Glossopteris*	Allan Hills	Weller Coal Measures

Pm 4948	9.84	*Glossopteris*	Allan Hills	Weller Coal Measures
Pm 4948	9.06	*Glossopteris*	Allan Hills	Weller Coal Measures
Pm 4948	11.41	*Glossopteris*	Allan Hills	Weller Coal Measures
Pm 4949	10.2	*Glossopteris*	Allan Hills	Weller Coal Measures
Pm 4956	10.45	*Glossopteris*	Allan Hills	Weller Coal Measures
Pm 4956	10.64	*Glossopteris*	Allan Hills	Weller Coal Measures
Pm 4956	10.72	*Glossopteris*	Allan Hills	Weller Coal Measures
Pm 4957	9.27	*Glossopteris*	Allan Hills	Weller Coal Measures
Pm 4957	12.65	*Glossopteris*	Allan Hills	Weller Coal Measures
Pm 4957	10.6	*Glossopteris*	Allan Hills	Weller Coal Measures
Pm 4999	9.78	*Glossopteris*	Allan Hills	Weller Coal Measures
Pm 5010b	11.17	*Glossopteris*	Allan Hills	Weller Coal Measures
Pm 5010b	9.56	*Glossopteris*	Allan Hills	Weller Coal Measures
Pm 5013	10.99	*Glossopteris*	Allan Hills	Weller Coal Measures
Pm 5014	9.35	*Glossopteris*	Allan Hills	Weller Coal Measures
Pm 5015	11.56	*Glossopteris*	Allan Hills	Weller Coal Measures
Pm 5031	9.6	*Glossopteris*	Allan Hills	Weller Coal Measures
Pm 5051a	9.06	*Glossopteris*	Allan Hills	Weller Coal Measures
Pm 5171	8.57	*Glossopteris*	Allan Hills	Weller Coal Measures
Pm 5176	11.64	*Glossopteris*	Allan Hills	Weller Coal Measures
Pm 5176	9.7	*Glossopteris*	Allan Hills	Weller Coal Measures
Pm 5178	13.5	*Glossopteris*	Allan Hills	Weller Coal Measures
Pm 5208	10.41	*Glossopteris*	Allan Hills	Weller Coal Measures
Pm 593	8.53	*Glossopteris*	Allan Hills	Weller Coal Measures

Pm 593	10.44	*Glossopteris*	Allan Hills	Weller Coal Measures
Pm 100	9.13	*Glossopteris*	Aztec Mt.	Weller Coal Measures
Pm 100	10.58	*Glossopteris*	Aztec Mt.	Weller Coal Measures
Pm 112	10.63	*Glossopteris*	Aztec Mt.	Weller Coal Measures
Pm 118	9.28	*Glossopteris*	Aztec Mt.	Weller Coal Measures
Pm 120	12.93	*Glossopteris*	Aztec Mt.	Weller Coal Measures
Pm 120	8.72	*Glossopteris*	Aztec Mt.	Weller Coal Measures
Pm 123	9.91	*Glossopteris*	Aztec Mt.	Weller Coal Measures
Pm 124	8.05	*Glossopteris*	Aztec Mt.	Weller Coal Measures
Pm 136a	10.32	*Glossopteris*	Aztec Mt.	Weller Coal Measures
Pm 143	9.28	*Glossopteris*	Aztec Mt.	Weller Coal Measures
Pm 143	9.6	*Glossopteris*	Aztec Mt.	Weller Coal Measures
Pm 34	8.98	*Glossopteris*	Aztec Mt.	Weller Coal Measures
Pm 35	10.81	*Glossopteris*	Aztec Mt.	Weller Coal Measures
Pm 36	10.44	*Glossopteris*	Aztec Mt.	Weller Coal Measures
Pm 38	8.93	*Glossopteris*	Aztec Mt.	Weller Coal Measures
Pm 40	8.69	*Glossopteris*	Aztec Mt.	Weller Coal Measures
Pm 41	10.2	*Glossopteris*	Aztec Mt.	Weller Coal Measures
Pm 43	8.81	*Glossopteris*	Aztec Mt.	Weller Coal Measures
Pm 50	8.35	*Glossopteris*	Aztec Mt.	Weller Coal Measures
Pm 50	9.49	*Glossopteris*	Aztec Mt.	Weller Coal Measures
Pm 5107	11.59	*Glossopteris*	Aztec Mt.	Weller Coal Measures
Pm 5120	11.72	*Glossopteris*	Aztec Mt.	Weller Coal Measures
Pm 5122a	12.06	*Glossopteris*	Aztec Mt.	Weller Coal Measures

Pm 5126	9.62	*Glossopteris*	Aztec Mt.	Weller Coal Measures
Pm 5127b	8.91	*Glossopteris*	Aztec Mt.	Weller Coal Measures
Pm 56	8.25	*Glossopteris*	Aztec Mt.	Weller Coal Measures
Pm 603b	9.16	*Glossopteris*	Aztec Mt.	Weller Coal Measures
Pm 63a	8.68	*Glossopteris*	Aztec Mt.	Weller Coal Measures
Pm 72	8.43	*Glossopteris*	Aztec Mt.	Weller Coal Measures
Pm 91	10.31	*Glossopteris*	Aztec Mt.	Weller Coal Measures
Pm 99	9.69	*Glossopteris*	Aztec Mt.	Weller Coal Measures
Pm 99	8.25	*Glossopteris*	Aztec Mt.	Weller Coal Measures
Pm 1720	10.06	*Glossopteris*	Bazargaon	Kamthi
Pm 1733	10.68	*Glossopteris*	Bazargaon	Kamthi
Pm 1733	5.05	*Glossopteris*	Bazargaon	Kamthi
Pm 2436	7.42	*Glossopteris*	Bowden Neve	Upper Buckley
Pm 2452b	8.4	*Glossopteris*	Bowden Neve	Upper Buckley
Pm 2452b	9.66	*Glossopteris*	Bowden Neve	Upper Buckley
Pm 2453a	8.83	*Glossopteris*	Bowden Neve	Upper Buckley
Pm 2453a	9.79	*Glossopteris*	Bowden Neve	Upper Buckley
Pm 2453b	10.02	*Glossopteris*	Bowden Neve	Upper Buckley
Pm 2460	11.33	*Glossopteris*	Bowden Neve	Upper Buckley
Pm 2470	8.7	*Glossopteris*	Bowden Neve	Upper Buckley
Pm 2472	9.88	*Glossopteris*	Bowden Neve	Upper Buckley
Pm 2486	8.2	*Glossopteris*	Bowden Neve	Upper Buckley
Pm 2487	9.27	*Glossopteris*	Bowden Neve	Upper Buckley
Pm 2511	6	*Glossopteris*	Bowden Neve	Upper Buckley
Pm 2553	6.7	*Glossopteris*	Bowden Neve	Upper Buckley
Pm 2553	6.46	*Glossopteris*	Bowden Neve	Upper Buckley
Pm 2448	10.37	*Glossopteris*	Canopy Cliffs	Upper Buckley
Pm 2448	6.23	*Glossopteris*	Canopy Cliffs	Upper Buckley
Pm 1436	6.74	*Glossopteris*	Clarkson Peak	Upper Buckley
Pm 1436	11.93	*Glossopteris*	Clarkson Peak	Upper Buckley
Pm 731	8.1	*Glossopteris*	Coalsack Bluff	Upper Buckley
Pm 731	7.1	*Glossopteris*	Coalsack Bluff	Upper Buckley
Pm 731	8.18	*Glossopteris*	Coalsack Bluff	Upper Buckley
Pm 731	6.75	*Glossopteris*	Coalsack Bluff	Upper Buckley
Pm 735	10.55	*Glossopteris*	Coalsack Bluff	Upper Buckley
Pm 736	8.02	*Glossopteris*	Coalsack Bluff	Upper Buckley
Pm 737	8.38	*Glossopteris*	Coalsack Bluff	Upper Buckley
Pm 737	8.45	*Glossopteris*	Coalsack Bluff	Upper Buckley

Pm 737	8.33	*Glossopteris*	Coalsack Bluff	Upper Buckley
Pm 738	7.68	*Glossopteris*	Coalsack Bluff	Upper Buckley
Pm 738	9.31	*Glossopteris*	Coalsack Bluff	Upper Buckley
Pm 738	5.97	*Glossopteris*	Coalsack Bluff	Upper Buckley
Pm 739	7	*Glossopteris*	Coalsack Bluff	Upper Buckley
Pm 739	7.24	*Glossopteris*	Coalsack Bluff	Upper Buckley
Pm 739	6.05	*Glossopteris*	Coalsack Bluff	Upper Buckley
Pm 739	7.02	*Glossopteris*	Coalsack Bluff	Upper Buckley
Pm 739	9.55	*Glossopteris*	Coalsack Bluff	Upper Buckley
Pm 739	7.67	*Glossopteris*	Coalsack Bluff	Upper Buckley
Pm 739	8.59	*Glossopteris*	Coalsack Bluff	Upper Buckley
Pm 739	7.13	*Glossopteris*	Coalsack Bluff	Upper Buckley
Pm 758	3.93	*Glossopteris*	Coalsack Bluff	Upper Buckley
Pm 758	9.93	*Glossopteris*	Coalsack Bluff	Upper Buckley
Pm 759	10.3	*Glossopteris*	Coalsack Bluff	Upper Buckley
Pm 759	10.15	*Glossopteris*	Coalsack Bluff	Upper Buckley
Pm 759	6.48	*Glossopteris*	Coalsack Bluff	Upper Buckley
Pm 759	8.9	*Glossopteris*	Coalsack Bluff	Upper Buckley
Pm 759	7.15	*Glossopteris*	Coalsack Bluff	Upper Buckley
Pm 760	8.71	*Glossopteris*	Coalsack Bluff	Upper Buckley
Pm 760	8.89	*Glossopteris*	Coalsack Bluff	Upper Buckley
Pm 760	8.71	*Glossopteris*	Coalsack Bluff	Upper Buckley
Pm 760	9.3	*Glossopteris*	Coalsack Bluff	Upper Buckley
Pm 760	8.71	*Glossopteris*	Coalsack Bluff	Upper Buckley
Pm 760	8.11	*Glossopteris*	Coalsack Bluff	Upper Buckley
Pm 761	9.07	*Glossopteris*	Coalsack Bluff	Upper Buckley
Pm 761	8.11	*Glossopteris*	Coalsack Bluff	Upper Buckley
Pm 761	6.84	*Glossopteris*	Coalsack Bluff	Upper Buckley
Pm 763	8.18	*Glossopteris*	Coalsack Bluff	Upper Buckley
Pm 763	8.01	*Glossopteris*	Coalsack Bluff	Upper Buckley
Pm 763	10.35	*Glossopteris*	Coalsack Bluff	Upper Buckley
Pm 778	8.19	*Glossopteris*	Coalsack Bluff	Upper Buckley
Pm 778	7.63	*Glossopteris*	Coalsack Bluff	Upper Buckley
Pm 778	9.67	*Glossopteris*	Coalsack Bluff	Upper Buckley
Pm 779	10.58	*Glossopteris*	Coalsack Bluff	Upper Buckley
Pm 788	10.44	*Glossopteris*	Coalsack Bluff	Upper Buckley
Pm 788	7.32	*Glossopteris*	Coalsack Bluff	Upper Buckley
Pm 788	8.03	*Glossopteris*	Coalsack Bluff	Upper Buckley
Pm 788	9.37	*Glossopteris*	Coalsack Bluff	Upper Buckley
Pm 789	8.5	*Glossopteris*	Coalsack Bluff	Upper Buckley
Pm 789	9.89	*Glossopteris*	Coalsack Bluff	Upper Buckley
Pm 790	9.83	*Glossopteris*	Coalsack Bluff	Upper Buckley
Pm 790	8.19	*Glossopteris*	Coalsack Bluff	Upper Buckley
Pm 790	9.15	*Glossopteris*	Coalsack Bluff	Upper Buckley
Pm 790	8.84	*Glossopteris*	Coalsack Bluff	Upper Buckley

Pm 790	10.37	*Glossopteris*	Coalsack Bluff	Upper Buckley
Pm 791b	10.25	*Glossopteris*	Coalsack Bluff	Upper Buckley
Pm 791b	8.76	*Glossopteris*	Coalsack Bluff	Upper Buckley
Pm 791b	10.93	*Glossopteris*	Coalsack Bluff	Upper Buckley
Pm 2053	9.7	*Glossopteris*	Crack Bluff	Queen Maud
Pm 2236	10.23	*Glossopteris*	Crack Bluff	Queen Maud
Pm 2244	7.53	*Glossopteris*	Crack Bluff	Queen Maud
Pm 2244	10.2	*Glossopteris*	Crack Bluff	Queen Maud
Pm 2244	12.5	*Glossopteris*	Crack Bluff	Queen Maud
Pm 2244	10.37	*Glossopteris*	Crack Bluff	Queen Maud
Pm 2244	7.42	*Glossopteris*	Crack Bluff	Queen Maud
Pm 2244	7.43	*Glossopteris*	Crack Bluff	Queen Maud
Pm 2244	9.71	*Glossopteris*	Crack Bluff	Queen Maud
Pm 2250a	5.36	*Glossopteris*	Crack Bluff	Queen Maud
Pm 2250a	7.41	*Glossopteris*	Crack Bluff	Queen Maud
Pm 2253	8.39	*Glossopteris*	Crack Bluff	Queen Maud
Pm 2254	7.1	*Glossopteris*	Crack Bluff	Queen Maud
Pm 2256	11.49	*Glossopteris*	Crack Bluff	Queen Maud
Pm 2280	8.58	*Glossopteris*	Crack Bluff	Queen Maud
Pm 2285	6.58	*Glossopteris*	Crack Bluff	Queen Maud
Pm 2287	8.68	*Glossopteris*	Crack Bluff	Queen Maud
Pm 2298	9.78	*Glossopteris*	Crack Bluff	Queen Maud
Pm 2340	10.01	*Glossopteris*	Crack Bluff	Queen Maud
Pm 2343	11.57	*Glossopteris*	Crack Bluff	Queen Maud
Pm 2344	10.74	*Glossopteris*	Crack Bluff	Queen Maud
Pm 2346	7.44	*Glossopteris*	Crack Bluff	Queen Maud
Pm 2356	8.37	*Glossopteris*	Crack Bluff	Queen Maud
Pm 2357	8.13	*Glossopteris*	Crack Bluff	Queen Maud
Pm 2358	9.29	*Glossopteris*	Crack Bluff	Queen Maud
Pm 4734	8.84	*Glossopteris*	Cranfield Peak	Lower Buckley
Pm 4736	9.52	*Glossopteris*	Cranfield Peak	Lower Buckley
Pm 4738	9.5	*Glossopteris*	Cranfield Peak	Lower Buckley
Pm 4740a	9.45	*Glossopteris*	Cranfield Peak	Lower Buckley
Pm 4740a	13.97	*Glossopteris*	Cranfield Peak	Lower Buckley
Pm 4740b	11.1	*Glossopteris*	Cranfield Peak	Lower Buckley
Pm 918	9.7	*Glossopteris*	Erehwon Nunatak	Erehwon beds
Pm 923a	7.36	*Glossopteris*	Erehwon Nunatak	Erehwon beds
Pm 937	8.11	*Glossopteris*	Erehwon Nunatak	Erehwon beds
Pm 937	6.22	*Glossopteris*	Erehwon Nunatak	Erehwon beds
Pm 938	6.91	*Glossopteris*	Erehwon Nunatak	Erehwon beds
Pm 938	8.4	*Glossopteris*	Erehwon Nunatak	Erehwon beds
Pm 940	8.12	*Glossopteris*	Erehwon Nunatak	Erehwon beds
Pm 941b	9.46	*Glossopteris*	Erehwon Nunatak	Erehwon beds
Pm 1400	9.1	*Glossopteris*	Graphite Peak	Upper Buckley
Pm 4711	8.35	*Glossopteris*	Graphite Peak	Upper Buckley

Pm 4713	13.06	*Glossopteris*	Graphite Peak	Upper Buckley
Pm 4713	11.41	*Glossopteris*	Graphite Peak	Upper Buckley
Pm 4790	7.95	*Glossopteris*	Graphite Peak	Upper Buckley
Pm 4819	10.53	*Glossopteris*	Graphite Peak	Upper Buckley
Pm 4820	10.48	*Glossopteris*	Graphite Peak	Upper Buckley
Pm 1223	12.74	*Glossopteris*	Horlick Mts.	Queen Maud
Pm 3834	8.12	*Glossopteris*	Horlick Mts.	Queen Maud
Pm 1088	7.72	*Glossopteris*	Illawarra Coal Measures	Illawarra Coal Measures
Pm 1088	9.46	*Glossopteris*	Illawarra Coal Measures	Illawarra Coal Measures
Pm 1088	8.38	*Glossopteris*	Illawarra Coal Measures	Illawarra Coal Measures
Pm 1088	6.95	*Glossopteris*	Illawarra Coal Measures	Illawarra Coal Measures
Pm 1089	7.23	*Glossopteris*	Illawarra Coal Measures	Illawarra Coal Measures
Pm 1089	9.69	*Glossopteris*	Illawarra Coal Measures	Illawarra Coal Measures
Pm 1090	5.03	*Glossopteris*	Illawarra Coal Measures	Illawarra Coal Measures
Pm 1090	5.72	*Glossopteris*	Illawarra Coal Measures	Illawarra Coal Measures
Pm 1093	5.44	*Glossopteris*	Illawarra Coal Measures	Illawarra Coal Measures
Pm 1093	6.66	*Glossopteris*	Illawarra Coal Measures	Illawarra Coal Measures
Pm 1093	7.41	*Glossopteris*	Illawarra Coal Measures	Illawarra Coal Measures
Pm 1093	6.03	*Glossopteris*	Illawarra Coal Measures	Illawarra Coal Measures
Pm 1094	9.07	*Glossopteris*	Illawarra Coal Measures	Illawarra Coal Measures
Pm 1094	7.79	*Glossopteris*	Illawarra Coal Measures	Illawarra Coal Measures
Pm 1094	8.05	*Glossopteris*	Illawarra Coal Measures	Illawarra Coal Measures
Pm 1094	5.4	*Glossopteris*	Illawarra Coal Measures	Illawarra Coal Measures
Pm 1096	8.84	*Glossopteris*	Illawarra Coal Measures	Illawarra Coal Measures
Pm 1096	6.72	*Glossopteris*	Illawarra Coal Measures	Illawarra Coal Measures
Pm 1736	6.62	*Glossopteris*	Illawarra Coal Measures	Illawarra Coal Measures
Pm 1737	6.33	*Glossopteris*	Illawarra Coal Measures	Illawarra Coal Measures
Pm 1738	7.77	*Glossopteris*	Illawarra Coal Measures	Illawarra Coal Measures

Pm 1739	7.3	*Glossopteris*	Illawarra Coal Measures	Illawarra Coal Measures
Pm 1739	7.51	*Glossopteris*	Illawarra Coal Measures	Illawarra Coal Measures
Pm 3	5.47	*Glossopteris*	Illawarra Coal Measures	Illawarra Coal Measures
Pm 3	7.47	*Glossopteris*	Illawarra Coal Measures	Illawarra Coal Measures
Pm 3	8.49	*Glossopteris*	Illawarra Coal Measures	Illawarra Coal Measures
Pm 169	10.33	*Glossopteris*	Kennar Valley	Weller Coal Measures
Pm 211	9.15	*Glossopteris*	Kennar Valley	Weller Coal Measures
Pm 234	10.02	*Glossopteris*	Kennar Valley	Weller Coal Measures
Pm 5407	6.44	*Glossopteris*	KwaZulu-Natal	Normandien
Pm 5407	12.36	*Glossopteris*	KwaZulu-Natal	Normandien
Pm 5407	5.45	*Glossopteris*	KwaZulu-Natal	Normandien
Pm 5407	10.81	*Glossopteris*	KwaZulu-Natal	Normandien
Pm 1121	12.5	*Glossopteris*	Laguna Polina	Upper La Golondrina
Pm 1127	9.42	*Glossopteris*	Laguna Polina	Upper La Golondrina
Pm 1142	9.02	*Glossopteris*	Laguna Polina	Upper La Golondrina
Pm 1142	11.99	*Glossopteris*	Laguna Polina	Upper La Golondrina
Pm 2040	7.51	*Glossopteris*	Leaia Ledge	Mt. Glossopteris
Pm 3945	7.69	*Glossopteris*	Leaia Ledge	Mt. Glossopteris
Pm 3947	7.13	*Glossopteris*	Leaia Ledge	Mt. Glossopteris
Pm 3950	10.65	*Glossopteris*	Leaia Ledge	Mt. Glossopteris
Pm 3957	8.29	*Glossopteris*	Leaia Ledge	Mt. Glossopteris
Pm 3973a	9.09	*Glossopteris*	Leaia Ledge	Mt. Glossopteris
Pm 3973a	7.65	*Glossopteris*	Leaia Ledge	Mt. Glossopteris
Pm 3976	8.25	*Glossopteris*	Leaia Ledge	Mt. Glossopteris
Pm 3990	6.4	*Glossopteris*	Leaia Ledge	Mt. Glossopteris
Pm 3991	9.21	*Glossopteris*	Leaia Ledge	Mt. Glossopteris
Pm 3992	8.81	*Glossopteris*	Leaia Ledge	Mt. Glossopteris
Pm 3993	9.98	*Glossopteris*	Leaia Ledge	Mt. Glossopteris
Pm 3997	10.85	*Glossopteris*	Leaia Ledge	Mt. Glossopteris
Pm 1161	11.06	*Glossopteris*	McIntyre Promontory	Lower Buckley
Pm 1161	9.5	*Glossopteris*	McIntyre Promontory	Lower Buckley
Pm 1166	10.28	*Glossopteris*	McIntyre Promontory	Lower Buckley
Pm 1167	10.13	*Glossopteris*	McIntyre Promontory	Lower Buckley
Pm 1168	10.32	*Glossopteris*	McIntyre Promontory	Lower Buckley
Pm 1168	14.47	*Glossopteris*	McIntyre Promontory	Lower Buckley
Pm 1181	8.73	*Glossopteris*	McIntyre Promontory	Lower Buckley
Pm 1181	9.55	*Glossopteris*	McIntyre Promontory	Lower Buckley
Pm 1182	12.15	*Glossopteris*	McIntyre Promontory	Lower Buckley
Pm 1183	9.35	*Glossopteris*	McIntyre Promontory	Lower Buckley

Pm 1183	8.87	*Glossopteris*	McIntyre Promontory	Lower Buckley
Pm 4014	8.28	*Glossopteris*	McIntyre Promontory	Lower Buckley
Pm 4016	11.94	*Glossopteris*	McIntyre Promontory	Lower Buckley
Pm 4016	7.18	*Glossopteris*	McIntyre Promontory	Lower Buckley
Pm 4021	7.23	*Glossopteris*	McIntyre Promontory	Lower Buckley
Pm 4023	9.49	*Glossopteris*	McIntyre Promontory	Lower Buckley
Pm 4023	16.27	*Glossopteris*	McIntyre Promontory	Lower Buckley
Pm 4024	8.32	*Glossopteris*	McIntyre Promontory	Lower Buckley
Pm 4752	9.29	*Glossopteris*	McIntyre Promontory	Lower Buckley
Pm 4757	9.4	*Glossopteris*	McIntyre Promontory	Lower Buckley
Pm 4762	13.6	*Glossopteris*	McIntyre Promontory	Lower Buckley
Pm 4762	9.82	*Glossopteris*	McIntyre Promontory	Lower Buckley
Pm 4766	13.17	*Glossopteris*	McIntyre Promontory	Lower Buckley
Pm 4767	12.76	*Glossopteris*	McIntyre Promontory	Lower Buckley
Pm 4769b	12.1	*Glossopteris*	McIntyre Promontory	Lower Buckley
Pm 1430	7.86	*Glossopteris*	McKay Cliffs	Mackellar or Fairchild
Pm 2593	8.48	*Glossopteris*	Mine Ledge	Mt. Glossopteris
Pm 2593	9.46	*Glossopteris*	Mine Ledge	Mt. Glossopteris
Pm 2594	8.15	*Glossopteris*	Mine Ledge	Mt. Glossopteris
Pm 2595	8.35	*Glossopteris*	Mine Ledge	Mt. Glossopteris
Pm 2600	8.37	*Glossopteris*	Mine Ledge	Mt. Glossopteris
Pm 2600	10.1	*Glossopteris*	Mine Ledge	Mt. Glossopteris
Pm 2600	7.9	*Glossopteris*	Mine Ledge	Mt. Glossopteris
Pm 2600	7.56	*Glossopteris*	Mine Ledge	Mt. Glossopteris
Pm 3790b	8.86	*Glossopteris*	Mine Ledge	Mt. Glossopteris
Pm 3790b	9.77	*Glossopteris*	Mine Ledge	Mt. Glossopteris
Pm 3792	7.9	*Glossopteris*	Mine Ledge	Mt. Glossopteris
Pm 3795	7.56	*Glossopteris*	Mine Ledge	Mt. Glossopteris
Pm 3796a	8.54	*Glossopteris*	Mine Ledge	Mt. Glossopteris
Pm 568	8.98	*Glossopteris*	Mine Ledge	Mt. Glossopteris
Pm 582	10.67	*Glossopteris*	Mine Ledge	Mt. Glossopteris
Pm 582	7.97	*Glossopteris*	Mine Ledge	Mt. Glossopteris
Pm 643	10.62	*Glossopteris*	Mine Ledge	Mt. Glossopteris
Pm 3693	7.27	*Glossopteris*	Moraine Ridge	Mt. Glossopteris
Pm 578b	12.81	*Glossopteris*	Moraine Ridge	Mt. Glossopteris
Pm 578b	13.2	*Glossopteris*	Moraine Ridge	Mt. Glossopteris
Pm 2836b	7.17	*Glossopteris*	Mt. Achernar	Upper Buckley
Pm 2836b	10.83	*Glossopteris*	Mt. Achernar	Upper Buckley
Pm 2836b	9.06	*Glossopteris*	Mt. Achernar	Upper Buckley
Pm 2842a	7.98	*Glossopteris*	Mt. Achernar	Upper Buckley
Pm 2842a	7	*Glossopteris*	Mt. Achernar	Upper Buckley
Pm 2842a	10.04	*Glossopteris*	Mt. Achernar	Upper Buckley
Pm 2842a	10.05	*Glossopteris*	Mt. Achernar	Upper Buckley
Pm 2842a	9.17	*Glossopteris*	Mt. Achernar	Upper Buckley
Pm 2842a	8.17	*Glossopteris*	Mt. Achernar	Upper Buckley

Pm 2842	8.41	*Glossopteris*	Mt. Achernar	Upper Buckley
Pm 2842	10.94	*Glossopteris*	Mt. Achernar	Upper Buckley
Pm 2842	8.2	*Glossopteris*	Mt. Achernar	Upper Buckley
Pm 2842	7.99	*Glossopteris*	Mt. Achernar	Upper Buckley
Pm 2850	8.14	*Glossopteris*	Mt. Achernar	Upper Buckley
Pm 2850	10.65	*Glossopteris*	Mt. Achernar	Upper Buckley
Pm 2910	7.94	*Glossopteris*	Mt. Achernar	Upper Buckley
Pm 2910	7.68	*Glossopteris*	Mt. Achernar	Upper Buckley
Pm 2912	10.44	*Glossopteris*	Mt. Achernar	Upper Buckley
Pm 2913	7.23	*Glossopteris*	Mt. Achernar	Upper Buckley
Pm 2913	7.91	*Glossopteris*	Mt. Achernar	Upper Buckley
Pm 2915	9.97	*Glossopteris*	Mt. Achernar	Upper Buckley
Pm 2932	7.16	*Glossopteris*	Mt. Achernar	Upper Buckley
Pm 2932	8.06	*Glossopteris*	Mt. Achernar	Upper Buckley
Pm 2937	9.21	*Glossopteris*	Mt. Achernar	Upper Buckley
Pm 2937	11.08	*Glossopteris*	Mt. Achernar	Upper Buckley
Pm 2937	9.88	*Glossopteris*	Mt. Achernar	Upper Buckley
Pm 2940	6.68	*Glossopteris*	Mt. Achernar	Upper Buckley
Pm 2940	8.48	*Glossopteris*	Mt. Achernar	Upper Buckley
Pm 2952	10.81	*Glossopteris*	Mt. Achernar	Upper Buckley
Pm 2962	12.21	*Glossopteris*	Mt. Achernar	Upper Buckley
Pm 2963	8.19	*Glossopteris*	Mt. Achernar	Upper Buckley
Pm 2984	5.34	*Glossopteris*	Mt. Achernar	Upper Buckley
Pm 2984	7.82	*Glossopteris*	Mt. Achernar	Upper Buckley
Pm 2984	10.3	*Glossopteris*	Mt. Achernar	Upper Buckley
Pm 2985a	7.09	*Glossopteris*	Mt. Achernar	Upper Buckley
Pm 2985a	10.6	*Glossopteris*	Mt. Achernar	Upper Buckley
Pm 2985a	9.81	*Glossopteris*	Mt. Achernar	Upper Buckley
Pm 2985b	9.13	*Glossopteris*	Mt. Achernar	Upper Buckley
Pm 2995	8.25	*Glossopteris*	Mt. Achernar	Upper Buckley
Pm 2995	9.2	*Glossopteris*	Mt. Achernar	Upper Buckley
Pm 2995	8.05	*Glossopteris*	Mt. Achernar	Upper Buckley
Pm 2995	8.82	*Glossopteris*	Mt. Achernar	Upper Buckley
Pm 2995	6.47	*Glossopteris*	Mt. Achernar	Upper Buckley
Pm 2995	8.62	*Glossopteris*	Mt. Achernar	Upper Buckley
Pm 2995	10.57	*Glossopteris*	Mt. Achernar	Upper Buckley
Pm 2997	9.58	*Glossopteris*	Mt. Achernar	Upper Buckley
Pm 3010b	8.87	*Glossopteris*	Mt. Achernar	Upper Buckley
Pm 3010b	10.49	*Glossopteris*	Mt. Achernar	Upper Buckley
Pm 3010b	7.98	*Glossopteris*	Mt. Achernar	Upper Buckley
Pm 3010b	12.52	*Glossopteris*	Mt. Achernar	Upper Buckley
Pm 3010b	5.02	*Glossopteris*	Mt. Achernar	Upper Buckley
Pm 3010b	8.21	*Glossopteris*	Mt. Achernar	Upper Buckley
Pm 3010b	10.48	*Glossopteris*	Mt. Achernar	Upper Buckley
Pm 3042a	9.19	*Glossopteris*	Mt. Achernar	Upper Buckley

Pm 3042a	9.77	*Glossopteris*	Mt. Achernar	Upper Buckley
Pm 3042a	10.48	*Glossopteris*	Mt. Achernar	Upper Buckley
Pm 3043	7.96	*Glossopteris*	Mt. Achernar	Upper Buckley
Pm 3043	8.22	*Glossopteris*	Mt. Achernar	Upper Buckley
Pm 3043	9.65	*Glossopteris*	Mt. Achernar	Upper Buckley
Pm 3043	6.13	*Glossopteris*	Mt. Achernar	Upper Buckley
Pm 3043	10.18	*Glossopteris*	Mt. Achernar	Upper Buckley
Pm 3043	8.63	*Glossopteris*	Mt. Achernar	Upper Buckley
Pm 3044	8.56	*Glossopteris*	Mt. Achernar	Upper Buckley
Pm 3044	7.88	*Glossopteris*	Mt. Achernar	Upper Buckley
Pm 3045	7.91	*Glossopteris*	Mt. Achernar	Upper Buckley
Pm 3046	10.93	*Glossopteris*	Mt. Achernar	Upper Buckley
Pm 3047	8.1	*Glossopteris*	Mt. Achernar	Upper Buckley
Pm 3047	8.71	*Glossopteris*	Mt. Achernar	Upper Buckley
Pm 3047	8.99	*Glossopteris*	Mt. Achernar	Upper Buckley
Pm 3050	7.85	*Glossopteris*	Mt. Achernar	Upper Buckley
Pm 3075	7.45	*Glossopteris*	Mt. Achernar	Upper Buckley
Pm 3075	7.55	*Glossopteris*	Mt. Achernar	Upper Buckley
Pm 3075	10.26	*Glossopteris*	Mt. Achernar	Upper Buckley
Pm 3101	9.37	*Glossopteris*	Mt. Achernar	Upper Buckley
Pm 3101	11.87	*Glossopteris*	Mt. Achernar	Upper Buckley
Pm 3101	9.73	*Glossopteris*	Mt. Achernar	Upper Buckley
Pm 3101	7.21	*Glossopteris*	Mt. Achernar	Upper Buckley
Pm 3103	7.93	*Glossopteris*	Mt. Achernar	Upper Buckley
Pm 3103	9.5	*Glossopteris*	Mt. Achernar	Upper Buckley
Pm 3220	8.34	*Glossopteris*	Mt. Achernar	Upper Buckley
Pm 3318	8.67	*Glossopteris*	Mt. Achernar	Upper Buckley
Pm 3318	9.53	*Glossopteris*	Mt. Achernar	Upper Buckley
Pm 3320	8.39	*Glossopteris*	Mt. Achernar	Upper Buckley
Pm 3320	8.94	*Glossopteris*	Mt. Achernar	Upper Buckley
Pm 3320	9.4	*Glossopteris*	Mt. Achernar	Upper Buckley
Pm 3422	7.51	*Glossopteris*	Mt. Achernar	Upper Buckley
Pm 3426	10.19	*Glossopteris*	Mt. Achernar	Upper Buckley
Pm 3427	7.25	*Glossopteris*	Mt. Achernar	Upper Buckley
Pm 3428	6.11	*Glossopteris*	Mt. Achernar	Upper Buckley
Pm 3429	10.33	*Glossopteris*	Mt. Achernar	Upper Buckley
Pm 5260	9.21	*Glossopteris*	Mt. Achernar	Upper Buckley
Pm 526	11.92	*Glossopteris*	Mt. Achernar	Upper Buckley
Pm 530	6.36	*Glossopteris*	Mt. Achernar	Upper Buckley
Pm 5892	13.09	*Glossopteris*	Mt. Achernar	Upper Buckley
Pm 5893a	9.24	*Glossopteris*	Mt. Achernar	Upper Buckley
Pm 5912a	8.1	*Glossopteris*	Mt. Achernar	Upper Buckley
Pm 5912a	7.22	*Glossopteris*	Mt. Achernar	Upper Buckley
Pm 5912a	9.64	*Glossopteris*	Mt. Achernar	Upper Buckley
Pm 5924a	6.18	*Glossopteris*	Mt. Achernar	Upper Buckley

Pm 5924a	9	*Glossopteris*	Mt. Achernar	Upper Buckley
Pm 5924a	8.25	*Glossopteris*	Mt. Achernar	Upper Buckley
Pm 5924b	10.48	*Glossopteris*	Mt. Achernar	Upper Buckley
Pm 5928a	7.63	*Glossopteris*	Mt. Achernar	Upper Buckley
Pm 5930a	7.6	*Glossopteris*	Mt. Achernar	Upper Buckley
Pm 5930a	7.63	*Glossopteris*	Mt. Achernar	Upper Buckley
Pm 5933b	7.07	*Glossopteris*	Mt. Achernar	Upper Buckley
Pm 5933b	11.08	*Glossopteris*	Mt. Achernar	Upper Buckley
Pm 5934a	6.82	*Glossopteris*	Mt. Achernar	Upper Buckley
Pm 5934a	6.56	*Glossopteris*	Mt. Achernar	Upper Buckley
Pm 5936	8.7	*Glossopteris*	Mt. Achernar	Upper Buckley
Pm 5946a	4.9	*Glossopteris*	Mt. Achernar	Upper Buckley
Pm 5946c	9.67	*Glossopteris*	Mt. Achernar	Upper Buckley
Pm 5949	7.61	*Glossopteris*	Mt. Achernar	Upper Buckley
Pm 5949	6.43	*Glossopteris*	Mt. Achernar	Upper Buckley
Pm 5949	9.16	*Glossopteris*	Mt. Achernar	Upper Buckley
Pm 5949	10.01	*Glossopteris*	Mt. Achernar	Upper Buckley
Pm 5956b	6.62	*Glossopteris*	Mt. Achernar	Upper Buckley
Pm 5973a	9.13	*Glossopteris*	Mt. Achernar	Upper Buckley
Pm 5973b	7.58	*Glossopteris*	Mt. Achernar	Upper Buckley
Pm 5974	8.5	*Glossopteris*	Mt. Achernar	Upper Buckley
Pm 5974	9.35	*Glossopteris*	Mt. Achernar	Upper Buckley
Pm 5974	8.09	*Glossopteris*	Mt. Achernar	Upper Buckley
Pm 5977a	8.81	*Glossopteris*	Mt. Achernar	Upper Buckley
Pm 5983b	6.15	*Glossopteris*	Mt. Achernar	Upper Buckley
Pm 5988b	8	*Glossopteris*	Mt. Achernar	Upper Buckley
Pm 5988c	4.56	*Glossopteris*	Mt. Achernar	Upper Buckley
Pm 5989a	6.8	*Glossopteris*	Mt. Achernar	Upper Buckley
Pm 5989a	7.46	*Glossopteris*	Mt. Achernar	Upper Buckley
Pm 5989a	7.49	*Glossopteris*	Mt. Achernar	Upper Buckley
Pm 5989c	6.78	*Glossopteris*	Mt. Achernar	Upper Buckley
Pm 6001	5.02	*Glossopteris*	Mt. Achernar	Upper Buckley
Pm 6001	6.47	*Glossopteris*	Mt. Achernar	Upper Buckley
Pm 6001	5.88	*Glossopteris*	Mt. Achernar	Upper Buckley
Pm 6030	10.58	*Glossopteris*	Mt. Achernar	Upper Buckley
Pm 6035b	6.56	*Glossopteris*	Mt. Achernar	Upper Buckley
Pm 6045c	7.96	*Glossopteris*	Mt. Achernar	Upper Buckley
Pm 6065	9.48	*Glossopteris*	Mt. Achernar	Upper Buckley
Pm 6065	8.58	*Glossopteris*	Mt. Achernar	Upper Buckley
Pm 6065	7.73	*Glossopteris*	Mt. Achernar	Upper Buckley
Pm 6067a	9.62	*Glossopteris*	Mt. Achernar	Upper Buckley
Pm 6067a	7.3	*Glossopteris*	Mt. Achernar	Upper Buckley
Pm 6067a	7.11	*Glossopteris*	Mt. Achernar	Upper Buckley
Pm 6067a	8.72	*Glossopteris*	Mt. Achernar	Upper Buckley
Pm 6068	11.63	*Glossopteris*	Mt. Achernar	Upper Buckley

Pm 6068	10.5	*Glossopteris*	Mt. Achernar	Upper Buckley
Pm 6068	7.69	*Glossopteris*	Mt. Achernar	Upper Buckley
Pm 6070	11.72	*Glossopteris*	Mt. Achernar	Upper Buckley
Pm 6070	11.52	*Glossopteris*	Mt. Achernar	Upper Buckley
Pm 6071a	10.18	*Glossopteris*	Mt. Achernar	Upper Buckley
Pm 6072	7.22	*Glossopteris*	Mt. Achernar	Upper Buckley
Pm 6072	8.38	*Glossopteris*	Mt. Achernar	Upper Buckley
Pm 6072	8.31	*Glossopteris*	Mt. Achernar	Upper Buckley
Pm 6074	7.25	*Glossopteris*	Mt. Achernar	Upper Buckley
Pm 6075	7.13	*Glossopteris*	Mt. Achernar	Upper Buckley
Pm 6077	10.55	*Glossopteris*	Mt. Achernar	Upper Buckley
Pm 6077	9.59	*Glossopteris*	Mt. Achernar	Upper Buckley
Pm 6077	9.94	*Glossopteris*	Mt. Achernar	Upper Buckley
Pm 6077	6.55	*Glossopteris*	Mt. Achernar	Upper Buckley
Pm 6077	8.87	*Glossopteris*	Mt. Achernar	Upper Buckley
Pm 6078a	7.31	*Glossopteris*	Mt. Achernar	Upper Buckley
Pm 6079a	10.97	*Glossopteris*	Mt. Achernar	Upper Buckley
Pm 6079a	10.57	*Glossopteris*	Mt. Achernar	Upper Buckley
Pm 6079b	6.92	*Glossopteris*	Mt. Achernar	Upper Buckley
Pm 6079b	7.17	*Glossopteris*	Mt. Achernar	Upper Buckley
Pm 6079b	9.61	*Glossopteris*	Mt. Achernar	Upper Buckley
Pm 6080	7.72	*Glossopteris*	Mt. Achernar	Upper Buckley
Pm 6080	7.87	*Glossopteris*	Mt. Achernar	Upper Buckley
Pm 6081	6.2	*Glossopteris*	Mt. Achernar	Upper Buckley
Pm 6082a	8.81	*Glossopteris*	Mt. Achernar	Upper Buckley
Pm 6083	8.47	*Glossopteris*	Mt. Achernar	Upper Buckley
Pm 6083	8.71	*Glossopteris*	Mt. Achernar	Upper Buckley
Pm 6084	6.35	*Glossopteris*	Mt. Achernar	Upper Buckley
Pm 6084	7.19	*Glossopteris*	Mt. Achernar	Upper Buckley
Pm 6084	6.92	*Glossopteris*	Mt. Achernar	Upper Buckley
Pm 6084	7.16	*Glossopteris*	Mt. Achernar	Upper Buckley
Pm 6085	8.54	*Glossopteris*	Mt. Achernar	Upper Buckley
Pm 6085	9.9	*Glossopteris*	Mt. Achernar	Upper Buckley
Pm 6087a	8.64	*Glossopteris*	Mt. Achernar	Upper Buckley
Pm 6087b	8.56	*Glossopteris*	Mt. Achernar	Upper Buckley
Pm 6088	9.1	*Glossopteris*	Mt. Achernar	Upper Buckley
Pm 6089	9.12	*Glossopteris*	Mt. Achernar	Upper Buckley
Pm 6092	7.82	*Glossopteris*	Mt. Achernar	Upper Buckley
Pm 6094	7.77	*Glossopteris*	Mt. Achernar	Upper Buckley
Pm 6094	8.82	*Glossopteris*	Mt. Achernar	Upper Buckley
Pm 6095	8.35	*Glossopteris*	Mt. Achernar	Upper Buckley
Pm 6095	9.73	*Glossopteris*	Mt. Achernar	Upper Buckley
Pm 6096	6.88	*Glossopteris*	Mt. Achernar	Upper Buckley
Pm 6096	10.24	*Glossopteris*	Mt. Achernar	Upper Buckley
Pm 6098	8.35	*Glossopteris*	Mt. Achernar	Upper Buckley

Pm 6100	9.18	*Glossopteris*	Mt. Achernar	Upper Buckley
Pm 6101	7.88	*Glossopteris*	Mt. Achernar	Upper Buckley
Pm 6102	10.07	*Glossopteris*	Mt. Achernar	Upper Buckley
Pm 6103	6.99	*Glossopteris*	Mt. Achernar	Upper Buckley
Pm 6104	9.33	*Glossopteris*	Mt. Achernar	Upper Buckley
Pm 6105	9.22	*Glossopteris*	Mt. Achernar	Upper Buckley
Pm 6107	9.1	*Glossopteris*	Mt. Achernar	Upper Buckley
Pm 6107	6.34	*Glossopteris*	Mt. Achernar	Upper Buckley
Pm 6108	8.01	*Glossopteris*	Mt. Achernar	Upper Buckley
Pm 6111	10.01	*Glossopteris*	Mt. Achernar	Upper Buckley
Pm 829	10.43	*Glossopteris*	Mt. Achernar	Upper Buckley
Pm 830	8.92	*Glossopteris*	Mt. Achernar	Upper Buckley
Pm 830	10.98	*Glossopteris*	Mt. Achernar	Upper Buckley
Pm 831	9.11	*Glossopteris*	Mt. Achernar	Upper Buckley
Pm 831	8.41	*Glossopteris*	Mt. Achernar	Upper Buckley
Pm 833	6.43	*Glossopteris*	Mt. Achernar	Upper Buckley
Pm 1452	10.57	*Glossopteris*	Mt. Baldwin	Takrouna
Pm 1452	10.69	*Glossopteris*	Mt. Baldwin	Takrouna
Pm 1453	10.48	*Glossopteris*	Mt. Baldwin	Takrouna
Pm 1454	7.12	*Glossopteris*	Mt. Baldwin	Takrouna
Pm 1454	11.43	*Glossopteris*	Mt. Baldwin	Takrouna
Pm 1455	11.32	*Glossopteris*	Mt. Baldwin	Takrouna
Pm 1455	10.42	*Glossopteris*	Mt. Baldwin	Takrouna
Pm 1455	12.07	*Glossopteris*	Mt. Baldwin	Takrouna
Pm 1456	9.8	*Glossopteris*	Mt. Baldwin	Takrouna
Pm 1457	9	*Glossopteris*	Mt. Baldwin	Takrouna
Pm 4356	9.33	*Glossopteris*	Mt. Bartlett	Upper Buckley
Pm 4356	10.44	*Glossopteris*	Mt. Bartlett	Upper Buckley
Pm 4358	6.32	*Glossopteris*	Mt. Bartlett	Upper Buckley
Pm 4359	10.7	*Glossopteris*	Mt. Bartlett	Upper Buckley
Pm 4361	4.77	*Glossopteris*	Mt. Bartlett	Upper Buckley
Pm 4010a	9.82	*Glossopteris*	Mt. Bastion	Mt. Bastion
Pm 4012	10.14	*Glossopteris*	Mt. Bastion	Mt. Bastion
Pm 4012	13.18	*Glossopteris*	Mt. Bastion	Mt. Bastion
Pm 4012	11.18	*Glossopteris*	Mt. Bastion	Mt. Bastion
Pm 4659	12.69	*Glossopteris*	Mt. Feather	Weller Coal Measures
Pm 4681a	15.91	*Glossopteris*	Mt. Feather	Weller Coal Measures
Pm 4681b	15.39	*Glossopteris*	Mt. Feather	Weller Coal Measures
Pm 4683	12.72	*Glossopteris*	Mt. Feather	Weller Coal Measures
Pm 857	8.59	*Glossopteris*	Mt. Feather	Weller Coal Measures

Pm 857	10.54	*Glossopteris*	Mt. Feather	Weller Coal Measures
Pm 857	10.9	*Glossopteris*	Mt. Feather	Weller Coal Measures
Pm 857	10.34	*Glossopteris*	Mt. Feather	Weller Coal Measures
Pm 858	8.69	*Glossopteris*	Mt. Feather	Weller Coal Measures
Pm 2617	8.87	*Glossopteris*	Mt. Glossopteris	Mt. Glossopteris
Pm 2619	10.68	*Glossopteris*	Mt. Glossopteris	Mt. Glossopteris
Pm 3881	9.09	*Glossopteris*	Mt. Glossopteris	Mt. Glossopteris
Pm 3881	5.23	*Glossopteris*	Mt. Glossopteris	Mt. Glossopteris
Pm 3889	7.51	*Glossopteris*	Mt. Glossopteris	Mt. Glossopteris
Pm 3889	10.41	*Glossopteris*	Mt. Glossopteris	Mt. Glossopteris
Pm 3889	8.95	*Glossopteris*	Mt. Glossopteris	Mt. Glossopteris
Pm 5462	12.11	*Glossopteris*	Mt. Gran	Mt. Bastion
Pm 5465	11.14	*Glossopteris*	Mt. Gran	Mt. Bastion
Pm 5466	11.02	*Glossopteris*	Mt. Gran	Mt. Bastion
Pm 5467	10.86	*Glossopteris*	Mt. Gran	Mt. Bastion
Pm 635	10.7	*Glossopteris*	Mt. Gran	Mt. Bastion
Pm 5307	6.07	*Glossopteris*	Mt. Howe	Queen Maud
Pm 5307	9.47	*Glossopteris*	Mt. Howe	Queen Maud
Pm 5310	7.18	*Glossopteris*	Mt. Howe	Queen Maud
Pm 5312	11.47	*Glossopteris*	Mt. Howe	Queen Maud
Pm 5317	6.82	*Glossopteris*	Mt. Howe	Queen Maud
Pm 5318	8.78	*Glossopteris*	Mt. Howe	Queen Maud
Pm 5321	8.57	*Glossopteris*	Mt. Howe	Queen Maud
Pm 5323	10.98	*Glossopteris*	Mt. Howe	Queen Maud
Pm 5327	10.82	*Glossopteris*	Mt. Howe	Queen Maud
Pm 5328a	9.16	*Glossopteris*	Mt. Howe	Queen Maud
Pm 5329a	8.08	*Glossopteris*	Mt. Howe	Queen Maud
Pm 5330a	5.94	*Glossopteris*	Mt. Howe	Queen Maud
Pm 5335	7.11	*Glossopteris*	Mt. Howe	Queen Maud
Pm 5336	8.48	*Glossopteris*	Mt. Howe	Queen Maud
Pm 5336	8.68	*Glossopteris*	Mt. Howe	Queen Maud
Pm 5337	8.02	*Glossopteris*	Mt. Howe	Queen Maud
Pm 5344	8.85	*Glossopteris*	Mt. Howe	Queen Maud
Pm 5345	8.88	*Glossopteris*	Mt. Howe	Queen Maud
Pm 4729	10.88	*Glossopteris*	Mt. Kinsey	Upper Buckley
Pm 1117	10.1	*Glossopteris*	Mt. MacPherson	Mackellar or Fairchild
Pm 1117	10.05	*Glossopteris*	Mt. MacPherson	Mackellar or Fairchild
Pm 541	8.17	*Glossopteris*	Mt. Picciotto	Lower Buckley
Pm 541	11.28	*Glossopteris*	Mt. Picciotto	Lower Buckley
Pm 547	11.51	*Glossopteris*	Mt. Picciotto	Lower Buckley

Pm 547	10.57	*Glossopteris*	Mt. Picciotto	Lower Buckley
Pm 547	13.15	*Glossopteris*	Mt. Picciotto	Lower Buckley
Pm 547	8.79	*Glossopteris*	Mt. Picciotto	Lower Buckley
Pm 549	9.08	*Glossopteris*	Mt. Picciotto	Lower Buckley
Pm 549	7.51	*Glossopteris*	Mt. Picciotto	Lower Buckley
Pm 553	12.62	*Glossopteris*	Mt. Picciotto	Lower Buckley
Pm 553	11.83	*Glossopteris*	Mt. Picciotto	Lower Buckley
Pm 555	12.24	*Glossopteris*	Mt. Picciotto	Lower Buckley
Pm 557	15.96	*Glossopteris*	Mt. Picciotto	Lower Buckley
Pm 557	9	*Glossopteris*	Mt. Picciotto	Lower Buckley
Pm 558	12.87	*Glossopteris*	Mt. Picciotto	Lower Buckley
Pm 558	12.48	*Glossopteris*	Mt. Picciotto	Lower Buckley
Pm 559	12.23	*Glossopteris*	Mt. Picciotto	Lower Buckley
Pm 566	11.07	*Glossopteris*	Mt. Picciotto	Lower Buckley
Pm 566	12.71	*Glossopteris*	Mt. Picciotto	Lower Buckley
Pm 566	9.29	*Glossopteris*	Mt. Picciotto	Lower Buckley
Pm 1360	8.07	*Glossopteris*	Mt. Ropar	Upper Buckley
Pm 1360	7.37	*Glossopteris*	Mt. Ropar	Upper Buckley
Pm 1360	8.53	*Glossopteris*	Mt. Ropar	Upper Buckley
Pm 1360	6.05	*Glossopteris*	Mt. Ropar	Upper Buckley
Pm 1360	8.28	*Glossopteris*	Mt. Ropar	Upper Buckley
Pm 813	7.64	*Glossopteris*	Mt. Rosenwald	Upper Buckley
Pm 822	7.39	*Glossopteris*	Mt. Rosenwald	Upper Buckley
Pm 823	8.19	*Glossopteris*	Mt. Rosenwald	Upper Buckley
Pm 823	9.8	*Glossopteris*	Mt. Rosenwald	Upper Buckley
Pm 3740b	7.62	*Glossopteris*	Mt. Schopf	Mt. Glossopteris
Pm 3741	8.84	*Glossopteris*	Mt. Schopf	Mt. Glossopteris
Pm 2201	10.46	*Glossopteris*	Mt. Sirius	Upper Buckley
Pm 2203	9.68	*Glossopteris*	Mt. Sirius	Upper Buckley
Pm 2203	9.35	*Glossopteris*	Mt. Sirius	Upper Buckley
Pm 2207	10.02	*Glossopteris*	Mt. Sirius	Upper Buckley
Pm 2207	7.5	*Glossopteris*	Mt. Sirius	Upper Buckley
Pm 2209	9.39	*Glossopteris*	Mt. Sirius	Upper Buckley
Pm 2209	8.99	*Glossopteris*	Mt. Sirius	Upper Buckley
Pm 2209	9.87	*Glossopteris*	Mt. Sirius	Upper Buckley
Pm 2209	8.56	*Glossopteris*	Mt. Sirius	Upper Buckley
Pm 3508	8.03	*Glossopteris*	Mt. Sirius	Upper Buckley
Pm 3510	9.79	*Glossopteris*	Mt. Sirius	Upper Buckley
Pm 3512	8.09	*Glossopteris*	Mt. Sirius	Upper Buckley
Pm 3512	5.99	*Glossopteris*	Mt. Sirius	Upper Buckley
Pm 3513	9.7	*Glossopteris*	Mt. Sirius	Upper Buckley
Pm 3513	10	*Glossopteris*	Mt. Sirius	Upper Buckley
Pm 3513	10.48	*Glossopteris*	Mt. Sirius	Upper Buckley
Pm 3513	10.54	*Glossopteris*	Mt. Sirius	Upper Buckley
Pm 3513	10.07	*Glossopteris*	Mt. Sirius	Upper Buckley

Pm 3513	10.86	*Glossopteris*	Mt. Sirius	Upper Buckley
Pm 3514	6.61	*Glossopteris*	Mt. Sirius	Upper Buckley
Pm 3514	10.11	*Glossopteris*	Mt. Sirius	Upper Buckley
Pm 3570	10.59	*Glossopteris*	Mt. Sirius	Upper Buckley
Pm 3570	9.85	*Glossopteris*	Mt. Sirius	Upper Buckley
Pm 3581	8.68	*Glossopteris*	Mt. Sirius	Upper Buckley
Pm 3581	7.48	*Glossopteris*	Mt. Sirius	Upper Buckley
Pm 3581	8.77	*Glossopteris*	Mt. Sirius	Upper Buckley
Pm 3583	8.59	*Glossopteris*	Mt. Sirius	Upper Buckley
Pm 3584	8.4	*Glossopteris*	Mt. Sirius	Upper Buckley
Pm 3586	11.39	*Glossopteris*	Mt. Sirius	Upper Buckley
Pm 3592	11.58	*Glossopteris*	Mt. Sirius	Upper Buckley
Pm 3592	7.05	*Glossopteris*	Mt. Sirius	Upper Buckley
Pm 3592	5.57	*Glossopteris*	Mt. Sirius	Upper Buckley
Pm 909	8.79	*Glossopteris*	Mt. Sirius	Upper Buckley
Pm 909	11.26	*Glossopteris*	Mt. Sirius	Upper Buckley
Pm 5304a	7.52	*Glossopteris*	Mt. Weaver	Queen Maud
Pm 5306	7.29	*Glossopteris*	Mt. Weaver	Queen Maud
Pm 5306	7.42	*Glossopteris*	Mt. Weaver	Queen Maud
Pm 5340	8.39	*Glossopteris*	Mt. Weaver	Queen Maud
Pm 5341	8.27	*Glossopteris*	Mt. Weaver	Queen Maud
Pm 5342	6.97	*Glossopteris*	Mt. Weaver	Queen Maud
Pm 2362	9.37	*Glossopteris*	Mt. Wild	Upper Buckley
Pm 2363	11.69	*Glossopteris*	Mt. Wild	Upper Buckley
Pm 2364	10.32	*Glossopteris*	Mt. Wild	Upper Buckley
Pm 2365	10.71	*Glossopteris*	Mt. Wild	Upper Buckley
Pm 2366	10.12	*Glossopteris*	Mt. Wild	Upper Buckley
Pm 2369	10.67	*Glossopteris*	Mt. Wild	Upper Buckley
Pm 5408	6.01	*Glossopteris*	Orange Free State	Normandien
Pm 4092a	10.9	*Glossopteris*	Pecora Nunatak	Pecora
Pm 4094	14.19	*Glossopteris*	Pecora Nunatak	Pecora
Pm 4102	12.71	*Glossopteris*	Pecora Nunatak	Pecora
Pm 4107	14.37	*Glossopteris*	Pecora Nunatak	Pecora
Pm 4166	9.8	*Glossopteris*	Pecora Nunatak	Pecora
Pm 4167a	11.44	*Glossopteris*	Pecora Nunatak	Pecora
Pm 4167a	7.49	*Glossopteris*	Pecora Nunatak	Pecora
Pm 4167a	14.06	*Glossopteris*	Pecora Nunatak	Pecora
Pm 4167b	9.15	*Glossopteris*	Pecora Nunatak	Pecora
Pm 4167d	13.19	*Glossopteris*	Pecora Nunatak	Pecora
Pm 4167g	10.16	*Glossopteris*	Pecora Nunatak	Pecora
Pm 4171d	17.13	*Glossopteris*	Pecora Nunatak	Pecora
Pm 4171d	8.15	*Glossopteris*	Pecora Nunatak	Pecora
Pm 4173	14.28	*Glossopteris*	Pecora Nunatak	Pecora
Pm 4173	11.73	*Glossopteris*	Pecora Nunatak	Pecora
Pm 4189c	13.6	*Glossopteris*	Pecora Nunatak	Pecora

Pm 4189c	14.87	*Glossopteris*	Pecora Nunatak	Pecora
Pm 4189c	15.35	*Glossopteris*	Pecora Nunatak	Pecora
Pm 4196	13.3	*Glossopteris*	Pecora Nunatak	Pecora
Pm 4284	12.76	*Glossopteris*	Pecora Nunatak	Pecora
Pm 4328	8.87	*Glossopteris*	Pecora Nunatak	Pecora
Pm 4330a	10.16	*Glossopteris*	Pecora Nunatak	Pecora
Pm 4330a	10.02	*Glossopteris*	Pecora Nunatak	Pecora
Pm 4330b	9.97	*Glossopteris*	Pecora Nunatak	Pecora
Pm 4330c	11.05	*Glossopteris*	Pecora Nunatak	Pecora
Pm 4332	13.24	*Glossopteris*	Pecora Nunatak	Pecora
Pm 4332	12	*Glossopteris*	Pecora Nunatak	Pecora
Pm 4333a	12.05	*Glossopteris*	Pecora Nunatak	Pecora
Pm 4335	12.19	*Glossopteris*	Pecora Nunatak	Pecora
Pm 4337a	11.46	*Glossopteris*	Pecora Nunatak	Pecora
Pm 4340	11.44	*Glossopteris*	Pecora Nunatak	Pecora
Pm 4344	13.49	*Glossopteris*	Pecora Nunatak	Pecora
Pm 4349	13.05	*Glossopteris*	Pecora Nunatak	Pecora
Pm 4381	12.24	*Glossopteris*	Pecora Nunatak	Pecora
Pm 4390ab	15.6	*Glossopteris*	Pecora Nunatak	Pecora
Pm 4409	12.42	*Glossopteris*	Pecora Nunatak	Pecora
Pm 4437b	11.98	*Glossopteris*	Pecora Nunatak	Pecora
Pm 614	10.76	*Glossopteris*	Pecora Nunatak	Pecora
Pm 615	10.56	*Glossopteris*	Pecora Nunatak	Pecora
Pm 412	10.63	*Glossopteris*	Polarstar Peak	Polarstar
Pm 412	10.14	*Glossopteris*	Polarstar Peak	Polarstar
Pm 412	10.99	*Glossopteris*	Polarstar Peak	Polarstar
Pm 412	9.05	*Glossopteris*	Polarstar Peak	Polarstar
Pm 413	9.5	*Glossopteris*	Polarstar Peak	Polarstar
Pm 413	9.37	*Glossopteris*	Polarstar Peak	Polarstar
Pm 413	8.77	*Glossopteris*	Polarstar Peak	Polarstar
Pm 416	7.93	*Glossopteris*	Polarstar Peak	Polarstar
Pm 416	10.37	*Glossopteris*	Polarstar Peak	Polarstar
Pm 419	10.37	*Glossopteris*	Polarstar Peak	Polarstar
Pm 419	7.88	*Glossopteris*	Polarstar Peak	Polarstar
Pm 419	10.35	*Glossopteris*	Polarstar Peak	Polarstar
Pm 419	10.22	*Glossopteris*	Polarstar Peak	Polarstar
Pm 419	8.42	*Glossopteris*	Polarstar Peak	Polarstar
Pm 420	10.02	*Glossopteris*	Polarstar Peak	Polarstar
Pm 420	8.92	*Glossopteris*	Polarstar Peak	Polarstar
Pm 420	9.32	*Glossopteris*	Polarstar Peak	Polarstar
Pm 420	10.24	*Glossopteris*	Polarstar Peak	Polarstar
Pm 4431	10.56	*Glossopteris*	Polarstar Peak	Polarstar
Pm 4431	10.84	*Glossopteris*	Polarstar Peak	Polarstar
Pm 4434	11.33	*Glossopteris*	Polarstar Peak	Polarstar
Pm 4434	12.9	*Glossopteris*	Polarstar Peak	Polarstar

Pm 4436	9.4	*Glossopteris*	Polarstar Peak	Polarstar
Pm 4442a	12.15	*Glossopteris*	Polarstar Peak	Polarstar
Pm 4442e	8.33	*Glossopteris*	Polarstar Peak	Polarstar
Pm 4443e	9.57	*Glossopteris*	Polarstar Peak	Polarstar
Pm 4444b	10.32	*Glossopteris*	Polarstar Peak	Polarstar
Pm 4445a	7.02	*Glossopteris*	Polarstar Peak	Polarstar
Pm 4449a	10.24	*Glossopteris*	Polarstar Peak	Polarstar
Pm 4449c	8.55	*Glossopteris*	Polarstar Peak	Polarstar
Pm 4449ef	9.39	*Glossopteris*	Polarstar Peak	Polarstar
Pm 4449h	8.98	*Glossopteris*	Polarstar Peak	Polarstar
Pm 4449j	9.59	*Glossopteris*	Polarstar Peak	Polarstar
Pm 4449j	10.04	*Glossopteris*	Polarstar Peak	Polarstar
Pm 4451	7.82	*Glossopteris*	Polarstar Peak	Polarstar
Pm 4453b	8.38	*Glossopteris*	Polarstar Peak	Polarstar
Pm 4464	8.52	*Glossopteris*	Polarstar Peak	Polarstar
Pm 4469b	8.21	*Glossopteris*	Polarstar Peak	Polarstar
Pm 4469e	9.99	*Glossopteris*	Polarstar Peak	Polarstar
Pm 4470a	8.2	*Glossopteris*	Polarstar Peak	Polarstar
Pm 4470c	7.84	*Glossopteris*	Polarstar Peak	Polarstar
Pm 4471a	7.74	*Glossopteris*	Polarstar Peak	Polarstar
Pm 4471b	9.84	*Glossopteris*	Polarstar Peak	Polarstar
Pm 4471d	10.04	*Glossopteris*	Polarstar Peak	Polarstar
Pm 4473a	9.97	*Glossopteris*	Polarstar Peak	Polarstar
Pm 4476	7.83	*Glossopteris*	Polarstar Peak	Polarstar
Pm 4477	8.52	*Glossopteris*	Polarstar Peak	Polarstar
Pm 4477	11.21	*Glossopteris*	Polarstar Peak	Polarstar
Pm 4480a	11.13	*Glossopteris*	Polarstar Peak	Polarstar
Pm 4481	9.22	*Glossopteris*	Polarstar Peak	Polarstar
Pm 4481	9.12	*Glossopteris*	Polarstar Peak	Polarstar
Pm 4486a	12.5	*Glossopteris*	Polarstar Peak	Polarstar
Pm 4487	8.69	*Glossopteris*	Polarstar Peak	Polarstar
Pm 4487	11.24	*Glossopteris*	Polarstar Peak	Polarstar
Pm 4489	11.22	*Glossopteris*	Polarstar Peak	Polarstar
Pm 4498	8.13	*Glossopteris*	Polarstar Peak	Polarstar
Pm 4498	8.89	*Glossopteris*	Polarstar Peak	Polarstar
Pm 4500	7.77	*Glossopteris*	Polarstar Peak	Polarstar
Pm 4501a	7.54	*Glossopteris*	Polarstar Peak	Polarstar
Pm 4502b	9.44	*Glossopteris*	Polarstar Peak	Polarstar
Pm 4504c	8.36	*Glossopteris*	Polarstar Peak	Polarstar
Pm 4504d	8.33	*Glossopteris*	Polarstar Peak	Polarstar
Pm 4505a	7.72	*Glossopteris*	Polarstar Peak	Polarstar
Pm 4505	10.42	*Glossopteris*	Polarstar Peak	Polarstar
Pm 4508	8.8	*Glossopteris*	Polarstar Peak	Polarstar
Pm 4513	8.8	*Glossopteris*	Polarstar Peak	Polarstar
Pm 4513	9.14	*Glossopteris*	Polarstar Peak	Polarstar

Pm 4515	8.15	*Glossopteris*	Polarstar Peak	Polarstar
Pm 4520	9.05	*Glossopteris*	Polarstar Peak	Polarstar
Pm 4525	8.89	*Glossopteris*	Polarstar Peak	Polarstar
Pm 4527	7.95	*Glossopteris*	Polarstar Peak	Polarstar
Pm 4528	8.43	*Glossopteris*	Polarstar Peak	Polarstar
Pm 4528	9.87	*Glossopteris*	Polarstar Peak	Polarstar
Pm 4553c	7.55	*Glossopteris*	Polarstar Peak	Polarstar
Pm 4554	6.04	*Glossopteris*	Polarstar Peak	Polarstar
Pm 4554	9.56	*Glossopteris*	Polarstar Peak	Polarstar
Pm 4557a	9.86	*Glossopteris*	Polarstar Peak	Polarstar
Pm 4557g	9.02	*Glossopteris*	Polarstar Peak	Polarstar
Pm 4557g	9.97	*Glossopteris*	Polarstar Peak	Polarstar
Pm 4558a	8.73	*Glossopteris*	Polarstar Peak	Polarstar
Pm 4564	10.24	*Glossopteris*	Polarstar Peak	Polarstar
Pm 4564	11.48	*Glossopteris*	Polarstar Peak	Polarstar
Pm 4565	8.45	*Glossopteris*	Polarstar Peak	Polarstar
Pm 4565	8.87	*Glossopteris*	Polarstar Peak	Polarstar
Pm 4566a	7.28	*Glossopteris*	Polarstar Peak	Polarstar
Pm 4566b	9.68	*Glossopteris*	Polarstar Peak	Polarstar
Pm 4568	7.81	*Glossopteris*	Polarstar Peak	Polarstar
Pm 4571	8.67	*Glossopteris*	Polarstar Peak	Polarstar
Pm 4571	8.16	*Glossopteris*	Polarstar Peak	Polarstar
Pm 4576a	9.17	*Glossopteris*	Polarstar Peak	Polarstar
Pm 4576a	10.11	*Glossopteris*	Polarstar Peak	Polarstar
Pm 4577b	8.13	*Glossopteris*	Polarstar Peak	Polarstar
Pm 4577b	8.75	*Glossopteris*	Polarstar Peak	Polarstar
Pm 4581c	9.49	*Glossopteris*	Polarstar Peak	Polarstar
Pm 4584a	8.43	*Glossopteris*	Polarstar Peak	Polarstar
Pm 4584a	5.37	*Glossopteris*	Polarstar Peak	Polarstar
Pm 4602	8.02	*Glossopteris*	Polarstar Peak	Polarstar
Pm 4604	9.34	*Glossopteris*	Polarstar Peak	Polarstar
Pm 4632	8.32	*Glossopteris*	Polarstar Peak	Polarstar
Pm 569a	7.86	*Glossopteris*	Polarstar Peak	Polarstar
Pm 569a	10.06	*Glossopteris*	Polarstar Peak	Polarstar
Pm 569b	8.38	*Glossopteris*	Polarstar Peak	Polarstar
Pm 570	9.88	*Glossopteris*	Polarstar Peak	Polarstar
Pm 570	10.22	*Glossopteris*	Polarstar Peak	Polarstar
Pm 574	10.22	*Glossopteris*	Polarstar Peak	Polarstar
Pm 574	7.56	*Glossopteris*	Polarstar Peak	Polarstar
Pm 576a	9.27	*Glossopteris*	Polarstar Peak	Polarstar
Pm 2238	10.21	*Glossopteris*	Roaring Cliffs	Queen Maud
Pm 2240	6.71	*Glossopteris*	Roaring Cliffs	Queen Maud
Pm 2270a	10.44	*Glossopteris*	Roaring Cliffs	Queen Maud
Pm 2270a	7.1	*Glossopteris*	Roaring Cliffs	Queen Maud
Pm 2270c	11.92	*Glossopteris*	Roaring Cliffs	Queen Maud

Pm 2270i	11.2	*Glossopteris*	Roaring Cliffs	Queen Maud
Pm 2270l	6.45	*Glossopteris*	Roaring Cliffs	Queen Maud
Pm 2270l	6.21	*Glossopteris*	Roaring Cliffs	Queen Maud
Pm 4048	9.24	*Glossopteris*	Robison Peak	Weller Coal Measures
Pm 4054	8.75	*Glossopteris*	Robison Peak	Weller Coal Measures
Pm 4055	7.56	*Glossopteris*	Robison Peak	Weller Coal Measures
Pm 4060	9.07	*Glossopteris*	Robison Peak	Weller Coal Measures
Pm 4835d	8.68	*Glossopteris*	Rubble Ridge	Queen Maud
Pm 4836	6.42	*Glossopteris*	Rubble Ridge	Queen Maud
Pm 4837	6.42	*Glossopteris*	Rubble Ridge	Queen Maud
Pm 4837	7.97	*Glossopteris*	Rubble Ridge	Queen Maud
Pm 4838b	7.36	*Glossopteris*	Rubble Ridge	Queen Maud
Pm 4841c	7.91	*Glossopteris*	Rubble Ridge	Queen Maud
Pm 4842a	8.13	*Glossopteris*	Rubble Ridge	Queen Maud
Pm 4844	8.64	*Glossopteris*	Rubble Ridge	Queen Maud
Pm 4849b	7.74	*Glossopteris*	Rubble Ridge	Queen Maud
Pm 4849b	9.37	*Glossopteris*	Rubble Ridge	Queen Maud
Pm 4851a	9.84	*Glossopteris*	Rubble Ridge	Queen Maud
Pm 4851a	9.8	*Glossopteris*	Rubble Ridge	Queen Maud
Pm 4856a	11.69	*Glossopteris*	Rubble Ridge	Queen Maud
Pm 4858	7.41	*Glossopteris*	Rubble Ridge	Queen Maud
Pm 4861a	7.15	*Glossopteris*	Rubble Ridge	Queen Maud
Pm 4861a	8.83	*Glossopteris*	Rubble Ridge	Queen Maud
Pm 4861e	9.44	*Glossopteris*	Rubble Ridge	Queen Maud
Pm 4862	8.26	*Glossopteris*	Rubble Ridge	Queen Maud
Pm 4862	8.81	*Glossopteris*	Rubble Ridge	Queen Maud
Pm 4863a	6.87	*Glossopteris*	Rubble Ridge	Queen Maud
Pm 4878	8.68	*Glossopteris*	Rubble Ridge	Queen Maud
Pm 2420	7.33	*Glossopteris*	Sandford Cliffs	Upper Buckley
Pm 2421b	8.91	*Glossopteris*	Sandford Cliffs	Upper Buckley
Pm 2421b	9.22	*Glossopteris*	Sandford Cliffs	Upper Buckley
Pm 2421d	6.49	*Glossopteris*	Sandford Cliffs	Upper Buckley
Pm 5425	7.79	*Glossopteris*	Sierra de Pillahuinco	Bonete
Pm 5432	11.84	*Glossopteris*	Sierra de Pillahuinco	Bonete
Pm 10	8.61	*Glossopteris*	Skaar Ridge	Upper Buckley
Pm 10	7.36	*Glossopteris*	Skaar Ridge	Upper Buckley
Pm 10	8.17	*Glossopteris*	Skaar Ridge	Upper Buckley
Pm 10	9.51	*Glossopteris*	Skaar Ridge	Upper Buckley
Pm 10	7.92	*Glossopteris*	Skaar Ridge	Upper Buckley
Pm 10	8.89	*Glossopteris*	Skaar Ridge	Upper Buckley
Pm 13	9.1	*Glossopteris*	Skaar Ridge	Upper Buckley
Pm 13	7.63	*Glossopteris*	Skaar Ridge	Upper Buckley

Pm 33	9.33	*Glossopteris*	Skaar Ridge	Upper Buckley
Pm 33	9.15	*Glossopteris*	Skaar Ridge	Upper Buckley
Pm 3657	5.6	*Glossopteris*	Skaar Ridge	Upper Buckley
Pm 3657	8.6	*Glossopteris*	Skaar Ridge	Upper Buckley
Pm 3657	11.07	*Glossopteris*	Skaar Ridge	Upper Buckley
Pm 3657	9.32	*Glossopteris*	Skaar Ridge	Upper Buckley
Pm 3659	8.96	*Glossopteris*	Skaar Ridge	Upper Buckley
Pm 3659	8.36	*Glossopteris*	Skaar Ridge	Upper Buckley
Pm 3659	10.97	*Glossopteris*	Skaar Ridge	Upper Buckley
Pm 3663	8.36	*Glossopteris*	Skaar Ridge	Upper Buckley
Pm 3663	10.83	*Glossopteris*	Skaar Ridge	Upper Buckley
Pm 3668	8.54	*Glossopteris*	Skaar Ridge	Upper Buckley
Pm 3668	7.81	*Glossopteris*	Skaar Ridge	Upper Buckley
Pm 3668	8.39	*Glossopteris*	Skaar Ridge	Upper Buckley
Pm 3668	7.45	*Glossopteris*	Skaar Ridge	Upper Buckley
Pm 3668	7.53	*Glossopteris*	Skaar Ridge	Upper Buckley
Pm 3671	9.92	*Glossopteris*	Skaar Ridge	Upper Buckley
Pm 3671	9.04	*Glossopteris*	Skaar Ridge	Upper Buckley
Pm 3671	7.58	*Glossopteris*	Skaar Ridge	Upper Buckley
Pm 3671	8.02	*Glossopteris*	Skaar Ridge	Upper Buckley
Pm 425	9.1	*Glossopteris*	Skaar Ridge	Upper Buckley
Pm 427	4.83	*Glossopteris*	Skaar Ridge	Upper Buckley
Pm 427	8.33	*Glossopteris*	Skaar Ridge	Upper Buckley
Pm 427	6.86	*Glossopteris*	Skaar Ridge	Upper Buckley
Pm 427	9.78	*Glossopteris*	Skaar Ridge	Upper Buckley
Pm 428	8.89	*Glossopteris*	Skaar Ridge	Upper Buckley
Pm 428	10.15	*Glossopteris*	Skaar Ridge	Upper Buckley
Pm 428	8.97	*Glossopteris*	Skaar Ridge	Upper Buckley
Pm 428	10.65	*Glossopteris*	Skaar Ridge	Upper Buckley
Pm 428	10.66	*Glossopteris*	Skaar Ridge	Upper Buckley
Pm 430	9.08	*Glossopteris*	Skaar Ridge	Upper Buckley
Pm 430	10.51	*Glossopteris*	Skaar Ridge	Upper Buckley
Pm 430	6.98	*Glossopteris*	Skaar Ridge	Upper Buckley
Pm 431	10.42	*Glossopteris*	Skaar Ridge	Upper Buckley
Pm 431	5.51	*Glossopteris*	Skaar Ridge	Upper Buckley
Pm 431	9.14	*Glossopteris*	Skaar Ridge	Upper Buckley
Pm 431	7.13	*Glossopteris*	Skaar Ridge	Upper Buckley
Pm 431	7.52	*Glossopteris*	Skaar Ridge	Upper Buckley
Pm 431	10.17	*Glossopteris*	Skaar Ridge	Upper Buckley
Pm 431	7.8	*Glossopteris*	Skaar Ridge	Upper Buckley
Pm 431	7.09	*Glossopteris*	Skaar Ridge	Upper Buckley
Pm 431	7.59	*Glossopteris*	Skaar Ridge	Upper Buckley
Pm 433	5.61	*Glossopteris*	Skaar Ridge	Upper Buckley
Pm 434	8.8	*Glossopteris*	Skaar Ridge	Upper Buckley
Pm 435	6.6	*Glossopteris*	Skaar Ridge	Upper Buckley

Pm 436	10.7	*Glossopteris*	Skaar Ridge	Upper Buckley
Pm 436	6.83	*Glossopteris*	Skaar Ridge	Upper Buckley
Pm 436	7.25	*Glossopteris*	Skaar Ridge	Upper Buckley
Pm 437	6.63	*Glossopteris*	Skaar Ridge	Upper Buckley
Pm 437	10.43	*Glossopteris*	Skaar Ridge	Upper Buckley
Pm 437	8.65	*Glossopteris*	Skaar Ridge	Upper Buckley
Pm 437	9.73	*Glossopteris*	Skaar Ridge	Upper Buckley
Pm 438	9.25	*Glossopteris*	Skaar Ridge	Upper Buckley
Pm 438	8.49	*Glossopteris*	Skaar Ridge	Upper Buckley
Pm 438	7.95	*Glossopteris*	Skaar Ridge	Upper Buckley
Pm 438	7.82	*Glossopteris*	Skaar Ridge	Upper Buckley
Pm 456	6.72	*Glossopteris*	Skaar Ridge	Upper Buckley
Pm 456	7.25	*Glossopteris*	Skaar Ridge	Upper Buckley
Pm 456	9.4	*Glossopteris*	Skaar Ridge	Upper Buckley
Pm 456	8.72	*Glossopteris*	Skaar Ridge	Upper Buckley
Pm 458	7.65	*Glossopteris*	Skaar Ridge	Upper Buckley
Pm 458	8.85	*Glossopteris*	Skaar Ridge	Upper Buckley
Pm 458	8.28	*Glossopteris*	Skaar Ridge	Upper Buckley
Pm 468	8.29	*Glossopteris*	Skaar Ridge	Upper Buckley
Pm 468	8.02	*Glossopteris*	Skaar Ridge	Upper Buckley
Pm 468	6.39	*Glossopteris*	Skaar Ridge	Upper Buckley
Pm 468	9.58	*Glossopteris*	Skaar Ridge	Upper Buckley
Pm 472	6.73	*Glossopteris*	Skaar Ridge	Upper Buckley
Pm 472	11.1	*Glossopteris*	Skaar Ridge	Upper Buckley
Pm 472	8.8	*Glossopteris*	Skaar Ridge	Upper Buckley
Pm 472	7.58	*Glossopteris*	Skaar Ridge	Upper Buckley
Pm 472	10.23	*Glossopteris*	Skaar Ridge	Upper Buckley
Pm 472	6.65	*Glossopteris*	Skaar Ridge	Upper Buckley
Pm 476	7.95	*Glossopteris*	Skaar Ridge	Upper Buckley
Pm 476	8.54	*Glossopteris*	Skaar Ridge	Upper Buckley
Pm 476	8.11	*Glossopteris*	Skaar Ridge	Upper Buckley
Pm 477	11.27	*Glossopteris*	Skaar Ridge	Upper Buckley
Pm 477	10.63	*Glossopteris*	Skaar Ridge	Upper Buckley
Pm 477	8.41	*Glossopteris*	Skaar Ridge	Upper Buckley
Pm 477	7.6	*Glossopteris*	Skaar Ridge	Upper Buckley
Pm 477	7.7	*Glossopteris*	Skaar Ridge	Upper Buckley
Pm 479	7.83	*Glossopteris*	Skaar Ridge	Upper Buckley
Pm 479	10.42	*Glossopteris*	Skaar Ridge	Upper Buckley
Pm 496	6.42	*Glossopteris*	Skaar Ridge	Upper Buckley
Pm 496	8.27	*Glossopteris*	Skaar Ridge	Upper Buckley
Pm 4	6.67	*Glossopteris*	Skaar Ridge	Upper Buckley
Pm 4	8.8	*Glossopteris*	Skaar Ridge	Upper Buckley
Pm 4	7.26	*Glossopteris*	Skaar Ridge	Upper Buckley
Pm 4	7.69	*Glossopteris*	Skaar Ridge	Upper Buckley
Pm 4	10.57	*Glossopteris*	Skaar Ridge	Upper Buckley

Pm 4	8.77	*Glossopteris*	Skaar Ridge	Upper Buckley
Pm 4	11.49	*Glossopteris*	Skaar Ridge	Upper Buckley
Pm 4	9.64	*Glossopteris*	Skaar Ridge	Upper Buckley
Pm 502	7.77	*Glossopteris*	Skaar Ridge	Upper Buckley
Pm 503	10.29	*Glossopteris*	Skaar Ridge	Upper Buckley
Pm 503	8.64	*Glossopteris*	Skaar Ridge	Upper Buckley
Pm 503	9.94	*Glossopteris*	Skaar Ridge	Upper Buckley
Pm 503	6.31	*Glossopteris*	Skaar Ridge	Upper Buckley
Pm 503	8.15	*Glossopteris*	Skaar Ridge	Upper Buckley
Pm 6118a	7.61	*Glossopteris*	Skaar Ridge	Upper Buckley
Pm 6118a	8.94	*Glossopteris*	Skaar Ridge	Upper Buckley
Pm 6118b	8.49	*Glossopteris*	Skaar Ridge	Upper Buckley
Pm 6119	5.97	*Glossopteris*	Skaar Ridge	Upper Buckley
Pm 6121a	7.88	*Glossopteris*	Skaar Ridge	Upper Buckley
Pm 6121a	8.81	*Glossopteris*	Skaar Ridge	Upper Buckley
Pm 6121b	7.8	*Glossopteris*	Skaar Ridge	Upper Buckley
Pm 6121b	7.42	*Glossopteris*	Skaar Ridge	Upper Buckley
Pm 6121c	7.98	*Glossopteris*	Skaar Ridge	Upper Buckley
Pm 6121d	5.17	*Glossopteris*	Skaar Ridge	Upper Buckley
Pm 6121d	9.88	*Glossopteris*	Skaar Ridge	Upper Buckley
Pm 6121d	10.91	*Glossopteris*	Skaar Ridge	Upper Buckley
Pm 6121d	8.96	*Glossopteris*	Skaar Ridge	Upper Buckley
Pm 6121d	7.65	*Glossopteris*	Skaar Ridge	Upper Buckley
Pm 6121d	7.28	*Glossopteris*	Skaar Ridge	Upper Buckley
Pm 6121d	10.01	*Glossopteris*	Skaar Ridge	Upper Buckley
Pm 6122	9.02	*Glossopteris*	Skaar Ridge	Upper Buckley
Pm 6122	9.47	*Glossopteris*	Skaar Ridge	Upper Buckley
Pm 6123	10.99	*Glossopteris*	Skaar Ridge	Upper Buckley
Pm 6123	7.66	*Glossopteris*	Skaar Ridge	Upper Buckley
Pm 6123	10.13	*Glossopteris*	Skaar Ridge	Upper Buckley
Pm 6123	8.02	*Glossopteris*	Skaar Ridge	Upper Buckley
Pm 6123	6.55	*Glossopteris*	Skaar Ridge	Upper Buckley
Pm 6124	7.01	*Glossopteris*	Skaar Ridge	Upper Buckley
Pm 6124	8.4	*Glossopteris*	Skaar Ridge	Upper Buckley
Pm 6125a	9.78	*Glossopteris*	Skaar Ridge	Upper Buckley
Pm 6125a	8.48	*Glossopteris*	Skaar Ridge	Upper Buckley
Pm 6125a	10.17	*Glossopteris*	Skaar Ridge	Upper Buckley
Pm 6125a	10.07	*Glossopteris*	Skaar Ridge	Upper Buckley
Pm 6125a	7.28	*Glossopteris*	Skaar Ridge	Upper Buckley
Pm 6125a	9.18	*Glossopteris*	Skaar Ridge	Upper Buckley
Pm 6125b	8.13	*Glossopteris*	Skaar Ridge	Upper Buckley
Pm 6125b	7.09	*Glossopteris*	Skaar Ridge	Upper Buckley
Pm 6126a	6.36	*Glossopteris*	Skaar Ridge	Upper Buckley
Pm 6126a	8.48	*Glossopteris*	Skaar Ridge	Upper Buckley
Pm 6127	5.44	*Glossopteris*	Skaar Ridge	Upper Buckley

Pm 6127	8.31	*Glossopteris*	Skaar Ridge	Upper Buckley
Pm 6127	7.58	*Glossopteris*	Skaar Ridge	Upper Buckley
Pm 6127	7.23	*Glossopteris*	Skaar Ridge	Upper Buckley
Pm 6128	8.57	*Glossopteris*	Skaar Ridge	Upper Buckley
Pm 6128	8.09	*Glossopteris*	Skaar Ridge	Upper Buckley
Pm 6128	7.8	*Glossopteris*	Skaar Ridge	Upper Buckley
Pm 6129a	12.29	*Glossopteris*	Skaar Ridge	Upper Buckley
Pm 6129a	8.37	*Glossopteris*	Skaar Ridge	Upper Buckley
Pm 6129b	7.86	*Glossopteris*	Skaar Ridge	Upper Buckley
Pm 6129b	6.07	*Glossopteris*	Skaar Ridge	Upper Buckley
Pm 6129b	6.38	*Glossopteris*	Skaar Ridge	Upper Buckley
Pm 6129b	6.37	*Glossopteris*	Skaar Ridge	Upper Buckley
Pm 6129b	10.15	*Glossopteris*	Skaar Ridge	Upper Buckley
Pm 6130	8.04	*Glossopteris*	Skaar Ridge	Upper Buckley
Pm 6131a	9.81	*Glossopteris*	Skaar Ridge	Upper Buckley
Pm 6131a	8.95	*Glossopteris*	Skaar Ridge	Upper Buckley
Pm 6131a	9.56	*Glossopteris*	Skaar Ridge	Upper Buckley
Pm 6131a	8.84	*Glossopteris*	Skaar Ridge	Upper Buckley
Pm 6131a	11.63	*Glossopteris*	Skaar Ridge	Upper Buckley
Pm 6131a	10.31	*Glossopteris*	Skaar Ridge	Upper Buckley
Pm 6131b	8.07	*Glossopteris*	Skaar Ridge	Upper Buckley
Pm 6131b	8.96	*Glossopteris*	Skaar Ridge	Upper Buckley
Pm 6131b	7.8	*Glossopteris*	Skaar Ridge	Upper Buckley
Pm 6132	7.89	*Glossopteris*	Skaar Ridge	Upper Buckley
Pm 6132	7.36	*Glossopteris*	Skaar Ridge	Upper Buckley
Pm 6132	6.81	*Glossopteris*	Skaar Ridge	Upper Buckley
Pm 6132	11.56	*Glossopteris*	Skaar Ridge	Upper Buckley
Pm 6132	6.63	*Glossopteris*	Skaar Ridge	Upper Buckley
Pm 6132	7.75	*Glossopteris*	Skaar Ridge	Upper Buckley
Pm 6132	6.13	*Glossopteris*	Skaar Ridge	Upper Buckley
Pm 6132	8.38	*Glossopteris*	Skaar Ridge	Upper Buckley
Pm 6132	6.84	*Glossopteris*	Skaar Ridge	Upper Buckley
Pm 6133a	7.6	*Glossopteris*	Skaar Ridge	Upper Buckley
Pm 6133a	7.89	*Glossopteris*	Skaar Ridge	Upper Buckley
Pm 6133a	8.49	*Glossopteris*	Skaar Ridge	Upper Buckley
Pm 6133a	7.9	*Glossopteris*	Skaar Ridge	Upper Buckley
Pm 6133a	8.57	*Glossopteris*	Skaar Ridge	Upper Buckley
Pm 6133a	7.89	*Glossopteris*	Skaar Ridge	Upper Buckley
Pm 6133b	7.47	*Glossopteris*	Skaar Ridge	Upper Buckley
Pm 6133b	9.85	*Glossopteris*	Skaar Ridge	Upper Buckley
Pm 6134b	9.77	*Glossopteris*	Skaar Ridge	Upper Buckley
Pm 6134b	10.67	*Glossopteris*	Skaar Ridge	Upper Buckley
Pm 6134c	9.09	*Glossopteris*	Skaar Ridge	Upper Buckley
Pm 6134c	8.18	*Glossopteris*	Skaar Ridge	Upper Buckley
Pm 6134c	6.71	*Glossopteris*	Skaar Ridge	Upper Buckley

Pm 6134c	6.66	*Glossopteris*	Skaar Ridge	Upper Buckley
Pm 6134c	7.23	*Glossopteris*	Skaar Ridge	Upper Buckley
Pm 6134c	6.99	*Glossopteris*	Skaar Ridge	Upper Buckley
Pm 6134d	7.62	*Glossopteris*	Skaar Ridge	Upper Buckley
Pm 6134d	8.14	*Glossopteris*	Skaar Ridge	Upper Buckley
Pm 6134d	9.54	*Glossopteris*	Skaar Ridge	Upper Buckley
Pm 6134e	8.87	*Glossopteris*	Skaar Ridge	Upper Buckley
Pm 6134e	8.96	*Glossopteris*	Skaar Ridge	Upper Buckley
Pm 6134e	11.56	*Glossopteris*	Skaar Ridge	Upper Buckley
Pm 6134f	7.1	*Glossopteris*	Skaar Ridge	Upper Buckley
Pm 6134f	8.61	*Glossopteris*	Skaar Ridge	Upper Buckley
Pm 6134g	7.92	*Glossopteris*	Skaar Ridge	Upper Buckley
Pm 6134g	9.68	*Glossopteris*	Skaar Ridge	Upper Buckley
Pm 6134g	8.66	*Glossopteris*	Skaar Ridge	Upper Buckley
Pm 6134h	8.24	*Glossopteris*	Skaar Ridge	Upper Buckley
Pm 6134h	8.84	*Glossopteris*	Skaar Ridge	Upper Buckley
Pm 6134h	8.44	*Glossopteris*	Skaar Ridge	Upper Buckley
Pm 6134h	8.42	*Glossopteris*	Skaar Ridge	Upper Buckley
Pm 6134h	6.71	*Glossopteris*	Skaar Ridge	Upper Buckley
Pm 6134h	10.78	*Glossopteris*	Skaar Ridge	Upper Buckley
Pm 6135	10.36	*Glossopteris*	Skaar Ridge	Upper Buckley
Pm 6135	8.75	*Glossopteris*	Skaar Ridge	Upper Buckley
Pm 6135	8.81	*Glossopteris*	Skaar Ridge	Upper Buckley
Pm 6136a	7.88	*Glossopteris*	Skaar Ridge	Upper Buckley
Pm 6136a	8.48	*Glossopteris*	Skaar Ridge	Upper Buckley
Pm 6136b	8.84	*Glossopteris*	Skaar Ridge	Upper Buckley
Pm 6136b	8.45	*Glossopteris*	Skaar Ridge	Upper Buckley
Pm 6136c	7.97	*Glossopteris*	Skaar Ridge	Upper Buckley
Pm 6136c	8.6	*Glossopteris*	Skaar Ridge	Upper Buckley
Pm 6136c	10.68	*Glossopteris*	Skaar Ridge	Upper Buckley
Pm 6136d	7.47	*Glossopteris*	Skaar Ridge	Upper Buckley
Pm 6137a	7.86	*Glossopteris*	Skaar Ridge	Upper Buckley
Pm 6137a	9.63	*Glossopteris*	Skaar Ridge	Upper Buckley
Pm 6137b	7.41	*Glossopteris*	Skaar Ridge	Upper Buckley
Pm 6137d	6.58	*Glossopteris*	Skaar Ridge	Upper Buckley
Pm 6137d	8.13	*Glossopteris*	Skaar Ridge	Upper Buckley
Pm 6138a	8.59	*Glossopteris*	Skaar Ridge	Upper Buckley
Pm 6138a	9.06	*Glossopteris*	Skaar Ridge	Upper Buckley
Pm 6138a	7.59	*Glossopteris*	Skaar Ridge	Upper Buckley
Pm 6138b	9.29	*Glossopteris*	Skaar Ridge	Upper Buckley
Pm 6138b	11.87	*Glossopteris*	Skaar Ridge	Upper Buckley
Pm 6138b	9.74	*Glossopteris*	Skaar Ridge	Upper Buckley
Pm 6138b	9.4	*Glossopteris*	Skaar Ridge	Upper Buckley
Pm 6138b	10.18	*Glossopteris*	Skaar Ridge	Upper Buckley
Pm 6138c	8.65	*Glossopteris*	Skaar Ridge	Upper Buckley

Pm 6138c	8.11	*Glossopteris*	Skaar Ridge	Upper Buckley
Pm 6138c	7.99	*Glossopteris*	Skaar Ridge	Upper Buckley
Pm 6139a	8.09	*Glossopteris*	Skaar Ridge	Upper Buckley
Pm 6139a	6.83	*Glossopteris*	Skaar Ridge	Upper Buckley
Pm 6139a	7.38	*Glossopteris*	Skaar Ridge	Upper Buckley
Pm 6139b	8.32	*Glossopteris*	Skaar Ridge	Upper Buckley
Pm 6139b	7.66	*Glossopteris*	Skaar Ridge	Upper Buckley
Pm 6140	12	*Glossopteris*	Skaar Ridge	Upper Buckley
Pm 6140	5.43	*Glossopteris*	Skaar Ridge	Upper Buckley
Pm 6140	8.31	*Glossopteris*	Skaar Ridge	Upper Buckley
Pm 6140	8.08	*Glossopteris*	Skaar Ridge	Upper Buckley
Pm 6141	8.24	*Glossopteris*	Skaar Ridge	Upper Buckley
Pm 6143a	7.75	*Glossopteris*	Skaar Ridge	Upper Buckley
Pm 6143a	12.03	*Glossopteris*	Skaar Ridge	Upper Buckley
Pm 6143a	12.62	*Glossopteris*	Skaar Ridge	Upper Buckley
Pm 6143a	11.61	*Glossopteris*	Skaar Ridge	Upper Buckley
Pm 6143c	7.15	*Glossopteris*	Skaar Ridge	Upper Buckley
Pm 6143c	10.83	*Glossopteris*	Skaar Ridge	Upper Buckley
Pm 6143c	9.63	*Glossopteris*	Skaar Ridge	Upper Buckley
Pm 6143c	9.32	*Glossopteris*	Skaar Ridge	Upper Buckley
Pm 6143c	11.4	*Glossopteris*	Skaar Ridge	Upper Buckley
Pm 6143c	7.99	*Glossopteris*	Skaar Ridge	Upper Buckley
Pm 6143d	5.83	*Glossopteris*	Skaar Ridge	Upper Buckley
Pm 6144a	10.34	*Glossopteris*	Skaar Ridge	Upper Buckley
Pm 6144a	10.04	*Glossopteris*	Skaar Ridge	Upper Buckley
Pm 6144c	9.39	*Glossopteris*	Skaar Ridge	Upper Buckley
Pm 6145a	11.63	*Glossopteris*	Skaar Ridge	Upper Buckley
Pm 6145a	7.74	*Glossopteris*	Skaar Ridge	Upper Buckley
Pm 6146a	5.44	*Glossopteris*	Skaar Ridge	Upper Buckley
Pm 6146a	9.97	*Glossopteris*	Skaar Ridge	Upper Buckley
Pm 6147a	11.51	*Glossopteris*	Skaar Ridge	Upper Buckley
Pm 6147a	8.34	*Glossopteris*	Skaar Ridge	Upper Buckley
Pm 6147a	11.53	*Glossopteris*	Skaar Ridge	Upper Buckley
Pm 6147a	7.16	*Glossopteris*	Skaar Ridge	Upper Buckley
Pm 6147a	8.18	*Glossopteris*	Skaar Ridge	Upper Buckley
Pm 6148a	9.1	*Glossopteris*	Skaar Ridge	Upper Buckley
Pm 6148a	10.32	*Glossopteris*	Skaar Ridge	Upper Buckley
Pm 6148a	10.04	*Glossopteris*	Skaar Ridge	Upper Buckley
Pm 6148a	10.45	*Glossopteris*	Skaar Ridge	Upper Buckley
Pm 6148a	9.69	*Glossopteris*	Skaar Ridge	Upper Buckley
Pm 6148a	9.03	*Glossopteris*	Skaar Ridge	Upper Buckley
Pm 6148a	12.13	*Glossopteris*	Skaar Ridge	Upper Buckley
Pm 6148b	9.08	*Glossopteris*	Skaar Ridge	Upper Buckley
Pm 6148b	9.97	*Glossopteris*	Skaar Ridge	Upper Buckley
Pm 6148b	8.49	*Glossopteris*	Skaar Ridge	Upper Buckley

Pm 6149a	6.95	*Glossopteris*	Skaar Ridge	Upper Buckley
Pm 6149b	10.18	*Glossopteris*	Skaar Ridge	Upper Buckley
Pm 6150b	9.88	*Glossopteris*	Skaar Ridge	Upper Buckley
Pm 6150b	7.1	*Glossopteris*	Skaar Ridge	Upper Buckley
Pm 6150b	8.67	*Glossopteris*	Skaar Ridge	Upper Buckley
Pm 6151a	7.66	*Glossopteris*	Skaar Ridge	Upper Buckley
Pm 6151a	9.32	*Glossopteris*	Skaar Ridge	Upper Buckley
Pm 6151a	11.48	*Glossopteris*	Skaar Ridge	Upper Buckley
Pm 6151a	8.98	*Glossopteris*	Skaar Ridge	Upper Buckley
Pm 6151a	8.81	*Glossopteris*	Skaar Ridge	Upper Buckley
Pm 6151b	10.35	*Glossopteris*	Skaar Ridge	Upper Buckley
Pm 6151c	7.27	*Glossopteris*	Skaar Ridge	Upper Buckley
Pm 6151c	11.22	*Glossopteris*	Skaar Ridge	Upper Buckley
Pm 6151d	9.51	*Glossopteris*	Skaar Ridge	Upper Buckley
Pm 6151d	8.98	*Glossopteris*	Skaar Ridge	Upper Buckley
Pm 6152a	8	*Glossopteris*	Skaar Ridge	Upper Buckley
Pm 6152a	10.23	*Glossopteris*	Skaar Ridge	Upper Buckley
Pm 6153a	6.21	*Glossopteris*	Skaar Ridge	Upper Buckley
Pm 6153b	8.8	*Glossopteris*	Skaar Ridge	Upper Buckley
Pm 6153b	9.65	*Glossopteris*	Skaar Ridge	Upper Buckley
Pm 6153b	9.78	*Glossopteris*	Skaar Ridge	Upper Buckley
Pm 6154a	9.13	*Glossopteris*	Skaar Ridge	Upper Buckley
Pm 6154c	7.69	*Glossopteris*	Skaar Ridge	Upper Buckley
Pm 6155b	8.21	*Glossopteris*	Skaar Ridge	Upper Buckley
Pm 6156a	9.2	*Glossopteris*	Skaar Ridge	Upper Buckley
Pm 6156a	8.86	*Glossopteris*	Skaar Ridge	Upper Buckley
Pm 6157	11.68	*Glossopteris*	Skaar Ridge	Upper Buckley
Pm 6157	8.16	*Glossopteris*	Skaar Ridge	Upper Buckley
Pm 6157	8.83	*Glossopteris*	Skaar Ridge	Upper Buckley
Pm 6159	5.69	*Glossopteris*	Skaar Ridge	Upper Buckley
Pm 6160	8.02	*Glossopteris*	Skaar Ridge	Upper Buckley
Pm 6162	7.34	*Glossopteris*	Skaar Ridge	Upper Buckley
Pm 6162	10.93	*Glossopteris*	Skaar Ridge	Upper Buckley
Pm 6162	10.9	*Glossopteris*	Skaar Ridge	Upper Buckley
Pm 6164	6.43	*Glossopteris*	Skaar Ridge	Upper Buckley
Pm 6164	10.28	*Glossopteris*	Skaar Ridge	Upper Buckley
Pm 6164	8.95	*Glossopteris*	Skaar Ridge	Upper Buckley
Pm 6165	8.51	*Glossopteris*	Skaar Ridge	Upper Buckley
Pm 6165	6.36	*Glossopteris*	Skaar Ridge	Upper Buckley
Pm 6165	13.39	*Glossopteris*	Skaar Ridge	Upper Buckley
Pm 6166	9.67	*Glossopteris*	Skaar Ridge	Upper Buckley
Pm 6166	12.02	*Glossopteris*	Skaar Ridge	Upper Buckley
Pm 6166	9.47	*Glossopteris*	Skaar Ridge	Upper Buckley
Pm 6167	9.61	*Glossopteris*	Skaar Ridge	Upper Buckley
Pm 6167	9.4	*Glossopteris*	Skaar Ridge	Upper Buckley

Pm 6170	6.94	*Glossopteris*	Skaar Ridge	Upper Buckley
Pm 6171	9.07	*Glossopteris*	Skaar Ridge	Upper Buckley
Pm 6173	11.23	*Glossopteris*	Skaar Ridge	Upper Buckley
Pm 6173	10.15	*Glossopteris*	Skaar Ridge	Upper Buckley
Pm 6174	8.83	*Glossopteris*	Skaar Ridge	Upper Buckley
Pm 6174	8.26	*Glossopteris*	Skaar Ridge	Upper Buckley
Pm 6177	7.62	*Glossopteris*	Skaar Ridge	Upper Buckley
Pm 6177	8.82	*Glossopteris*	Skaar Ridge	Upper Buckley
Pm 6178	7.85	*Glossopteris*	Skaar Ridge	Upper Buckley
Pm 6179	9.68	*Glossopteris*	Skaar Ridge	Upper Buckley
Pm 6179	9.68	*Glossopteris*	Skaar Ridge	Upper Buckley
Pm 6179	10.74	*Glossopteris*	Skaar Ridge	Upper Buckley
Pm 6179	7.6	*Glossopteris*	Skaar Ridge	Upper Buckley
Pm 6179	10.66	*Glossopteris*	Skaar Ridge	Upper Buckley
Pm 6180	10.68	*Glossopteris*	Skaar Ridge	Upper Buckley
Pm 6181	8.71	*Glossopteris*	Skaar Ridge	Upper Buckley
Pm 6184a	9.92	*Glossopteris*	Skaar Ridge	Upper Buckley
Pm 6184a	9.88	*Glossopteris*	Skaar Ridge	Upper Buckley
Pm 6184a	8.15	*Glossopteris*	Skaar Ridge	Upper Buckley
Pm 6186	8.26	*Glossopteris*	Skaar Ridge	Upper Buckley
Pm 6188	10.81	*Glossopteris*	Skaar Ridge	Upper Buckley
Pm 6188	11.41	*Glossopteris*	Skaar Ridge	Upper Buckley
Pm 6188	7.83	*Glossopteris*	Skaar Ridge	Upper Buckley
Pm 6189	4.44	*Glossopteris*	Skaar Ridge	Upper Buckley
Pm 6189	7.33	*Glossopteris*	Skaar Ridge	Upper Buckley
Pm 6189	8.55	*Glossopteris*	Skaar Ridge	Upper Buckley
Pm 6189	8.01	*Glossopteris*	Skaar Ridge	Upper Buckley
Pm 6190	9.21	*Glossopteris*	Skaar Ridge	Upper Buckley
Pm 6190	7.41	*Glossopteris*	Skaar Ridge	Upper Buckley
Pm 6191	11.31	*Glossopteris*	Skaar Ridge	Upper Buckley
Pm 6191	10.81	*Glossopteris*	Skaar Ridge	Upper Buckley
Pm 6192	9.23	*Glossopteris*	Skaar Ridge	Upper Buckley
Pm 6194	6.69	*Glossopteris*	Skaar Ridge	Upper Buckley
Pm 6195	9.89	*Glossopteris*	Skaar Ridge	Upper Buckley
Pm 6196	9.52	*Glossopteris*	Skaar Ridge	Upper Buckley
Pm 6196	6.66	*Glossopteris*	Skaar Ridge	Upper Buckley
Pm 6198	10.53	*Glossopteris*	Skaar Ridge	Upper Buckley
Pm 6198	8.54	*Glossopteris*	Skaar Ridge	Upper Buckley
Pm 6198	8.27	*Glossopteris*	Skaar Ridge	Upper Buckley
Pm 6201	8.75	*Glossopteris*	Skaar Ridge	Upper Buckley
Pm 6201	11.46	*Glossopteris*	Skaar Ridge	Upper Buckley
Pm 6201	10.84	*Glossopteris*	Skaar Ridge	Upper Buckley
Pm 6202	8.42	*Glossopteris*	Skaar Ridge	Upper Buckley
Pm 6202	9.84	*Glossopteris*	Skaar Ridge	Upper Buckley
Pm 6202	8.6	*Glossopteris*	Skaar Ridge	Upper Buckley

Pm 6202	9.62	*Glossopteris*	Skaar Ridge	Upper Buckley
Pm 6215	9.5	*Glossopteris*	Skaar Ridge	Upper Buckley
Pm 6216	7.18	*Glossopteris*	Skaar Ridge	Upper Buckley
Pm 6217	10.52	*Glossopteris*	Skaar Ridge	Upper Buckley
Pm 6219a	8.15	*Glossopteris*	Skaar Ridge	Upper Buckley
Pm 6219a	9.04	*Glossopteris*	Skaar Ridge	Upper Buckley
Pm 6219a	8.1	*Glossopteris*	Skaar Ridge	Upper Buckley
Pm 6219a	8.33	*Glossopteris*	Skaar Ridge	Upper Buckley
Pm 6219a	9.44	*Glossopteris*	Skaar Ridge	Upper Buckley
Pm 6219a	9.87	*Glossopteris*	Skaar Ridge	Upper Buckley
Pm 6220a	8.97	*Glossopteris*	Skaar Ridge	Upper Buckley
Pm 6220a	8.6	*Glossopteris*	Skaar Ridge	Upper Buckley
Pm 6220g	8.22	*Glossopteris*	Skaar Ridge	Upper Buckley
Pm 6220i	8.59	*Glossopteris*	Skaar Ridge	Upper Buckley
Pm 6220l	8.02	*Glossopteris*	Skaar Ridge	Upper Buckley
Pm 6221aa	8.15	*Glossopteris*	Skaar Ridge	Upper Buckley
Pm 6221a	7.69	*Glossopteris*	Skaar Ridge	Upper Buckley
Pm 6221a	7.57	*Glossopteris*	Skaar Ridge	Upper Buckley
Pm 6221bb	5.63	*Glossopteris*	Skaar Ridge	Upper Buckley
Pm 6221bb	6.8	*Glossopteris*	Skaar Ridge	Upper Buckley
Pm 6221l	7.58	*Glossopteris*	Skaar Ridge	Upper Buckley
Pm 6221l	7.66	*Glossopteris*	Skaar Ridge	Upper Buckley
Pm 6221l	8.12	*Glossopteris*	Skaar Ridge	Upper Buckley
Pm 6221l	8.51	*Glossopteris*	Skaar Ridge	Upper Buckley
Pm 6221o	6.31	*Glossopteris*	Skaar Ridge	Upper Buckley
Pm 6221y	6.94	*Glossopteris*	Skaar Ridge	Upper Buckley
Pm 6221z	7.04	*Glossopteris*	Skaar Ridge	Upper Buckley
Pm 6224	10.42	*Glossopteris*	Skaar Ridge	Upper Buckley
Pm 6227	8.35	*Glossopteris*	Skaar Ridge	Upper Buckley
Pm 6228	10.1	*Glossopteris*	Skaar Ridge	Upper Buckley
Pm 657	8.74	*Glossopteris*	Skaar Ridge	Upper Buckley
Pm 657	11.48	*Glossopteris*	Skaar Ridge	Upper Buckley
Pm 658	6.18	*Glossopteris*	Skaar Ridge	Upper Buckley
Pm 658	7.71	*Glossopteris*	Skaar Ridge	Upper Buckley
Pm 659	7.51	*Glossopteris*	Skaar Ridge	Upper Buckley
Pm 659	9.15	*Glossopteris*	Skaar Ridge	Upper Buckley
Pm 659	9.53	*Glossopteris*	Skaar Ridge	Upper Buckley
Pm 659	9.64	*Glossopteris*	Skaar Ridge	Upper Buckley
Pm 659	8.56	*Glossopteris*	Skaar Ridge	Upper Buckley
Pm 659	8.86	*Glossopteris*	Skaar Ridge	Upper Buckley
Pm 7	9.05	*Glossopteris*	Skaar Ridge	Upper Buckley
Pm 7	8.12	*Glossopteris*	Skaar Ridge	Upper Buckley
Pm 7	7.24	*Glossopteris*	Skaar Ridge	Upper Buckley
Pm 7	6.04	*Glossopteris*	Skaar Ridge	Upper Buckley
Pm 9a	9.69	*Glossopteris*	Skaar Ridge	Upper Buckley

Pm 9b	10.52	*Glossopteris*	Skaar Ridge	Upper Buckley
Pm 9c	9.21	*Glossopteris*	Skaar Ridge	Upper Buckley
Pm 1456	10.05	*Glossopteris*	Terrace Ridge	Mt. Glossopteris
Pm 1727	10.81	*Glossopteris*	Terrace Ridge	Mt. Glossopteris
Pm 3675a	8.91	*Glossopteris*	Terrace Ridge	Mt. Glossopteris
Pm 3676	8.48	*Glossopteris*	Terrace Ridge	Mt. Glossopteris
Pm 3682b	9.29	*Glossopteris*	Terrace Ridge	Mt. Glossopteris
Pm 3688	10.64	*Glossopteris*	Terrace Ridge	Mt. Glossopteris
Pm 3688	9.5	*Glossopteris*	Terrace Ridge	Mt. Glossopteris
Pm 3698	7.82	*Glossopteris*	Terrace Ridge	Mt. Glossopteris
Pm 3699b	6.12	*Glossopteris*	Terrace Ridge	Mt. Glossopteris
Pm 3699b	9.16	*Glossopteris*	Terrace Ridge	Mt. Glossopteris
Pm 3699b	8.72	*Glossopteris*	Terrace Ridge	Mt. Glossopteris
Pm 3699b	7.49	*Glossopteris*	Terrace Ridge	Mt. Glossopteris
Pm 3699b	8.41	*Glossopteris*	Terrace Ridge	Mt. Glossopteris
Pm 3699b	9.49	*Glossopteris*	Terrace Ridge	Mt. Glossopteris
Pm 3699b	8.22	*Glossopteris*	Terrace Ridge	Mt. Glossopteris
Pm 3699b	7.22	*Glossopteris*	Terrace Ridge	Mt. Glossopteris
Pm 3699b	7.74	*Glossopteris*	Terrace Ridge	Mt. Glossopteris
Pm 3700	9.53	*Glossopteris*	Terrace Ridge	Mt. Glossopteris
Pm 3701a	10.4	*Glossopteris*	Terrace Ridge	Mt. Glossopteris
Pm 3701a	8.12	*Glossopteris*	Terrace Ridge	Mt. Glossopteris
Pm 3701a	8.04	*Glossopteris*	Terrace Ridge	Mt. Glossopteris
Pm 3701b	7.22	*Glossopteris*	Terrace Ridge	Mt. Glossopteris
Pm 3702	9.31	*Glossopteris*	Terrace Ridge	Mt. Glossopteris
Pm 3702	6.73	*Glossopteris*	Terrace Ridge	Mt. Glossopteris
Pm 3702	7.18	*Glossopteris*	Terrace Ridge	Mt. Glossopteris
Pm 3702	10.57	*Glossopteris*	Terrace Ridge	Mt. Glossopteris
Pm 3703	10.27	*Glossopteris*	Terrace Ridge	Mt. Glossopteris
Pm 3706	7.66	*Glossopteris*	Terrace Ridge	Mt. Glossopteris
Pm 3706	10.64	*Glossopteris*	Terrace Ridge	Mt. Glossopteris
Pm 3716	10.27	*Glossopteris*	Terrace Ridge	Mt. Glossopteris
Pm 3723	10.2	*Glossopteris*	Terrace Ridge	Mt. Glossopteris
Pm 3723	6.49	*Glossopteris*	Terrace Ridge	Mt. Glossopteris
Pm 3723	6.45	*Glossopteris*	Terrace Ridge	Mt. Glossopteris
Pm 3724	7.69	*Glossopteris*	Terrace Ridge	Mt. Glossopteris
Pm 3737	10.91	*Glossopteris*	Terrace Ridge	Mt. Glossopteris
Pm 3739	12.24	*Glossopteris*	Terrace Ridge	Mt. Glossopteris
Pm 3746	5.63	*Glossopteris*	Terrace Ridge	Mt. Glossopteris
Pm 3753	6.37	*Glossopteris*	Terrace Ridge	Mt. Glossopteris
Pm 3758	8.61	*Glossopteris*	Terrace Ridge	Mt. Glossopteris
Pm 577	5.99	*Glossopteris*	Terrace Ridge	Mt. Glossopteris
Pm 577	10.9	*Glossopteris*	Terrace Ridge	Mt. Glossopteris
Pm 577	8.07	*Glossopteris*	Terrace Ridge	Mt. Glossopteris
Pm 581	11.97	*Glossopteris*	Terrace Ridge	Mt. Glossopteris

Pm 585	11.46	*Glossopteris*	Terrace Ridge	Mt. Glossopteris
Pm 585	9.27	*Glossopteris*	Terrace Ridge	Mt. Glossopteris
Pm 585	9.37	*Glossopteris*	Terrace Ridge	Mt. Glossopteris
Pm 2695	8.43	*Glossopteris*	Tillite Ridge	Weaver
Pm 2695	10.25	*Glossopteris*	Tillite Ridge	Weaver
Pm 2699	7.71	*Glossopteris*	Tillite Ridge	Weaver
Pm 2778	7.88	*Glossopteris*	Tillite Ridge	Weaver
Pm 2779	12.67	*Glossopteris*	Tillite Ridge	Weaver
Pm 2808	9.06	*Glossopteris*	Tillite Ridge	Weaver
Pm 2809	10.88	*Glossopteris*	Tillite Ridge	Weaver
Pm 2811	10.72	*Glossopteris*	Tillite Ridge	Weaver
Pm 2820	10.1	*Glossopteris*	Tillite Ridge	Weaver
Pm 2821	11.3	*Glossopteris*	Tillite Ridge	Weaver
Pm 2822	11.03	*Glossopteris*	Tillite Ridge	Weaver
Pm 5389	8.96	*Glossopteris*	Waterberg Coal Field	Ecca Group
Pm 5390	7.13	*Glossopteris*	Waterberg Coal Field	Ecca Group
Pm 5397	9.06	*Glossopteris*	Waterberg Coal Field	Ecca Group
Pm 5417	8.25	*Glossopteris*	Zimbabwe	Wankie Sandstone
Pm 5419	11.18	*Glossopteris*	Zimbabwe	Wankie Sandstone
Pm 1436	7.79	*Noeggerathiopsis*	Clarkson Peak	Upper Buckley
Pm 155b	5.52	*Noeggerathiopsis*	Kennar Valley	Weller Coal Measures
Pm 167	5.89	*Noeggerathiopsis*	Kennar Valley	Weller Coal Measures
Pm 230	7.02	*Noeggerathiopsis*	Kennar Valley	Weller Coal Measures
Pm 232	5.23	*Noeggerathiopsis*	Kennar Valley	Weller Coal Measures
Pm 234	6.06	*Noeggerathiopsis*	Kennar Valley	Weller Coal Measures
Pm 235	5.85	*Noeggerathiopsis*	Kennar Valley	Weller Coal Measures
Pm 235	6.87	*Noeggerathiopsis*	Kennar Valley	Weller Coal Measures
Pm 4672	8.55	*Noeggerathiopsis*	Mt. Feather	Weller Coal Measures
Pm 4027	9.33	*Noeggerathiopsis*	Robison Peak	Weller Coal Measures
Pm 3744	6.62	*Noeggerathiopsis*	Terrace Ridge	Mt. Glossopteris
Pm 2750	6.56	*Noeggerathiopsis*	Tillite Ridge	Weaver
Pm 2827	5.49	*Noeggerathiopsis*	Tillite Ridge	Weaver

Appendix I. Table II. Leaf Venation Density for Triassic Leaves Analyzed

Specimen Number	Venation Density (mm mm-2)	Genus	Locality	Formation
T 1902	4.92	*Cladophlebis*	Mt. Wisting	Fremouw
T 1904	4.74	*Cladophlebis*	Mt. Wisting	Fremouw
T 1217	4.53	*Dejerseya*	Alfie's Elbow	FreFalla
T 124	6.7	*Dejerseya*	Mt. Falla	Falla
T 124	4.71	*Dejerseya*	Mt. Falla	Falla
T 171	4.69	*Dejerseya*	Mt. Falla	Falla
T 46	4.86	*Dejerseya*	Mt. Falla	Falla
T 58	4.19	*Dejerseya*	Mt. Falla	Falla
T 6221	4.52	*Dejerseya*	Mt. Falla	Falla
T 6229	5.29	*Dejerseya*	Mt. Falla	Falla
T 1009	4.88	*Dicroidium*	Alfie's Elbow	FreFalla
T 1013	4.91	*Dicroidium*	Alfie's Elbow	FreFalla
T 1013	4.49	*Dicroidium*	Alfie's Elbow	FreFalla
T 1015	5.96	*Dicroidium*	Alfie's Elbow	FreFalla
T 1017	4.8	*Dicroidium*	Alfie's Elbow	FreFalla
T 1018	6.63	*Dicroidium*	Alfie's Elbow	FreFalla
T 1034	4.96	*Dicroidium*	Alfie's Elbow	FreFalla
T 1042	4.59	*Dicroidium*	Alfie's Elbow	FreFalla
T 1043	5.78	*Dicroidium*	Alfie's Elbow	FreFalla
T 1043	5.29	*Dicroidium*	Alfie's Elbow	FreFalla
T 1048	4.64	*Dicroidium*	Alfie's Elbow	FreFalla
T 1063	5.03	*Dicroidium*	Alfie's Elbow	FreFalla
T 1075	5.96	*Dicroidium*	Alfie's Elbow	FreFalla
T 1097	5.19	*Dicroidium*	Alfie's Elbow	FreFalla
T 1124	6.37	*Dicroidium*	Alfie's Elbow	FreFalla
T 1129	5.47	*Dicroidium*	Alfie's Elbow	FreFalla
T 1130	5.16	*Dicroidium*	Alfie's Elbow	FreFalla
T 1133	3.95	*Dicroidium*	Alfie's Elbow	FreFalla
T 1147	4.9	*Dicroidium*	Alfie's Elbow	FreFalla
T 1155	4.81	*Dicroidium*	Alfie's Elbow	FreFalla
T 1161	4.54	*Dicroidium*	Alfie's Elbow	FreFalla
T 1161	4.46	*Dicroidium*	Alfie's Elbow	FreFalla
T 1164	4.53	*Dicroidium*	Alfie's Elbow	FreFalla
T 1200	5.28	*Dicroidium*	Alfie's Elbow	FreFalla
T 1200	5.05	*Dicroidium*	Alfie's Elbow	FreFalla
T 1205	3.74	*Dicroidium*	Alfie's Elbow	FreFalla
T 1205	4.29	*Dicroidium*	Alfie's Elbow	FreFalla
T 1209	4.64	*Dicroidium*	Alfie's Elbow	FreFalla
T 1209	5.29	*Dicroidium*	Alfie's Elbow	FreFalla

T 1217	5.31	*Dicroidium*	Alfie's Elbow	FreFalla
T 1219	4.01	*Dicroidium*	Alfie's Elbow	FreFalla
T 1227	3.9	*Dicroidium*	Alfie's Elbow	FreFalla
T 1228	5.08	*Dicroidium*	Alfie's Elbow	FreFalla
T 1241	4.41	*Dicroidium*	Alfie's Elbow	FreFalla
T 1242	5.1	*Dicroidium*	Alfie's Elbow	FreFalla
T 1247a	3.54	*Dicroidium*	Alfie's Elbow	FreFalla
T 1251	5.69	*Dicroidium*	Alfie's Elbow	FreFalla
T 1254	4.64	*Dicroidium*	Alfie's Elbow	FreFalla
T 1264c	5.51	*Dicroidium*	Alfie's Elbow	FreFalla
T 1273	5.17	*Dicroidium*	Alfie's Elbow	FreFalla
T 1290	4.15	*Dicroidium*	Alfie's Elbow	FreFalla
T 1311	5.47	*Dicroidium*	Alfie's Elbow	FreFalla
T 1375	4.26	*Dicroidium*	Alfie's Elbow	FreFalla
T 1375	4.9	*Dicroidium*	Alfie's Elbow	FreFalla
T 1389	3.84	*Dicroidium*	Alfie's Elbow	FreFalla
T 1397	5.28	*Dicroidium*	Alfie's Elbow	FreFalla
T 1409	4.79	*Dicroidium*	Alfie's Elbow	FreFalla
T 1413	3.8	*Dicroidium*	Alfie's Elbow	FreFalla
T 1416c	4.02	*Dicroidium*	Alfie's Elbow	FreFalla
T 1420	3.73	*Dicroidium*	Alfie's Elbow	FreFalla
T 1434	4.2	*Dicroidium*	Alfie's Elbow	FreFalla
T 1473	3.99	*Dicroidium*	Alfie's Elbow	FreFalla
T 1473	4.08	*Dicroidium*	Alfie's Elbow	FreFalla
T 1498	4.89	*Dicroidium*	Alfie's Elbow	FreFalla
T 5539	3.7	*Dicroidium*	Alfie's Elbow	FreFalla
T 5541	4.24	*Dicroidium*	Alfie's Elbow	FreFalla
T 5555	4.14	*Dicroidium*	Alfie's Elbow	FreFalla
T 5555	2.72	*Dicroidium*	Alfie's Elbow	FreFalla
T 5596b	4.58	*Dicroidium*	Alfie's Elbow	FreFalla
T 1969	5.17	*Dicroidium*	Allan Hills	Lashly
T 1971	4.61	*Dicroidium*	Allan Hills	Lashly
T 206	3.73	*Dicroidium*	Allan Hills	Lashly
T 247	4.66	*Dicroidium*	Allan Hills	Lashly
T 247	4.64	*Dicroidium*	Allan Hills	Lashly
T 247	3.68	*Dicroidium*	Allan Hills	Lashly
T 253	3.95	*Dicroidium*	Allan Hills	Lashly
T 253	3.81	*Dicroidium*	Allan Hills	Lashly
T 254	3.19	*Dicroidium*	Allan Hills	Lashly
T 255	5.3	*Dicroidium*	Allan Hills	Lashly
T 257	3.7	*Dicroidium*	Allan Hills	Lashly
T 259	6.8	*Dicroidium*	Allan Hills	Lashly
T 271	3.52	*Dicroidium*	Allan Hills	Lashly
T 271	3.62	*Dicroidium*	Allan Hills	Lashly
T 416	4.48	*Dicroidium*	Allan Hills	Lashly

T 417	3.9	*Dicroidium*	Allan Hills	Lashly
T 439	3.48	*Dicroidium*	Allan Hills	Lashly
T 441	3.64	*Dicroidium*	Allan Hills	Lashly
T 449	4.58	*Dicroidium*	Allan Hills	Lashly
T 460	4.43	*Dicroidium*	Allan Hills	Lashly
T 464	5.13	*Dicroidium*	Allan Hills	Lashly
T 464	3.7	*Dicroidium*	Allan Hills	Lashly
T 521	5.01	*Dicroidium*	Allan Hills	Lashly
T 527	6.27	*Dicroidium*	Allan Hills	Lashly
T 527	4.91	*Dicroidium*	Allan Hills	Lashly
T 537	5.53	*Dicroidium*	Allan Hills	Lashly
T 541	4.84	*Dicroidium*	Allan Hills	Lashly
T 545	5.34	*Dicroidium*	Allan Hills	Lashly
T 561	5.75	*Dicroidium*	Allan Hills	Lashly
T 562	4.13	*Dicroidium*	Allan Hills	Lashly
T 562	5.63	*Dicroidium*	Allan Hills	Lashly
T 570	4.71	*Dicroidium*	Allan Hills	Lashly
T 573	5.29	*Dicroidium*	Allan Hills	Lashly
T 587	5.64	*Dicroidium*	Allan Hills	Lashly
T 587	5.14	*Dicroidium*	Allan Hills	Lashly
T 591	4.75	*Dicroidium*	Allan Hills	Lashly
T 597	4.38	*Dicroidium*	Allan Hills	Lashly
T 598	5.45	*Dicroidium*	Allan Hills	Lashly
T 604	5.13	*Dicroidium*	Allan Hills	Lashly
T 608	4.86	*Dicroidium*	Allan Hills	Lashly
T 608	5.73	*Dicroidium*	Allan Hills	Lashly
T 6159	4.76	*Dicroidium*	Allan Hills	Lashly
T 615	4.69	*Dicroidium*	Allan Hills	Lashly
T 633	5.57	*Dicroidium*	Allan Hills	Lashly
T 662	4.49	*Dicroidium*	Allan Hills	Lashly
T 662	4.36	*Dicroidium*	Allan Hills	Lashly
T 677	5.03	*Dicroidium*	Allan Hills	Lashly
T 708	4.82	*Dicroidium*	Allan Hills	Lashly
T 714	6.26	*Dicroidium*	Allan Hills	Lashly
T 722a	4.97	*Dicroidium*	Allan Hills	Lashly
T 749	4.92	*Dicroidium*	Allan Hills	Lashly
T 766	4.36	*Dicroidium*	Allan Hills	Lashly
T 769	4.41	*Dicroidium*	Allan Hills	Lashly
T 773	5.38	*Dicroidium*	Allan Hills	Lashly
T 790	6.3	*Dicroidium*	Allan Hills	Lashly
T 878	5.47	*Dicroidium*	Allan Hills	Lashly
T 883	4.26	*Dicroidium*	Allan Hills	Lashly
T 884	6.53	*Dicroidium*	Allan Hills	Lashly
T 888	4.7	*Dicroidium*	Allan Hills	Lashly
T 2095	6.4	*Dicroidium*	Dinmore	Blackstone

T 2098	6.29	*Dicroidium*	Dinmore	Blackstone
T 2099	5.93	*Dicroidium*	Dinmore	Blackstone
T 2099	5.99	*Dicroidium*	Dinmore	Blackstone
T 2099	6.04	*Dicroidium*	Dinmore	Blackstone
T 2101	5.09	*Dicroidium*	Dinmore	Blackstone
T 2102	6.28	*Dicroidium*	Dinmore	Blackstone
T 2109	6.64	*Dicroidium*	Dinmore	Blackstone
T 2114	5.6	*Dicroidium*	Dinmore	Blackstone
T 2117	5.43	*Dicroidium*	Dinmore	Blackstone
T 2117	6.08	*Dicroidium*	Dinmore	Blackstone
T 2120	6.45	*Dicroidium*	Dinmore	Blackstone
T 2120	4.8	*Dicroidium*	Dinmore	Blackstone
T 2122	5.66	*Dicroidium*	Dinmore	Blackstone
T 2124	5.5	*Dicroidium*	Dinmore	Blackstone
T 5412a	4.3	*Dicroidium*	Fremouw Peak	Fremouw
T 5414	4.87	*Dicroidium*	Fremouw Peak	Fremouw
T 5414	5.07	*Dicroidium*	Fremouw Peak	Fremouw
T 188	4.77	*Dicroidium*	Gordon Valley	Fremouw
T 26	4.76	*Dicroidium*	Gordon Valley	Fremouw
T 26	5.23	*Dicroidium*	Gordon Valley	Fremouw
T 26	3.59	*Dicroidium*	Gordon Valley	Fremouw
T 29	4.82	*Dicroidium*	Gordon Valley	Fremouw
T 29	5.99	*Dicroidium*	Gordon Valley	Fremouw
T 33	4.46	*Dicroidium*	Gordon Valley	Fremouw
T 1823	5.89	*Dicroidium*	Marshall Mountains	Falla
T 1826	4.64	*Dicroidium*	Marshall Mountains	Falla
T 1855	4.57	*Dicroidium*	Marshall Mountains	Falla
T 1865	3.64	*Dicroidium*	Marshall Mountains	Falla
T 1865	4.64	*Dicroidium*	Marshall Mountains	Falla
T 1865	5.11	*Dicroidium*	Marshall Mountains	Falla
T 6253	5.82	*Dicroidium*	Marshall Mountains	Falla
T 6254	4.77	*Dicroidium*	Marshall Mountains	Falla
T 6259	5.3	*Dicroidium*	Marshall Mountains	Falla
T 6261	4.92	*Dicroidium*	Marshall Mountains	Falla
T 6280	6.89	*Dicroidium*	Marshall Mountains	Falla

T 6287	5.14	*Dicroidium*	Marshall Mountains	Falla
T 6302	5.17	*Dicroidium*	Marshall Mountains	Falla
T 6304	4.99	*Dicroidium*	Marshall Mountains	Falla
T 6307	5.27	*Dicroidium*	Marshall Mountains	Falla
T 6308	4.07	*Dicroidium*	Marshall Mountains	Falla
T 6313	5.88	*Dicroidium*	Marshall Mountains	Falla
T 5897	4.23	*Dicroidium*	Molteno	Molteno
T 109	5.18	*Dicroidium*	Mt. Falla	Falla
T 123	5.76	*Dicroidium*	Mt. Falla	Falla
T 124	5.49	*Dicroidium*	Mt. Falla	Falla
T 144	5.27	*Dicroidium*	Mt. Falla	Falla
T 163	4.04	*Dicroidium*	Mt. Falla	Falla
T 163	5.16	*Dicroidium*	Mt. Falla	Falla
T 1743	4.57	*Dicroidium*	Mt. Falla	Falla
T 1752	5.54	*Dicroidium*	Mt. Falla	Falla
T 1776a	4.64	*Dicroidium*	Mt. Falla	Falla
T 1776a	4.14	*Dicroidium*	Mt. Falla	Falla
T 1776b	4.35	*Dicroidium*	Mt. Falla	Falla
T 178	3.21	*Dicroidium*	Mt. Falla	Falla
T 1811	4.3	*Dicroidium*	Mt. Falla	Falla
T 50	3.61	*Dicroidium*	Mt. Falla	Falla
T 5921	5.81	*Dicroidium*	Mt. Falla	Falla
T 6005	5.39	*Dicroidium*	Mt. Falla	Falla
T 6007	4.26	*Dicroidium*	Mt. Falla	Falla
T 6051	5.56	*Dicroidium*	Mt. Falla	Falla
T 6234	4.01	*Dicroidium*	Mt. Falla	Falla
T 6237	3.4	*Dicroidium*	Mt. Falla	Falla
T 64	4.09	*Dicroidium*	Mt. Falla	Falla
T 80	4.19	*Dicroidium*	Mt. Falla	Falla
T 80	4.81	*Dicroidium*	Mt. Falla	Falla
T 1519	4.31	*Dicroidium*	Shapeless Mountain	Lashly
T 1520	3.66	*Dicroidium*	Shapeless Mountain	Lashly
T 1523	5.33	*Dicroidium*	Shapeless Mountain	Lashly
T 1557	4.45	*Dicroidium*	Shapeless Mountain	Lashly
T 1565	4.22	*Dicroidium*	Shapeless Mountain	Lashly

T 1567	4.51	*Dicroidium*	Shapeless Mountain	Lashly
T 1571	4.11	*Dicroidium*	Shapeless Mountain	Lashly
T 1577	4.28	*Dicroidium*	Shapeless Mountain	Lashly
T 1610	5.83	*Dicroidium*	Shapeless Mountain	Lashly
T 1618	4.71	*Dicroidium*	Shapeless Mountain	Lashly
T 1627a	5.27	*Dicroidium*	Shapeless Mountain	Lashly
T 1663	3.97	*Dicroidium*	Shapeless Mountain	Lashly
T 1144	2.45	*Heidiphyllum*	Alfie's Elbow	FreFalla
T 1144	2.67	*Heidiphyllum*	Alfie's Elbow	FreFalla
T 1220	2.18	*Heidiphyllum*	Alfie's Elbow	FreFalla
T 1220	2.21	*Heidiphyllum*	Alfie's Elbow	FreFalla
T 1273	2.2	*Heidiphyllum*	Alfie's Elbow	FreFalla
T 1273	3	*Heidiphyllum*	Alfie's Elbow	FreFalla
T 1311	3.04	*Heidiphyllum*	Alfie's Elbow	FreFalla
T 1311	1.97	*Heidiphyllum*	Alfie's Elbow	FreFalla
T 1313	1.94	*Heidiphyllum*	Alfie's Elbow	FreFalla
T 1357	2.08	*Heidiphyllum*	Alfie's Elbow	FreFalla
T 1402	2.9	*Heidiphyllum*	Alfie's Elbow	FreFalla
T 1420	2.77	*Heidiphyllum*	Alfie's Elbow	FreFalla
T 1420	2.93	*Heidiphyllum*	Alfie's Elbow	FreFalla
T 1424	4.3	*Heidiphyllum*	Alfie's Elbow	FreFalla
T 1463	1.89	*Heidiphyllum*	Alfie's Elbow	FreFalla
T 1466a	2.79	*Heidiphyllum*	Alfie's Elbow	FreFalla
T 1474	1.94	*Heidiphyllum*	Alfie's Elbow	FreFalla
T 5555	2.95	*Heidiphyllum*	Alfie's Elbow	FreFalla
T 206	3.88	*Heidiphyllum*	Allan Hills	Lashly
T 213	4.02	*Heidiphyllum*	Allan Hills	Lashly
T 243	3.45	*Heidiphyllum*	Allan Hills	Lashly
T 256	3.38	*Heidiphyllum*	Allan Hills	Lashly
T 272	2.84	*Heidiphyllum*	Allan Hills	Lashly
T 275	2.9	*Heidiphyllum*	Allan Hills	Lashly
T 362	1.83	*Heidiphyllum*	Allan Hills	Lashly
T 384	1.86	*Heidiphyllum*	Allan Hills	Lashly
T 393	1.99	*Heidiphyllum*	Allan Hills	Lashly
T 582	3.42	*Heidiphyllum*	Allan Hills	Lashly
T 615	3.03	*Heidiphyllum*	Allan Hills	Lashly
T 634	3.08	*Heidiphyllum*	Allan Hills	Lashly
T 651	2.77	*Heidiphyllum*	Allan Hills	Lashly
T 5895	3.06	*Heidiphyllum*	Molteno	Molteno
T 5897	1.98	*Heidiphyllum*	Molteno	Molteno

T 5902	3.02	*Heidiphyllum*	Molteno	Molteno
T 5902	1.92	*Heidiphyllum*	Molteno	Molteno
T 5904	3.03	*Heidiphyllum*	Molteno	Molteno
T 5909	3.02	*Heidiphyllum*	Molteno	Molteno
T 5910	2.15	*Heidiphyllum*	Molteno	Molteno
T 124	2.95	*Heidiphyllum*	Mt. Falla	Falla
T 143	3.25	*Heidiphyllum*	Mt. Falla	Falla
T 163	2.31	*Heidiphyllum*	Mt. Falla	Falla
T 39	1.99	*Heidiphyllum*	Mt. Falla	Falla
T 39	3.09	*Heidiphyllum*	Mt. Falla	Falla
T 45	3.01	*Heidiphyllum*	Mt. Falla	Falla
T 5896	3.67	*Heidiphyllum*	Mt. Falla	Falla
T 5896	2.46	*Heidiphyllum*	Mt. Falla	Falla
T 5896	2.99	*Heidiphyllum*	Mt. Falla	Falla
T 58	2.89	*Heidiphyllum*	Mt. Falla	Falla
T 58	2.97	*Heidiphyllum*	Mt. Falla	Falla
T 59	2.44	*Heidiphyllum*	Mt. Falla	Falla
T 6220	2.69	*Heidiphyllum*	Mt. Falla	Falla
T 6229	2.9	*Heidiphyllum*	Mt. Falla	Falla
T 85	1.86	*Heidiphyllum*	Mt. Falla	Falla
T 93	3.14	*Heidiphyllum*	Mt. Falla	Falla
T 1241	4.44	*Osmunda*	Alfie's Elbow	FreFalla
T 380	4.87	*Osmunda*	Allan Hills	Lashly
T 380	4.74	*Osmunda*	Allan Hills	Lashly
T 432a	4.31	*Osmunda*	Allan Hills	Lashly
T 437	3.78	*Osmunda*	Allan Hills	Lashly
T 448	4.7	*Osmunda*	Allan Hills	Lashly
T 455	4.53	*Osmunda*	Allan Hills	Lashly
T 5833	4.27	*Osmunda*	Allan Hills	Lashly
T 5834	4.78	*Osmunda*	Allan Hills	Lashly
T 694	4.78	*Osmunda*	Allan Hills	Lashly
T 2114	6.01	*Sphenobaiera*	Dinmore	Blackstone
T 1857	3.47	*Sphenobaiera*	Marshall Mountains	Falla
T 1868	4.05	*Sphenobaiera*	Marshall Mountains	Falla
T 5654	4.04	*Sphenobaiera*	Mt. Falla	Falla
T 1241	3.54	*Taeniopteris*	Alfie's Elbow	FreFalla
T 1389	5.97	*Taeniopteris*	Alfie's Elbow	FreFalla
T 1424	3.83	*Taeniopteris*	Alfie's Elbow	FreFalla
T 858	6.22	*Taeniopteris*	Allan Hills	Lashly
T 861	7.2	*Taeniopteris*	Allan Hills	Lashly
T 861	6.8	*Taeniopteris*	Allan Hills	Lashly
T 868	8.81	*Taeniopteris*	Allan Hills	Lashly
T 2104-5	7.08	*Taeniopteris*	Dinmore	Blackstone
T 2112	4.6	*Taeniopteris*	Dinmore	Blackstone

T 2113	5.84	*Taeniopteris*	Dinmore	Blackstone
T 2123	4.06	*Taeniopteris*	Dinmore	Blackstone
T 1868	4.65	*Taeniopteris*	Marshall Mountains	Falla
T 1869	6.68	*Taeniopteris*	Marshall Mountains	Falla
T 6270	6.07	*Taeniopteris*	Marshall Mountains	Falla
T 6096b	6.54	*Taeniopteris*	Mt. Bumstead	Lashly
T 6397	3.86	*Taeniopteris*	Mt. Falla	Falla
T 6398	3.22	*Taeniopteris*	Mt. Falla	Falla
T 6398	3.41	*Taeniopteris*	Mt. Falla	Falla
T 6398	3.55	*Taeniopteris*	Mt. Falla	Falla
T 6404	4.63	*Taeniopteris*	Mt. Falla	Falla
T 5889	4.35	*Taeniopteris*	Umkomaas Valley	Molteno

Appendix II: LMA Data

Appendix II. Table I. Leaf Mass Per Area (LMA) for Glossopteris Leaves Analyzed

Specimen Number	LMA (g m-2)	Locality	Formation
Pm 342	176.2	Allan Hills	Weller Coal Measures
Pm 342	126.9	Allan Hills	Weller Coal Measures
Pm 343	114.1	Allan Hills	Weller Coal Measures
Pm 359	131.8	Allan Hills	Weller Coal Measures
Pm 359	131.3	Allan Hills	Weller Coal Measures
Pm 374	94.9	Allan Hills	Weller Coal Measures
Pm 374	113.8	Allan Hills	Weller Coal Measures
Pm 389	117.4	Allan Hills	Weller Coal Measures
Pm 389	132.8	Allan Hills	Weller Coal Measures
Pm 390	137.3	Allan Hills	Weller Coal Measures
Pm 390	104.5	Allan Hills	Weller Coal Measures
Pm 390	120.8	Allan Hills	Weller Coal Measures
Pm 393	124.9	Allan Hills	Weller Coal Measures
Pm 393	155	Allan Hills	Weller Coal Measures
Pm 395a	111.7	Allan Hills	Weller Coal Measures
Pm 399	139.1	Allan Hills	Weller Coal Measures
Pm 4934	86.2	Allan Hills	Weller Coal Measures
Pm 4943	130.6	Allan Hills	Weller Coal Measures
Pm 4947	99.8	Allan Hills	Weller Coal Measures

Pm 4948	85.1	Allan Hills	Weller Coal Measures
Pm 4956	108.6	Allan Hills	Weller Coal Measures
Pm 4962	114.3	Allan Hills	Weller Coal Measures
Pm 100	117.8	Aztec Mt.	Weller Coal Measures
Pm 112	127.1	Aztec Mt.	Weller Coal Measures
Pm 112	146	Aztec Mt.	Weller Coal Measures
Pm 38	106.5	Aztec Mt.	Weller Coal Measures
Pm 41	100.1	Aztec Mt.	Weller Coal Measures
Pm 71	100.5	Aztec Mt.	Weller Coal Measures
Pm 74	97.9	Aztec Mt.	Weller Coal Measures
Pm 89	135.5	Aztec Mt.	Weller Coal Measures
Pm 93	92.8	Aztec Mt.	Weller Coal Measures
Pm 1733	116	Bazargaon	Kamthi
Pm 2275b	114.1	Coalsack Bluff	Upper Buckley
Pm 827a	114.3	Leaia Ledge	Mt. Glossopteris
Pm 528	108.5	Mt. Achernar	Upper Buckley
Pm 4683	116.2	Mt. Feather	Weller Coal Measures
Pm 321	111.8	Mt. Fleming	Weller Coal Measures
Pm 1358b	105.5	Mt. Ropar	Upper Buckley
Pm 5315a	103.4	Mt. Weaver	Queen Maud
Pm 2383	95.8	Mt. Wild	Upper Buckley
Pm 4558a	108.7	Polarstar Peak	Polarstar
Pm 4565	112.4	Polarstar Peak	Polarstar
Pm 4566a	113.7	Polarstar Peak	Polarstar
Pm 4571	112.5	Polarstar Peak	Polarstar
13677 H	112.6	Skaar Ridge	Upper Buckley
Pm 3657	108.9	Skaar Ridge	Upper Buckley
Pm 426	107.1	Skaar Ridge	Upper Buckley
Pm 432	109.1	Skaar Ridge	Upper Buckley
Pm 465	105.4	Skaar Ridge	Upper Buckley
Pm 480	102	Skaar Ridge	Upper Buckley
Pm 6119	98.2	Skaar Ridge	Upper Buckley
Pm 6119	116.2	Skaar Ridge	Upper Buckley
Pm 6121c	116.7	Skaar Ridge	Upper Buckley

Pm 6124	81.4	Skaar Ridge	Upper Buckley
Pm 6125a	92.6	Skaar Ridge	Upper Buckley
Pm 6125a	123	Skaar Ridge	Upper Buckley
Pm 6125c	88.3	Skaar Ridge	Upper Buckley
Pm 6125c	116.8	Skaar Ridge	Upper Buckley
Pm 6125c	110.4	Skaar Ridge	Upper Buckley
Pm 6128	103.4	Skaar Ridge	Upper Buckley
Pm 6128	119.5	Skaar Ridge	Upper Buckley
Pm 6129a	108.3	Skaar Ridge	Upper Buckley
Pm 6130	99.6	Skaar Ridge	Upper Buckley
Pm 6130	120.2	Skaar Ridge	Upper Buckley
Pm 6131	102.1	Skaar Ridge	Upper Buckley
Pm 6131	118.9	Skaar Ridge	Upper Buckley
Pm 6131	126.6	Skaar Ridge	Upper Buckley
Pm 6131	118.6	Skaar Ridge	Upper Buckley
Pm 6132	106.3	Skaar Ridge	Upper Buckley
Pm 6132	123.2	Skaar Ridge	Upper Buckley
Pm 6133a	86.7	Skaar Ridge	Upper Buckley
Pm 6133a	119.1	Skaar Ridge	Upper Buckley
Pm 6133a	107.8	Skaar Ridge	Upper Buckley
Pm 6133a	97	Skaar Ridge	Upper Buckley
Pm 6133a	113.1	Skaar Ridge	Upper Buckley
Pm 6133a	95.6	Skaar Ridge	Upper Buckley
Pm 6134a	84.1	Skaar Ridge	Upper Buckley
Pm 6134a	89	Skaar Ridge	Upper Buckley
Pm 6134c	97.7	Skaar Ridge	Upper Buckley
Pm 6134c	105.7	Skaar Ridge	Upper Buckley
Pm 6134d	140	Skaar Ridge	Upper Buckley
Pm 6134d	115	Skaar Ridge	Upper Buckley
Pm 6134g	123.4	Skaar Ridge	Upper Buckley
Pm 6137a	116.4	Skaar Ridge	Upper Buckley
Pm 6137d	135.1	Skaar Ridge	Upper Buckley
Pm 6138a	114.7	Skaar Ridge	Upper Buckley
Pm 6138a	132.6	Skaar Ridge	Upper Buckley
Pm 6138b	104	Skaar Ridge	Upper Buckley
Pm 6138b	138.3	Skaar Ridge	Upper Buckley
Pm 6139a	135.2	Skaar Ridge	Upper Buckley
Pm 6139a	147.1	Skaar Ridge	Upper Buckley
Pm 6139a	105.8	Skaar Ridge	Upper Buckley
Pm 6140	121.8	Skaar Ridge	Upper Buckley
Pm 6140	120.1	Skaar Ridge	Upper Buckley
Pm 6140	117.6	Skaar Ridge	Upper Buckley
Pm 6140	114.9	Skaar Ridge	Upper Buckley
Pm 6140	123.2	Skaar Ridge	Upper Buckley
Pm 6140	92.7	Skaar Ridge	Upper Buckley

Pm 6141	109.5	Skaar Ridge	Upper Buckley
Pm 6141	106.5	Skaar Ridge	Upper Buckley
Pm 6143a	91.7	Skaar Ridge	Upper Buckley
Pm 6143a	104.6	Skaar Ridge	Upper Buckley
Pm 6143c	109.5	Skaar Ridge	Upper Buckley
Pm 6144a	113.7	Skaar Ridge	Upper Buckley
Pm 6144a	113.3	Skaar Ridge	Upper Buckley
Pm 6145a	119.1	Skaar Ridge	Upper Buckley
Pm 6145a	115	Skaar Ridge	Upper Buckley
Pm 6145a	121.8	Skaar Ridge	Upper Buckley
Pm 6146a	103.7	Skaar Ridge	Upper Buckley
Pm 6146a	113.7	Skaar Ridge	Upper Buckley
Pm 6149a	171.3	Skaar Ridge	Upper Buckley
Pm 6150a	136.2	Skaar Ridge	Upper Buckley
Pm 6150b	129.3	Skaar Ridge	Upper Buckley
Pm 6151a	125	Skaar Ridge	Upper Buckley
Pm 6151c	114.5	Skaar Ridge	Upper Buckley
Pm 6152a	120.8	Skaar Ridge	Upper Buckley
Pm 6152a	78.8	Skaar Ridge	Upper Buckley
Pm 6152a	126.8	Skaar Ridge	Upper Buckley
Pm 6156a	135.1	Skaar Ridge	Upper Buckley
Pm 6156a	108.1	Skaar Ridge	Upper Buckley
Pm 6156b	94.6	Skaar Ridge	Upper Buckley
Pm 6157	117.6	Skaar Ridge	Upper Buckley
Pm 6159	111.6	Skaar Ridge	Upper Buckley
Pm 6163	115.4	Skaar Ridge	Upper Buckley
Pm 6164	95.7	Skaar Ridge	Upper Buckley
Pm 6167	116	Skaar Ridge	Upper Buckley
Pm 6167	114.8	Skaar Ridge	Upper Buckley
Pm 6174	112.1	Skaar Ridge	Upper Buckley
Pm 6174	136.2	Skaar Ridge	Upper Buckley
Pm 6175	139.5	Skaar Ridge	Upper Buckley
Pm 6179	73.2	Skaar Ridge	Upper Buckley
Pm 6181	84	Skaar Ridge	Upper Buckley
Pm 6181	109.2	Skaar Ridge	Upper Buckley
Pm 6181	112.6	Skaar Ridge	Upper Buckley
Pm 6183	98	Skaar Ridge	Upper Buckley
Pm 6184a	110	Skaar Ridge	Upper Buckley
Pm 6188	94.8	Skaar Ridge	Upper Buckley
Pm 6198	98	Skaar Ridge	Upper Buckley
Pm 6202	134.5	Skaar Ridge	Upper Buckley
Pm 6219a	114	Skaar Ridge	Upper Buckley
Pm 6219a	124.3	Skaar Ridge	Upper Buckley
Pm 6219a	103	Skaar Ridge	Upper Buckley
Pm 6219a	124.9	Skaar Ridge	Upper Buckley

Pm 6219a	117.3	Skaar Ridge	Upper Buckley
Pm 6219a	99.1	Skaar Ridge	Upper Buckley
Pm 6219a	110.9	Skaar Ridge	Upper Buckley
Pm 6219a	120.5	Skaar Ridge	Upper Buckley
Pm 6219b	125.2	Skaar Ridge	Upper Buckley
Pm 6219b	104.6	Skaar Ridge	Upper Buckley
Pm 6219b	115.5	Skaar Ridge	Upper Buckley
Pm 6220abc	118.4	Skaar Ridge	Upper Buckley
Pm 6220ab	108.4	Skaar Ridge	Upper Buckley
Pm 6220ab	112.3	Skaar Ridge	Upper Buckley
Pm 6220ab	98.1	Skaar Ridge	Upper Buckley
Pm 6220ab	101	Skaar Ridge	Upper Buckley
Pm 6220ab	101.1	Skaar Ridge	Upper Buckley
Pm 6220ab	123.9	Skaar Ridge	Upper Buckley
Pm 6220ab	93.3	Skaar Ridge	Upper Buckley
Pm 6220ac	91.5	Skaar Ridge	Upper Buckley
Pm 6220ado	124.9	Skaar Ridge	Upper Buckley
Pm 6220bf	108.2	Skaar Ridge	Upper Buckley
Pm 6220bf	124.2	Skaar Ridge	Upper Buckley
Pm 6220cd	100.9	Skaar Ridge	Upper Buckley
Pm 6221a	105	Skaar Ridge	Upper Buckley
Pm 6221a	114.8	Skaar Ridge	Upper Buckley
Pm 6221a	84.7	Skaar Ridge	Upper Buckley
Pm 6221l	128.5	Skaar Ridge	Upper Buckley
Pm 6221l	102.3	Skaar Ridge	Upper Buckley
Pm 6221l	141.5	Skaar Ridge	Upper Buckley
Pm 6221mq	99.9	Skaar Ridge	Upper Buckley
Pm 6221mq	109.1	Skaar Ridge	Upper Buckley
Pm 6221oq	91.4	Skaar Ridge	Upper Buckley
Pm 6221o	124.1	Skaar Ridge	Upper Buckley
Pm 6221ro	97.4	Skaar Ridge	Upper Buckley
Pm 6221rt	123.2	Skaar Ridge	Upper Buckley
Pm 6230	102.5	Skaar Ridge	Upper Buckley
Pm 3677	124.2	Terrace Ridge	Mt. Glossopteris
Pm 3697	108.5	Terrace Ridge	Mt. Glossopteris
Pm 3699b	122.9	Terrace Ridge	Mt. Glossopteris
Pm 3726	94.1	Terrace Ridge	Mt. Glossopteris
Pm 3736	91.3	Terrace Ridge	Mt. Glossopteris
Pm 3896	99.9	Terrace Ridge	Mt. Glossopteris
Pm 3899	105.6	Terrace Ridge	Mt. Glossopteris
Pm 3902	103.9	Terrace Ridge	Mt. Glossopteris

Appendix III: Python scripts

```
# Leaf Hydraulic Analysis
# Written in Python 2.7
# Andrew B. Schwendemann
import glob
import math
import os
from time import strftime
from xlrd import open_workbook
from xlwt import Workbook,Style

class StoredData:
    def
__init__(self,specimen_num=None,locality=None,leaf=None,species=None,Dv=None,dy=None,
Kleaf=None,gs=None,Pc=None,instWUE=None,intrWUE=None):
        self.specimen_num = specimen_num
        self.locality = locality
        self.leaf = leaf
        self.species = species
        self.Dv = Dv # mm mm^-2
        self.dy = dy # um
        self.Kleaf = Kleaf # mmol m^-2 s^-1 MPa^-1
        self.gs = gs # mmol H20 m^-2 s^-1
        self.Pc = Pc # umol CO2 m^-2 s^-1
        self.instWUE = instWUE # umol CO2/mmol H20 kPa
        self.intrWUE = intrWUE # umol CO2/mmol H2O
    def displayInput(self):
        print "\nSpecimen num: {}".format(self.specimen_num)
        print "Locality: {}".format(self.locality)
        print "Species: {}".format(self.species)
        print self.leaf
        print "Dv = {}".format(self.Dv)
        print "dy = {} \n".format(self.dy)
    def displayOutput(self):
        print "\nSpecimen num: {}".format(self.specimen_num)
        print "Species: {}".format(self.species)
        print self.leaf
        print "Kleaf = {}".format(self.Kleaf)
        print "gs = {}".format(self.gs)
        print "Pc = {}".format(self.Pc)
        print "Inst. WUE = {}".format(self.instWUE)
        print "Intr. WUE = {} \n".format(self.intrWUE)

def calcK_leaf(vein_den, leaf_thick): # calcK_leaf(Dv,dy)
```

```
    dx = 650.0/vein_den
    dm = (math.pi/2.0)*math.sqrt((math.pow(dx,2.0)+math.pow(leaf_thick,2.0)))
    kleaf = 12670.0*math.pow(dm,-1.27)
    return kleaf

def calcWUE(press_def, stomatal_c,A): # calcWUE(v,gs,Pc)
    instantaneous = A/(press_def*stomatal_c) # umol CO2/mmol H20 kPa
    intrinsic = A/stomatal_c # umol CO2/mmol H2O - better
    return (instantaneous,intrinsic)

def calcPc(kleaf): # calcPC(K_leaf) - uses regression equation
    return -0.0226*math.pow(kleaf,2) + 1.32*kleaf - 0.26

def calc_gs(kleaf,press_def,water_pot): # calc_gs(K_leaf, v, Psi_leaf)
    atm_press = 101.3 #kPa
    return (kleaf*water_pot)/(press_def/atm_press) # in mmol m^-2 s^-1

def convGenus(lng_str): # convGenus(instance.species)
    found_sp = False
    for char in lng_str:
        if char.isspace() == True:
            genus = lng_str.split(' ')[0]
            found_sp = True
            break
    if found_sp == False:
        genus = lng_str
    return genus

def file_check(inp_list,geol_dict,log_file,stor_err): #file_check(data_list,dictionary,log,flerr)
    temp = geol_dict.values()
    geol_list = []
    misloc = []
    misinp = []
    for i in temp:
        geol_list = geol_list + i
    for entry in inp_list: # make sure we have time/location/formation data for all inputed
measurements
        if entry not in geol_list:
            if entry not in stor_err['locmis']:
                stor_err['locmis'].append(entry)
                print '{} is missing locality information.'.format(entry)
                log_file.write('\t{} is missing locality information.\n'.format(entry))
    for entry in geol_list: # makes sure all localities we have data for are in input files
        if entry not in inp_list:
            if entry not in stor_err['inpmis']:
```

```
            stor_err['inpmis'].append(entry)
            print '{} has no input files to make use of the stored data.'.format(entry)
            log_file.write('\t{} has no input files to make use of the stored data.\n'.format(entry))
    return stor_err

def error_log(counter,failures,localities,stratigraphy,geography,time):
#error_log(output_counter,zero_files,locality_list,formations,latitudes,geotime)
    flerr = {'locmis':[],'inpmis':[]}
    log = open('Dv_hydraulics.log', 'a')
    log.write('\n\nExecuted: {}\n'.format(strftime("%Y-%m-%d %H.%M")))
    log.write('\t{} output files created.\n'.format(counter))
    print "\nDone.\n{} output files created.".format(counter)
    if len(failures) == 0:
        print 'All input files passed quality control.\n'
        log.write('\tAll input files passed quality control.\n')
    else:
        print 'The following input files failed quality control:\n'
        log.write('\tThe following input files failed quality control:\n')
        for entry in failures:
            print '\t{}'.format(entry)
            log.write('\t\t{}\n'.format(entry))
        print '\n'
    flerr = file_check(localities,stratigraphy,log,flerr)
    flerr = file_check(localities,geography,log,flerr)
    flerr = file_check(localities,time,log,flerr)
    log.close()

def min_max(leaf,stored_data): # min_max(taxon,data_list)
    min_max_dict = {}
    print '\n{}\n-------------------------'.format(leaf)
    for instance in stored_data:
        if convGenus(instance.species) == leaf:
            if instance.locality in min_max_dict:
                if instance.Dv < min_max_dict[instance.locality][0]:
                    min_max_dict[instance.locality][0] = instance.Dv
                if instance.Dv > min_max_dict[instance.locality][1]:
                    min_max_dict[instance.locality][1] = instance.Dv
            else:
                min_max_dict[instance.locality] = [instance.Dv,instance.Dv]
    for entry in min_max_dict:
        print entry
        print '\tMin: {}\n\tMax: {}'.format(min_max_dict[entry][0],min_max_dict[entry][1])

def build_dictionary(rd_sheet,data_type): # build_dictionary(sheet,string)
    dict = {}
```

```
    if data_type == 'str':
        for col in range(rd_sheet.ncols):
            dict[str(rd_sheet.cell(0,col).value)] = []
            for row in range(1,rd_sheet.nrows):
                if rd_sheet.cell(row,col).value != '':
                    dict[rd_sheet.cell(0,col).value].append(str(rd_sheet.cell(row,col).value))
        if 'TBD' in dict:
            del dict['TBD'] # removes localities with partial data; will show up in the log
    elif data_type == 'flt':
        for col in range(rd_sheet.ncols):
            dict[str(rd_sheet.cell(0,col).value)] = []
            for row in range(1,rd_sheet.nrows):
                if rd_sheet.cell(row,col).value != '':
                    dict[rd_sheet.cell(0,col).value].append(float(rd_sheet.cell(row,col).value))
    return dict


data_list = []
zero_files = []
# magnification:1 um = value px
wkbkconv = open_workbook('Unit Conversions.xls')
unit_conversions = build_dictionary(wkbkconv.sheet_by_name('Compound Scope'),'flt')
grid_size = 5.0 # mm
scale_bar = 10.0 # mm
dy = 140.0 # vary from 70 to 140 um
v = 2.0 #kPa
Psi_leaf = 0.4 #MPa
vein_counter = 0


# input specimen number, locality, leaf, species, Dv, dy if applicable
cwd_path = os.path.abspath('')
for infile in glob.glob(os.path.join(cwd_path,'Measurements Formated','Dv*.xls')):
    filename = os.path.split(infile)[1]
    site, block1 = filename.split('{')
    site = site[3:-1]
    block1a, block1b = block1.split('[')
    spec_num, leafdelim = block1a.split('}')
    leafdelim = leafdelim[1:-1]
    taxonomic_data, mag = block1b.split(']')
    mag = mag[1:-4]
    wb = open_workbook(infile)
    Dv_list = []
    for sheet in wb.sheets():
        duplicate = False
```

```
        for row in range(sheet.nrows - 1):
            vein_counter += 1
            vein_length = sheet.cell(row+1,3).value
            Dv_list.append(vein_length)
            if vein_length == 0:
                zero_files.append(filename)
        vein_counter -= 1
        for i in range(0,len(data_list)):
            if data_list[i].specimen_num == spec_num:
                if data_list[i].leaf == leafdelim:
                    if (data_list[i].species == taxonomic_data) and (mag[-2:] != 'dy'):
                        duplicate = True
                        if spec_num[0:1].isdigit() == False: # finds compression fossils
                            conversion = scale_bar/Dv_list[-1]
                            del Dv_list[-1]
                            data_list[i].Dv.append((sum(Dv_list)*conversion)/grid_size)
                        elif spec_num[0:1].isdigit() == True: # finds permineralized fossils
                            data_list[i].Dv.append(((sum(Dv_list)/unit_conversions[mag[0:-
2]])/1000.0)/grid_size)
                    elif (data_list[i].species == taxonomic_data) and (mag[-2:] == 'dy'):
                        duplicate = True
                        data_list[i].dy = (sum(Dv_list)/len(Dv_list))/unit_conversions[mag[0:-3]]
        if duplicate == False:
            if spec_num[0:1].isdigit() == False: # finds new compression fossils
                conversion = scale_bar/Dv_list[-1]
                del Dv_list[-1]
                data_list.append(StoredData(spec_num,site,leafdelim,taxonomic_data,
[(sum(Dv_list)*conversion)/grid_size],dy))
            elif spec_num[0:1].isdigit() == True: # finds new permineralized fossils
                data_list.append(StoredData(spec_num,site,leafdelim,taxonomic_data,
[((sum(Dv_list)/unit_conversions[mag[0:-2]])/1000.0)/grid_size]))

# averages the Dv for each specimen -> each grid is averaged into one value for that leaf
for instance in data_list:
    instance.Dv = sum(instance.Dv)/len(instance.Dv)

# calculates other values from Dv
for object in data_list:
    object.Kleaf = calcK_leaf(object.Dv, object.dy)
    object.gs = calc_gs(object.Kleaf,v,Psi_leaf)
    object.Pc = calcPc(object.Kleaf)
    object.instWUE, object.intrWUE = calcWUE(v,object.gs,object.Pc)

# locality:genus
genus_summary = {}
```

```
for instance in data_list:
    if instance.locality not in genus_summary:
        genus_summary[instance.locality] = []
        genus_summary[instance.locality].append(convGenus(instance.species))
    elif instance.locality in genus_summary:
        genus_found = False
        genus_var = convGenus(instance.species)
        for genera in genus_summary[instance.locality]:
            if genera == genus_var:
                genus_found = True
                break
        if genus_found == False:
            genus_summary[instance.locality].append(genus_var)

# genus:locality
local_genus = {}
for instance in data_list:
    genus_var = convGenus(instance.species)
    if genus_var not in local_genus:
        local_genus[genus_var] = []
        local_genus[genus_var].append(instance.locality)
    elif genus_var in local_genus:
        locality_found = False
        for location in local_genus[genus_var]:
            if location == instance.locality:
                locality_found = True
                break
        if locality_found == False:
            local_genus[genus_var].append(instance.locality)


output_counter = 0

# Creates dictionaries for output files
wkbk_flt = open_workbook('FormLatTime_list.xls')
formations = build_dictionary(wkbk_flt.sheet_by_name('Formations'),'str')
latitudes = build_dictionary(wkbk_flt.sheet_by_name('Latitudes'),'str')
geotime = build_dictionary(wkbk_flt.sheet_by_name('GeoTime'),'str')

genus_list = sorted(local_genus.keys())
locality_list = sorted(genus_summary.keys())
for taxon in genus_list:
    min_max(taxon,data_list)

# in locality:genus format
```

```
# Data summary as txt file
file_string = 'Summary of ' + strftime("%Y-%m-%d %H.%M") + " run.Dv.txt"
output_file = open(os.path.join(cwd_path,'Summary Output',file_string),'w')
output_file.write("Analyzed {} leaves \n".format(len(data_list)))
output_file.write('Measured {} veins \n'.format(vein_counter))
output_file.write('\nLocalities ({}):\n'.format(len(locality_list)))
for gen_list in genus_summary:
    genus_summary[gen_list] = sorted(genus_summary[gen_list])
for locations in locality_list:
    book = Workbook()
    output_file.write('\n\t' + locations)
    output_file.write(' ({} species)\n\n'.format(len(genus_summary[locations])))
    for taxon in genus_summary[locations]:
        output_file.write('\t\t' + taxon)
        sheet1 = book.add_sheet(taxon)
        sheet1.col(0).width = 8000
        sheet1.col(1).width = 5000
        sheet1.col(8).width = 5000
        sheet1.col(9).width = 4500
        sheet1.row(0).write(0,'Specimen #')
        sheet1.row(0).write(1,'Species')
        sheet1.row(0).write(2,'Leaf')
        sheet1.row(0).write(3,'Dv')
        sheet1.row(0).write(4,'dy')
        sheet1.row(0).write(5,'K_leaf')
        sheet1.row(0).write(6,'g_s')
        sheet1.row(0).write(7,'Pc')
        sheet1.row(0).write(8,'Instantaneous WUE')
        sheet1.row(0).write(9,'Intrinsic WUE')
        row = 1
        counter=sumDv=sumdy=sumKleaf=sumgs=sumPc=sumIns=sumInt = 0
        for object in data_list:
            if (object.locality == locations) and (convGenus(object.species) == taxon):
                counter += 1
                sheet1.row(row).write(0,object.specimen_num)
                sheet1.row(row).write(1,object.species)
                sheet1.row(row).write(2,object.leaf)
                sheet1.row(row).write(3,object.Dv)
                sumDv += object.Dv
                sheet1.row(row).write(4,object.dy)
                sumdy += object.dy
                sheet1.row(row).write(5,object.Kleaf)
                sumKleaf += object.Kleaf
                sheet1.row(row).write(6,object.gs)
                sumgs += object.gs
```

```
            sheet1.row(row).write(7,object.Pc)
            sumPc += object.Pc
            sheet1.row(row).write(8,object.instWUE)
            sumIns += object.instWUE
            sheet1.row(row).write(9,object.intrWUE)
            sumInt += object.intrWUE
            row += 1
        row += 2
        sheet1.row(row).write(0,'Average:')
        sheet1.row(row).write(3,sumDv/counter)
        sheet1.row(row).write(4,sumdy/counter)
        sheet1.row(row).write(5,sumKleaf/counter)
        sheet1.row(row).write(6,sumgs/counter)
        sheet1.row(row).write(7,sumPc/counter)
        sheet1.row(row).write(8,sumIns/counter)
        sheet1.row(row).write(9,sumInt/counter)
        output_file.write(': Dv = {}, Kleaf = {} ({}
leaves)\n'.format(sumDv/counter,sumKleaf/counter,counter))
    file_string = locations + "_Genus Leaf Hydraulics " + strftime("%Y-%m-%d %H.%M") +
".xls"
    book.save(os.path.join(cwd_path,'Locality Output',file_string))
    output_counter += 1
output_file.close()
output_counter += 1

# in genus:locality format
for taxon in local_genus:
    book = Workbook()
    for location in local_genus[taxon]:
        sheet1 = book.add_sheet(location)
        sheet1.col(0).width = 8000
        sheet1.col(1).width = 5000
        sheet1.col(8).width = 5000
        sheet1.col(9).width = 4500
        sheet1.row(0).write(0,'Specimen #')
        sheet1.row(0).write(1,'Species')
        sheet1.row(0).write(2,'Leaf')
        sheet1.row(0).write(3,'Dv')
        sheet1.row(0).write(4,'dy')
        sheet1.row(0).write(5,'K_leaf')
        sheet1.row(0).write(6,'g_s')
        sheet1.row(0).write(7,'Pc')
        sheet1.row(0).write(8,'Instantaneous WUE')
        sheet1.row(0).write(9,'Intrinsic WUE')
        row = 1
```

```
        counter=sumDv=sumdy=sumKleaf=sumgs=sumPc=sumIns=sumInt = 0
        for object in data_list:
            if (object.locality == location) and (convGenus(object.species) == taxon):
                counter += 1.0
                sheet1.row(row).write(0,object.specimen_num)
                sheet1.row(row).write(1,object.species)
                sheet1.row(row).write(2,object.leaf)
                sheet1.row(row).write(3,object.Dv)
                sumDv += object.Dv
                sheet1.row(row).write(4,object.dy)
                sumdy += object.dy
                sheet1.row(row).write(5,object.Kleaf)
                sumKleaf += object.Kleaf
                sheet1.row(row).write(6,object.gs)
                sumgs += object.gs
                sheet1.row(row).write(7,object.Pc)
                sumPc += object.Pc
                sheet1.row(row).write(8,object.instWUE)
                sumIns += object.instWUE
                sheet1.row(row).write(9,object.intrWUE)
                sumInt += object.intrWUE
                row += 1
        row += 2
        sheet1.row(row).write(0,'Average:')
        sheet1.row(row).write(3,sumDv/counter)
        sheet1.row(row).write(4,sumdy/counter)
        sheet1.row(row).write(5,sumKleaf/counter)
        sheet1.row(row).write(6,sumgs/counter)
        sheet1.row(row).write(7,sumPc/counter)
        sheet1.row(row).write(8,sumIns/counter)
        sheet1.row(row).write(9,sumInt/counter)
    file_string = taxon + " Leaf Hydraulics " + strftime("%Y-%m-%d %H.%M") + ".xls"
    book.save(os.path.join(cwd_path,'Genus Output',file_string))
    output_counter += 1

# Averages all genera regardless of locality
book = Workbook()
for taxon in genus_list:
    sheet1 = book.add_sheet(taxon)
    sheet1.col(0).width = 8000
    sheet1.col(1).width = 5000
    sheet1.col(8).width = 5000
    sheet1.col(9).width = 4500
    sheet1.row(0).write(0,'Specimen #')
    sheet1.row(0).write(1,'Species')
```

```
    sheet1.row(0).write(2,'Leaf')
    sheet1.row(0).write(3,'Dv')
    sheet1.row(0).write(4,'dy')
    sheet1.row(0).write(5,'K_leaf')
    sheet1.row(0).write(6,'g_s')
    sheet1.row(0).write(7,'Pc')
    sheet1.row(0).write(8,'Instantaneous WUE')
    sheet1.row(0).write(9,'Intrinsic WUE')
    row = 1
    counter=sumDv=sumdy=sumKleaf=sumgs=sumPc=sumIns=sumInt = 0
    for object in data_list:
        if (convGenus(object.species) == taxon):
            counter += 1.0
            sheet1.row(row).write(0,object.specimen_num)
            sheet1.row(row).write(1,object.species)
            sheet1.row(row).write(2,object.leaf)
            sheet1.row(row).write(3,object.Dv)
            sumDv += object.Dv
            sheet1.row(row).write(4,object.dy)
            sumdy += object.dy
            sheet1.row(row).write(5,object.Kleaf)
            sumKleaf += object.Kleaf
            sheet1.row(row).write(6,object.gs)
            sumgs += object.gs
            sheet1.row(row).write(7,object.Pc)
            sumPc += object.Pc
            sheet1.row(row).write(8,object.instWUE)
            sumIns += object.instWUE
            sheet1.row(row).write(9,object.intrWUE)
            sumInt += object.intrWUE
            row += 1
    row += 2
    sheet1.row(row).write(0,'Average:')
    sheet1.row(row).write(3,sumDv/counter)
    sheet1.row(row).write(4,sumdy/counter)
    sheet1.row(row).write(5,sumKleaf/counter)
    sheet1.row(row).write(6,sumgs/counter)
    sheet1.row(row).write(7,sumPc/counter)
    sheet1.row(row).write(8,sumIns/counter)
    sheet1.row(row).write(9,sumInt/counter)
file_string = "All Genera Leaf Hydraulics " + strftime("%Y-%m-%d %H.%M") + ".xls"
book.save(os.path.join(cwd_path,'Summary Output',file_string))
output_counter += 1

# Averages Dv of a genus for each formation
```

```
for taxon in genus_list:
    book = Workbook()
    for formation in formations:
        sheet1 = book.add_sheet(formation)
        sheet1.col(0).width = 8000
        sheet1.col(1).width = 5000
        sheet1.col(2).width = 5000
        sheet1.col(9).width = 5000
        sheet1.col(10).width = 4500
        sheet1.row(0).write(0,'Specimen #')
        sheet1.row(0).write(1,'Locality')
        sheet1.row(0).write(2,'Species')
        sheet1.row(0).write(3,'Leaf')
        sheet1.row(0).write(4,'Dv')
        sheet1.row(0).write(5,'dy')
        sheet1.row(0).write(6,'K_leaf')
        sheet1.row(0).write(7,'g_s')
        sheet1.row(0).write(8,'Pc')
        sheet1.row(0).write(9,'Instantaneous WUE')
        sheet1.row(0).write(10,'Intrinsic WUE')
        row = 1
        counter=sumDv=sumdy=sumKleaf=sumgs=sumPc=sumIns=sumInt = 0
        for object in data_list:
            if (object.locality in formations[formation]) and (convGenus(object.species) == taxon):
                counter += 1.0
                sheet1.row(row).write(0,object.specimen_num)
                sheet1.row(row).write(1,object.locality)
                sheet1.row(row).write(2,object.species)
                sheet1.row(row).write(3,object.leaf)
                sheet1.row(row).write(4,object.Dv)
                sumDv += object.Dv
                sheet1.row(row).write(5,object.dy)
                sumdy += object.dy
                sheet1.row(row).write(6,object.Kleaf)
                sumKleaf += object.Kleaf
                sheet1.row(row).write(7,object.gs)
                sumgs += object.gs
                sheet1.row(row).write(8,object.Pc)
                sumPc += object.Pc
                sheet1.row(row).write(9,object.instWUE)
                sumIns += object.instWUE
                sheet1.row(row).write(10,object.intrWUE)
                sumInt += object.intrWUE
                row += 1
        row += 2
```

```
        if counter > 0:
            sheet1.row(row).write(0,'Average:')
            sheet1.row(row).write(4,sumDv/counter)
            sheet1.row(row).write(5,sumdy/counter)
            sheet1.row(row).write(6,sumKleaf/counter)
            sheet1.row(row).write(7,sumgs/counter)
            sheet1.row(row).write(8,sumPc/counter)
            sheet1.row(row).write(9,sumIns/counter)
            sheet1.row(row).write(10,sumInt/counter)
    file_string = "Formations - " + taxon + " Leaf Hydraulics " + strftime("%Y-%m-%d %H.
%M") + ".xls"
    book.save(os.path.join(cwd_path,"Formation Output",file_string))
    output_counter += 1

for taxon in genus_list:
    book = Workbook()
    sheet1 = book.add_sheet('Data')
    sheet1.col(0).width = 5000
    sheet1.row(0).write(0,'Specimen Number')
    sheet1.col(1).width = 5000
    sheet1.row(0).write(1,'Dv')
    sheet1.col(1).width = 5000
    sheet1.row(0).write(2,'Genus')
    sheet1.col(2).width = 5000
    sheet1.row(0).write(3,'Locality')
    sheet1.row(0).write(4,'time_bin')
    sheet1.row(0).write(5,'lat_bin')
    sheet1.col(5).width = 8000
    sheet1.row(0).write(6,'Formation')
    row = 1
    for object in data_list:
        if (convGenus(object.species) == taxon):
            known_locality = False
            for time in geotime:
                if object.locality in geotime[time]:
                    if taxon == 'Noeggerathiopsis':
                        if time == 'Early':
                            early['Dv'].append(object.Dv)
                            early['Kleaf'].append(object.Kleaf)
                            early['gs'].append(object.gs)
                            early['Pc'].append(object.Pc)
                            early['Int'].append(object.intrWUE)
                        elif time == 'Middle':
                            middle['Dv'].append(object.Dv)
                            middle['Kleaf'].append(object.Kleaf)
```

```
                middle['gs'].append(object.gs)
                middle['Pc'].append(object.Pc)
                middle['Int'].append(object.intrWUE)
            elif time == 'Late':
                late['Dv'].append(object.Dv)
                late['Kleaf'].append(object.Kleaf)
                late['gs'].append(object.gs)
                late['Pc'].append(object.Pc)
                late['Int'].append(object.intrWUE)
            sheet1.row(row).write(4,time)
            known_locality = True
            break
        if known_locality:
            for bin in latitudes:
                if object.locality in latitudes[bin]:
                    sheet1.row(row).write(5,bin)
                    break
            for name in formations:
                if object.locality in formations[name]:
                    sheet1.row(row).write(6,name)
                    break
            sheet1.row(row).write(0,object.specimen_num)
            sheet1.row(row).write(1,object.Dv)
            sheet1.row(row).write(2,convGenus(object.species))
            sheet1.row(row).write(3,object.locality)
            row += 1
    book.save(os.path.join(cwd_path,'ANOVA Output',file_string))
    file_string = "ANOVA Master " + taxon + " " + strftime("%Y-%m-%d %H.%M") + ".xls"
    output_counter += 1

error_log(output_counter,zero_files,locality_list,formations,latitudes,geotime)
```

 # LMA Analysis
 # Written in Python 2.7

```
# Andrew B. Schwendemann

import glob
import math
from time import strftime
from xlrd import open_workbook
from xlwt import Workbook, Style

class RecordClass: # structure for leaf data
    def __init__(self,
specimen_num=None,locality=None,leaf=None,species=None,pet_width=None,surf_area=None
,LMA=None,partial=None):
        self.specimen_num = specimen_num
        self.locality = locality
        self.leaf = leaf
        self.species = species
        self.pet_width = pet_width # in cm
        self.surf_area = surf_area # in cm^2
        self.LMA = LMA # in g m^-2
        self.partial = partial # partial solution of LMA used for prediction interval
    def display_record_data(self):
        print "\nFor specimen: %s \n" % self.specimen_num
        print "\tLocality: %s" % self.locality
        print "\tSpecies: %s" % self.species
        print self.leaf
        print "\tPetiole width = %g cm" % self.pet_width
        print "\tSurface area = %g cm^2" % self.surf_area
    def display_record_LMA(self):
        print "\nFor specimen: %s \n" % self.specimen_num
        print "\tSpecies: %s" % self.species
        print self.leaf
        print "\tPartial solution: %g" % self.partial
        print "\tLMA = %g g m^-2" % self.LMA


def display_all_records(record_list): # prints raw data from list of class objects
    for j in range(0, len(record_list)):
        record_list[j].display_record_data()
    return

def display_all_LMA(record_list): # prints LMA from class list of records
    for k in range(0, len(record_list)):
        record_list[k].display_record_LMA()
    return
```

```
def calculate_LMA(PW, SA, b, a): # calculates the LMA and writes to record
    partial = math.log10(math.pow(PW,2)/SA)
    multcoeff = partial*b + a
    lma = math.pow(10,multcoeff)
    return (lma,partial)

def determine_LLS(record_tuple): # calculates LLS
    if record_tuple[0] <= 51.5: # 95% of species in this LMA range have LLS in this range
        return " < 12 months"
    if record_tuple[0] > 51.5: # 87% of species in this LMA range have LLS in this range
        return " > 12 months"

def convGenus(lng_str):
    found_sp = False
    for char in lng_str:
        if char.isspace() == True:
            genus,sp_epithet = lng_str.split(' ')
            found_sp = True
            break
    if found_sp == False:
        genus = lng_str
    return genus

def calculate_stats(record_list): # calculates stats from regression analysis
    # calculates mean LMA for all elements in list
    total = 0
    for j in range(0, len(record_list),2):
        total += record_list[j]
    average = total/(len(record_list)/2)

    # calculates Prediction Interval
    Syx2 = 0.0231325 # Royer et al. (2010)
    students = 1.986 # two-tailed t-value for (n-2) degrees of freedom (calibration set n) # Royer
et al. (2010)
    x_calib = -2.473 # Royer et al. (2010)
    sum_squares = 17.76 # Royer et al. (2010)
    n = 95 # Royer et al. (2010)
    k = len(record_list)/2
    sum = 0
    for q in range(1, len(record_list),2):
        sum += record_list[q]
    xi = sum/k

    plus_minus = students*(math.pow(Syx2*((1.0/k)+(1.0/n)+(math.pow(xi-
x_calib,2.0)/sum_squares)),0.5))
```

```
    PI_plus = math.pow(10.0,math.log10(average) + plus_minus)
    PI_minus = math.pow(10.0, math.log10(average) - plus_minus)
    return (average, PI_minus, PI_plus)


# regression data from previous analysis
reg_coeff = 0.3076 # Royer et al.(2010)
intercept = 3.015  # Royer et al.(2010)

class_list = []
scale_bar = 1.0
summary = {}
locality_dict = {}
# magnification:1 um = value px
unit_conversions =
{'15.62':0.49,'20':0.6,'50':1.45,'62.5':1.8,'80':2.32,'100':2.98,'125':3.6,'160':4.62,'200':5.85,'250':7.
26,'320':9.24,'400':11.8,'500':14.7,'640':18.5,'1600':46.7,'1008':29.5,'787.5':23,'1125':35.3,'1000':2
8.8,'12.5':0.38,'630':18.4}


for infile in glob.glob("LMA_Input*.xls"):

    site, block1 = infile.split('{')
    site = site[10:-1]
    block1a, block1b = block1.split('[')
    spec_num, leafdelim = block1a.split('}')
    leafdelim = leafdelim[1:-1]
    taxonomic_data, mag = block1b.split(']')
    mag = mag[1:-4]
    wb = open_workbook(infile)
    if locality_dict.has_key(site) == False:
        locality_dict[site] = []
        locality_dict[site].append(taxonomic_data)
    elif locality_dict.has_key(site) == True:
        taxon_found = False
        for i in range(0,len(locality_dict[site])):
            if locality_dict[site][i] == taxonomic_data:
                taxon_found = True
        if taxon_found == False:
            locality_dict[site].append(taxonomic_data)

    for sheet in wb.sheets():

class_list.append(RecordClass(spec_num,site,leafdelim,taxonomic_data,sheet.cell(1,3).value,she
et.cell(2,1).value))
```

```
        conversion = scale_bar/sheet.cell(3,3).value
        class_list[-1].pet_width = class_list[-1].pet_width*conversion
        class_list[-1].surf_area = class_list[-1].surf_area*conversion
        lma_sol = calculate_LMA(class_list[-1].pet_width, class_list[-1].surf_area, reg_coeff,
intercept)
        class_list[-1].LMA = lma_sol[0]
        class_list[-1].partial = lma_sol[1]

# code to test for regional differences
local_factors = {}
for i in range(0,len(class_list)):
    if local_factors.has_key(class_list[i].species) == False:
        local_factors[class_list[i].species] = {class_list[i].locality:[]}
        local_factors[class_list[i].species][class_list[i].locality].append(class_list[i].LMA)
        local_factors[class_list[i].species][class_list[i].locality].append(class_list[i].partial)
    elif local_factors.has_key(class_list[i].species) == True:
        locality_found = False
        for location in local_factors[class_list[i].species]:
            if location == class_list[i].locality:
                locality_found = True
                local_factors[class_list[i].species][location].append(class_list[i].LMA)
                local_factors[class_list[i].species][location].append(class_list[i].LMA)
        if locality_found == False:
            local_factors[class_list[i].species][class_list[i].locality] = []
            local_factors[class_list[i].species][class_list[i].locality].append(class_list[i].LMA)
            local_factors[class_list[i].species][class_list[i].locality].append(class_list[i].partial)

# tests for regional differences by genus
local_genus = {}
for i in range(0,len(class_list)):
    genera_var = convGenus(class_list[i].species)
    if local_genus.has_key(genera_var) == False:
        local_genus[genera_var] = {class_list[i].locality:[]}
        local_genus[genera_var][class_list[i].locality].append(class_list[i].LMA)
        local_genus[genera_var][class_list[i].locality].append(class_list[i].partial)
    elif local_genus.has_key(genera_var) == True:
        locality_found = False
        for location in local_genus[genera_var]:
            if location == class_list[i].locality:
                locality_found = True
                local_genus[genera_var][location].append(class_list[i].LMA)
                local_genus[genera_var][location].append(class_list[i].partial)
        if locality_found == False:
            local_genus[genera_var][class_list[i].locality] = []
            local_genus[genera_var][class_list[i].locality].append(class_list[i].LMA)
```

```
        local_genus[genera_var][class_list[i].locality].append(class_list[i].partial)

# code that groups by genus
genus_summary = {}
for i in range(0,len(class_list)):
   if genus_summary.has_key(class_list[i].locality) == False:
      genera_var = convGenus(class_list[i].species)
      genus_summary[class_list[i].locality] = {genera_var:[]}
      genus_summary[class_list[i].locality][genera_var].append(class_list[i].LMA)
      genus_summary[class_list[i].locality][genera_var].append(class_list[i].partial)
   elif genus_summary.has_key(class_list[i].locality) == True:
      genus_found = False
      for genus in genus_summary[class_list[i].locality]:
         genera_var = convGenus(class_list[i].species)
         if genus == genera_var:
            genus_found = True
            genus_summary[class_list[i].locality][genera_var].append(class_list[i].LMA)
            genus_summary[class_list[i].locality][genera_var].append(class_list[i].partial)
      if genus_found == False:
         genus_summary[class_list[i].locality][genera_var] = []
         genus_summary[class_list[i].locality][genera_var].append(class_list[i].LMA)
         genus_summary[class_list[i].locality][genera_var].append(class_list[i].partial)

# setup summary dictionary
for i in range(0,len(class_list)):
   if class_list[i].locality not in summary:
      summary[class_list[i].locality] = {class_list[i].species:[]}
      summary[class_list[i].locality][class_list[i].species].append(class_list[i].LMA)
      summary[class_list[i].locality][class_list[i].species].append(class_list[i].partial)
   elif class_list[i].locality in summary:
      taxon_found = False
      for taxon in summary[class_list[i].locality]:
         if taxon == class_list[i].species:
            taxon_found = True
            summary[class_list[i].locality][taxon].append(class_list[i].LMA)
            summary[class_list[i].locality][taxon].append(class_list[i].partial)
      if taxon_found == False:
         summary[class_list[i].locality][class_list[i].species] = []
         summary[class_list[i].locality][class_list[i].species].append(class_list[i].LMA)
         summary[class_list[i].locality][class_list[i].species].append(class_list[i].partial)

# move through dictionary for stat calculations
for location in summary:
   for taxon in summary[location]:
      summary[location][taxon] = calculate_stats(summary[location][taxon])
```

```
for taxon in local_factors:
    for location in local_factors[taxon]:
        local_factors[taxon][location] = calculate_stats(local_factors[taxon][location])

# Output to xls file
for location in summary:
    book = Workbook()
    for taxon in summary[location]:
        sheet1 = book.add_sheet(taxon)
        sheet1.col(0).width = 8000
        sheet1.row(0).write(0,'Specimen #')
        sheet1.row(0).write(1,'Leaf')
        sheet1.row(0).write(2,'PW')
        sheet1.row(0).write(3,'SA')
        sheet1.row(0).write(4,'LMA')
        row = 1
        for i in range(0,len(class_list)):
            if (class_list[i].locality == location) and (class_list[i].species == taxon):
                sheet1.row(row).write(0,class_list[i].specimen_num)
                sheet1.row(row).write(1,class_list[i].leaf)
                sheet1.row(row).write(2,round(class_list[i].pet_width,2))
                sheet1.row(row).write(3,round(class_list[i].surf_area,1))
                sheet1.row(row).write(4,round(class_list[i].LMA,1))
                row += 1
        sheet1.row(row+1).write(0,"Data generated with: log_10(LMA) = %g*log_10(PW^2/A) +
%g \n \n" % (reg_coeff, intercept))
        sheet1.row(row+2).write(0,"Average LMA = %g g m^-2, n = %d" % (summary[location]
[taxon][0], row-1))
        sheet1.row(row+3).write(0,"LLS for average LMA is %s" %
determine_LLS(summary[location][taxon]))
        sheet1.row(row+4).write(0,"Prediction Interval = %g to %g g m^-2" % (summary[location]
[taxon][1], summary[location][taxon][2]))
    book.save(location + ' LMA ' + strftime("%Y-%m-%d %H.%M") + ".xls")
```